Synthesis of a Glycosidase Inhibitor and a Potential Phosphoglucomutase Inhibitor, Expression of the Corresponding Proteins, and their Evaluation Using Kinetics or ^{19}F-NMR Spectroscopy

by

Madison A. Carroll

Submitted in partial fulfilment of the requirements
for the degree of Master of Science

at

Dalhousie University
Halifax, Nova Scotia
June 2018

Table of Contents

List of Tables

List of Figures

Abstract

The inhibition and reactivation of several naturally prevalent enzymes has many pharmaceutical applications. A glycosidase inhibitor, 2,4-dinitrophenyl 2-deoxy-2-fluoro-β-D-glucopyranose (**6**), was synthesized and its kinetics evaluated with the Family-3 retaining glycosidases, DesR, EryBI, and Hsero1941. **6** displayed quantitative inactivation of DesR and EryBI after two hours and 54% inactivation of Hsero1941 after 16 hours. Various acceptors were screened in attempts to observe transglycosylation activity from the enzymes.

β-phosphoglucomutase (βPGM) is an essential enzyme for energy metabolism in cells. A W216F mutant βPGM was produced and its transition state analogue (TSA) complexation with metal fluorides and phospho- or phosphono-glucosides was monitored using ^{19}F NMR spectroscopy. Molar ratios of metal fluoride and complexed 5FW24 were observed spectroscopically, indicating that metal fluorides are representative of the transition states. A novel potential inhibitor of βPGM, diammonium 3-deoxy-3-fluoro-β-D-glucopyranosylmethylphosphonate (**21**), was synthesized which is expected to lead to improved ratios of complexed: free βPGM during TSA complexation.

List of Abbreviations and symbols used

A/B	acid/base
AcCl	acetyl chloride
Ac_2O	acetic anhydride
AIBN	azobisisobutyronitrile
Ala	alanine
Amp	ampicillin
Anh.	anhydrous
Asp	aspartic acid
βG1P	β-glucose 1-phosphate
βG16P	β-glucose 1,6-bisphosphate
βPGM	β-phosphoglucomutase
^{13}C	carbon
CAZy	Carbohydrate-Active enZYmes
COSY	COrrelation SpectroscopY
c. v.	column volume
δ	chemical shift in ppm
DABCO	1,4-diazabicyclo[2.2.2]octane
DAST	diethylaminosulfur trifluoride
ddH_2O	distilled deionized water
DIPEA	*N*,*N*-diisopropylethylamine
DMAP	4-dimethylaminopyridine

DMF	dimethylformamide
DMP	Dess-Martin Periodinane
DNA	deoxyribonucleic acid
DNFB	2,4-dinitrofluorobenzene
dNTP	deoxynucleotide
DTT	dithiothreitol
ε	extinction coefficient
EDTA	ethylenediaminetetracetic acid
^{19}F	fluorine
5-FW	5-fluorotryptophan
5FWβPGM	5-fluorotryptophan labelled βPGM
G1CF$_s$P	(*S*)-1-β-phosphonofluoromethylene-1-deoxy-D-glucopyranose
G1CP	β-D-glucopyranosylmethylphosphonate
G6P	glucose 6-phosphate
Gln	glutamine
Glu	glutamic acid
Gly	glycine
^{1}H	proton
$\{^{1}H\}$	proton decoupled
h	hours
HAD	Haloalkanoic Acid Dehalogenase
HEPES	4-(2-hydroxyethyl)-1-piperazineethanesulfonic acid

HSQC	Heteronuclear Single Quantum Correlation
HMBC	Heteronuclear Multiple-Bond Correlation
ITPG	isopropyl β-D-1-thiogalactopyranoside
kDa	kilodaltons
kb	kilobases
LB	lysogeny broth
LB_{Amp}	lysogeny broth containing ampicillin (100 μg/mL)
LB_{kan}	lysogeny broth containing kanamycin (50 μg/mL)
Leu	leucine
min	minutes
MWCO	molecular weight cut-off
NMR	nuclear magnetic resonance
Nu	nucleophilic
OAc	acetate
OD	optical density
^{31}P	phosphorus
PAGE	polyacrylamide gel electrophoresis
PBS	phosphate buffered saline
pNP-glc	para-nitrophenyl glucopyranoside
pNP-GlcNAc	para-nitrophenyl *N*-acetyl-β-D-glucosaminide
R_f	retention factor
rpm	revolutions per minute

sat. aq.	saturated aqueous solution
SDS	sodium dodecyl sulfate
SOC	super optimal broth with catabolite repression
TAE	tris base, acetic acid, and EDTA
TBAF	tetrabutylammonium fluoride
TBAI	tetrabutylammonium iodide
THF	tetrahydrofuran
Thr	threonine
TLC	thin layer chromatography
TMSI	trimethyl silyl iodide
Tris	tris(hydroxymethyl)aminomethane
TSA	transition state analogue
UV	ultraviolet

Acknowledgements

First, I would like to thank my supervisor Dr. David Jakeman for his insight and advice as well as his encouragement throughout these projects. I would also like to thank my committee members, Dr. Bruce Grindley and Dr. Alex Speed, for reading this thesis and for providing helpful suggestions for my research.

I would like to acknowledge the past and present members of the Jakeman lab group who have assisted me throughout my MSc. A special thanks goes to Dr. Diogo Ducatti who worked on the DesR and Hsero1941 acceptor screening with me and taught me much about enzyme kinetics. Another thank you goes to Salman Alsharif who synthesized some of the materials for scale-up of the diammonium 3-deoxy-3-fluoro-β-D-glucopyranosylmethylphosphonate (**21**) synthesis. I would also like to acknowledge Jian-She Zhu and Stephanie Forget for their assistance in learning new lab techniques both in synthetic chemistry and microbiology.

I would also like to acknowledge Xiao Feng who acquired all of the high resolution mass spectra and Mike Lumsden who was able to answer any questions I had about the acquisition of the NMR spectra. I would like to thank Matthew Bowler from the European Molecular Biology Laboratory in Grenoble, France who acquired the X-ray crystallographic data of the β-phosphoglucomutase. Finally, I would like to thank the Natural Sciences and Engineering Council of Canada, the Nova Scotia Health Research Foundation, and the Nova Scotia Research and Innovation Graduate Scholarship for helping to fund my research.

Chapter 1. Introduction

1.1. Glycosidases

Glycosidases, or glycoside hydrolases, are enzymes which cleave the glycosidic linkage between carbohydrates or between a carbohydrate and an aglycone.[1] The glycosidic linkage is one of the strongest type of bonds that occurs in natural biopolymers: for example, the half-life for the spontaneous hydrolysis of cellulose is five million years. Glycoside hydrolases can catalyze hydrolysis reactions with half-lives as short as 6.9×10^{-4} seconds.[2] These enzymes are necessary for the degradation of biomass and for many antipathogenic and pathogenic functions. They are also required for many regular cellular functions such as glycoprotein biosynthesis.[3] Glycosidases function primarily by either a retaining or an inverting mechanism. Inverting glycosidases create a product with the opposite stereochemistry from the reactant at the anomeric centre. Retaining glycosidases catalyze reactions in two steps, each of which includes an inversion, so that overall the stereochemistry is retained (Figure 1).[2]

Retaining glycosidases have two catalytic carboxylic acid residues in their active site. One of these residues (an aspartic acid or glutamic acid) acts as a nucleophile and the other acts as an acid/base. The nucleophilic residue attacks the anomeric position of the glycosyl substrate, forming a covalent bond with C1. Simultaneously, the substituent on C1 leaves and is protonated by the acid/base residue.[4] The species bound in the active site is a glycosyl-enzyme intermediate[5] which can either undergo hydrolysis or transglycosylation.[4] Hydrolysis (Figure 1) occurs when the acid/base residue removes a proton from water, after which the resulting hydroxide attacks the anomeric position of the donor sugar, breaking the glycosyl-enzyme bond. A product having a hydroxyl group at

the anomeric position and the same stereochemistry as the reactant is produced.[4] Transglycosylation (Figure 2) may occur if an appropriate sugar or alcohol acceptor is present. The acid/base residue deprotonates the acceptor, which then attacks the anomeric position of the donor sugar, breaking the glycosyl-enzyme bond and forming an ether linkage. Thus, the product maintains the same stereochemistry at the anomeric position as the reactant, with the acceptor bound to C1.[4]

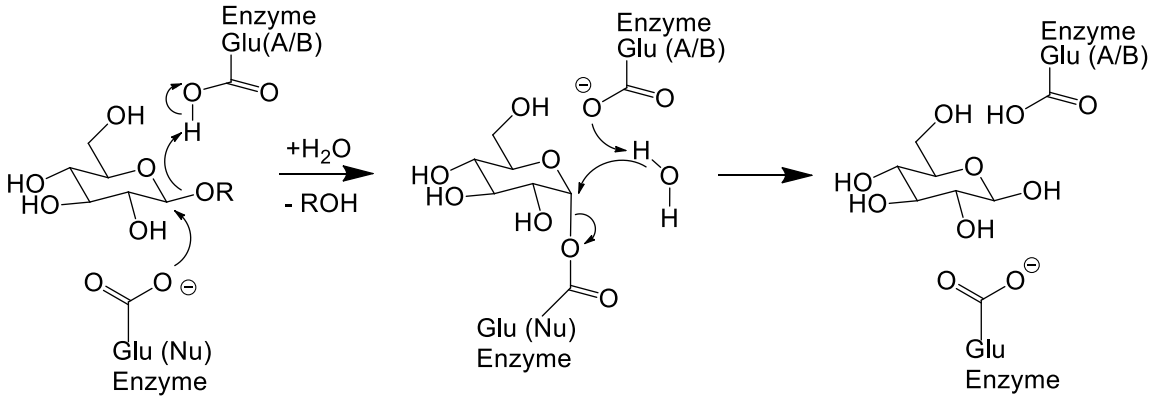

Figure 1. Hydrolysis of a β-D-glucopyranosyl substrate in the active site of a retaining glycosidase.

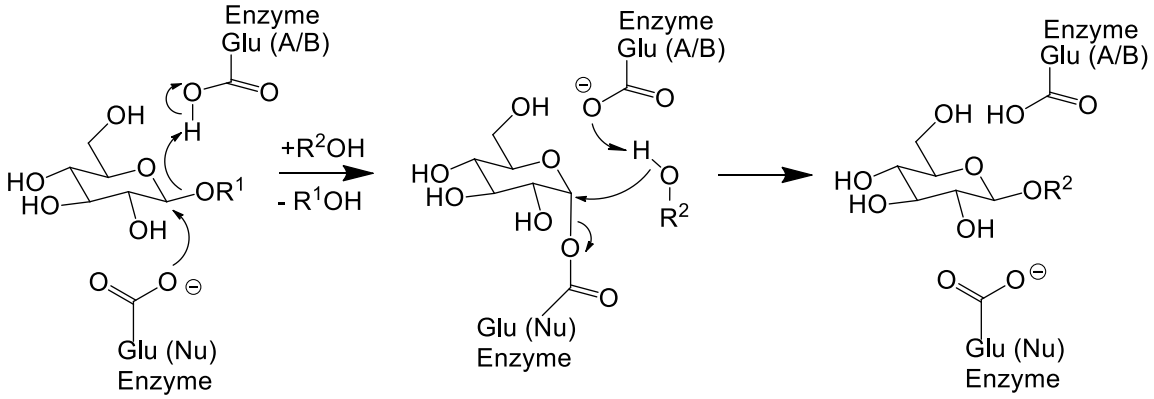

Figure 2. Transglycosylation of a β-D-glucopyranosyl substrate in the active site of a retaining glycosidase, where R^2OH is an alcohol ($R^2 \neq H$).

If capable of catalyzing the transglycosylation of a donor sugar with an acceptor sugar, a retaining glycosidase can be utilized for oligosaccharide synthesis.[6] However, the

hydrolysis reaction will compete with the transglycosylation reaction, reducing the yield. A method to avoid this involves using a glycosynthase to catalyze the transglycosylation reaction instead. A glycosynthase is a glycosidase where the nucleophilic catalytic residue has been mutated to a non-nucleophilic residue such as serine, alanine, or glycine.[4,6] Glycosynthase mutants can catalyze transglycosylation whilst disabling hydrolysis if a suitable acceptor is present. An example of a glycosynthase-catalyzed reaction is depicted in Figure 3, where the C1-F bond is more stable than the C1-enzyme bond formed when a nucleophilic residue is present in the active site (Figures 1 and 2) and cannot be hydrolyzed by water. The C1-F bond will only be cleaved if a strong nucleophile is present (ie. a deprotonated acceptor), leading to transglycosylation. Reactions catalyzed by glycosynthases proceed by an inverting mechanism (Figure 3). The use of glycosynthases as catalysts offers a single-step method of oligosaccharide synthesis using mild conditions.[4]

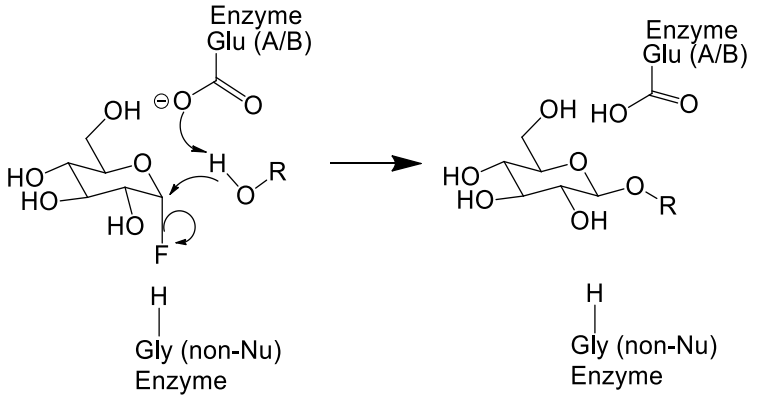

Figure 3. Transglycosylation reaction catalyzed by a glycosynthase mutant

1.2. DesR, EryBI, and Hsero1941 enzymes

Three enzymes were used in inactivation studies and as catalysts in attempted transglycosylation reactions. Two of the enzymes, DesR and EryBI, are Family-3 retaining glycosidases, cloned from *Steptomyces venezuelae* and *Saccharopolyspora erythraea*,

respectively.[7,8] The third, Hsero1941, is a Family-3 β-*N*-acetylglucosaminidase from *Herbaspirillum seropedicae* SmR1.[9] DesR and EryBI were selected to be studied as they catalyze the glycolysis of glucosylated antibiotics in their respective host organisms,[8,10] a process which could be exploited for pharmaceutical purposes. Hsero1941 has not been studied as extensively, however, as an *N*-acetyglucosaminidase from Family 3, it could potentially prove useful in drug design as Family 3 *N*-acetyglucosaminidases are reported to be producers of metabolic intermediates used in the regulation of β-lactamase expression, as well as catalysts in cell wall recycling in both Gram-positive and Gram-negative bacteria.[9] Previous studies in the Jakeman lab have explored the inhibition of DesR by macrolide antibiotics[7] and evaluated the glycosidase activity of EryBI using several aryl glycosides as substrates.[8] Hsero1941 has been studied in the Jakeman lab as well, for its phosphorolytic and hydrolytic activity.[9] The current work focuses on the reverse reactions of DesR, EryBI, and Hsero1941 which involve forming glycosidic linkages rather than cleaving them.

The source of DesR, *Steptomyces venezuelae* is a gram-positive bacterium that produces the antibiotics methymycin and picromycin. As a self-resistance mechanism, the antibiotics are glucosylated to inactivate them while they remain in the cell. Once transported outside the cell, DesR reactivates the antibiotics by hydrolyzing the glucose moiety.[10] Three DesR mutants were previously produced in the Jakeman lab with the goal of using them to catalyze the formation of β-(1-2)-glycosidic linkages. However, the mutants proved to be incapable of glycosynthase activity.[7] This study attempted transglycosylation using the wild-type DesR glucosidase, a 2-deoxy-2-fluoro donor sugar (*vide infra*), and various acceptors.

It is postulated that EryBI in *Saccharopolyspora erythraea* serves an analogous purpose as DesR in *S. venezuelae*. *S. erythraea* produces the macrolide antibiotic erythromycin which is present in the glucosylated form inside the cells. EryBI is thought to be responsible for the cleavage of this glycosidic linkage which reactivates erythromycin.[8] Potential glycosynthase mutants of EryBI were produced in the Jakeman lab; one of which displayed catalytic glycosynthase activity by forming a β-(1,2)-glycosidic linkage between an α-glycosyl fluoride and the macrolide antibiotic erythromycin.[8] In this study, transglycosylation was attempted using the wild-type EryBI glucosidase, a 2-deoxy-2-fluoro donor sugar (*vide infra*), and erythromycin as well as various other acceptors, in attempts to expand the scope of these catalysts.

The source of Hsero 1941, *Herbaspirillum seropedicae* SmR1 is a nitrogen-fixing bacterium which possesses 23 genes coding for glycoside hydrolases. Two of these glycosidases belong to Carbohydrate-Active EnZYmes (CAZy) Family 3, one of which is Hsero1941. As backdrop to this thesis, Dr. Diogo Ducatti showed that Hsero1941 acts as a glycoside hydrolase with a retaining mechanism. Further, the enzyme was shown to exhibit a broad aglycone site specificity.[9] In this study, Hsero1941 was utilized in attempts to catalyze transglycosylation reactions with a 2-deoxy-2-fluoro sugar donor.

1.3. 2,4-Dinitrophenyl 2-deoxy-2-fluoro-β-D-glucopyranose

2-deoxy-2-fluoro sugars have been reported as substrates and as inhibitors of glycosidases as well as donor sugars in successful β-glucosidase catalyzed transglycosylation reactions.[11] They have been used as donor sugars by glycosynthases to aid in the synthesis of oligosaccharides as well.[12] The presence of the ^{19}F nucleus makes them useful for labelling the active sites of enzymes, meaning complexation can be monitored using ^{19}F

NMR spectroscopy. X-ray analysis of covalent glycosyl-enzyme intermediates has also been performed using 2-deoxy-2-fluoro sugars as substrates.[13]

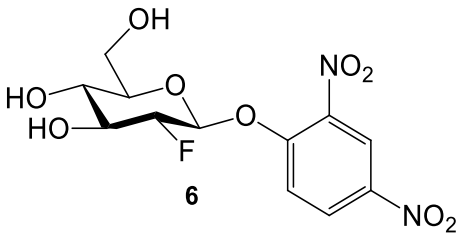

Figure 4. 2,4-dinitrophenyl 2-deoxy-2-fluoro-β-D-glucopyranose (**6**)

The 2-deoxy-2-fluoro sugar, 2,4-dinitrophenyl 2-deoxy-2-fluoro-β-D-glucopyranose (**6**), was synthesized and used for the inhibition of DesR, EryBI, and Hsero1941. **6** has been previously synthesized by Blanchard et al. for use in aglycone specificity screening.[5] **6** was used to inhibit six retaining glycosidases: *Agrobacterium sp.* β-glucosidase, *Xanthomonas manihotis* β-galactosidase, *Bacillus circulans* β-galactosidase, *Cellulomonas fimi* β-mannosidase, *Cellulomonas fimi* glucanase/xylanase, and *Streptomyces lividans* cellulase. The enzymes were found to form hydrolysis-resistant glycosyl-enzyme intermediates with **6**. This is an example of covalent inactivation, where a covalent bond between the substrate and an amino acid of the active site is formed, as opposed to non-covalent inactivation where the substrate is held in place by weaker forces such as hydrogen bonds or electrostatic interactions.[5,14] After successful covalent inactivation of the enzymes with **6**, reactivation experiments were conducted using sugars as acceptors, which found aryl glycosides, especially para-nitrophenyl glycosides, to be the most effective at reactivating the glycosidases.[5] In the current work, **6** is used to inactivate three other retaining glycosidases: DesR, EryBI, and Hsero1941. This is followed by attempted reactivation of the glycosidases via transglycosylation reactions where **6** acts as

the donor sugar and various hydroxyl-containing compounds (sugars, alcohols, macrolide antibiotics, etc.) are used as potential acceptors.

1.4. β-phosphoglucomutase

Another class of enzymes which we chose to study along with glycosidases, based on its prevalence in biological functions and use as a potential drug target, are phosphate transfer enzymes, specifically β-phosphoglucomutase (βPGM). Phosphate transfer enzymes play key roles in many biological processes; for example thymidine kinase aids with DNA synthesis by catalyzing the transfer of a phosphate group from adenosine triphosphate (ATP) to the deoxynucleoside thymidine.[15] Catalytic phosphoryl transfer enzymes are essential as the spontaneous hydrolysis of phosphate groups is extremely slow and these enzymes can accelerate it by a factor of 10^{21}.[16] βPGM is considered a phosphate transfer mutase, which is a phosphoryl transfer enzyme that catalyzes the intramolecular transfer of a phosphate group.[17] βPGM was studied specifically, as it is the best characterized hexose 1-phosphate mutase and plays the important function of catalyzing the production of glucose 6-phosphate, a universal source of cellular energy.[16] It is an isomerase belonging to the Haloalkanoic Acid Dehalogenase (HAD) superfamily,[18] all members of which have a core catalytic domain comprised of three layers of repeating β-α units, with typical Rosmann fold topology. The phosphomutases of this superfamily have two aspartic acid residues in the active site, one which acts as a nucleophile and the other as an acid/base. Both aspartic acid residues also contribute to coordinating a single Mg^{2+} cofactor.[18] Most members of the HAD superfamily have inserts at two positions on the core domain, termed caps. These caps can be in an “open” or “closed” conformation thanks to the increased mobility provided by a single helical turn and a beta hairpin motif located directly

downstream from the first β-strand of the core Rossmanoid fold.[18] β-phosphoglucomutase is a unique enzyme of this superfamily which has a cap domain capable of binding two different substrates and catalyzing two reactions sequentially.[16,19] βPGM catalyzes the transfer of a phosphate group from β-glucose 1-phosphate (βG1P) to produce glucose 6-phosphate (G6P), proceeding though a β-glucose 1,6-bisphosphate (βG16P) intermediate as well as two transition states (Figure 5).[16]

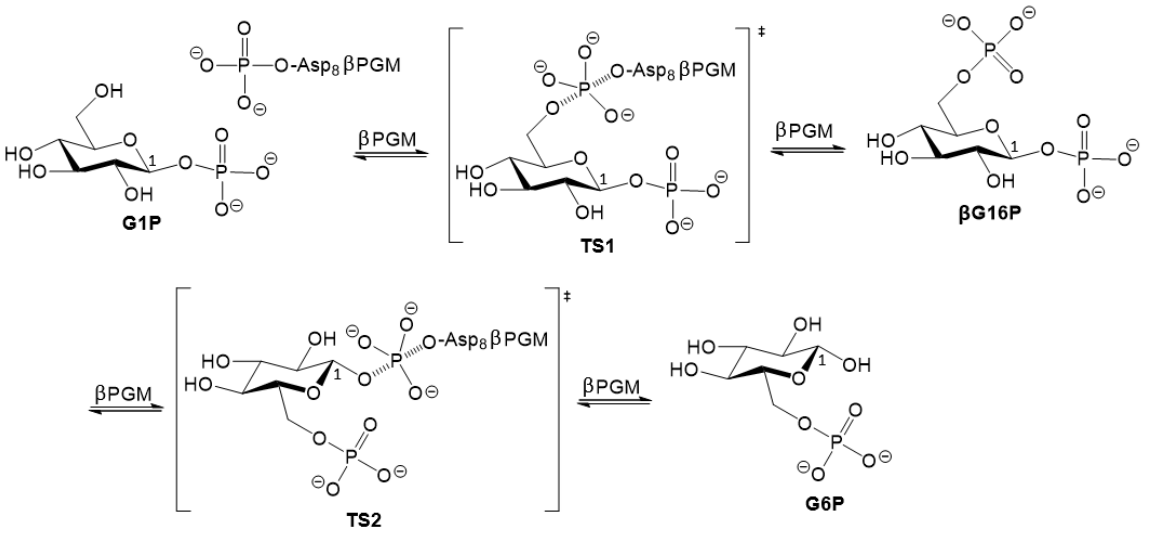

Figure 5. βPGM catalyzed conversion of β-glucose 1-phosphate to β-glucose 6-phosphate. (The anomeric centre is labelled as "1".)

This reaction is necessary for the synthesis of cell wall polysaccharides in bacteria as well as being essential for energy metabolism.[20] In its "cap-closed" conformation, the acid/base aspartic acid residue of βPGM is oriented so that it may form a hydrogen bond with the C1 oxygen of the substrate, stabilizing the complex. In the "cap-open" conformation, the aspartic acid is trapped outside of the active site where it interacts with Thr16 and Ala17 residues instead.[21] When βPGM binds β-G1P, it changes from its cap open conformation to its cap closed conformation, reverting back to its cap open form only upon the generation

of βG16P. This intermediate is released by the enzyme, reorients itself in the active site, and then binds to the enzyme again in the opposite orientation, converting the enzyme to its cap closed conformation. Finally, release of the product G6P regenerates the cap open conformation.[21,22]

1.5. Transition state analogues of β-phosphoglucomutase complexes

To learn more about an enzyme's mechanism, it is often desirable to study the transition state(s). However, it is not feasible to trap an enzyme in a transition state due to the high energy required to remain in this state.[23] The lifetime of a transition state is ephemeral, lasting only a few femtoseconds.[24] Instead, researchers use transition state analogues (TSA) to form longer lasting enzyme complexes, allowing for the study of this high-energy state.[24,25] Metal fluorides, such as AlF_4^- and MgF_3^-, have been reported to form stable complexes with phosphoryl transfer enzymes.[26] In some enzymes, such as β-phosphoglucomutase, this results in inhibition.[27] AlF_4^- and MgF_3^- both act as mimics of the phosphoryl group which is being transferring the between β-phosphoglucomutase nucleophilic aspartic acid residue (Asp_8) and the substrate during the transition states. Upon binding in the active site of βPGM, MgF_3^- adopts a trigonal-bipyramidal geometry and AlF_4^- an octahedral geometery.[27]

Transition state analogue complexes including a metal fluoride (either MgF_3^- or AlF_4^-), the enzyme βPGM, and a glucopyranosyl phosphate/phosphonate substrate are studied in this work. TSAs of both transition states are investigated. During the βPGM catalyzed conversion of βG1P to G6P, the first transition state is higher in free energy than the second transition state.[16] Due to this high free energy of the first transition state, AlF_4^- and MgF_3^- can not form stable complexes with βG1P. AlF_4^- and MgF_3^- with G6P will,

however, form transition state analogues of the more energetically favorable second transition state (βG16P conversion to G6P).[16,28] Methylene phosphonates (such as β-D-glucopyranosylmethylphosphonate), which are non-covalent inhibitors of βPGM and are non-hydrolysable, may be used along with AlF_4^- or MgF_3^- to mimic the first transition state.[16]

A convenient method for observing the formation of these transition state analogue complexes is to label a relevant amino acid of the enzyme with ^{19}F and subject the reaction mixture to ^{19}F NMR spectroscopy. For βPGM, tryptophan was selected as the amino acid to be labelled as βPGM possesses only two tryptophan residues which are located in the regions surrounding the active site: W216 (in the core domain) and W24 (in the cap domain). Previously in the Jakeman group, the two tryptophan residues were replaced with 5-fluorotryptophan residues to allow for the monitoring of TSA complexation using ^{19}F NMR spectroscopy. Along with the wild-type 5FWβPGM, a 5FWβPGM-His-W24F mutant was made (using site-directed mutagenesis), containing a single 5-fluorotryptophan residue, with a phenylalanine residue in place of the W24. The TSA complexes with 5FWβPGM-His-W24F have previously been studied using ^{19}F NMR spectroscopy.[19] The present study focuses on the 5FWβPGM-His-W216F mutant (where the W216 residue has been replaced with phenylalanine) and the monitoring of its TSA complexation using ^{19}F NMR spectroscopy. This study will also involve the synthesis of diammonium 3-deoxy-3-fluoro-β-D-glucopyranosylmethylphosphonate, a compound which is expected to form a transition state analogue 1 (TSA1) complex with βPGM. It is expected that the fluorine on C3 will give improved binding, due to its strong hydrogen bonding capability, compared to that previously observed with β-D-glucopyranosylmethylphosphonate.

1.6. Research aims

Project 1. Synthesis of 2,4-dinitrophenyl 2-deoxy-2-fluoro-β-D-glucopyranose and application as a covalent inactivator of DesR glucosidase, EryBI glucosidase, and Hsero1941 β-*N*-acetylglucosaminidase

1. Synthesize 2,4-dinitrophenyl 2-deoxy-2-fluoro-β-D-glucopyranose (**6**).
2. Test the ability of **6** to inactivate DesR, EryBI, and Hsero1941 using kinetic assays.
3. Compile a library of potential alcohol and sugar acceptors and screen these for the ability to participate in transglycosylation reactions (ie. reactivate the enzymes).

Project 2. The expression of ^{19}F-labelled β-phosphoglucomutase and the study of its transition state analogues

1. Prepare appropriate expression vector for βPGM-His-W216F using site-directed mutagenesis.
2. Prepare and purify recombinant ^{19}F- labelled βPGM-His-W216F protein by incorporating 5-fluorotryptophan.
3. Acquire ^{19}F NMR spectra of the protein to observe transition state analogue complexation.

Project 3. Synthesis of diammonium 3-deoxy-3-fluoro-β-D-glucopyranosylmethyl-phosphonate

1. Synthesize the potential βPGM inhibitor diammonium 3-deoxy-3-fluoro-β-D-glucopyranosylmethylphosphonate (**21**, Figure 6).

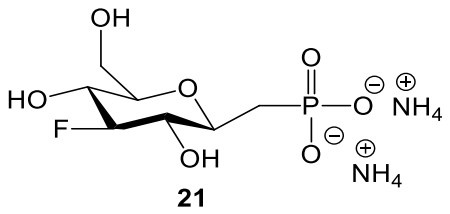

Figure 6. Diammonium 3-deoxy-3-fluoro-β-D-glucopyranosylmethylphosphonate (**21**)

Chapter 2. Results and Discussion of the synthesis and application of a covalent inactivator of DesR, EryBI, and Hsero1941 glycosidases

2.1. Synthesis of 2,4-dinitrophenyl 2-deoxy-2-fluoro-β-D-glucopyranose (6)

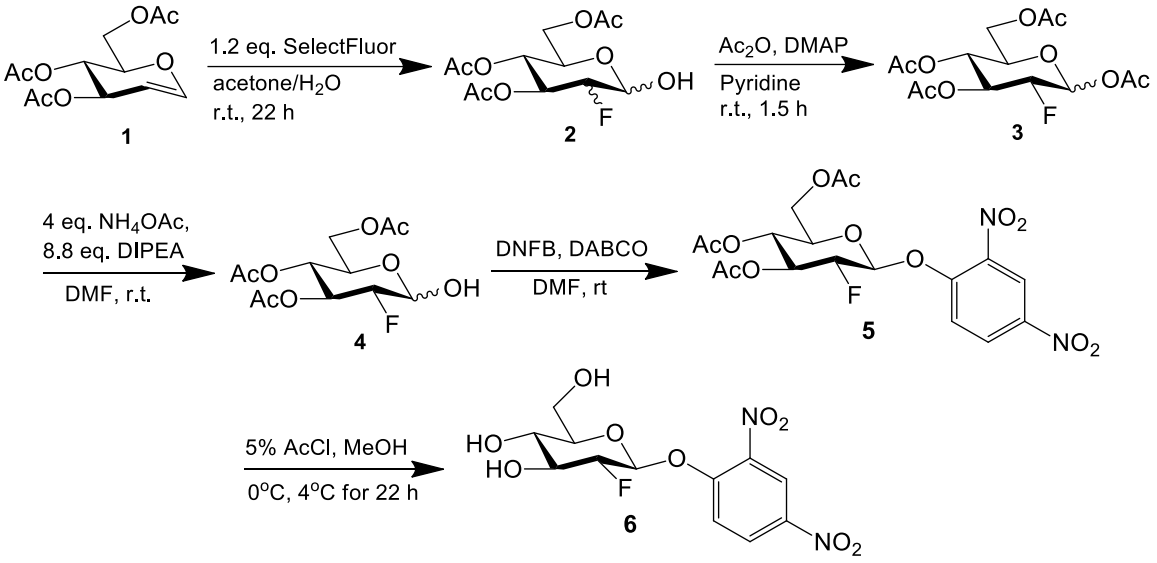

Figure 7. Synthesis of 2,4-dinitrophenyl 2-deoxy-2-fluoro-β-D-glucopyranose (**6**) in five steps

2,4-Dinitrophenyl 2-deoxy-2-fluoro-β-D-glucopyranose (**6)** was synthesized in five steps using procedures from the literature (Figure 7).[29-31] First, tri-*O*-acetyl-D-glucal (**1**) was subjected to a fluorination at C2, using Selectfluor® in acetone/water.[29] The product mixture, containing four diastereomers of 2-deoxy-2-fluoro-3,4,6-tri-*O*-acetyl-D-manno/glucopyranose (**2**), was directly subjected to the next reaction. The anomeric position of **2** was acetylated, using acetic anhydride in pyridine and catalytic DMAP,[29] to allow for chromatographic separation where **3** was isolated (21% over the first two steps). The gluco configured products **3** were then subjected to a selective deprotection at the anomeric position, using ammonium acetate and *N*,*N*-diisopropylethylamine (DIPEA) in DMF,[30] to yield **4** (75%). A 2,4-dinitrophenyl group was then attached to the anomeric

hydroxyl group of **4** by adding 2,4-dinitrofluorobenzene (DNFB) and 1,4-diazabicyclo[2.2.2]octane (DABCO) in DMF[31] to give **5** (52%). Compound **5** was then globally deprotected using 5% acetyl chloride in methanol,[31] which produced HCl in situ to hydrolyze the acetyl groups, giving **6** (92%).

Once synthesized, the compounds (**2**-**6**) were characterized using NMR spectroscopy and by comparing this data to data reported in the literature. Compound **2** was subjected to ^{19}F NMR spectroscopy and compounds **3-6** were characterized using ^{19}F, COSY, and ^{1}H NMR spectroscopy. **2** had four signals in its ^{19}F NMR spectrum (Appendix A): -201.0, -202.4, -204.0, and -219.7 ppm, corresponding to β-gluco, α-gluco, α-manno, and β-manno configured products, respectively, consistent with reported data.[29]

The ^{19}F{^{1}H} NMR spectrum of **3** (Figure 8A) had two signals, -201.0 and -202.3 ppm, corresponding to β-gluco and α-gluco configured products, respectively, as reported in the literature.[29] In the ^{1}H NMR spectrum (Figure 8B), peaks corresponding to α-gluco configured (major) and β-gluco configured (minor) products were also observed. It was possible to tell which signals belonged to protons of the α-configured product versus the β-configured product as the integrations displayed a 1α: 0.6β ratio. The acetyl group protons for both anomers produced several overlapping singlets around 2.01 ppm, integrating to a total of 12 α protons plus 12 β protons. The anomeric protons of the α and β anomers (for compounds **3**-**5**) could be differentiated by the fact that the β was expected to be shifted further upfield and to be split into a doublet of doublets (coupling with both H2 and F), whereas the α appears further downfield and split into a doublet (coupling with H2 only).[29-31]

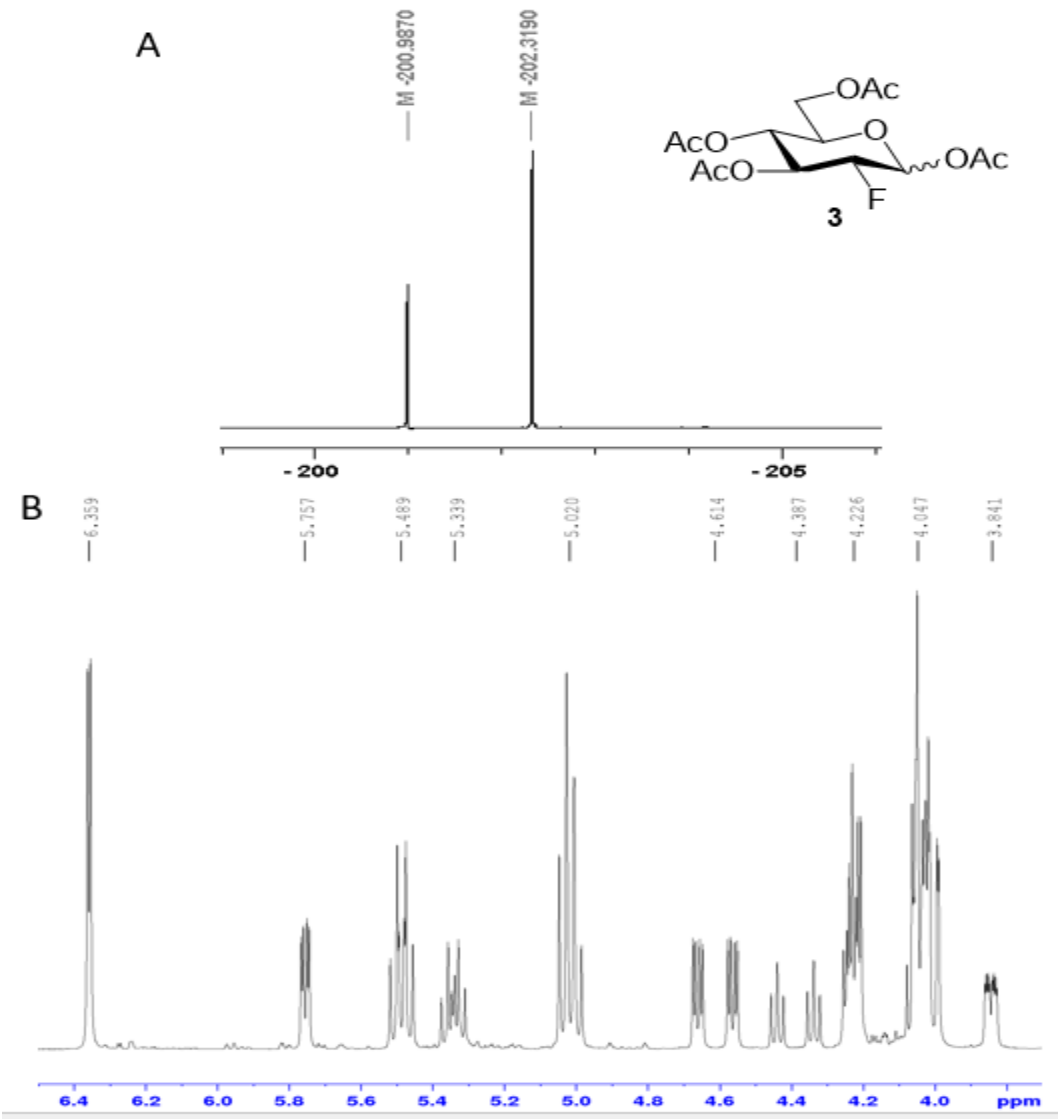

Figure 8. NMR spectra of 1,3,4,6-tetra-*O*-acetyl-2-deoxy-2-fluoro-D-glucopyranose (**3**). **A)** $^{19}F\{^{1}H\}$ (470MHz, $CDCl_3$) **B)** ^{1}H (500 MHz, $CDCl_3$).

For the β-configured **3**, the anomeric proton signal was identified as the doublet of doublets at 5.76 ppm which coupled with the H2 ($^{3}J_{H1-H2}$= 8.0 Hz) and the fluorine ($^{3}J_{H1-F}$= 3.1 Hz) on the neighbouring carbon. H2 produced the doublet of triplets at 4.39 ppm which coupled vicinally to fluorine ($^{2}J_{H2-F}$= 50.7 Hz) as well as geminally to H1 and H3 (^{3}J= 8.6 Hz). The doublet of triplets at 5.34 ppm was identified as H3, which coupled to the fluorine on the next carbon over ($^{3}J_{H3-F}$= 14.4 Hz) as well as to H1 and H2 (^{3}J= 9.2 Hz). H4 produced one

of the triplets at 5.02 ppm. COSY correlations indicated that H5 caused the multiplet at 3.84 ppm and that one of the H6 signals appeared within the multiplet at 4.05 ppm. The other H6 signal appears within the multiplet at 4.23 ppm.

For the α-configured **3**, the anomeric proton was identified as the doublet at 6.36 ppm which coupled to H2 ($^3J_{H1-H2}$= 4.0 Hz). H2 caused the doublet of doublet of doublets at 4.61 ppm which coupled to H1 (^3J= 4.0 Hz), H3 (^3J= 9.6 Hz), and fluorine (^3J= 48.5 Hz). The doublet of triplets at 5.49 ppm was caused by H3 which coupled with fluorine (^2J= 12.2 Hz) as well as the protons on both neighbouring carbons (^3J= 9.5 Hz). H4 produced the other triplet at 5.02 ppm (which overlapped with the H4β signal). H5 and one H6 produced signals which fell within the multiplet at 4.05 ppm. The other H6 signal was present within the multiplet at 4.23 ppm.

The ^{19}F NMR spectrum of **4** (Figure 9A) displayed two peaks, -199.3 and -199.9 ppm, corresponding to β-gluco and α-gluco configured products (0.4β: 1α), consistent with the reported signals.[30] In the ^1H NMR spectrum (Figure 9B), peaks corresponding to α-gluco configured (major) and β-gluco configured (minor) products were observed in a 1α: 0.4β ratio, congruous with the ratio observed in the ^{19}F NMR spectrum. The acetyl group protons for both anomers appear as a group of overlapping singlets at 2.03 ppm, integrating to 9 α protons plus 9 β protons. For the β-configured product, the anomeric proton was identified as the doublet of doublets at 4.89 ppm which coupled to the neighbouring H2 ($^3J_{H1-H2}$= 7.5 Hz) as well as participating in coupling with fluorine ($^3J_{H1-F}$= 2.2 Hz). The signal which appears to be a triplet at 4.30 ppm is in fact the left half of a doublet of triplets centered at 4.27 ppm, caused by H2. Coupling with H1 and H3 (^3J= 8.5 Hz) produced the

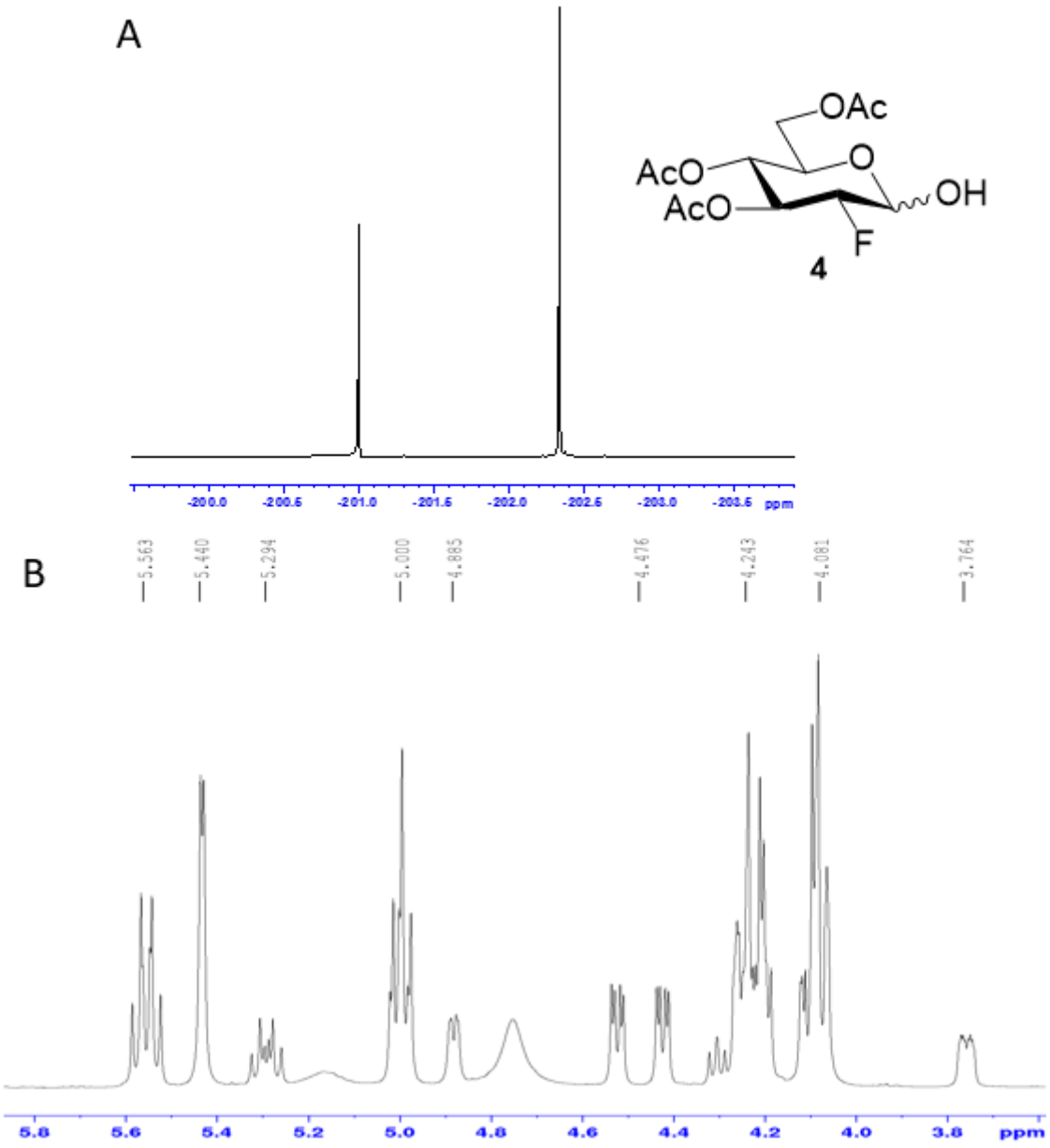

Figure 9. NMR Spectra of 2-deoxy-2-fluoro-3,4,6-tri-*O*-acetyl-D-glucopyranose (**4**). **A)** ^{19}F (470 MHz, $CDCl_3$) **B)** ^{1}H (500 MHz, $CDCl_3$).

triplet and coupling with fluorine caused the doublet, which should have a coupling constant of about 50 Hz. However, the doublet is not visible in this spectrum due to overlap with the multiplet at 4.24 ppm. H3 was identified as the multiplet at 5.29 ppm, H4 as part of the multiplet at 4.99 ppm, and H5 as the multiplet at 3.76 ppm. The signals for the two

H6 are located within the multiplets at 4.08 and 4.24 ppm. For the α-configured product, the anomeric proton was identified as the doublet at 5.44 ppm, which coupled with H2 ($^3J_{H1\text{-}H2}$= 3.4 Hz). H2 was identified as the doublet of doublet of doublets at 4.48 ppm, which coupled with H1 ($^3J_{H1\text{-}H2}$= 3.6 Hz), H3 ($^3J_{H2\text{-}H3}$= 9.6 Hz), and fluorine ($^2J_{H2\text{-}F}$= 49.7 Hz). The multiplet at 5.56 ppm is caused by H3. H4 is part of the multiplet at 4.99 ppm (overlapping with the H4β signal). H5 and both H6 signals are located within the multiplets at 4.08 and 4.24 ppm. Residual ethyl acetate was also visible in this spectrum, having signals at 1.26, 2.05, and 4.12 ppm, thus the sample was dried for longer on the vacuum line before proceeding with the next reaction.

The ^{19}F NMR spectrum of **5** (Figure 10A) displayed two peaks, -198.7 and -201.6, corresponding to β-gluco and α-gluco configured products (5β: 1α), respectively, as reported in the literature.[31] In the ^1H NMR spectrum (Figure 10B), peaks corresponding to α-gluco configured (minor) and β-gluco configured (major) products were observed in a 1α: 5β ratio, the same ratio as in the ^{19}F NMR spectrum. For the β-configured product, the anomeric proton was determined to be the multiplet at 5.48 ppm. The H2 signal was found to be the doublet of multiplets at 4.72 ppm, where the doublet was caused by coupling with fluorine ($^2J_{H2\text{-}F}$= 50.1 Hz). H3 was assigned as the multiplet at 5.44 ppm and the signal produced by H4 was located within the multiplet at 5.16 ppm. H5 and both H6 signals were part of the multiplet at 4.15 ppm. The aromatic protons H3', H5', and H6', produced signals at 8.75 (m), 8.46 (m), and 7.45 (d) ppm. H3' was located between the two nitro groups therefore it experienced the most deshielding and the signal was shifted furthest downfield. H6' was not adjacent to any nitro groups and was located close enough to only one proton for coupling to occur, therefore it was identified as the doublet at 7.45 ppm. H5' would be

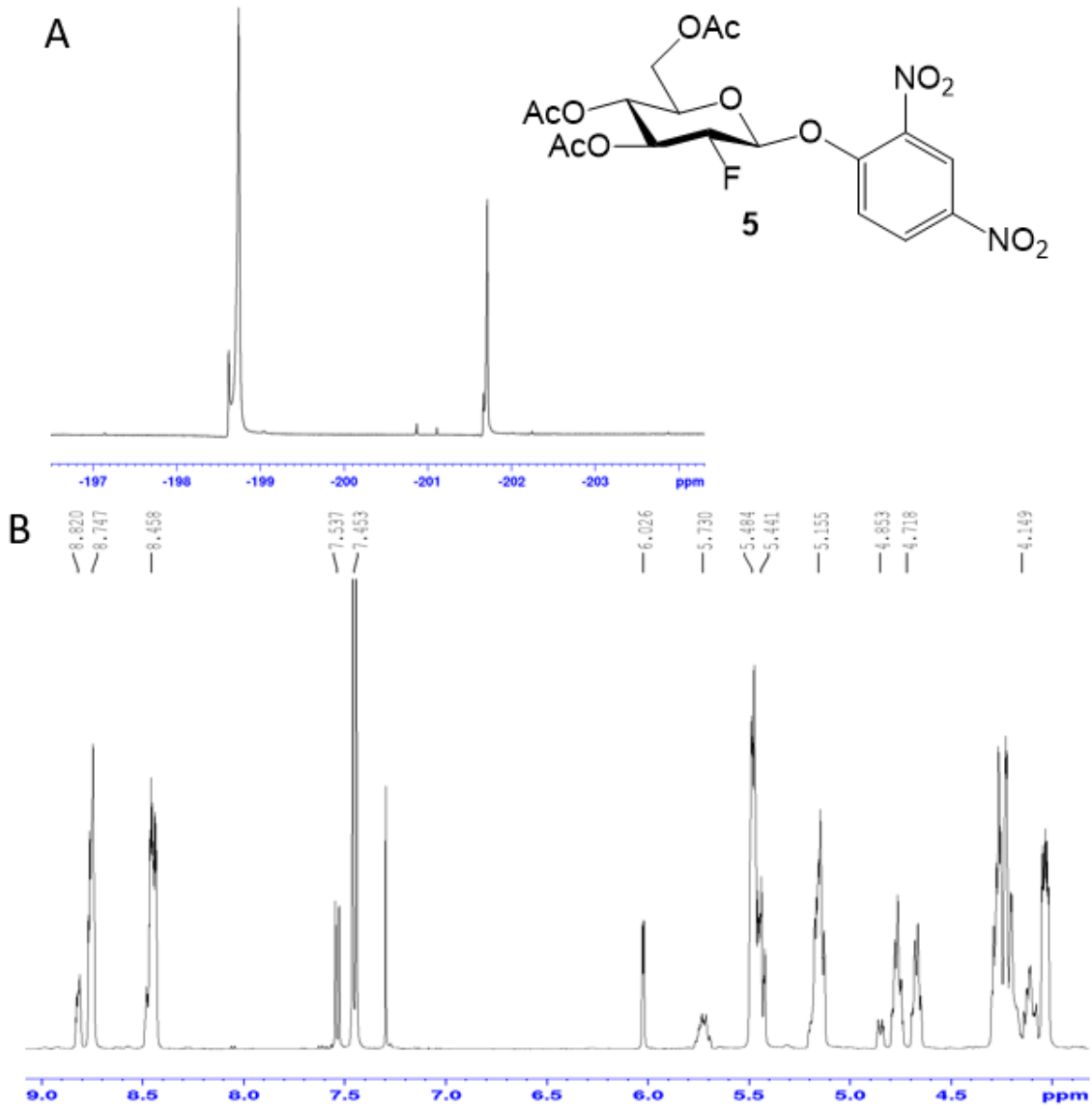

Figure 10. NMR Spectra of 2,4-dinitrophenyl 2-deoxy-2-fluoro-3,4,6-tri-*O*-acetyl-D-glucopyranose (**5**). **A)** $^{19}F\{^{1}H\}$ (470 MHz, $CDCl_3$) **B)** ^{1}H (500 MHz, $CDCl_3$).

expected to have a chemical shift somewhere between that of H3' and H6' due to its proximity to one nitro group, therefore it was assigned as the signal at 8.46 ppm. For the α-configured product, the anomeric proton was found to be the doublet at 6.03 ppm which coupled with H2 ($^{3}J_{H1\text{-}H2}$= 3.6 Hz). H2 was identified as the multiplet at 4.85 ppm and H3 as the multiplet at 5.73 ppm. The signal for H4 resided within the multiplet at 5.16 ppm

(overlapping with H4β). The H5 and H6 protons were all located within the multiplet at 4.15 ppm. The aromatic protons H3', H5', and H6', produced signals at 8.82 (m), 8.46 (m), and 7.54 (d) ppm, respectively. The signal at 8.46 ppm contained the two overlapping signals of H5'α and H5'β.

The ^{19}F NMR spectrum of **6** (Figure 11A) displayed two peaks, -201.1 and -203.5, corresponding to the β-gluco and α-gluco products (5β: 1α), respectively, as reported in the literature.[31] In the ^{1}H NMR spectrum (Figure 11B), peaks corresponding to α-gluco configured (minor) and β-gluco configured (major) products were observed in a 1α: 5β ratio, consistent with the ratio observed in the ^{19}F NMR spectrum. The peaks corresponding to the acetyl groups around 2.05 ppm were no longer present after the deprotection reaction. For the desired β-configured product, the anomeric proton was assigned as the doublet of doublets at 5.59 ppm which coupled with H2 ($^{3}J_{H1\text{-}H2}$= 7.5 Hz) and fluorine ($^{3}J_{H1\text{-}F}$= 2.9 Hz). H2 was identified as the doublet of triplets at 4.37 ppm which coupled with H1 and H3 (^{3}J = 7.6 Hz) as well as fluorine ($^{3}J_{H2\text{-}F}$= 51.6 Hz). The signal for H3 appeared in the multiplet centered at 3.80 ppm along with one of the H6 signals. The triplet at 3.52 ppm was produced by H4, which coupled with H3 and H5 (^{3}J= 9.5 Hz). H5 was assigned as the multiplet at 3.67 ppm. The second H6 produced a doublet of doublets at 3.97 ppm which coupled to H5 ($^{3}J_{H5\text{-}H6b}$= 2.1 Hz) and to the other H6 proton ($^{2}J_{H6a\text{-}H6b}$= 12.2 Hz). The aromatic protons H3', H5', and H6' were responsible for the signals at 8.74 (d), 8.50 (dd), and 7.67 (d) ppm, respectively.

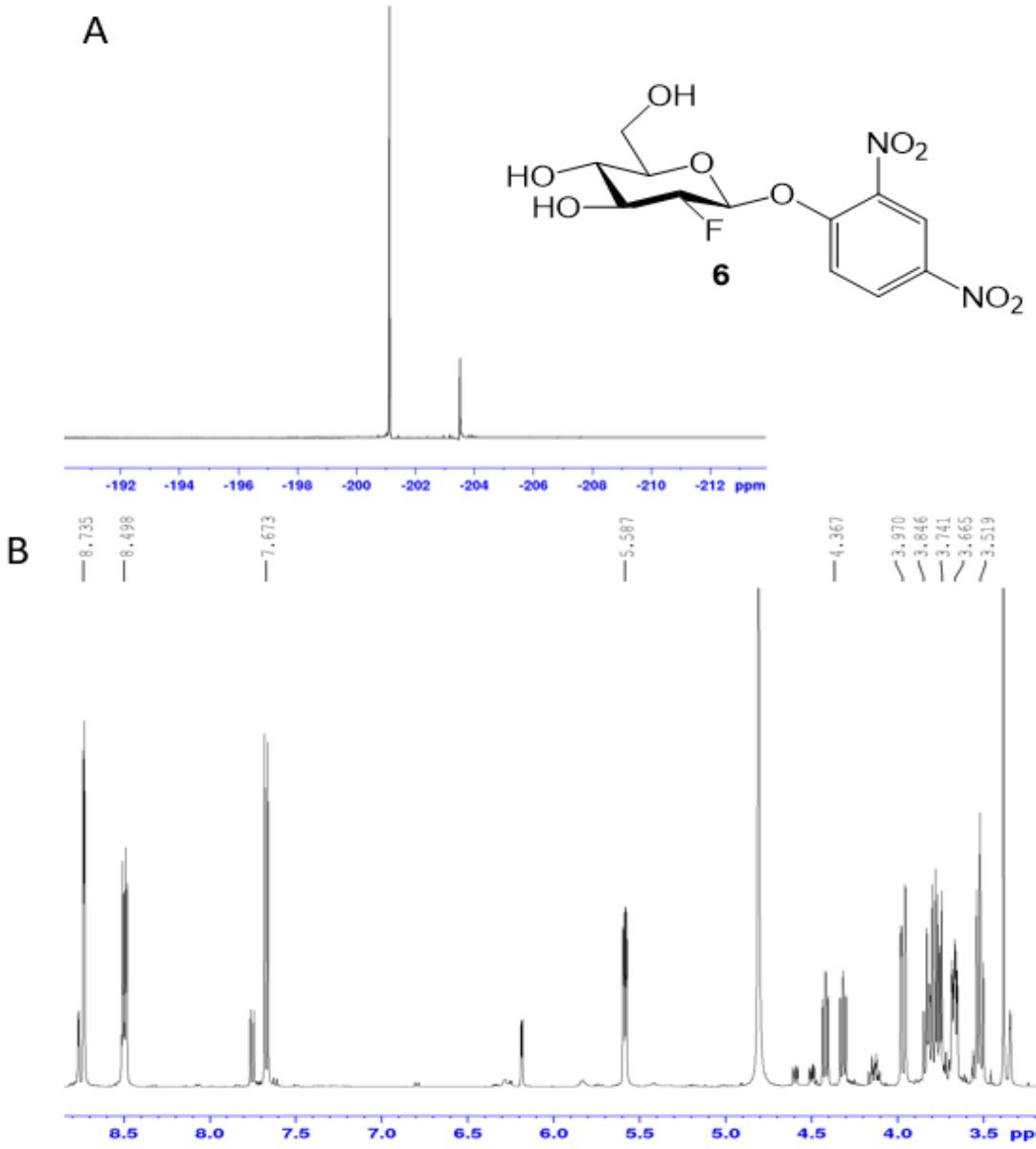

Figure 11. NMR spectra of 2,4-dinitrophenyl 2-deoxy-2-fluoro-β-D-glucopyranose (**6**). **A)** $^{19}F\{^{1}H\}$ (500 MHz, CD_3OD) **B)** ^{1}H (500 MHz, CD_3OD).

Throughout the synthesis and characterization of compounds **2**-**6** several trends were recognized in the NMR spectra of these compounds, facilitating the assignment of the α and β anomers (Table 1). Since **2** was the only compound which included manno-configured species, only trends for the gluco-configured species are discussed. For all compounds, both the ^{1}H δ of the anomeric proton and the ^{19}F δ were shifted further

downfield for the α anomer than for the β anomer. The anomeric proton signals of the β-configured compounds all had greater multiplicities than the α-configured compounds, due to a more favourable angle allowing for vicinal coupling between H1 and the fluorine on C2 as well as coupling with H2. All of the α-configured anomeric protons were doublets as their only coupling partner was H2. The β: α ratio in table 1 was calculated by comparing the integrations of the β- and α-configured anomeric protons of the same compound. In the synthesis of **3** and **4**, it was found that the formation of the α anomer was favoured over the β, whereas in the synthesis of **5** and **6**, β was favoured over α. Since compounds **3** and **4** had small heteroaromatic substituents (acetyl or hydroxyl) at the anomeric position, the anomeric effect dominated, making it more favourable for these substituents to be in the axial position (α-configured).[32] With the introduction of the bulky 2,4-dinitrophenyl group in **5**, steric hinderance has outweighed the anomeric effect, leading to the substituent preferring an equatorial position (β-configured).

Compound	δ of β-gluco anomer (^{1}H δ is for anomeric H)	δ of α-gluco anomer (^{1}H δ is for anomeric H)	β:α ratio
2	^{19}F: -201.0	^{19}F: -202.4	-
3	^{19}F: -201.0 ^{1}H: 5.76 (dd)	^{19}F: -202.3 ^{1}H: 6.36 (d)	0.6: 1
4	^{19}F: -199.3 ^{1}H: 4.89 (dd)	^{19}F: -199.9 ^{1}H: 5.44 (d)	0.4: 1
5	^{19}F: -198.7 ^{1}H: 5.48 (m)	^{19}F: -201.6 ^{1}H: 6.03 (d)	5: 1
6	^{19}F: -201.1 ^{1}H: 5.59 (dd)	^{19}F: -203.5 ^{1}H: 6.19 (d)	5: 1

Table 1. Summary of important NMR data for synthetic compounds **2**-**6**: Comparison of the ^{19}F chemical shifts as well as ^{1}H chemical shifts and multiplicities of the anomeric protons for the α- and β-gluco anomers.

2.2. Kinetic studies of the inhibition of DesR, Hsero1941, and EryBI

Compound **6** has been reported to inhibit six different retaining glycosidases.[5] In this study, **6** was kinetically evaluated with three other retaining glycosidases, DesR, EryBI, and Hsero1941. To determine if **6** was capable of inactivating DesR, two reactions were set up. The first reaction involved incubating DesR with **6** for two hours in phosphate-buffered saline (PBS), after which the mixture was subjected to centrifugal filtration (using a 10 000 MWCO centrifugal filter) to remove excess **6**. Then, a substrate for DesR, para-nitrophenyl glucopyranoside (pNP-glc), was added to the DesR-**6** mixture and time-dependent inhibition was monitored at 400 nm over a period of five minutes (Figure 12). The second reaction involved identical conditions without any **6**, to be used as a control (Figure 12). The control reaction mixture displayed a positive slope, as the absorbance increased with time. Since the wild-type DesR was uninhibited, it continued to bind and hydrolyze pNP-glc, releasing para-nitrophenolate ions which led to the increase in absorbance at 400 nm. The DesR which was incubated with **6** displayed a slope of zero, meaning that it was not hydrolyzing any pNP-glc. This indicated that DesR was completely inactivated by **6** after two hours of incubation.

Inactivation and control reactions were set up for the second enzyme, Hsero1941. These involved incubating Hsero1941 with **6** in HEPES buffer for 16 hours before adding the substrate para-nitrophenyl *N*-acetyl-β-D-glucosaminide (pNP-GlcNAc) and measuring the time-dependent inhibition over a period of three minutes (Figure 13). For the control reactions, **6** was omitted. The control reaction mixture had a positive slope (0.090 min^{-1}) as Hsero1941 continued to hydrolyze pNP-GlcNAc, increasing the concentration of para-nitrophenolate ions and therefore, the absorbance reading. The plot of absorbance vs time

for the reaction mixture containing **6** had a positive slope (0.042 min^{-1}) approximately half that of the wild-type Hsero1941 reaction mixture. The decrease in activity indicated that Hsero1941 was partially inactivated by **6**.

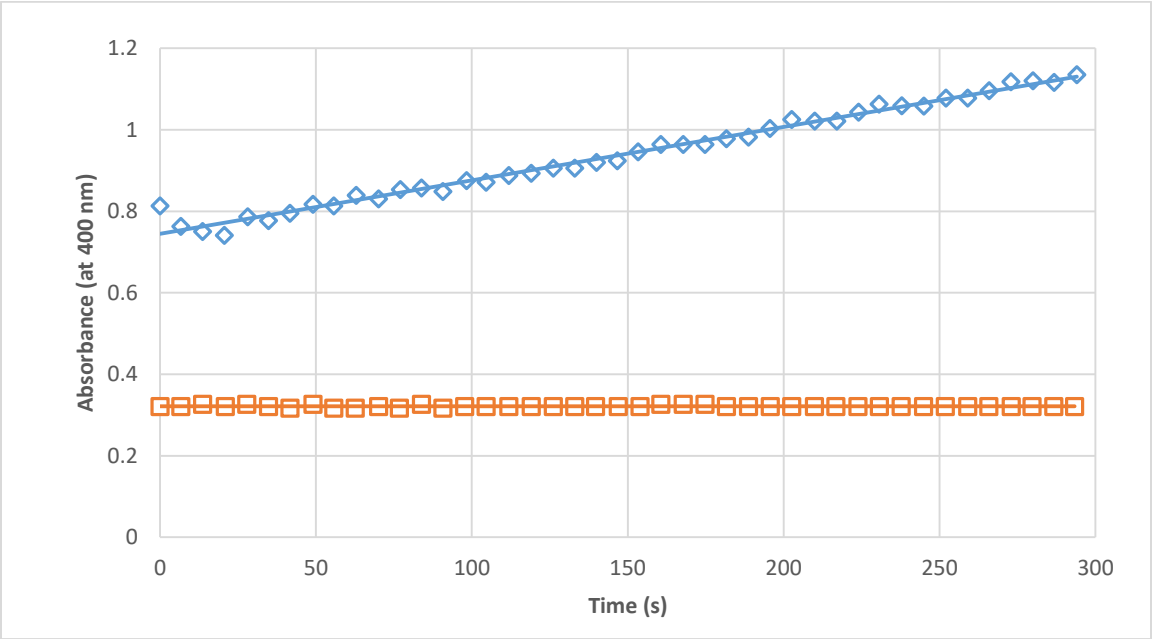

Figure 12. Time-dependent inhibition of DesR incubated with **6** (orange squares) and the wild-type DesR control (blue diamonds)

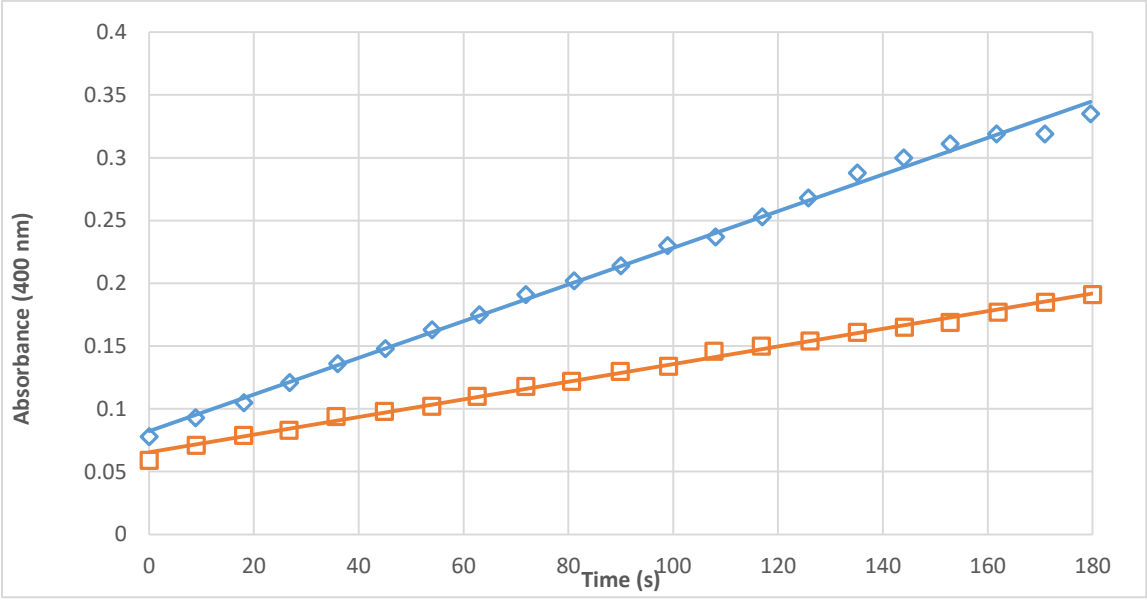

Figure 13. Time-dependent inhibition of Hsero1941 incubated with **6** (orange squares) and wild-type Hsero1941 control (blue diamonds)

Reactions using the third enzyme, EryBI, and **6** were set up along with a control in the absence of **6**. The reaction mixtures were incubated for two hours, after which the substrate pNP-glc was added and absorbance vs time was measured at 400 nm over a period of five minutes (Figure 14). The control reaction mixture presented a positive slope, indicating that EryBI continued to hydrolyze the substrate pNP-glc. The reaction mixture where EryBI was incubated with **6** displayed a slope of zero, indicating that EryBI was quantitatively inactivated by **6** after two hours. Once it was determined that **6** was capable of (completely or partially) inactivating DesR, Hsero1941, and EryBI, screening for acceptors which could reactivate the enzymes could commence.

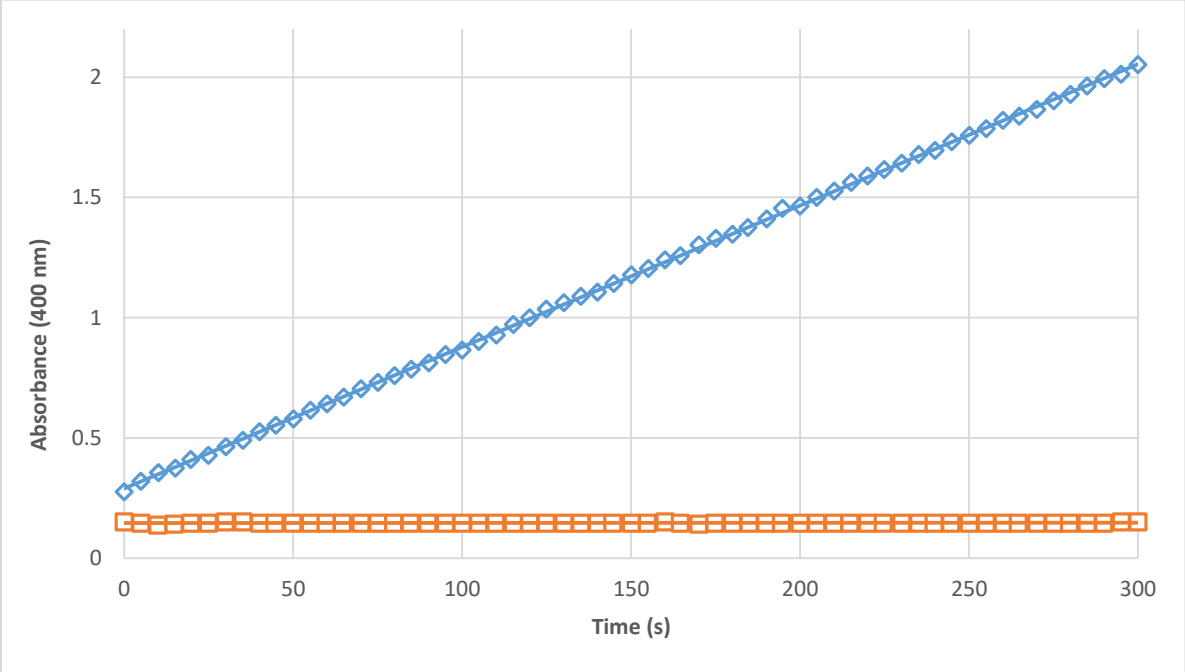

Figure 14. Time-dependent inhibition of EryBI by **6** (orange squares) and the wild-type EryBI control (blue diamonds)

2.3. Acceptor screening for the reactivation of DesR

DesR was inactivated by **6** using the same method as previously described (see Chapter 2.2). After the two hour incubation period, the DesR/**6** complex solution was purified via

ultrafiltration (4ºC, 10 000 MWCO centrifugal filter), washing with PBS (50 mM, pH= 7.6, 4 x 400 µL) to remove any excess **6**. The recovered DesR/inactivator solution was incubated for an additional 3-24 hours along with solutions of potential acceptors in the wells of a 96-well plate. (When reactivation was not successful in any of the reaction mixtures incubated for three hours, the incubation time was increased to 24 hours.) After the incubation period, pNP-glc was added to the reaction mixture and absorbance vs time was measured over a period of five minutes at 400 nm. 26 acceptors were screened, including monosaccharides, disaccharides, macrolide antibiotics, amino acids, alcohols, and hydroxylamines (full list of acceptors in Chapter 5.4.2). Control reactions involving the wild-type DesR and the inactivated DesR without an acceptor were also included. All potential acceptor reaction mixtures produced absorbance vs time plots with slopes of zero, indicating that DesR remained inactivated. Therefore, none of the potential acceptors tested were appropriate acceptors for the reactivation of DesR.

2.4. Acceptor screening for the reactivation of Hsero1941

Hsero1941 was (partially) inactivated by **6** using the method described previously (in Chapter 2.2). Then, the Hsero1941/**6** solution was purified via ultrafiltration (4ºC, 10 000 MWCO centrifugal filter), washing with HEPES buffer (50 mM, pH= 7.2, 4 x 400 µL) to remove excess **6**. Next, the enzyme/inactivator solution was incubated for three hours with potential acceptors in HEPES buffer in the wells of a 96-well plate. Control reactions containing no acceptors were also included. After the incubation period, pNP-GlcNAc was added and absorbance vs time was measured over a period of five minutes at 400 nm. 35 potential acceptors were screened for the reactivation of Hsero1941 (list in Chapter 5.4.3). 30 of the compounds led to higher activity than that of inactivated Hsero1941 and five

produced lower activity than inactivated Hsero1941 (Figure 15). Activity was defined as absorbance at 400 nm divided by time (in seconds). Percent reactivation was defined by the equation:

$$\% \text{ reactivation} = \left(\frac{\text{activity of inhibited enzyme with acceptor}}{\text{activity of inhibited enzyme}} - 1\right) \times 100$$

Compounds having high % reactivation, such as L-serine, are those which are most likely acceptors which can reactivate Hsero1941. Fifteen of the tested compounds produced a % reactivation of 40 or higher. These acceptors are those that have the potential to be used in single-step glycosynthase-catalyzed syntheses.

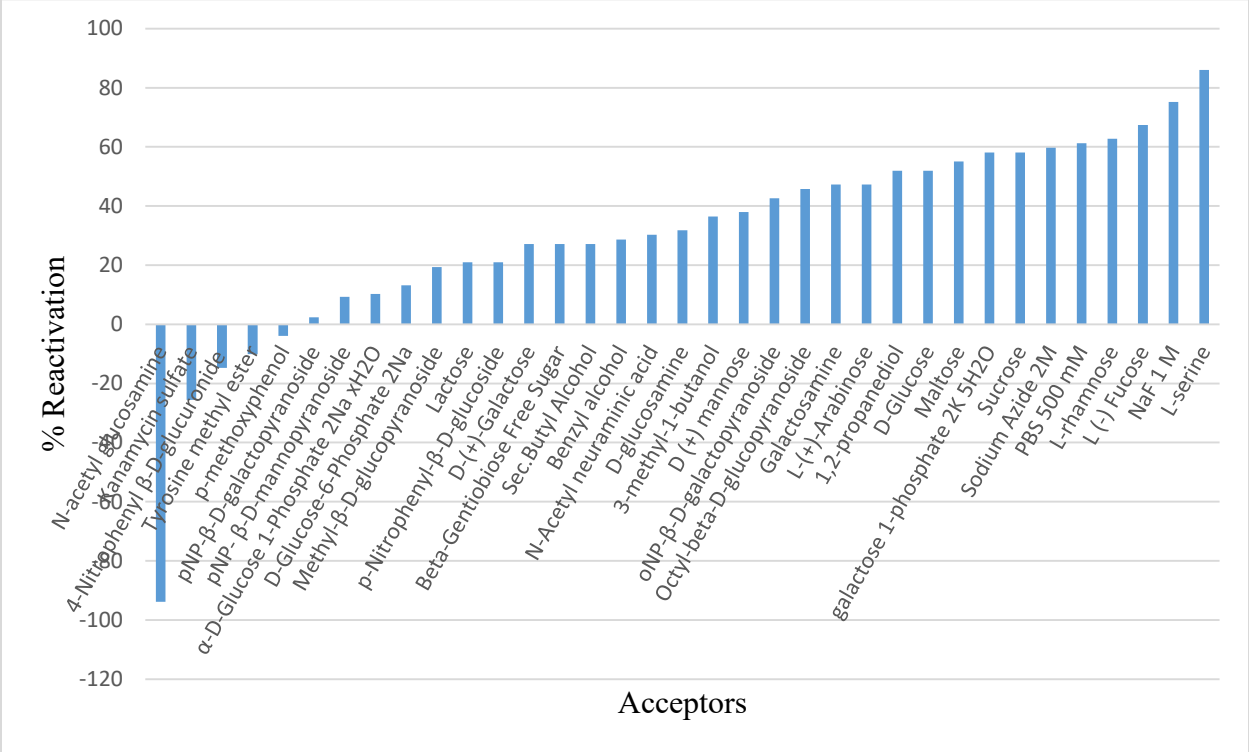

Figure 15. Reactivation of Hsero1941 by potential acceptors

2.5. Acceptor screening for the reactivation of EryBI

EryBI was inactivated by **6** using the same method as described in Chapter 2.2. The solution of enzyme/inactivator was purified via ultrafiltration (4ºC, 10 000 MWCO centrifugal filter), washing with PBS buffer (225 mM, pH= 7.6, 4 x 400 µL), after the two hour incubation period. The recovered EryBI/**6** solution was then incubated overnight (17-18 hours) with solutions of potential acceptors in the wells of a 96-well plate. Finally, pNP-glc was added to each well and absorbance at 400 nm vs time was measured over a period of five minutes. Control reactions involving the wild-type EryBI and the inactivated EryBI with no acceptor were also included in the screening process. 46 different potential acceptors were tested (full list in Chapter 5.4.4), none of which were successful in the reactivation of EryBI. Of all the potential acceptors screened, erythromycin was thought to be the most likely to succeed due to the fact that it has been shown to act as an acceptor for an EryBI glycosynthase mutant, EryBI D257G.[8] Next, acceptor screening was conducted using only erythromycin as the potential acceptor whilst varying other conditions such as the duration of incubation and period of time over which time-dependent inhibition was measured. Incubation periods ranging between 24 and 125 hours still did not lead to the reactivation of EryBI, with the absorbance at 400 nm being measured for a period of 30 minutes after the addition of pNP-glc. It has been reported that erythromycin is capable of inhibiting DesR.[7] Since EryBI is homologous to DesR, it was hypothesized that erythromycin could be an inhibitor of EryBI as well. To verify this hypothesis, aliquots of wild-type EryBI in PBS were incubated with or without erythromycin overnight. After this, pNP-glc was added and time-dependent inhibition was monitored at 400 nm. The EryBI which was incubated with erythromycin demonstrated only 16% of the activity of the

control, indicating that erythromycin is an inhibitor of EryBI (Figure 16). This made it unable to determine whether erythromycin acts as an acceptor for the reactivation of EryBI as the inactivation observed could be due to EryBI binding with **6** or with erythromycin. No definitive conclusions could be drawn from the screening of erythromycin as a potential acceptor.

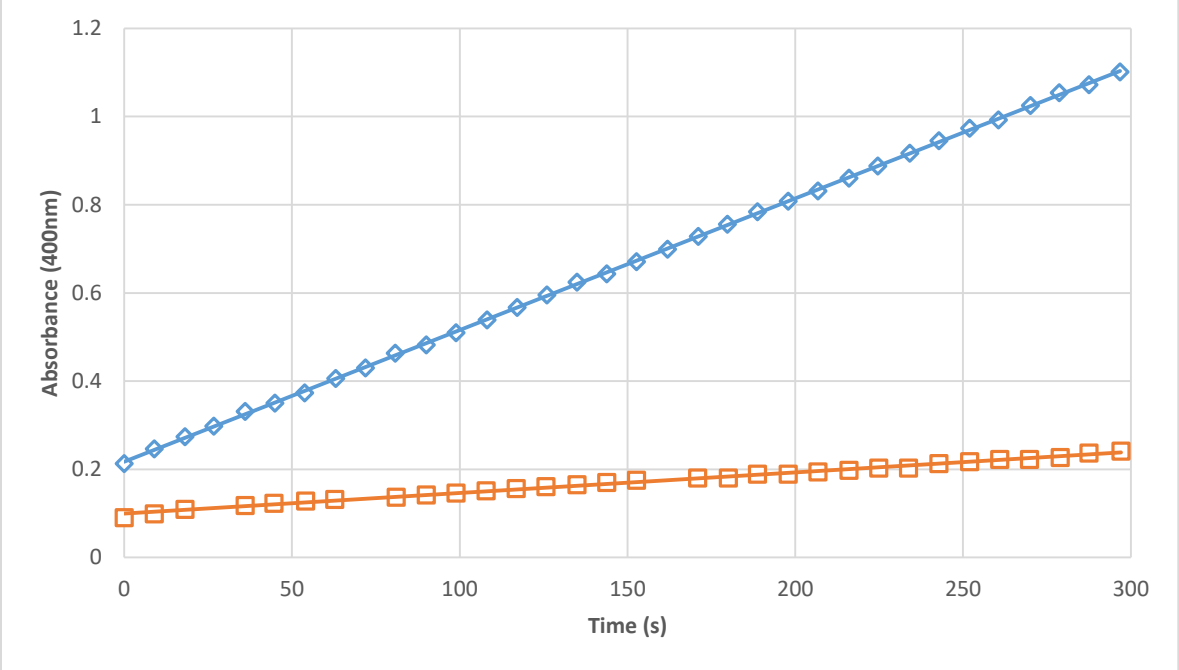

Figure 16. Time-dependent inhibition of EryBI by erythromycin (orange squares) and wild-type EryBI control (blue diamonds)

It was found that **6** inhibited DesR and EryBI completely, with none of the acceptors screened succeeding in reactivating the glucosidases. In order to find a suitable reactivator for DesR and EryBI in future studies, a weaker inhibitor would need to be used. Several preliminary hits for the reactivation of Hsero1941 were found and collection of further kinetic data will be needed to confirm them. The isolation of the Hsero1941-catalyzed transglycosylation products can also be used as proof of reaction in future.

Chapter 3. Results and Discussion of the expression of ^{19}F-labelled β-phosphoglucomutase and the study of its transition state analogues

3.1. Preparation of β-phosphoglucomutase mutants

In order to easily purify β-phosphoglucomutase via (Ni) affinity chromatography and to observe its transition state analogue complexation using ^{19}F NMR spectroscopy, several mutations have been introduced into the wild-type pET22b(+)_*pgmB* plasmids throughout the course of this project. The plasmids resulting from these mutations and the proteins which were produced upon translation are summarized in table 2.

Plasmid	Description of protein	Source
pET22b(+)_*pgmB*	Wild-type βPGM	Gift from the University of Sheffield[28]
pET22b(+)_*pgmB*-His	Wild-type βPGM with SacI site incorporated to allow for the production of a His_6-tag	Produced previously in the Jakeman group[19]
pET22b(+)_*pgmB*-His-W24F	βPGM with SacI site incorporated and with phenylalanine replacing tryptophan 24	Produced previously in the Jakeman group[19]
pET22b(+)_*pgmB*-His-W216F	βPGM with SacI site incorporated and with phenylalanine replacing tryptophan 216	Produced during the current study

Table 2. Overview of the plasmids and the corresponding proteins translated in Chapter 3.

3.2. Expression of wild-type (His_6-tagged) βPGM

The βPGM enzyme can be produced recombinantly in *E. coli* BL21 (DE3) by inserting *pgmB*, the gene encoding β-phosphoglucomutase in *Lactococcus lactis,* into the multiple cloning site of the expression vector pET22b(+).[33] Previously in the Jakeman lab, a

mutation was introduced into pET22b(+)_*pgmB* (received as a gift from the University of Sheffield[28]), where the C-terminal stop codon was changed to a glutamic acid residue in order to produce a βPGM protein having a C-terminal His_6-tag.[19] The presence of this C-terminal His_6-tag allowed for facile purification of the protein using nickel affinity chromatography. In the current study, plasmid digestion was performed using the restriction enzymes SacI and HindIII to confirm the presence of the SacI site (Figure 18A). This DNA cleavage site was incorporated to confirm read-through of the genetic sequence encoding the C-terminal His_6-tag. 1% agarose gel electrophoresis was used to view the digestion products (Figure 17). The bands at 0.6 kb and 5.4 kb observed for the pET22b(+)_*pgmB*-His plasmid indicated that it possessed SacI and HindIII restriction sites. A pET22b(+)_*pgmB* plasmid having a HindIII restriction site but no SacI site would have a single linearized band at 6.0 kb. This confirmed the identity of the plasmid for the subsequent genetic manipulations.

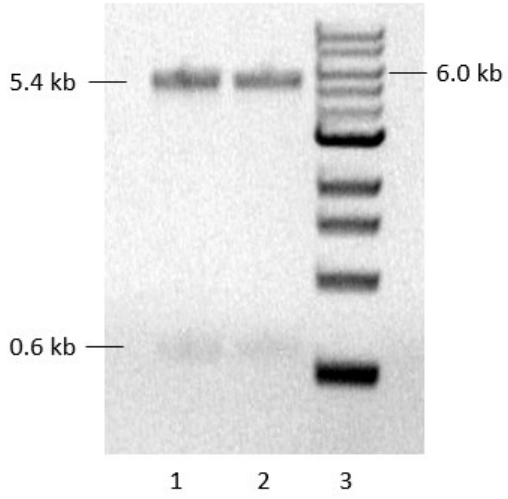

Figure 17. 1% agarose gel of pET22b(+)_*pgmB*-His plasmids digested with SacI and HindIII restriction enzymes. 1) & 2) pET22b(+)_*pgmB*-His plasmid digested with SacI and HindIII, 3) 1 kb DNA ladder.

3.3. Preparation of pET22b(+)_*pgmB*-His-W216F via site-directed mutagenesis

The βPGM protein contains two tryptophan residues, W216 (in the core domain) and W24 (in the cap domain). In previous work by the Jakeman group, the wild-type 5FWβPGM and a 5FWβPGM-His-W24F mutant were produced and ^{19}F NMR spectra of their TSA complexes were acquired.[19] The spectrum of the wild-type contained multiple signals and the W24F mutant was not useful for monitoring TSA complexation as the 5-fluorotryptophan (5-FW) residue (present as 5FW216) was too far from the active site to see a change in the ^{19}F chemical shift upon complexation. On the other hand, ^{19}F-labelling of the W24 residue abutting the active site was expected to produce a ^{19}F NMR signal that would change in chemical shift and enable monitoring of TSA complexation. In order to label only the W24 residue, a 5FWβPGM-His-W216F mutant was prepared.

In order to express the 5FWβPGM-His-W216F mutant protein, it was required to prepare the corresponding expression vector: pET22b(+)_*pgmB*-His-W216F. This was accomplished by conducting site-directed mutagenesis on the pET22b(+)_*pgmB*-His plasmid, which incorporated a phenylalanine residue in place of a tryptophan residue on the enzyme core domain (W216) as well incorporating a new restriction site: the introduction of a second PstI site (Figure 18A). This new restriction site allows for the identification of the mutant plasmid using digestion with restriction enzymes. Removing one of the tryptophan residues allows for the ^{19}F-labelling of a single residue (W24) under appropriate culture conditions.[16] The mutations were introduced using PCR amplification of oligonucleotide primers that replaced the wild-type TGG (translating to tryptophan) with a TTT codon (translating to phenylalanine) and the wild-type CTTCAA sequence with the CTGCAG sequence for PstI (where both sets of codons are translated as leucine

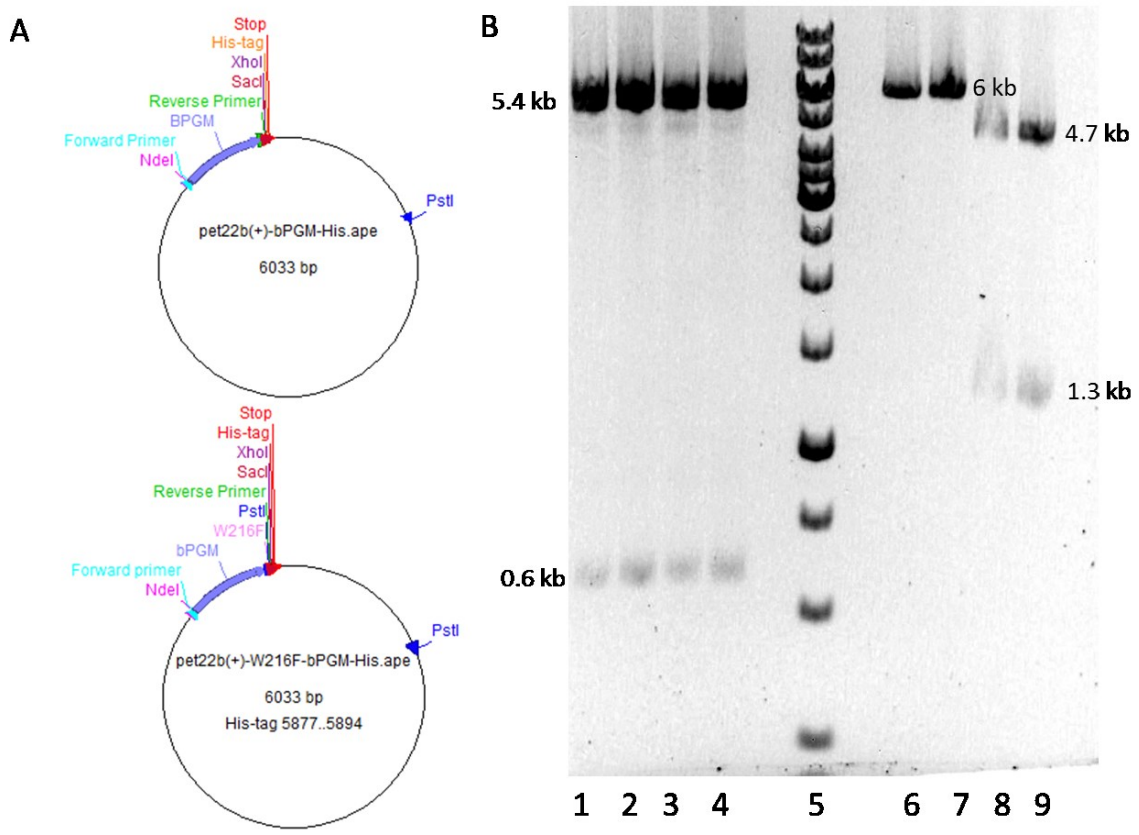

Figure 18. A) Plasmid maps of pET22b(+)_*pgmB*-His (top) and pET22b(+)_*pgmB*-His-W216F (bottom). **B)** 1% agarose gel of pET22b(+)_*pgmB*-His-W216F plasmids digested with restriction enzymes. 1-4) pET22b(+)_*pgmB*-His-W216F digestion with SacI and HindIII, 5) 1 kb DNA ladder, 6-7) PstI digest of pET22b(+)_*pgmB*-His, containing only one PstI site, 8-9) PstI digest of pET22b(+)_*pgmB*-His-W216F, containing two PstI sites.

glutamine). Plasmids were isolated from transformed cells following the general procedure (described in Chapter 5.1.2). To confirm the appropriate mutations were present, plasmid digestion with SacI and HindIII was conducted as well as plasmid digestion with PstI. The digestion products were viewed by running the DNA using 1% agarose gel electrophoresis (Figure 18B). Lanes 1-4 are the products of the SacI and HindIII digest, where bands at 0.6 kb and 5.4 kb indicate that the plasmids contain a SacI and HindIII site, indicating that the constructs contain C-terminal His_6-tags. Lanes 6-7 show the product of a digest with PstI where the plasmid does not contains only one PstI site. Lanes 8-9 show the products of a

PstI digest, having bands at 1.3 kb and 4.7 kb, indicating the presence of two PstI sites. Since the second PstI site was introduced in the same site-directed mutagenesis which incorporated the W216F mutation, the presence of the additional PstI site confirmed the presence of the W216F mutation. The pET22b(+)_*pgmB*-His and pET22b(+)_*pgmB*-His-W216F plasmid constructs were confirmed by DNA sequencing.

Once it had been confirmed that the expression vector pET22b(+)_*pgmB*-His-W216F was successfully prepared, *E.coli* BL21 (DE3) competent cells were transformed with the expression vector. Plasmids were then isolated and digested with SacI and HindIII as well as PstI, ensuring the appropriate mutations were present. The plates of *E.coli* BL21 (DE3) pET22b_*pgmB*-His-W216F were used to grow cultures and make glycerol stocks to be used for protein production.

3.4. Overexpression and purification of W216F 5FWβPGM-His mutant

5-Fluorotryptophan was incorporated into W216F-His-βPGM following the procedure by Crowley et al. for the incorporation of 5-FW into proteins.[34] In order to inhibit the biosynthesis of aromatic amino acids (ie. tryptophan), glyphosate was added to the media during protein production, since glyphosate is an inhibitor of 5-enolpyruvoylshikimate-3-phosphate synthase (EPSP), the enzyme responsible for catalyzing the penultimate step (an enolpyruvoyl transfer) in aromatic amino acid biosynthesis.[35] The media was then supplemented with DL-5-fluorotryptophan as the ^{19}F source, as well as unlabelled tyrosine and L-phenylalanine. *E.coli* BL21 (DE3) pET22b(+)_*pgmB*-His-W216F was grown in minimal media with the aforementioned supplements, as well as IPTG to induce production of the 5-FW protein. After induction, a band at 25 kDa was observed by SDS-PAGE gel, corresponding to the molecular weight of βPGM (Figure 19). Cell pellets were isolated,

lysed, and purified by Ni affinity chromatography. SDS-PAGE was used to determine that the protein was eluted in fractions 6-8, where bands of 25 kDa were observed (Figure 20). These tubes were combined, concentrated, and de-salted, exchanging the buffer from imidazole to HEPES. The protein was further concentrated to 1.9 mM and dithithreitol (DTT) was added to make the stock solution used in the NMR experiments.

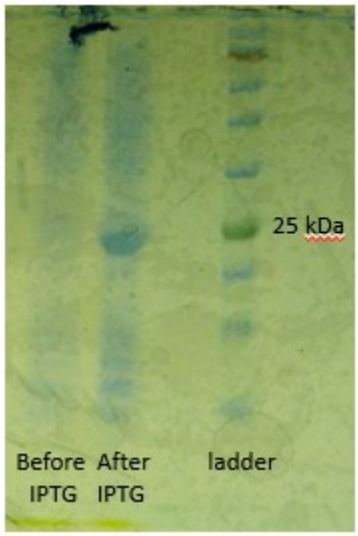

Figure 19. SDS-PAGE gel of *E.coli* BL21 (DE3) pET22b(+)_*pgmB*-His-W216F culture before and after IPTG induction.

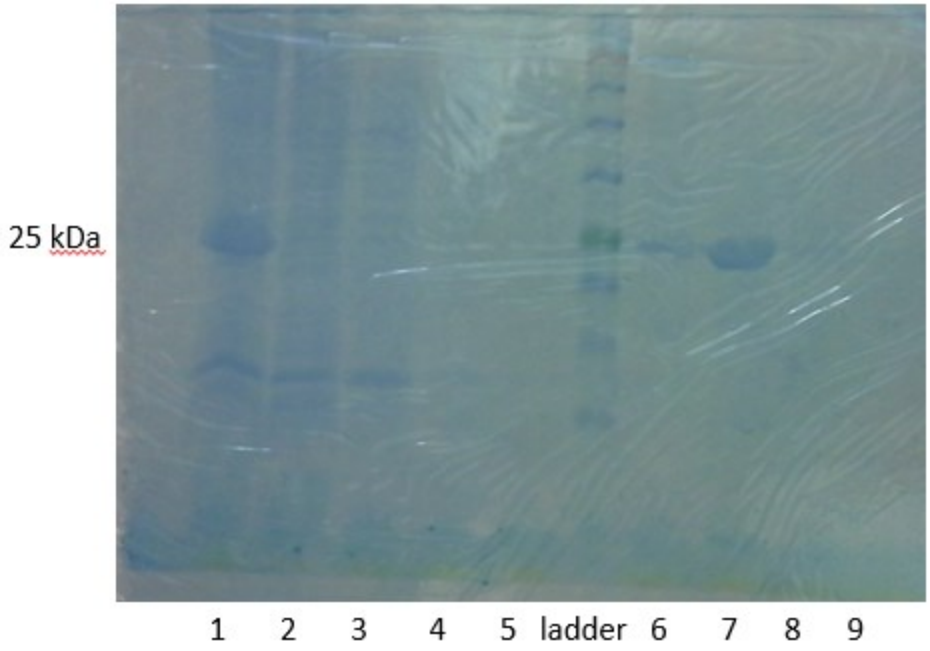

Figure 20. SDS-PAGE gel of nickel column fractions collected during W216F 5FWβPGM-His purification, where fractions 6-8 containing the desired protein.

3.5. ^{19}F NMR spectroscopy of W216F 5FWβPGM-His Transition State Analogue complexes

Excerpts of this section were taken from the 2017 *Chem. Sci.* manuscript "Observing enzyme ternary transition state analogue complexes by ^{19}F NMR spectroscopy," by Anna Ampaw, Madison Carroll, Jill von Velsen, Debabrata Bhattasali, Alejandro Cohen, Matthew W. Bowler, and David L. Jakeman.[36]

The ^{19}F NMR spectrum of the wild-type 5FWβPGM (produced by a previous member of the Jakeman lab) along with NH_4F and $MgCl_2$ in HEPES buffer/ D_2O) is shown in Figure 21A.[19] The peaks at -123.5 and -125 ppm were caused by the two 5FW residues, however, it was not known which signal corresponds to which residue from this spectrum. The spectrum of the W24F 5FWβPGM mutant was also acquired previously in the lab,

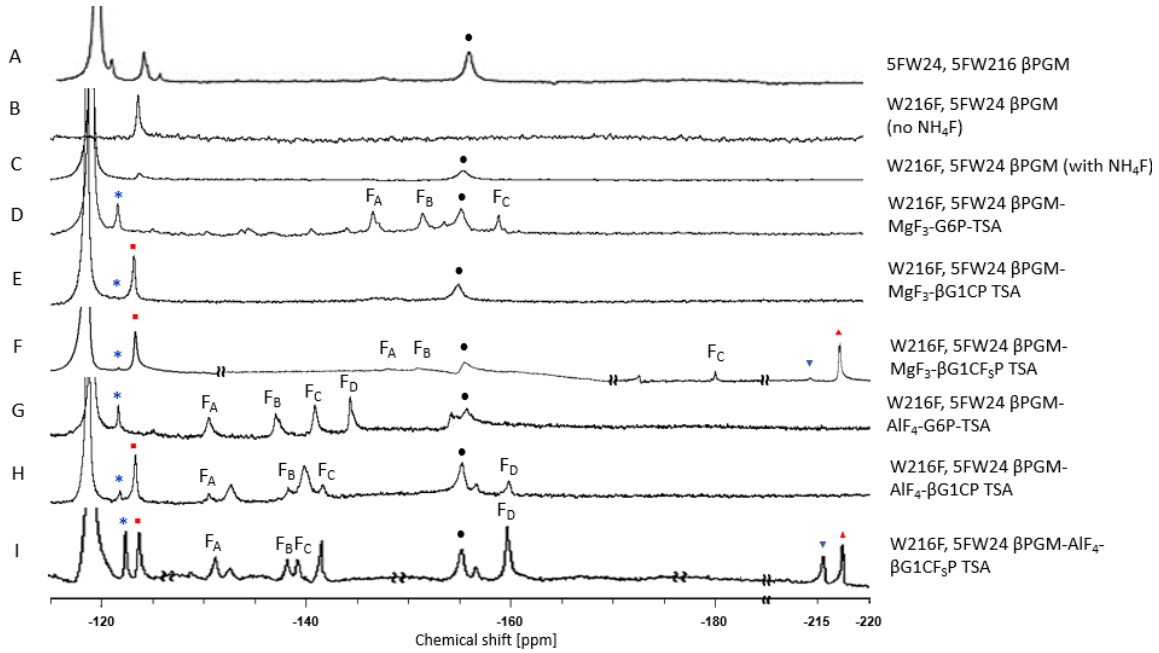

Figure 21. $^{19}F\{^{1}H\}$ NMR spectra of the wild-type 5FWβPGM, the W216F 5FWβPGM mutant, and its TSA1 and TSA2 complexes. Blue asterisks (*) are TSA 5FW24 resonances, red squares (▪) are apo 5FW24 resonances, black circles (•) are free MgF_3^-, blue inverse triangles (▼) are complexed $G1CF_sP$ ligands, red triangles (▲) are free $G1CF_sP$. (A) wild-type 5FWβPGM; (B) W216F 5FWβPGM; (C) W216F 5FWβPGM with NH_4F and $MgCl_2$; (D) W216F 5FWβPGM-MgF_3^--G6P TSA complex; (E) W216F 5FWβPGM-MgF_3^--G1CP TSA complex; (F) W216F 5FWβPGM-MgF_3^--$G1CF_sP$ TSA complex; (G) W216F 5FWβPGM-AlF_4^--G6P TSA complex; (H) W216F 5FWβPGM-AlF_4^--G1CP TSA complex; (I) W216F 5FWβPGM-AlF_4^--$G1CF_sP$ TSA complex. Sample A contains 0.5 mM protein, 5 mM $MgCl_2$, 10 mM NH_4F, and 10% D_2O in HEPES buffer (50 mM, pH=7.2). Sample B contains 1.6 mM protein and 10% D_2O in HEPES buffer. Samples C-I contain 1.6 mM protein, 5 mM $MgCl_2$, 10 mM NH_4F, and 10% D_2O in HEPES buffer. Samples D-I also contain 5 mM substrate. Samples G-I also contain 1 equivalent $AlCl_3$.

showing two equal height signals at -123.5 and -125 ppm, allowing for the assignment of both of these signals as 5FW216.[19] This, along with crystallographic data (Figure 22A), suggested that 5FW216 exists in two different conformation in the ground state, due to an indole ring flip. Although the W24F mutant enzyme was useful for the assignment of the 5FW216 NMR signals, it could not be used to monitor TSA complexation. As the 5FW216 residue is distal from the active site, no change in ^{19}F chemical shift was observed for the

5FW216 residue upon complexation. In the current project, ^{19}F NMR spectra of the W216F 5FWβPGM mutant and its TSA complexes were acquired as the chemical shift of 5FW24 in the cap domain was expected to change upon complexation due to its proximity to the active site (Figure 21).

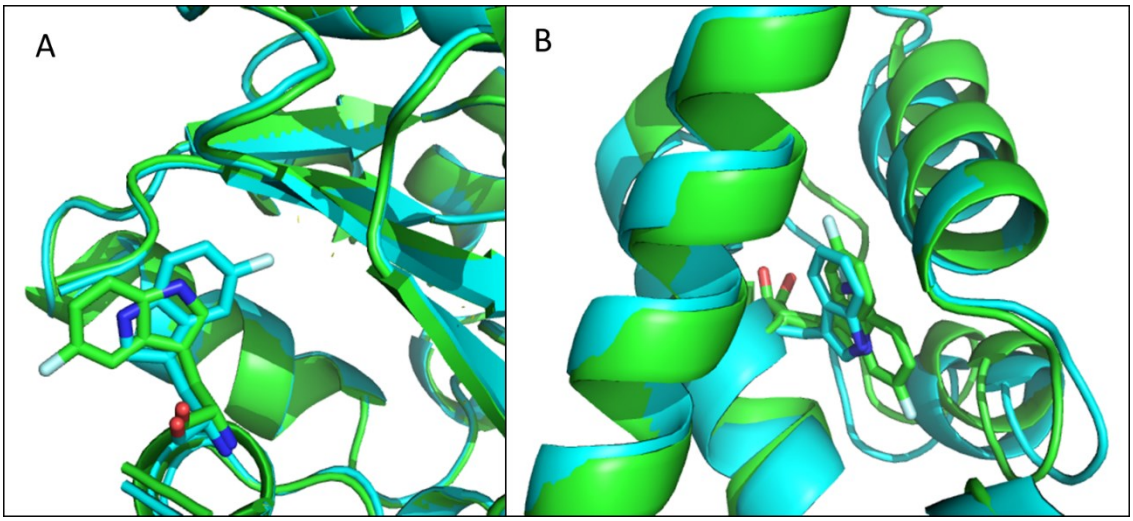

Figure 22. Crystal structures of the W216 and W24 residues in 5FWβPGM.
A) Alternative conformations of 5FW216 observed in the monoclinic crystal form.
B) Alternative conformation of 5FW24 in the cap domain of the open structure.

Analysis of the $^{19}F\{^{1}H\}$ NMR spectrum of the W216F 5FWβPGM mutant alone indicated that the 5FW24 residue in the cap-open (apo) conformation produced a signal at -123.7 ppm (Figure 21B). Therefore, the broad appearance of the signal at -123.5 ppm in the wild-type protein can be explained by the overlap of the 5FW24 and 5FW216 signals. 5FW216 produced two signals as the tryptophan undergoes an aromatic ring flip, resulting in two different conformations with distinct ^{19}F signals. The presence of a single resonance for the 5FW24 residue indicated that it exists in only one conformation in the ground-state. It is worth noting that the crystal structure (Figure 22B) actually shows two conformations for 5FW24 in the ground state, however, the occupancy of the alternative conformation is very low at only 10%. The addition of NH_4F and $MgCl_2$ in the next spectrum produced

signals at -119 and -155 ppm, corresponding to free F^- and MgF_3^-, respectively (Figure 21C).

TSA2 complexes of the W216F mutant were formed using glucose-6-phosphate (G6P, Figure 23), with both MgF_3^--G6P and AlF_4^--G6P being formed, as confirmed by the appearance of three or four new metal-fluoride resonances, respectively (Figure 21D and G). In both cases, the signal for the 5FW24 residue shifted to -121.7 ppm, indicating that the fluorine became more deshielded when the enzyme transitioned into its cap-closed form. Two of the MgF_3^- ^{19}F nuclei appeared to be in a similar chemical environment, interacting with several amino acids in the active site, and therefore had chemical shifts in close proximity at -146.8 and -151.7 ppm. The third ^{19}F nucleus is that which was coordinated to the catalytic magnesium, causing the signal to appear further upfield at -159.2 ppm.[16] The AlF_4^--G6P TSA complex displayed distinct signals of -130.5, -137.1, -140.9, and -144.3 ppm for the bound metal-fluoride ^{19}F nuclei. Once again, the most shielded ^{19}F nucleus was that bound to the catalytic magnesium.

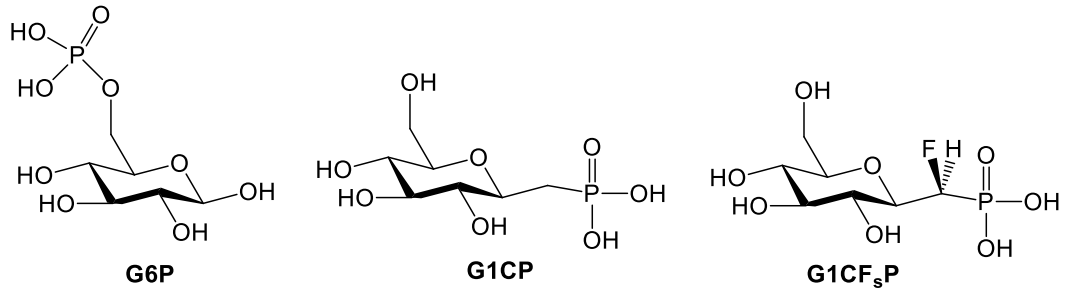

Figure 23. Substrates used in TSA2 and TSA1 complexes with W216F 5FWβPGM.

TSA1 complexes of the W216F mutant were also formed by using either β-D-glucopyranosylmethylphosphonate (G1CP, Figure 23) or (*S*)-1-β-phosphonofluoro-methylene-1-deoxy-D-glucopyranose ($G1CF_sP$, Figure 23) along with MgF_3^- or AlF_4^-. In all of the TSA complex spectra, changing to the cap-closed configuration caused a

downfield shift of the 5FW24 signal (Table 3). The differences observed in $\Delta\delta_F$ can be attributed to the difference in orientation of sugar rings in the active site between G6P, G1CP, and G1CF$_s$P complexes. In both the MgF_3^- and AlF_4^- TSA complexes, similar chemical shifts were observed for the metal-fluoride ^{19}F nuclei to those observed in the G6P TSA spectra. The intensity of these peaks in the AlF_4^- TSA spectra was much greater than in the MgF_3^- TSA spectra, as was the ratio of the 5FW24 complexed enzyme to 5FW24 apo enzyme, indicating the enzyme binds more readily with the tetrafluoroaluminate than the trifluoromagnesate. This is consistent with previous reports of the wild-type βPGM forming AlF_4^- complexes preferentially over MgF_3^- complexes.[27] In the G1CF$_s$P TSA spectra, the ratio of bound to free protein was mirrored by the ratio of bound to free G1CF$_s$P, which displayed signals at -215 (s) and -217 (d), respectively. The intensity of these resonances was also comparable to the intensity of the bound metal fluorides. This is the first time ^{19}F NMR spectroscopy has been used to probe the enzyme, ligand, and metal fluoride complex, demonstrating that the molar ratios of each species are comparable and additionally the metal fluorides are representative of the transition state. In the spectrum of each complex, the integrations of the metal fluoride resonances were equivalent to the integration of the complexed 5FW24 peak, for both the MgF_3^- and the AlF_4^- complexes, an occurrence which has not been previously reported.

The crystal structure of 5FWβPGM with MgF_3^- and G6P showed by electron density that the 5FW residues had been incorporated (Figure 24A) and that similar conformations were observed for the ^{19}F-labelled and wild-type residues (Figure 24B). When the structure of a second crystal form of the 5FWβPGM-MgF_3^--G6P complex was determined, it was observed that the W216 residue existed in two equally populated

Fig. #	5FWβPGM W216F TSA complex	5FW24 δ_{apo} (ppm)	5FW24 $\delta_{complexed}$ (ppm)	$\Delta\delta_F$ (ppm)
20D	MgF_3^--G6P	-123.7	-121.7	2.0
20G	AlF_4^--G6P	-123.7	-121.7	2.0
20E	MgF_3^--βG1CP	-123.4	-121.3	2.1
20H	AlF_4^--βG1CP	-123.4	-121.5	1.6
20F	MgF_3^--βG1CF$_S$P	-123.2	-121.5	1.7
20I	AlF_4^--βG1CF$_S$P	-123.7	-122.4	1.3

Table 3. ^{19}F NMR chemical shifts of 5-FWβPGM W216F in apo and complexed enzyme conformations of step 1 and step 2 MgF_3^- and AlF_4^- TSA complexes.

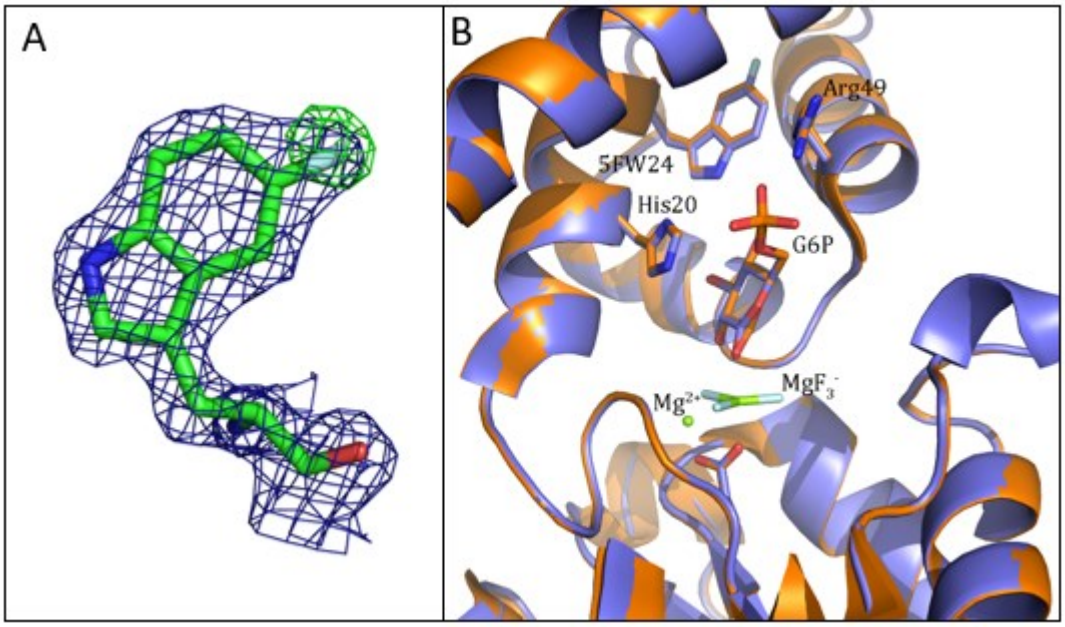

Figure 24. A) Electron density for 5FW216. Clear positive density was observed for fluorine (green mesh around the light blue atom.) **B)** Overlay of ^{19}F-labelled and unlabelled W24 in the βPGM-MgF_3^--G6P complexes (^{19}F-labelled in gold, wild-type in purple). No difference in structure was observed between labelled and unlabelled.

conformations (Figure 22A) which corroborated the assignment of two ^{19}F NMR resonances as signals produced by 5FW216. The wild-type βPGM W216 residue exists in a single conformation, therefore, the observation of two conformations for the 5FW216 residue of the ^{19}F-labelled enzyme is potentially an artefact produced by the incorporation of the unnatural amino acid 5-fluorotryptophan.

The W216F 5FWβPGM mutant protein was used to form TSA1 and TSA2 complexes. The assignment of complexes using ^{19}F NMR spectroscopy was done with great ease compared to the wild-type 5FWβPGM as only one signal was observed for free 5FW24 and one signal for complexed 5FW24. The resonances of complexed 5FW24 were observed in equal integrations to the metal fluoride resonances in all spectra, indicating that the chosen method was appropriate for measuring the extent of TSA complexation. In the TSA2 complex (with G6P) spectra, complete complexation was observed, however, of the TSA1 complexes (with G1CP or G1CF$_S$P), the best complexation observed (the AlF_4^--G1CF$_S$P complex) was only 50%. This leaves room for future work where different substrates are tried with AlF_4^- and W216F 5FWβPGM to increase the amount of complexation.

Chapter 4. Results and Discussion of the Synthesis of Diammonium 3-deoxy-3-fluoro-β-D-glucopyranosylmethylphosphonate (21)

In this study, a novel potential inhibitor of β-phosphoglucomutase, diammonium 3-deoxy-3-fluoro-β-D-glucopyranosylmethylphosphonate (**21**), was synthesized and fully characterized. This compound is structurally similar to the previously studied 5FW-W216F 5FWβPGM substrate G1CP[36,37] (see Chapter 3.5), with the only difference being a fluorine atom in place of the hydroxyl group on C3 of G1CP. This substitution of a fluorine for a hydroxyl group could lead to better binding in the active site, due to the increased electronegativity of fluorine, leading to improved hydrogen bonding with the leucine 44, serine 52, and tryptophan 24 residues in this area of the active site[16]. This stronger binding of **21** in the active site is expected to produce a **21**-W216F 5FWβPGM complex more stable than those studied in Chapter 3 and therefore we anticipate greater conversion of apo to cap-closed enzyme to be observed in the ^{19}F NMR spectrum of the **21**-W216F 5FWβPGM transition-state analogue complex than we observed for the TSA complexes studied in Chapter 3.

The synthetic scheme for **21** was devised based on methods which were successful in previous syntheses of fluorinated phosphates and phosphonates in the Jakeman lab.[16,37,38] Eight fluorinated α-D-glucopyranosyl 1-phosphate analogues were previously synthesized using a four-step synthetic strategy: 1) fluorine addition to the monosaccharide, 2) selective anomeric deprotection, 3) phosphorylation of the anomeric hydroxyl group, and 4) global deprotection.[38] A similar synthetic strategy was employed in the synthesis of **21**, with the exception of the third step being phosphonylation rather that phosphorylation. The starting material selected was diacetone-D-glucose (**7**) as it is inexpensive and easy to procure. To

eventually produce **21**, **7** must be converted to its pyranose form, which has a free hydroxyl group at the anomeric position, therefore an additional step of selective anomeric protection was added between steps one and two. The five key steps in the synthesis of **21** are demonstrated retrosynthetically in Figure 25.

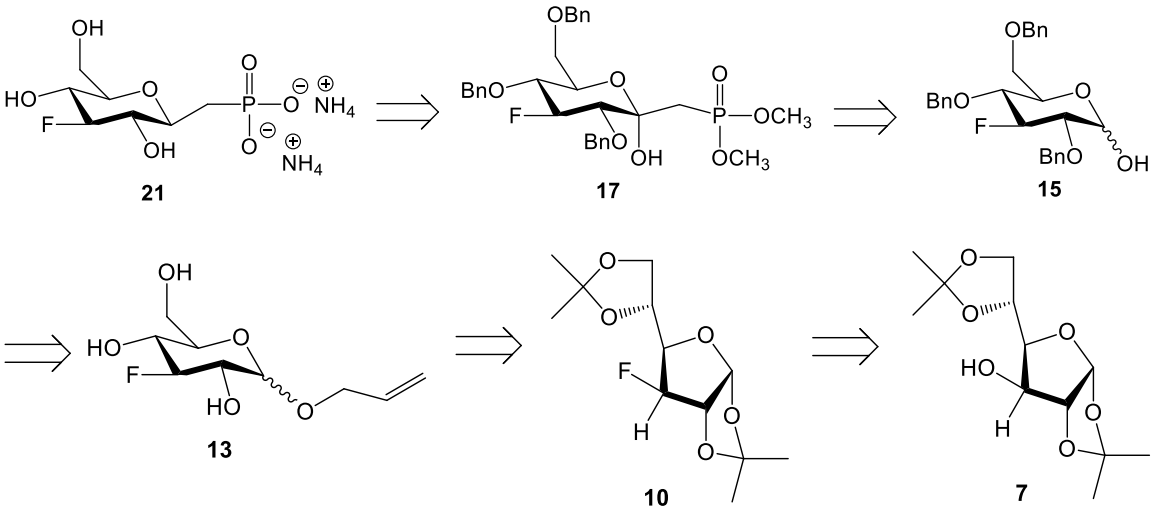

Figure 25. Five major steps in the retrosynthesis of **21**

Diammonium 3-deoxy-3-fluoro-β-D-glucopyranosylmethylphosphonate (**21**), was synthesized in twelve steps (Figure 26). Compounds **8-11** were synthesized as previously described in the literature[39-44], whereas **12-21** were novel compounds, synthesized by applying techniques described for similar transformations. The first functional group to be installed was the fluorine on C3. To introduce this functionality in the equatorial position, the stereochemistry at C3 of the starting material, diacetone-D-glucose (**7**), had to be inverted. This was accomplished by first oxidizing **7** at the C3 hydroxyl using Dess-Martin Periodinane (DMP) in CH_2Cl_2 with sodium bicarbonate, producing **8**, which was then reduced using sodium borohydride in ethanol-water, thus inverting the stereochemistry, producing **9** (94% over two steps).[39] The fluorine was then incorporated into **9** either by fluoro-de-hydroxylation using diethylaminosulfur trifluoride (DAST) in CH_2Cl_2-pyridine

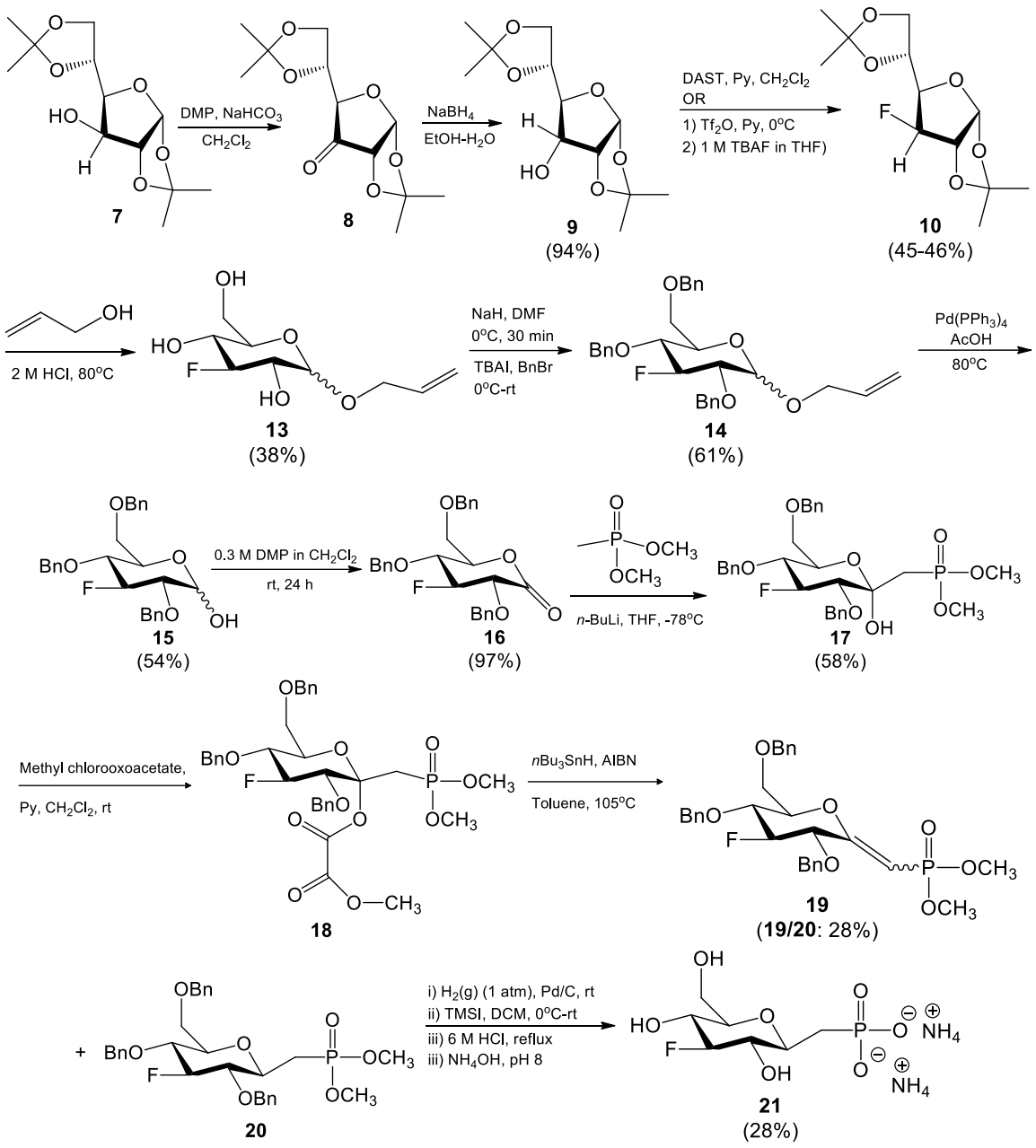

Figure 26. Twelve-step synthesis of diammonium 3-deoxy-3-fluoro-β-D-glucopyranosylmethylphosphonate (**21**)

(45% yield)[40-42] or by consecutive nucleophilic substitution reactions using triflic anhydride followed by tetrabutylammonium fluoride (TBAF), giving **10** (46% yield)[44]. Next, the furanose **10** would be converted to a pyranose ring and the anomeric hydroxyl group would be protected. A methoxy group was chosen as the protecting group for the C1

hydroxyl as it required different deprotection conditions than benzyl groups, allowing the other hydroxyl groups (on C2, C4, and C6) to be protected using benzyl groups. After all of the hydroxyl groups were protected, the methoxy group at C1 could be deprotected selectively, leaving a single hydroxyl group available for phosphonylation. The transformation of **10** to the C1-protected pyranose was accomplished by refluxing in methanol with acetyl chloride, yielding **11** (66%)[43] (Figure 27). The three benzyl protecting groups on C2, C4, and C6 were then introduced to **11** using sodium hydride and benzyl bromide in dry dimethyl formamide (DMF) with tetrabutylammonium iodide (TBAI) as a catalyst,[45] making **12** (72%) (Figure 27). Unfortunately, selective deprotection of the methyl glucoside **12** was not accomplished using literature conditions[46,47] or several variations thereof, therefore an alternate route starting from **10** was implemented (Figure 26). For this route, an allyl ether was selected as the protecting group for C1 since the conditions for its deprotection differed than those used for benzyl deprotection along with the fact that it is a relatively easy protecting group to remove.[48] Using HCl in allyl alcohol, the acetal **10** was converted to a pyranose ring and an allyl group was introduced at the anomeric position,[49,50] giving **13** (38%). The three benzyl protecting groups were introduced using the same method described for the production of **12**, making **14** (61%). Next, the anomeric allyl group was to be selectively deprotected. To accomplish this, the allyl group was isomerized to a prop-1-en-1-yl group and hydrolyzed in one pot, using $Pd(PPh_3)_4$ as a catalyst along with acetic acid as both co-catalyst and solvent,[51] to give **15** (54%). The subsequent functionality to be introduced would be the phosphono group at the anomeric position. This transformation was performed by oxidizing **15** to the lactone **16** (97%) using DMP in CH_2Cl_2,[52] followed by phosphonylation using dimethyl

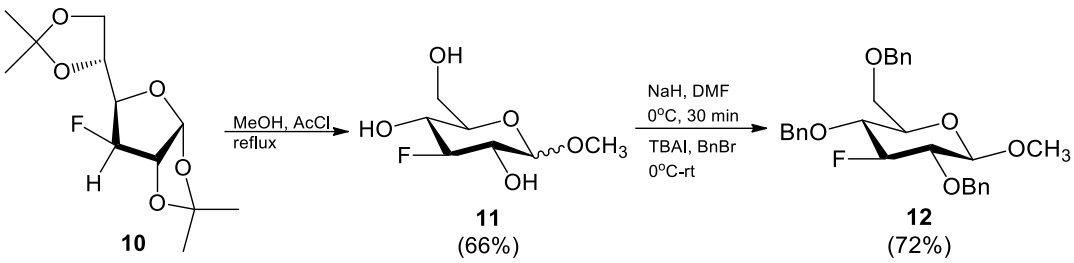

Figure 27. Synthesis of **11** and **12** from **10**.

methylphosphonate with *n*-butyllithium[37] to give **17** (58%). The axial hydroxyl group which was introduced during the phosphonylation was unwanted in the final product, therefore the next step was to reduce it. Triethyl silane reduction of the hemi-acetal was unsuccessful and consequently a two-step method was implemented. First, an oxalate ester was formed at the anomeric position of **17** by addition of methyl chlorooxoacetate in CH_2Cl_2-pyridine.[16] Second, the crude oxalate ester, **18**, was subjected to a radical reaction using azobisisobutyronitrile (AIBN) and nBu$_3$SnH in refluxing toluene,[16] to give a mixture of **19** and **20** (28%). The **19**/**20** mixture was hydrogenated over a period of four hours using H_2 gas (1 atm) and catalytic Pd/C in order to saturate the double bond[37] of **19** converting the entire mixture to **20**. Once the double bond was saturated, the only remaining transformations needed to obtain the final product were global deprotection and ion-exchange. The benzyl and methyl groups of **20** were deprotected using TMSI followed by refluxing with HCl, respectively, and the phosphonate functionality was converted to the ammonium salt form by titrating with ammonium hydroxide (pH= 8)[37] to give the final product **21** (28%). The yield for the final step has the potential to be improved in future syntheses as a much higher yield (66%) is reported for similar transformations in the literature.[37] During the current synthesis, **19**/**20** were recovered several times after failed hydrogenation attempts using different conditions, leading to residual loss which negatively impacted the yield.

The conversion of **7** to **8** was determined to be complete when the starting material could no longer be observed by TLC and was replaced by a spot with a higher R_f value. Crude **8** was directly subjected to reduction, producing **9**. This material was characterized using ^{1}H NMR spectroscopy (Figure 28) as well as 2-dimensional ^{1}H-^{1}H COSY, and found to be consistent with the reported ^{1}H NMR spectrum.[39] The doublet at 5.80 ppm was identified as the the anomeric proton, which showed only one COSY correlation: to the H2 triplet at 4.61 ppm. H2 also coupled to a multiplet, integrating to 3H, at 4.04 ppm which was found to contain the signal for H3 as well as the signal for H4. H4 then correlated to a multiplet, integrating to 1H, at 4.30 ppm which was identified as H5. H5 in turn, correlated to the two diastereotopic H6 protons: the first overlapped with the H3 and H4 signals at 4.04 ppm and the second produced a doublet of doublets at 3.81 ppm. This doublet of

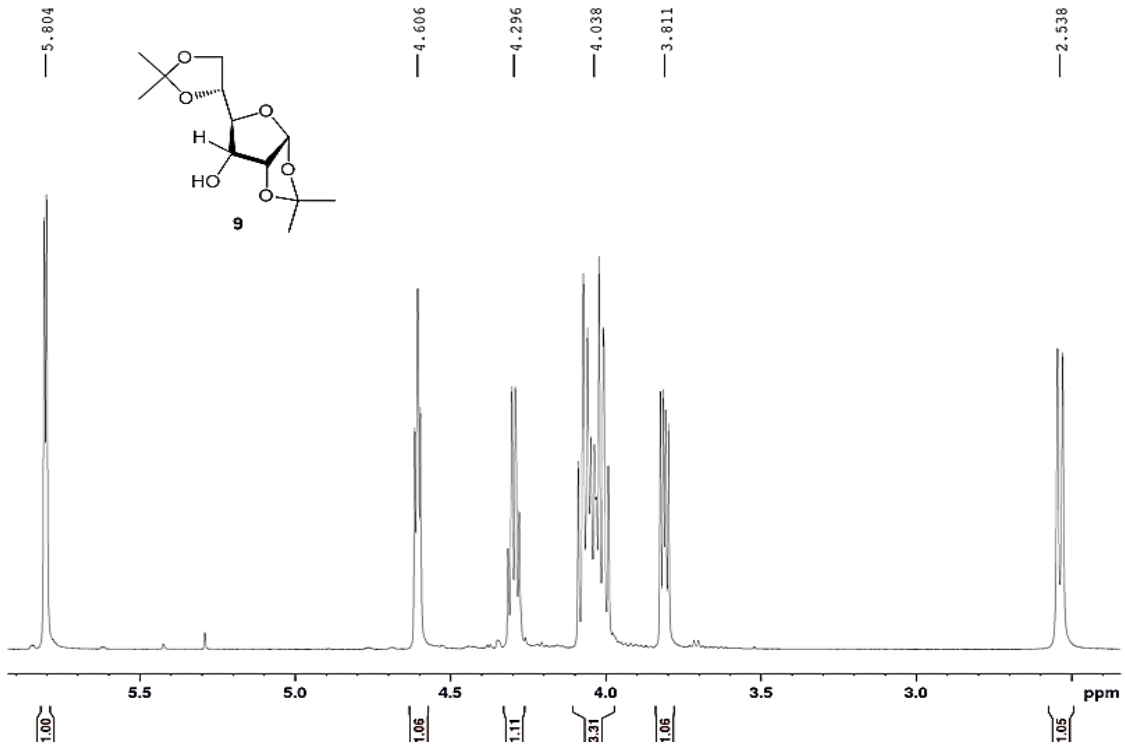

Figure 28. ^{1}H NMR (500 MHz, $CDCl_3$) spectrum of 1,2: 5,6-di-*O*-isopropylidene-α-D-allofuranose (**9**)

doublets showed coupling characteristic of diastereotopic protons on a furanose ring ($^{2}J_{H6a-H6b}$= 8.5 Hz) as well as coupling with H5 ($^{3}J_{H5-H6b}$= 4.8 Hz). The four singlets at 1.57, 1.46, 1.38, and 1.37 ppm integrated to 3H each and were assigned as the methyl groups of the two isopropylidene moieties (Appendix B for full spectrum).

10 and **11** were characterized using ^{19}F, ^{1}H, and ^{1}H-^{1}H COSY NMR spectroscopy. The ^{19}F NMR spectrum of **10** (Figure 29A) had only one peak at -207.7 ppm, confirming the presence of a single mono-fluorinated species. The peak was a doublet of doublet of doublets due to geminal coupling with H3 ($^{2}J_{H3-F}$= 49.9 Hz) as well as vicinal coupling with H2 ($^{3}J_{H2-F}$= 10.6 Hz) and H4 ($^{3}J_{H4-F}$= 29.2 Hz). The ^{1}H NMR spectrum of **10** (Figure 29B) was consistent with the reported data.[40] The anomeric proton was identified as the doublet at 5.95 ppm which correlated to only one other peak: the doublet of doublets at 4.69 ppm, which was assigned as H2. The H2 coupling constant of 10.7 Hz was indicative of vicinal coupling with fluorine whilst the smaller coupling constant of 3.7 Hz was due to coupling with the H1. Coupling was not observed between H2 and H3, however, H3 was identified as the signal at 5.00 ppm by its splitting pattern (doublet of doublets) characteristic of a proton geminal to a fluorine ($^{2}J_{H-F}$= 50.0 Hz) as well as vicinal to a proton ($^{3}J_{H3-H4}$= 2.3 Hz). H3 correlated to H4 whose signal appeared within the 3H multiplet at 4.08 ppm. H4 in turn, correlated to the multiplet at 4.28 ppm, integrating to 1H, leading to the assignment of this signal as H5. Finally, H5 correlated to the two H6 protons whose signals arose within the multiplet at 4.08 ppm.

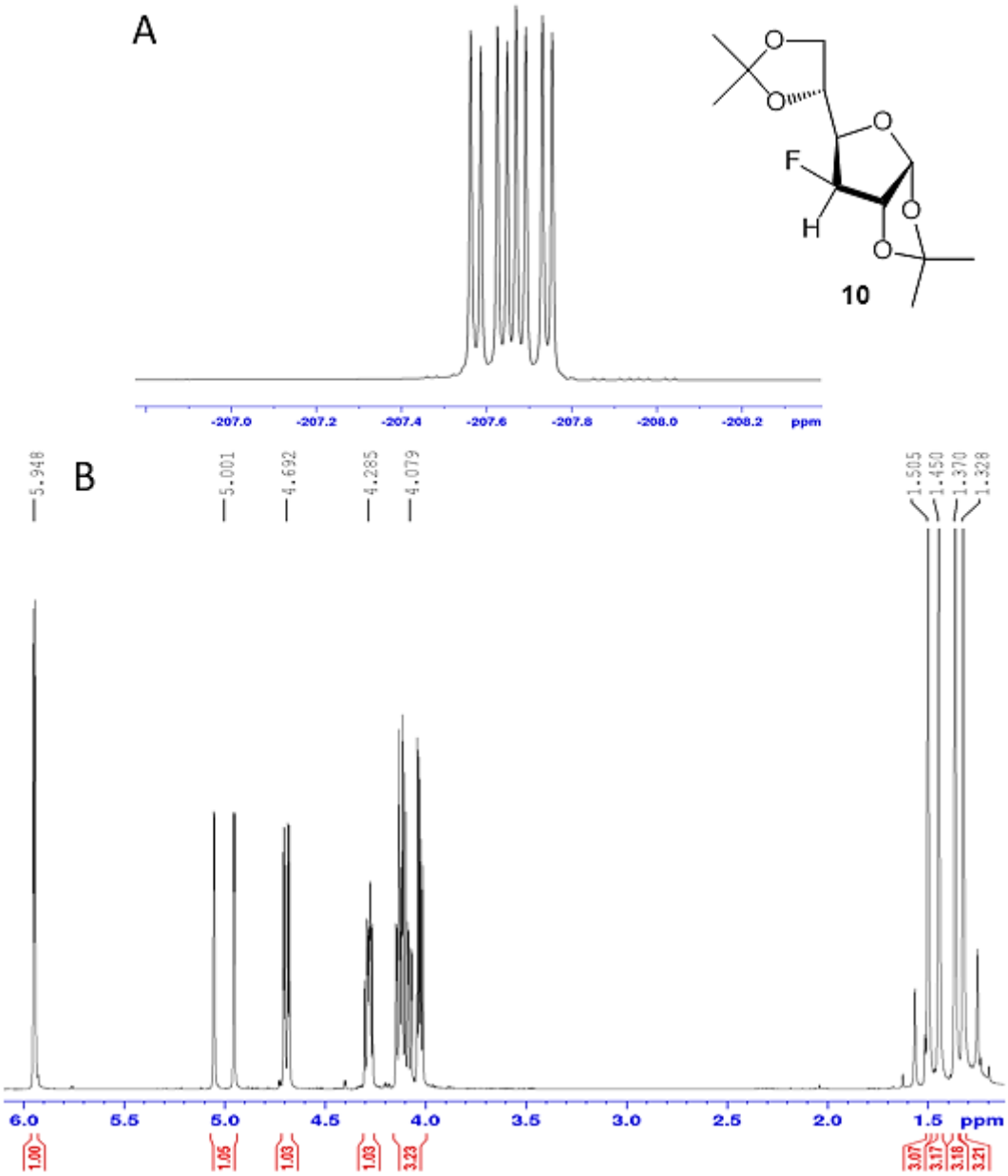

Figure 29. NMR spectra of 3-deoxy-3-fluoro- 1,2: 5,6-di-*O*-isopropylidene-α-D-glucofuranose (**10**). **A)** ^{19}F (470 MHz, $CDCl_3$) **B)** ^{1}H (500 MHz, $CDCl_3$).

The ^{19}F NMR spectrum of **11** (Figure 30A) contained two signals, both doublets of triplets, at -196.6 and -200.6 ppm. These were assigned as the β and α anomers of **11**, respectively as the α-configured **11** has been reported in the literature.[53] In both signals,

there was a coupling constant of 13 Hz due to vicinal coupling with H2 and H4, as well as a coupling constant of 53-54 Hz due to geminal coupling with H3. In the ^{1}H NMR spectrum of **11** (Figure 30B), the signals for the α and β anomers were present in a 2:1 ratio. Consistent with the reported data,[53] the anomeric proton of the major (α) product was identified as the apparent triplet at 4.82 ppm, which coupled vicinally to H2 as well as (long-range) coupling with fluorine, both with coupling constants of 3.5 Hz. The doublet of triplets at 4.53 ppm was identified as the signal for H3α. This signal overlapped with another doublet of triplets at 4.41 ppm, caused by H3β. The anomeric proton for the minor (β) anomer was identified as the doublet at 4.26 ppm, with a coupling constant of 7.8 Hz, characteristic of axial-axial proton coupling. The remaining ring protons (H2, H4, H6a, H6b) of both anomers produced indistinct signals appearing in the multiplet from 3.97-3.62 ppm. The methoxy substituents on C1 produced singlets, integrating to 3H, which appeared at 3.58 and 3.44 ppm for the β and α anomers, respectively. Several peaks were present between 0.00 and 2.50 ppm (not shown) due to impurities which proved impossible to remove by extraction or column chromatography.

Compounds **12-17, 19,** and **21** were fully characterized using ^{19}F and/or $^{19}F\{^{1}H\}$, ^{1}H, $^{13}C\{^{1}H\}$, COSY, and HSQC NMR spectroscopy as well as high resolution mass spectrometry. Additionally, $^{31}P\{^{1}H\}$ NMR spectra were acquired for compounds **17**-**21**.

The successful synthesis of **12** was confirmed by the ESI+ mass spectrum, which contained a peak at 489.2055 corresponding to the molecular ion plus sodium (Appendix D). The ^{19}F NMR spectrum of **12** contained only one signal: an apparent doublet of triplets at -188.7 ppm, indicating that a single anomer was present (Figure 31A). The ^{1}H NMR spectrum confirmed that this was the β anomer, as indicated by the appearance of the H1

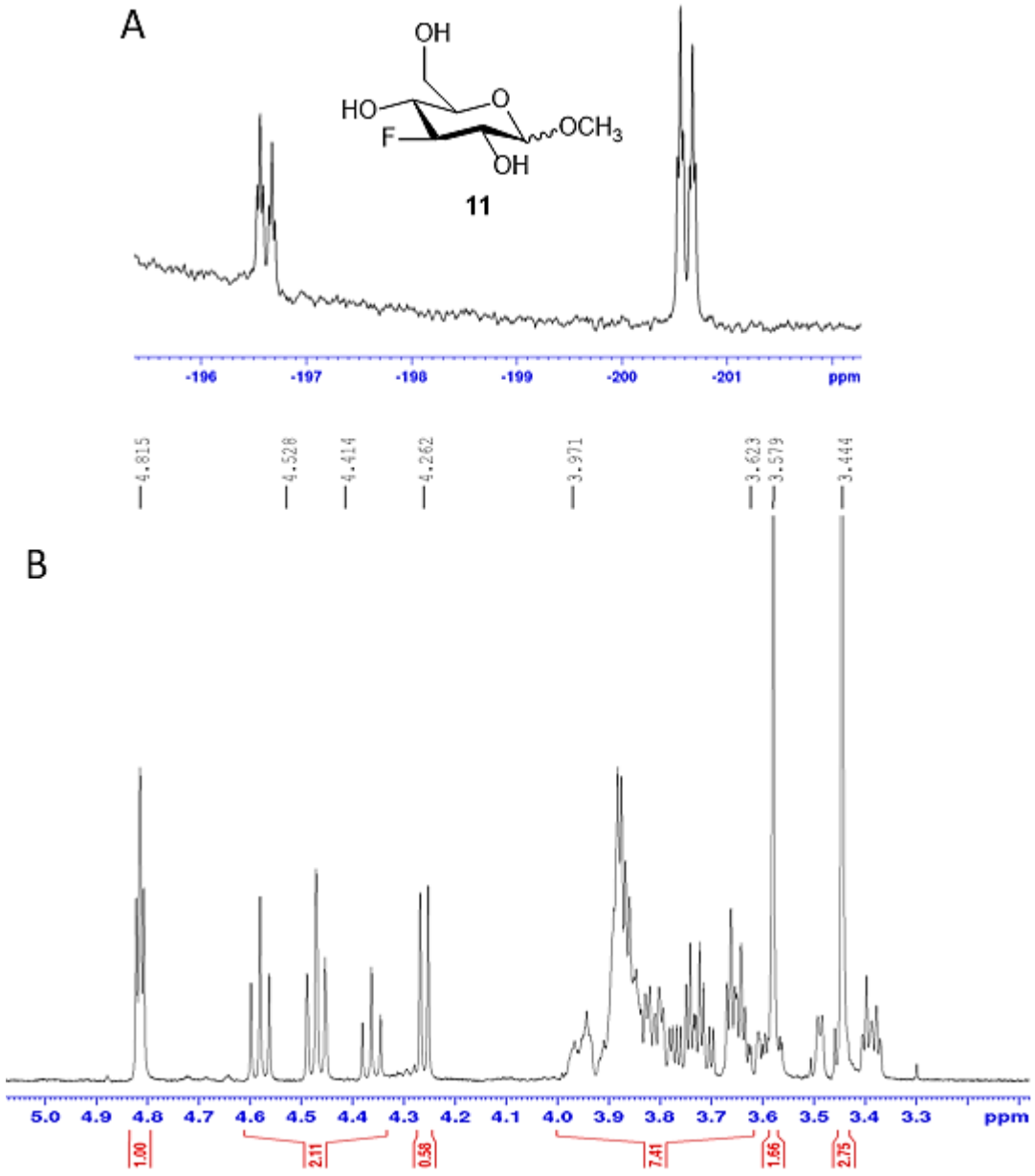

Figure 30. NMR spectra of methyl 3-deoxy-3-fluoro-α/β-D-glucopyranoside (**11**). **A)** ^{19}F (470 MHz, $CDCl_3$) **B)** ^{1}H (500 MHz, $CDCl_3$).

signal at 4.40 ppm as a doublet with a coupling constant of 7.8 Hz (Figure 31B). The signals produced by the carbohydrate protons and the methoxy protons were observed with similar chemical shifts to those of **11**. In addition to these peaks, six doublets corresponding to the benzyl methylene protons were observed from 5.00-4.87 and 4.75-4.64 ppm. The aromatic

protons of the benzyl groups produced a multiplet at 7.44 ppm (Appendix B for full spectrum) which integrated to 15H, confirming three benzyl groups were present. The $^{13}C\{^{1}H\}$ NMR spectrum (Appendix C) was also fully assigned (see Chapter 5.8).

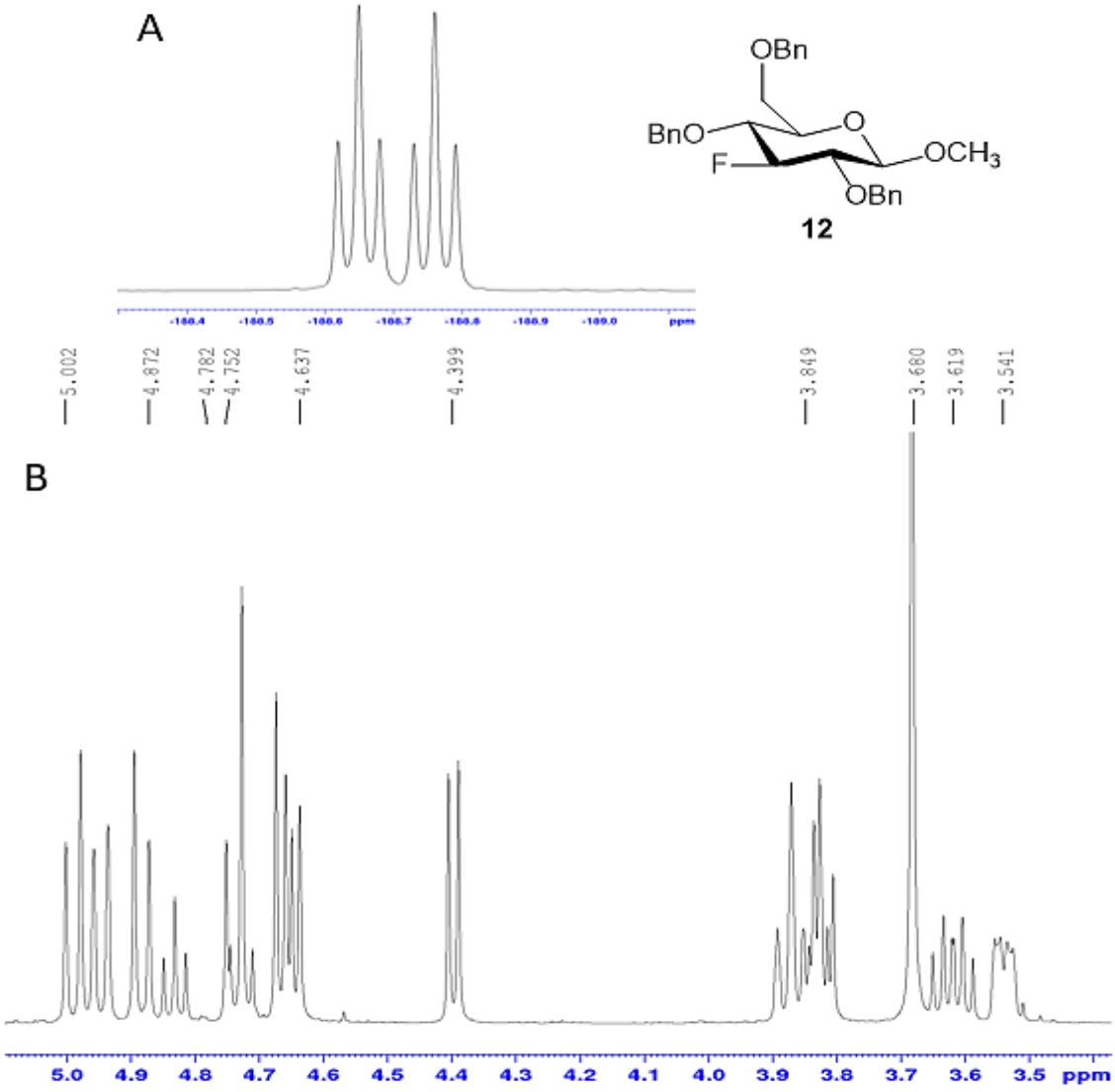

Figure 31. NMR spectra of methyl 2,4,6-tri-*O*-benzyl-3-deoxy-3-fluoro-β-D-glucopyranoside (**12**). **A)** ^{19}F (470 MHz, $CDCl_3$) **B)** ^{1}H (500 MHz, $CDCl_3$).

The appropriate mass for **13** was found in its ESI+ mass spectrum, which contained a peak at 285.0801 corresponding to the molecular ion plus sodium (Appendix D). The ^{19}F NMR spectrum contained two doublets of triplets (-196.1 and -200.3 ppm), present in a 1:1

ratio, indicating that both α and β anomers were synthesized (Figure 32A). The ^{1}H NMR corroborated that equal quantities of α and β anomers were formed (Figure 32B). The newly introduced allyl group produced multiplets at 5.99, 5.37, 5.21, and within 4.43-4.05 ppm which were assigned by comparing to a literature spectrum of allyl alcohol.[54] The two furthest upfield allyl signals (within 4.43-4.05 ppm) were assigned as the methylene H1'a and H1'b. The furthest downfield allyl signal (at 5.99 ppm) was assigned as H2', leaving the two remaining allyl signals at 5.37 and 5.21 ppm to be assigned as the vinylic H3'a and H3'b. The anomeric protons for the α and β configured products were identified as the signals at 4.91 (t) and 4.37 (d) ppm, respectively, based on their coupling constants of 3.5 Hz and 7.9 Hz, respectively. COSY correlations were used to identify the remaining carbohydrate signals. The doublet of triplets clearly visible at 4.54 ppm was assigned as H3α whereas the signal for H3β fell within the multiplet of overlapping signals from 4.43 to 4.05 ppm. The H5 protons were identified as the two multiplets furthest up-field in the carbohydrate region at 3.47 and 3.30 ppm. The remaining protons (H2, H4, H6a, and H6b of both anomers) produced overlapping signals, which integrated to a total of 8H, in the region from 3.94-3.56 ppm. The ^{13}C{^{1}H} NMR spectrum (Appendix C) was also fully assigned (see Chapter 5.8), corroborating that **13** was formed.

The ^{19}F{^{1}H} NMR spectrum of **14** contained two signals, -188.7 and -192.8 ppm, indicating the presence of both anomers (Figure 33A). In the ^{1}H NMR spectrum of **14** (Figure 33B), the expected aromatic benzyl signals were present as a multiplet centered at 7.39 ppm, integrating to 16H (with the integration being one proton too high as the signals overlapped with the residual chloroform peak). The allyl protons were assigned as the multiplets (integrating to 1H each) at 6.00, 5.28, 4.21, and 4.06 ppm which appeared in

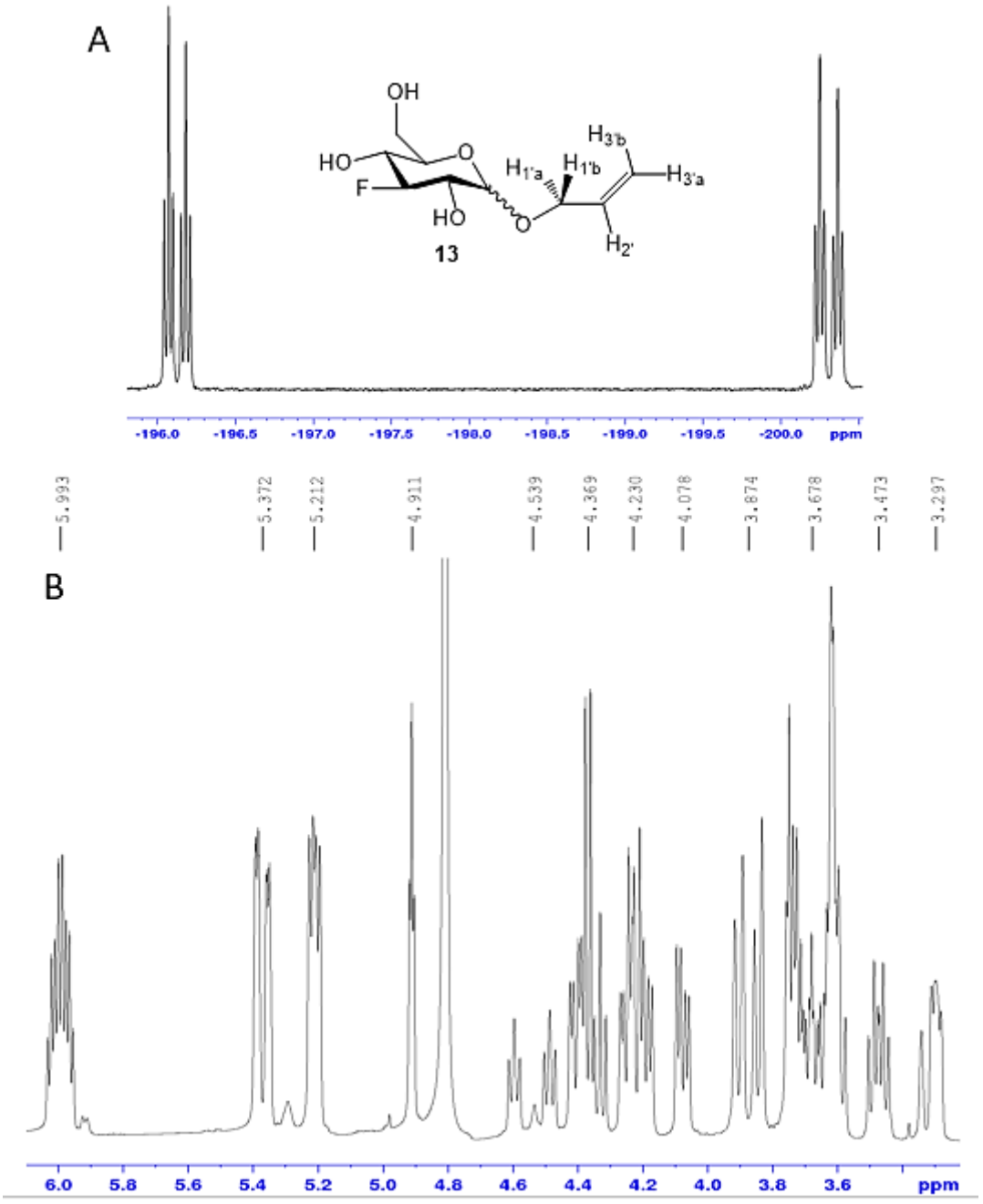

Figure 32. NMR spectra of allyl 3-deoxy-3-fluoro-D-glucopyranoside (**13**). **A)** ^{19}F (470 MHz, CD_3OD), **B)** ^{1}H (500 MHz, CD_3OD).

the same order as described in **13**. The carbohydrate protons and the methylene units of the benzyl groups produced overlapping signals which were difficult to assign distinctly. With the assistance of the COSY spectrum, the multiplet from 5.15 to 4.48 ppm was found to contain the signals for H3, H1, and the six methylene protons. The remaining carbohydrate

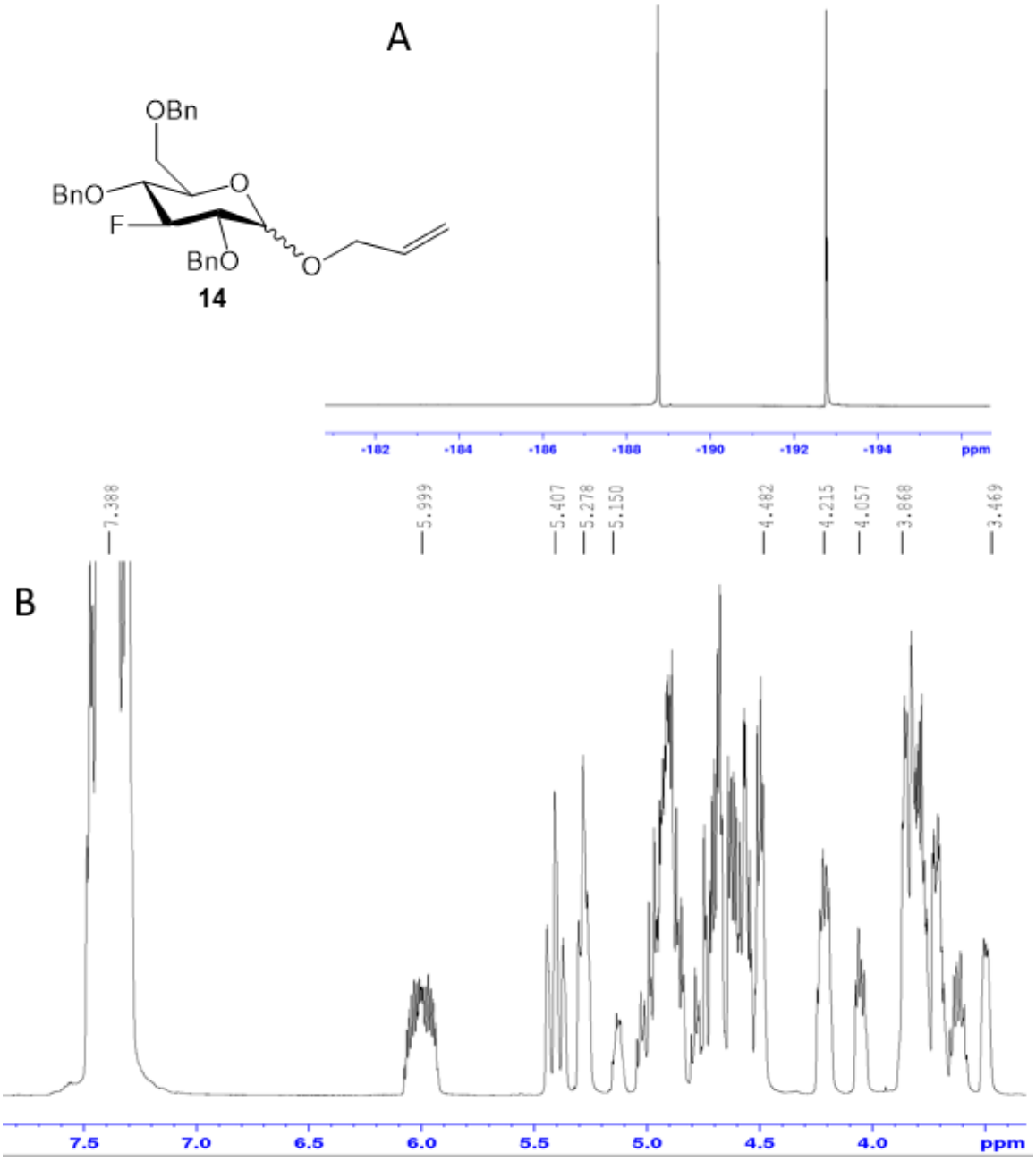

Figure 33. NMR spectra of allyl 2,4,6-tri-*O*-benzyl-3-deoxy-3-fluoro-D-glucopyranoside (**14**). **A)** $^{19}F\{^{1}H\}$ (470 MHz, $CDCl_3$), **B)** ^{1}H (500 MHz, $CDCl_3$).

protons (H2, H4, H5, H6a, and H6b) produced signals in the range of 3.87 to 3.47 ppm. The $^{13}C\{^{1}H\}$ NMR spectrum (Appendix C) was also assigned, using HSQC correlations (see Chapter 5.8). The most definitive indicator of product formation was the ESI+ high

resolution mass spectrum, where a peak at 515.2191, the appropriate mass for the molecular ion plus sodium, was observed (Appendix D).

The high resolution mass spectrum (ESI+) of **15** indicated that the desired product was synthesized with the appearance of a peak at 475.1884, corresponding to the molecular ion plus sodium (Appendix D). Two signals, -189.0 and -193.8 ppm, were present in the ^{19}F NMR spectrum of **15**, indicating the presence of β and α anomers, respectively (1β: 4α, Figure 34A). By ^{1}H NMR, only the major α anomer was observed distinctly and completely assigned (Figure 34B). The four allyl signals had disappeared. The anomeric proton appeared as a triplet at 5.27 ppm due to similar coupling constants (~3.7 Hz) for axial-equatorial vicinal coupling with H2 and W-coupling with fluorine. A COSY correlation indicated that H2 corresponded to the signal at 3.67 ppm, which overlapped with other signals in a multiplet. H3 was identified as the doublet of triplets at 4.99 ppm based on its characteristic splitting pattern ($^{3}J_{HH}$ = 8.7 Hz, $^{2}J_{HF}$= 53.6 Hz). The COSY spectrum showed a correlation between the H3 signal and a multiplet at 3.77 ppm, identifying it as H4. H4 only correlated back to a multiplet ranging from 3.59 to 3.82 ppm, which included itself and H2. As the entire multiplet integrated to 5H, it was concluded that the yet unidentified signals of H5, H6a, and H6b were included. The $^{13}C\{^{1}H\}$ NMR spectrum (Appendix C) of the α anomer was also assigned, confirming the successful synthesis of **15** (see Chapter 5.8).

In the $^{19}F\{^{1}H\}$ NMR spectrum of **16**, the appearance of a new peak at -183.5 ppm and the disappearance of both starting material peaks indicated that a single new product was formed (Figure 35A). The ^{1}H NMR spectrum of **16** (Figure 35B) showed that the anomeric proton of the starting material (5.27 ppm) had disappeared. H3 was identified as

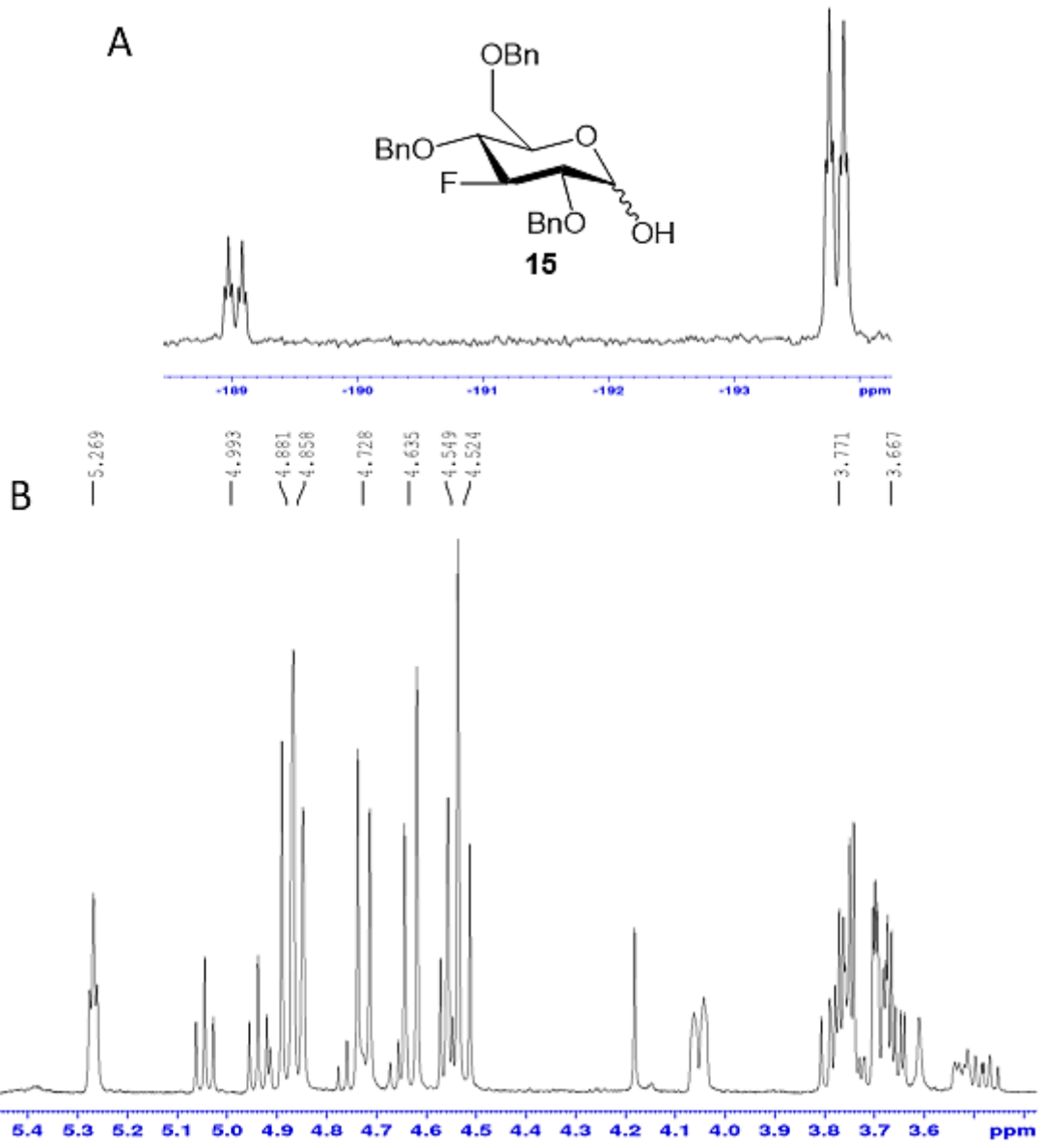

Figure 34. NMR spectra of 2,4,6-tri-*O*-benzyl-3-deoxy-3-fluoro-D-glucopyranose (**15**). **A)** ^{19}F (470 MHz, $CDCl_3$), **B)** ^{1}H (500 MHz, $CDCl_3$).

the signal at 4.92 ppm based on its characteristic doublet of triplet splitting pattern and downfield chemical shift caused by the geminal fluorine. COSY correlations were observed between H3 and signals at 4.21 and 4.12 ppm, meaning that they could each correspond to either H2 or H4. The doublet of doublets at 4.21 ppm was assigned as H2 since this proton was expected to couple only with H3 and fluorine. The doublet of doublet

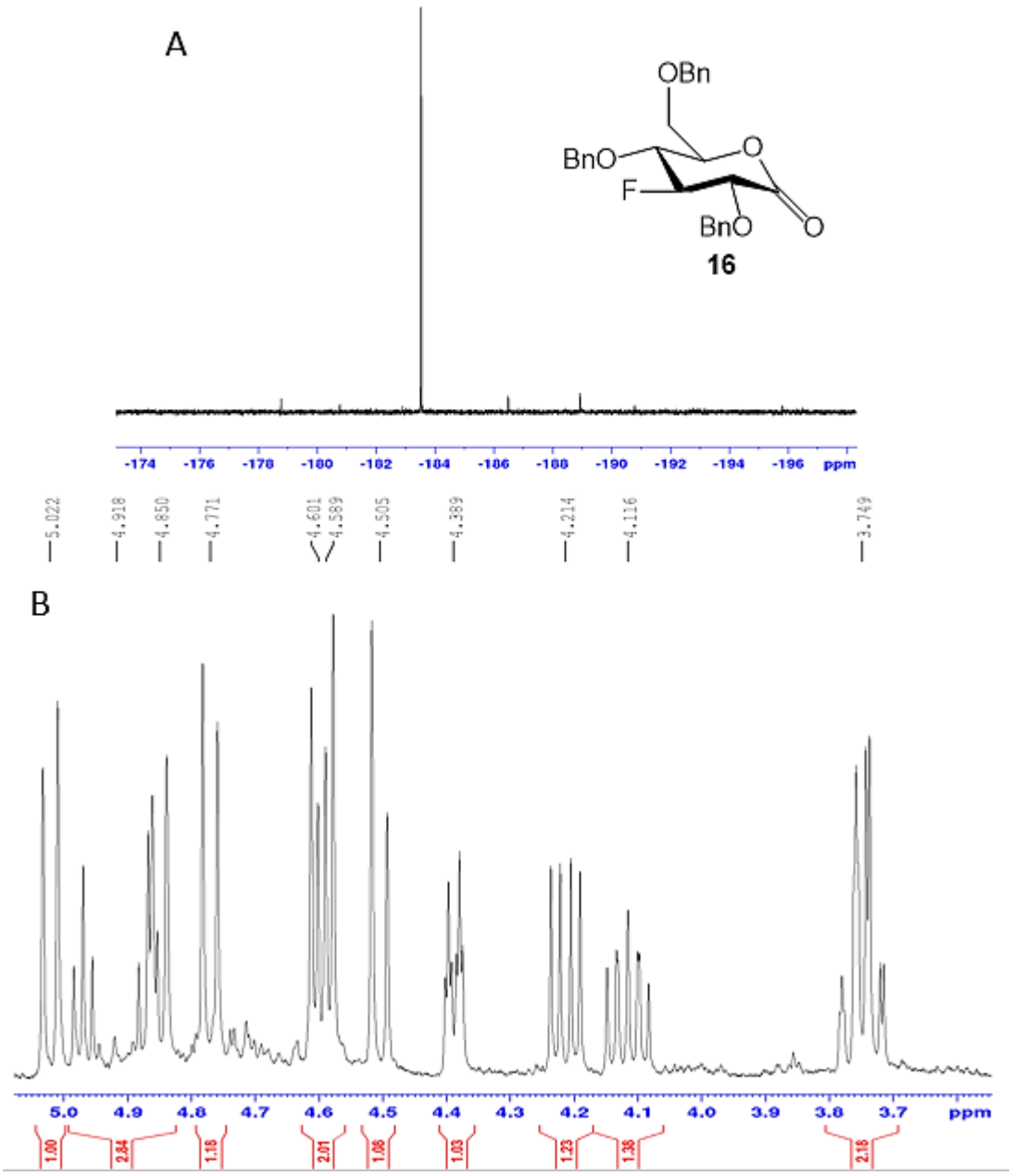

Figure 35. NMR spectra of 2,4,6-tri-*O*-benzyl-3-deoxy-3-fluoro-D-gluconolactone (**16**). **A)** $^{19}F\{^{1}H\}$ (470 MHz, $CDCl_3$), **B)** ^{1}H (500 MHz, $CDCl_3$).

of doublets at 4.12 ppm was assigned as H4 as this proton was expected to couple with H5 as well as H3 and fluorine. H4 correlated to the doublet of triplets at 4.39 ppm which lead to its assignment as H5. The only other coupling partner of H5 was the multiplet at 3.75 ppm, integrating to 2H, which was assigned as the overlapping signals of H6a and H6b. The $^{13}C\{^{1}H\}$ NMR spectrum (Appendix C) was assigned (see Chapter 5.8) with the help

of an HSQC spectrum. An HMBC spectrum demonstrated the correlation between the lactone carbon (C1, 168 ppm) and H2, confirming the formation of the desired gluconolactone **16**. The ESI+ high resolution mass spectrum (Appendix D) corroborated this when a *m/z* of 473.1719 corresponding to [**16**+Na]$^+$ was found.

The $^{31}P\{^1H\}$ (Figure 36A) and $^{19}F\{^1H\}$ (Figure 36B) NMR spectra of **17** each indicated the formation of a single new species. In the $^{19}F\{^1H\}$ NMR spectrum, a doublet at -192.2 ppm was observed, having a coupling constant of 4.1 Hz, due to five-bond coupling with phosphorus. In the $^{31}P\{^1H\}$ NMR spectrum, the minor peak at 31.6 ppm was caused by residual dimethyl methylphosphonate and the major peak, an apparent singlet at 30.7 ppm, was caused by the product. Although the $^{31}P\{^1H\}$ product peak appeared as a singlet, it should in fact be a doublet, due to coupling with fluorine, however, the line width of the $^{31}P\{^1H\}$ peak was broader than the P-F coupling constant of 4.1 Hz, so the splitting pattern was not observed. The ^1H NMR spectrum (Figure 36C) indicated the formation of the desired product. The hydroxyl group on the anomeric carbon was observed as a singlet at 5.81 ppm, which was consistent with the anomeric hydroxyl chemical shift in the NMR spectrum of a similar compound.[37] The doublets at 3.68 and 3.65 ppm, integrating to three protons each, were identified as the two methoxy substituents bound to the phosphorus. The doublet of doublets at 2.46 ppm and 1.78 ppm were assigned as H1'a and H1'b, which was also consistent with the aforementioned literature spectrum. The COSY spectrum along with the ^1H NMR spectrum were used to assign the carbohydrate signals, starting with the doublet of triplets produced by H3 at 5.11 ppm. From here, correlations to H2 (doublet of doublets at 3.36 ppm) and H4 (multiplet at 3.80 ppm) were observed. The H5 (multiplet at 4.07 ppm) was assigned based on its COSY correlation to H4. COSY

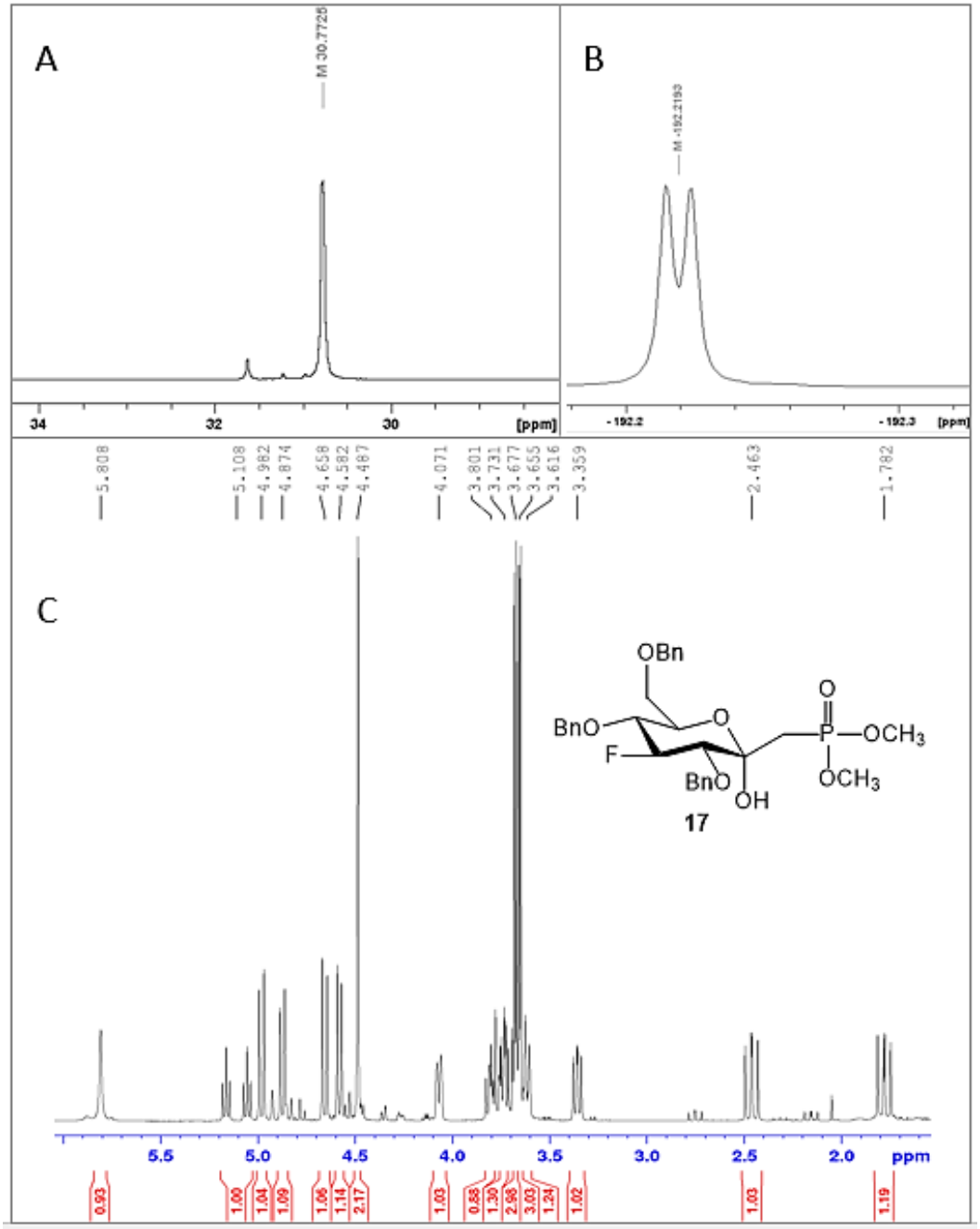

Figure 36. NMR spectra of 1-(dimethyl phosphonatylmethyl)-2,4,6-tri-*O*-benzyl-3-deoxy-3-fluoro-α-D-glucopyranose (**17**). **A)** $^{31}P\{^{1}H\}$ (202 MHz, $CDCl_3$), **B)** $^{19}F\{^{1}H\}$ (470 MHz, $CDCl_3$), **C)** ^{1}H (500 MHz, $CDCl_3$).

correlations to H6a and H6b were not observed, however, the HSQC spectrum indicated that the peaks at 3.73 and 3.61 ppm corresponded to CH_2 protons on the same carbon, so these were assigned as the diastereotopic H6 protons. The $^{13}C\{^{1}H\}$ NMR spectrum

(Appendix C) was consistent with the identification of the product as **17** (assignment in Chapter 5.8). The ESI+ high resolution mass spectrum (Appendix D) confirmed that **17** had been formed when the *m/z* of 597.2017, corresponding to [**17**+Na]$^+$ was found.

Compound **18** was characterized using $^{31}P\{^1H\}$ and $^{19}F\{^1H\}$ NMR as well as LRMS. The $^{31}P\{^1H\}$ (Figure 37A) and $^{19}F\{^1H\}$ (Figure 37B) NMR spectra of **18** each indicated the formation of a new species as well as complete consumption of the starting material. The low resolution ESI+ mass spectrum (Appendix D) found the appropriate mass for the oxalate ester **18** plus sodium, *m/z* = 683.2, as the major species. Due to instability observed for similar oxalate esters during column chromatography, the crude **18** was subjected to the next reaction without further purification or characterization.

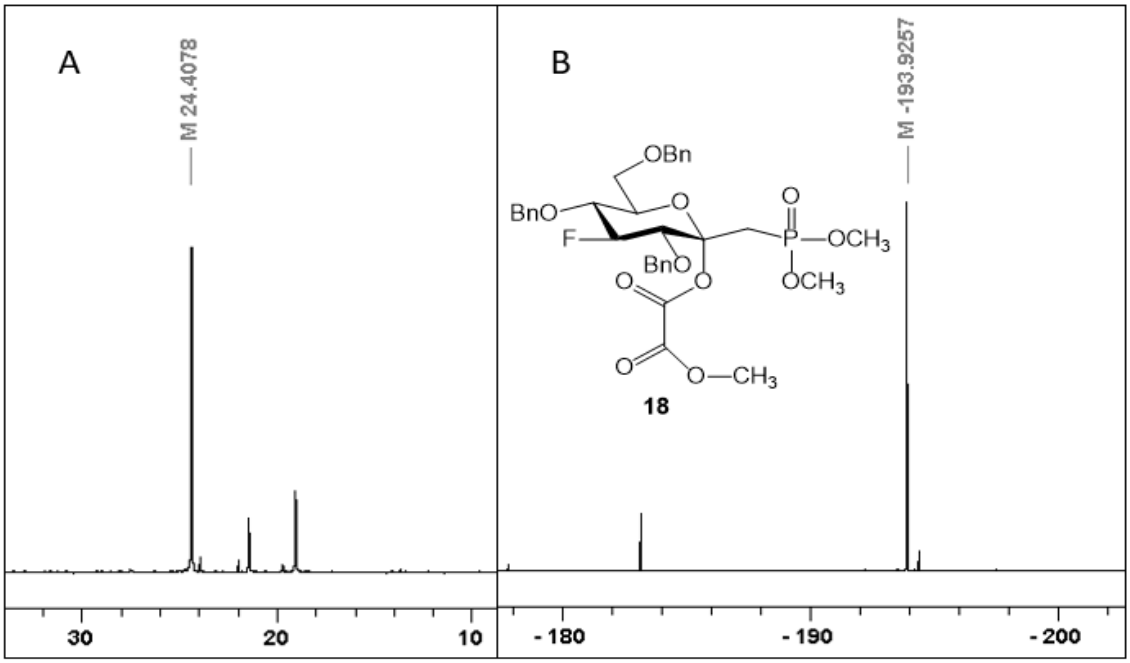

Figure 37. NMR spectra of (methyl oxalyl) 1-(dimethyl phosphonatylmethyl)-2,4,6-tri-*O*-benzyl-3-deoxy-3-fluoro-α-D-glucopyranose (**18**). **A)** $^{31}P\{^1H\}$ (202 MHz, $CDCl_3$), **B)** $^{19}F\{^1H\}$ (470 MHz, $CDCl_3$).

A single species was indicated by the appearance of one new signal in each the $^{31}P\{^1H\}$ and $^{19}F\{^1H\}$ NMR spectra of **19** (Figure 38A and 38B, respectively). The ^1H NMR

spectrum (Figure 38C) indicated that the double bond between C1 and C1' had been formed by the appearance of a doublet of doublets at 5.57 ppm, a signal caused by the alkenyl proton H1. A lack of protons on C1 was corroborated by the fact that the H2 signal, at 5.17 ppm, was merely split into a doublet as the sole neighbouring proton was H3. The doublet of triplets at 4.99 ppm was assigned as H3 as its coupling constant of 46.9 Hz was indicative of positioning geminal to the fluorine. COSY correlation lead to the identification of H4 as the doublet of doublet of doublets at 3.90 ppm. This signal in turn correlated to H5, a multiplet at 4.60 ppm which overlapped with the methylene signals. The two phosphorus-bound methoxy groups produced doublets, integrating to 3H each, at 3.75 and 3.72 ppm, both with $^{2}J_{H\text{-}P}$= 11.4 Hz. H6a was identified as the doublet at 3.80 ppm, next to the $P(OCH_3)_2$ peaks, while H6b overlapped with the aforementioned peaks (at 3.72 ppm). Although the H6b signal was somewhat obscured, the geminal coupling constant of the diastereotopic protons was clearly observed in the H6a signal as $^{2}J_{H6a\text{-}H6b}$= 11.3 Hz. The $^{13}C\{^{1}H\}$ NMR spectrum (Appendix C) was also assigned (see Chapter 5.8), using the HSQC and HMBC spectra, confirming the proposed structure. Finally, a high resolution spectrum mass (ESI+) was obtained (Appendix D), where the *m/z* for **19** plus sodium (597.1906) was found. Where a single set of signals was observed in the ^{1}H NMR as well as a single signal in each of the heteroatom NMR spectra, it can be concluded that a single either E or Z isomer of **19** was formed. However, the geometry about the double bond was not determined as the same coupling constant between H1 and P would be expected for both isomers, nor is there a literature spectrum with which to compare the chemical shifts of E versus Z isomers.

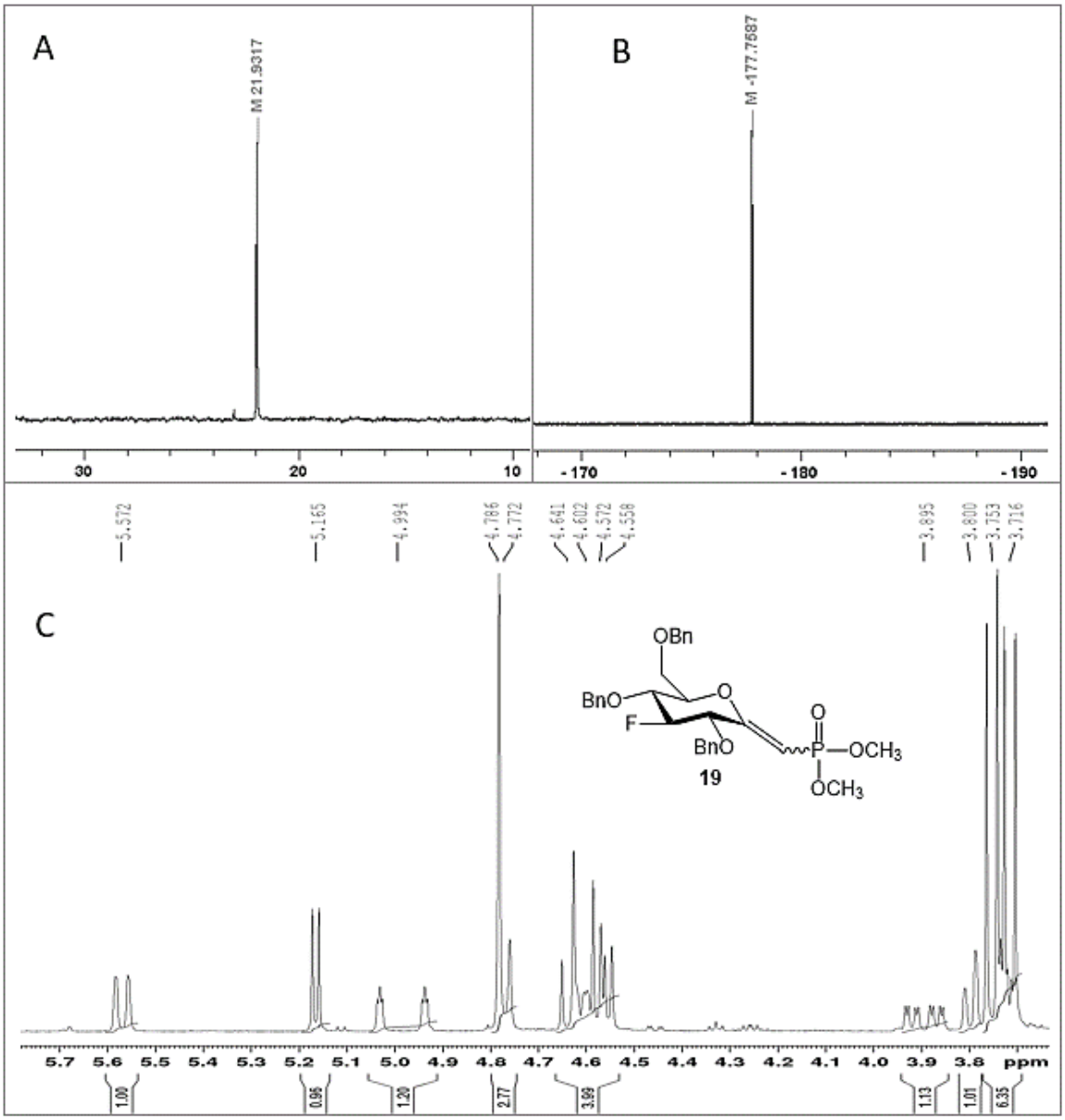

Figure 38. NMR spectra of (E/Z)-1-(dimethylphosphonomethylene)-2,4,6-tri-*O*-benzyl-1,3-deoxy-3-fluoro-D-glucopyranosyl-2-ylidene (**19**). **A)** $^{31}P\{^{1}H\}$ (202 MHz, $CDCl_3$), **B)** $^{19}F\{^{1}H\}$ (470 MHz, $CDCl_3$), **C)** ^{1}H (500 MHz, $CDCl_3$).

20 was not isolated as a pure compound, but rather as a mixture with **19**. This was indicated by the ESI+ high resolution mass spectrum (Appendix D) where *m/z*= 581.2063 and 579.1920 were found, corresponding to **20** plus sodium and **19** plus sodium, respectively. In the $^{31}P\{^{1}H\}$ NMR spectrum, a new signal (which was assigned as **20**) was observed at 31.0 ppm as well as the known signal for **19** at 21.9 ppm (Figure 39A and

Appendix E). The $^{19}F\{^{1}H\}$ NMR spectrum also displayed the signal for **19**, at -177.7 ppm and a new signal at -185.3 ppm, which was assigned as **20** (Figure 39B and Appendix A). In the ^{1}H NMR spectrum of the **19**/**20** mixture (Figure 39C) the doublet of doublets at 5.57 ppm, corresponding to the alkenyl proton of **19** had decreased in size (compared to the spectrum of pure **19**, Figure 38C), integrating to only 0.24 H. Two new signals (both ddd) at 2.33 and 1.92 ppm, integrating to 1 H each, were identified as the diastereotopic CH_2-P protons of **20**. These two protons demonstrated COSY correlations to each other and to the P-OCH_3 signals at 3.66 ppm. The presence of these distinctive protons confirmed that both **19** and **20** were present in this mixture. Comparing the integrations of the **20** C<u>H</u>-P signal at 1.92 ppm and the **19** =C<u>H</u>-P signal at 5.57 ppm, it was concluded that **20** and **19** were present in a 4:1 ratio. This differs from the ratio reported in the synthesis of the non-fluorinated versions of **19** and **20** (having a hydroxyl group at C3 instead of F), using triethylsilane reduction, where the quantity of saturated compound produced was greater than the quantity of unsaturated compound (reported ratios varied from 1:8 to 1:30, unsaturated: saturated).[37,55] This indicates that either fluorination at C3 affects the reactivity at the C1 and C1' positions to favor formation of the unsaturated compound or that the preference for unsaturated compound is a result of using different reaction conditions than in the literature.

The $^{31}P\{^{1}H\}$ and $^{19}F\{^{1}H\}$ NMR spectra of **21** each indicated the presence of a single new species, with signals at 21.3 and -192.8, respectively (Figures 40A and 40B, respectively). The high resolution mass spectrum (ESI-) displayed the expected peak for **21** minus a proton, *m/z*= 259.0377 (Appendix D). The ^{1}H NMR spectrum of **21** (Figure 40C) was assigned with the help of COSY and HSQC spectra. The H1'a and H1'b signals

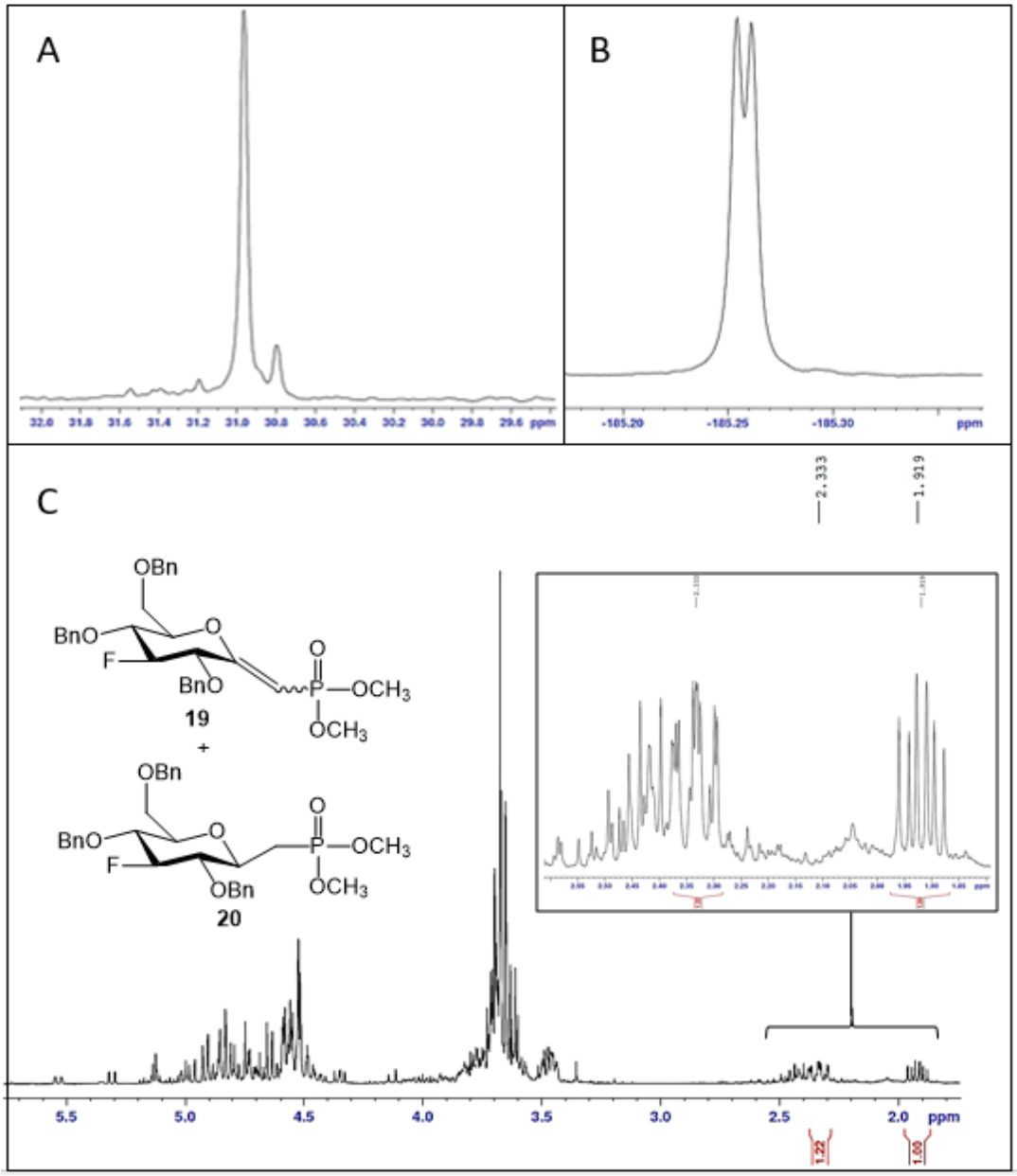

Figure 39. NMR spectra of (E/Z)-1-(dimethylphosphonomethylene)-2,4,6-tri-*O*-benzyl-1,3-deoxy-3-fluoro-D-glucopyranosyl-2-ylidene (**19**) and 2,4,6-tri-*O*-benzyl-3-deoxy-3-fluoro-β-D-glucopyranosylmethylphosphonate (**20**) mixture; relevant signals of **20** have been picked**. A)** $^{31}P\{^{1}H\}$ (202 MHz, $CDCl_3$), **B)** $^{19}F\{^{1}H\}$ (470 MHz, $CDCl_3$), **C)** ^{1}H (500 MHz, $CDCl_3$).

were easily identified as those at 2.23 and 1.90 ppm since they appeared furthest upfield and correlated to each other. The signal at 4.47 ppm was assigned as H3 as it was a doublet of triplets including a coupling constant of 53.3 Hz, indicative of geminal coupling with

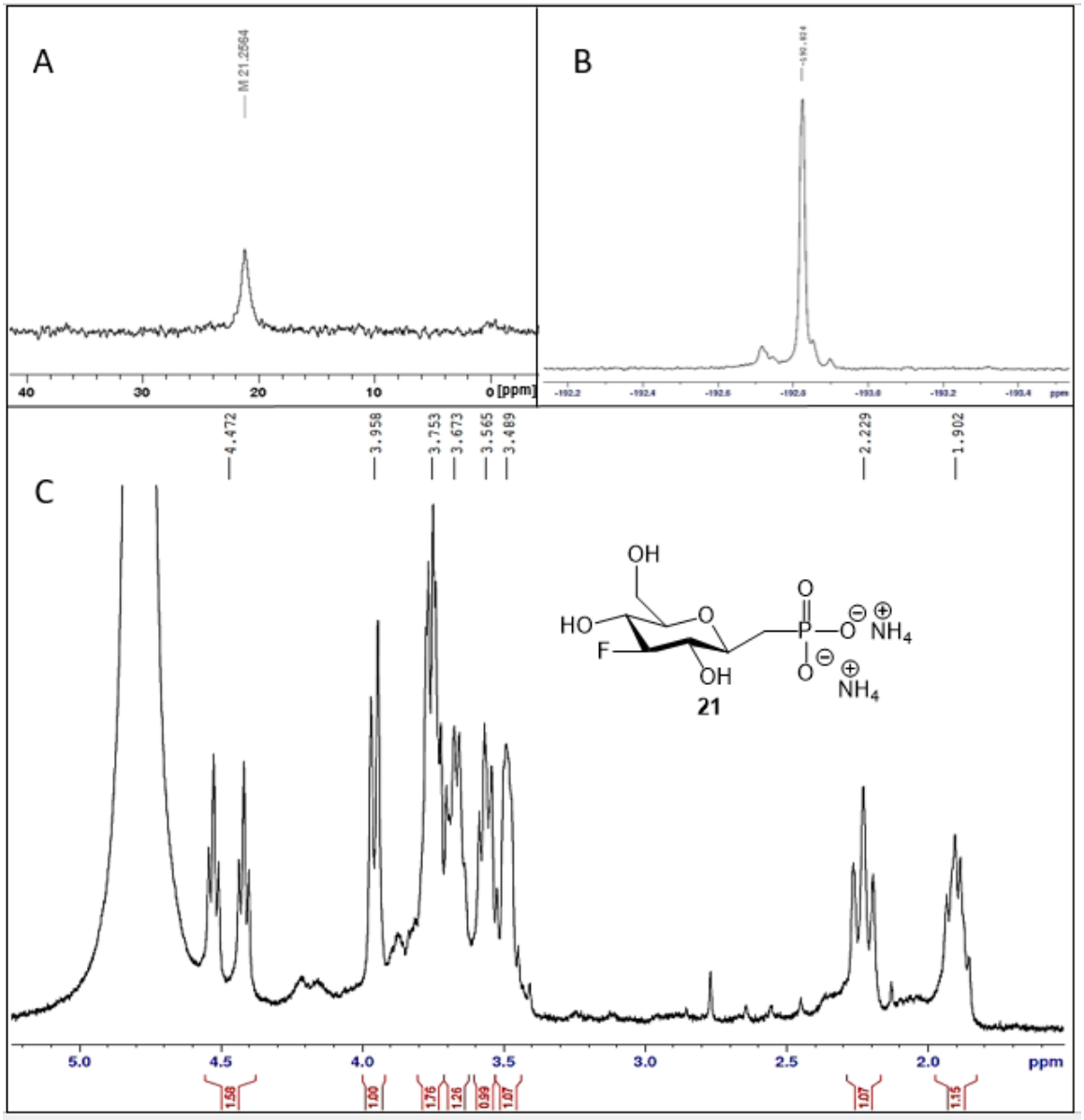

Figure 40. NMR spectra of diammonium 3-deoxy-3-fluoro-β-D-glucopyranosylmethylphosphonate (**21**). **A)** $^{31}P\{^{1}H\}$ (202 MHz, $CDCl_3$), **B)** $^{19}F\{^{1}H\}$ (470 MHz, $CDCl_3$), **C)** ^{1}H (500 MHz, $CDCl_3$).

fluorine. H3 correlated to a multiplet, integrating to 2 H, at 3.75 ppm as well as the 1 H multiplet at 3.57 ppm, indicating that these were the signals for H2 and H4. H5 was identified as the signal at 3.49 ppm based on its high multiplicity and it being the signal furthest upfield in the carbohydrate region. The signal at 3.75 ppm correlated to to H5 as well as back to H3, leading to its assignment as H4. This also lead to the conclusion that

the signal at 3.57 ppm must belong to H2. H2 in turn appeared to correlate to the neighbouring signal at 3.67 ppm, integrating to 1 H, leading to the assignment of this signal as H1. The doublet at 3.96 ppm ($^{2}J_{H\text{-}H}$= 12.0 Hz) was assigned as H6a as the coupling constant was typical of geminal coupling between diastereotopic protons. H6a displayed a COSY correlation to the 2 H multiplet at 3.75 ppm, leading to the assignment of the second proton in this multiplet as H6b. This assignment was also consistent with the fact that the 3.75 ppm multiplet correlated to H5. HSQC confirmed that the signals at 3.75 ppm and 3.96 ppm belonged to CH_2 protons on the same carbon. The $^{13}C\{^{1}H\}$ NMR spectrum was also fully assigned (Appendix C), using HSQC. The C1' signal was not visible in the $^{13}C\{^{1}H\}$ NMR spectrum, however it was identified as having a chemical shift of 31.1 ppm based on the HSQC correlations of H1'a and H1'b (2.23 and 1.90 ppm) on the x-axis with 31.1 ppm on the y-axis (Appendix F).

The new potential βPGM substrate **21** was successfully synthesized in twelve steps. **21** will be kinetically evaluated for its ability to inhibit W216F 5FWβPGM-His and a crystal structure of the **21**-W216F 5FWβPGM-His complex will be acquired. **21** can also be used in the ^{19}F NMR-monitored TSA complexation study where we anticipitate it to provide greater conversion of the protein from its apo to complexed form than observed with the previous substrates.

Chapter 5. Experimental

5.1. General procedures

5.1.1. Equipment and general laboratory practices

Reactions were performed in oven-dried glassware and monitored for completion using thin layer chromatography (TLC). Reactions under an inert atmosphere were conducted using nitrogen gas. Glass-backed normal phase silica TLC plates (Silicycle) were visualized using UV light, *p*-anisaldehyde stain, or potassium permanganate stain. NMR spectra were obtained using Bruker AV-300 or AV-500 instruments at Dalhousie University's NMR-3 facility. For kinetic studies, a Molecular Devices Spectromax 384 UV spectrometer was used for data acquisition and Softmax® Pro Version 4.8 software was used for data analysis. High resolution mass spectra were acquired by Xiao Feng on the Bruker microTOF Focus Mass Spectrometer, using an ESI+ or ESI- source, at Dalhousie University's mass spectrometry laboratory.

5.1.2. Plasmid isolation

The Bio Basic Inc. EZ-10 Spin Column MiniPrep kit was used for plasmid isolation, following the procedure detailed in the enclosed brochure. Before beginning the plasmid isolation procedure, RNAse A solution (240 μL) was added to Solution I (12 mL) and ethanol (160 mL) was added to Solution III (40 mL). 1.5-2 mL samples of overnight *E. coli* harbouring the plasmid of interest were centrifuged (2 minutes, 12,000 rpm). The supernatant was discarded and the cell pellets were taken up in Solution I (100 μL), mixed, and held at room temperature for 1 minute. VisualLyse (1 μL) was added to the mixture. Solution II (200 μL) was added and the tube gently inverted 4-6 times to mix, turning the

mixture a homogenous blue. The mixture was allowed to sit for 1 minute before adding Solution III (350 µL) and gently mixing. The mixture was let sit 1 minute, after which the solution became clear and colourless with fluffy white precipitate at the bottom of the tube. The tube was centrifuged (5 minutes, 12,000 rpm) and the supernatant transferred to an EZ-10 column which was centrifuged again (2 minutes, 10,000 rpm). The flow-through was removed, Wash Solution (750 µL) was applied to the column, and the column was centrifuged (2 minutes, 10,000 rpm). The wash step was then repeated a second time. The flow-through was discarded and the column was centrifuged (1 minute, 10,000 rpm). The column was transferred to a new 1.5 mL microcentrifuge tube. Elution buffer (50 µL) was applied to the centre of the column and kept at room temperature for 2 minutes before centrifuging (2 minutes, 10,000 rpm). The flow-through containing the purified plasmid was then stored at -20ºC.

5.1.3. Agarose gel electrophoresis (1%)

Agarose (300 mg) and TAE buffer (1X, 30 mL) were combined and heated until all the agarose was dissolved. Once cooled to just above room temperature, the agarose solution was poured into the gel template. The gel was allowed to set 20 minutes before removing the ladder. Samples were prepared by adding 2 µL purple gel loading dye (6x, NEB) to each 10 µL DNA sample. Samples (12 µL) and 1 kb DNA ladder (2.5 µL, NEB) were added to the wells. The gel was run in TAE buffer (1X) with ethidium bromide (30 µg) with an applied voltage of 120 V for 30-40 minutes. The gel was visualized using UV light.

5.1.4. Sodium dodecyl sulfide polyacrylamide gel electrophoresis (SDS-PAGE)

The SDS-gel was composed of a resolving solution and a stacking solution. The resolving solution was made by combining sterile distilled deionized water (ddH_2O, 1.24 mL),

resolving buffer (1.37 mL, 1.5 M Tris·HCl, pH = 8.8), acrylamide solution (2.75 mL, 30% acrylamide, 0.8% bisacrylamide), sodium dodecyl sulfate (SDS, 27.5 μL, 20% w/v), ammonium persulfate (APS, 110 μL, 10%), and tetramethylethylenediamine (TEMED, 6 μL). The resolving solution was added to the template, covered with isopropanol, and allowed to set. The stacking solution was made by combining ddH_2O (1.11 mL), stacking buffer (500 μL, 0.5 M Tris·HCl, pH = 6.8), acrylamide solution (340 μL), SDS (10 μL, 20%), APS (60 μL, 10%), and TEMED (6.5 μL). The isopropanol was drained off and the stacking solution was added to the template on top of the solidified resolving solution. The plastic comb was placed in the stacking solution and it was allowed to set. Samples were prepared by adding SDS-PAGE loading dye (5 μL, 2X) to each protein sample (5 μL). The gel was removed from template and placed in the electrophoresis apparatus, immersed in SDS-PAGE running buffer (1X). Samples (10 μL each) and prestained protein ladder (3 μL, NEB, 11-250 kDa) were loaded into the wells of the gel. A voltage of 150 V was applied for one hour. The gel was visualized using protein stain (Sci-Med Inc.).

5.1.5. Cell lysis for protein purification

Cell pellets were thawed and suspended in imidazole buffer (16 mL, 25 mM). Glycerol (3 mL), Triton X (1 mL, 10% solution), lysozyme (0.5 mg/mL), and DNAse (1 μg/mL) were added to the mixture. The mixture was stirred in a bath of shaved ice for 30 minutes. The cell lysate (5 times 5s, 50% amplitude) was sonicated using a microprobe sonicator. The cell lysate was centrifuged (10 minutes, 13,000 rpm) and the supernatant was collected for further purification.

5.1.6. Nickel column stripping and recharging

A 5 mL HisTrap column (Amersham Biosciences) was used. The column was prepared for use by stripping and recharging in the following manner: The column was washed with 2-3 column volumes (c. v.) of distilled water, 3-4 c. v. of stripping buffer, 4-5 c. v. distilled water, and then 2 c. v. NaOH (1 M). The column was stored at 4ºC for 1 hour and then washed with 4-5 c. v. distilled water, 2 c. v. $NiSO_4$ (0.1 M), 4 c. v. distilled water, and 3-4 c. v. imidazole buffer (25 mM). Stored at 4ºC until use.

5.1.7. Preparation of Media and buffers

Lysogeny broth (LB)

Tryptone (10 g), NaCl (10 g), and yeast extract (5 g) were dissolved in 1 L distilled water. Adjusted the pH to 7.5 using NaOH (1 M) and autoclaved the broth.

LB agar

Agar (15 g) was added to 1 L lysogeny broth prior to autoclaving.

Minimal growth media

$NaH_2PO_4 \cdot 2H_2O$ (15.6 g/L) and $K_2HPO_4 \cdot 3H_2O$ (7.9 g/L) were added to 1 L distilled water. The pH was adjusted to 7.3 using NaOH (1 M) and the media was autoclaved. The following components were added in the form of filter-sterilized solutions (made with distilled deionized water) to the 1 L of media before use: NH_4Cl (1 g), glucose (2 g), $MgSO_4$ (4 mmol), and $FeSO_4$ (1.8 μmol).

NZY^+ broth

Casein hydrolysate (NZ amine, 1 g), yeast extract (0.5 g), and NaCl (0.5 g) were dissolved in 100 mL distilled deionized water. The pH was adjusted to 7.5 by adding NaOH (1 M) and the broth autoclaved. The following solutions were made in distilled deionized water,

filter-sterilized, and added to the broth before use: $MgCl_2$ (1.25 mL of 1M), $MgSO_4$ (1.25 mL of 1M), and glucose (2.0 mL of 20% w/v).

Imidazole buffer (25 mM)

NaCl (300 mM), Tris base (20 mM), and imidazole (25 mM) were dissolved in 500 mL distilled water. The pH was adjusted to 8.0 by adding HCl (1 M) and the buffer was filter-sterilized.

Imidazole buffer (250 mM, 500 mL)

NaCl (300 mM), Tris base (20 mM), and imidazole (250 mM) were dissolved in 500 mL distilled water. The pH was adjusted to 8.0 by adding HCl (1 M) and the buffer was filter-sterilized.

HEPES buffer (50 mM)

4-(2-hydroxyethyl)-1-piperazineethanesulfonic acid (HEPES, 1.1915 g) was dissolved in 100 mL distilled water. Adjusted the pH to 7.2 by adding NaOH (1 M) and autoclaved the buffer.

Phosphate buffered saline (PBS, 500 mM)

$NaH_2PO_4 \cdot 2H_2O$ (7.80 g/ 100 mL) and NaCl (8.48 g/100 mL) were dissolved in 100 mL distilled water. The pH was adjusted to 7.6 by adding HCl (1 M) and the buffer autoclaved.

TAE buffer (1X)

Tris-acetate (40 mM) and EDTA (1 mM) were combined in distilled water. The pH should be 8.2.

SDS-PAGE loading dye (2X)

Tris·HCl (20 mM, pH = 6.8, 10 mL), glycerol (3 mL), β-mercaptoethanol (15 mL), and bromophenol blue (1.8 g) were added to 100 mL distilled deionized water.

SDS-PAGE running buffer (10X)

Sodium dodecyl sulfate (10 g/L), Tris (30 g/L), and glycine (144.1 g/L) were dissolved in distilled water.

Stripping buffer

Na_3PO_4 (20 mM), NaCl (0.5 M), and EDTA (50 mM) were combined in distilled water. The pH was adjusted to 7.4 by adding HCl (1 M) and the buffer was filter-sterilized.

5.2. Overexpression and purification of DesR, EryBI, and Hsero1941 enzymes

The overexpression and purification procedure for EryBI is described, following a reported procedure used for DesR.[7] The overexpression and purification of DesR and Hsero1941 were conducted in a similar manner.

LB_{kan} (LB containing 50 μg/mL kanamycin, 25 mL) was inoculated with EryBI glycerol stock (25 μL). This was grown overnight at 37°C with shaking (250 rpm). Then, the culture (3 x 3 mL) was used to inoculate flasks of LB_{kan} (3 x 300 mL). These were incubated at 37°C with shaking until OD_{600} = 0.6-0.8. A "before IPTG sample" (500 μL aliquot) was taken out and centrifuged, collecting the cell pellet and storing it at -20°C. Isopropyl β-D-1-thiogalactopyranoside (IPTG, 1 mM) was added to the flasks and they were incubated at 17°C with shaking overnight. The next day, an "after IPTG" (148.0 μL aliquot) was removed and centrifuged, collecting and freezing the cell pellet. The contents of the flasks were centrifuged (3700 rpm, 1 hour), supernatant discarded, and cell pellets stored at -70 °C. The "before IPTG" and "after IPTG" samples were prepared for SDS-PAGE according to the general procedure and heated to 95°C for 10 minutes. SDS-PAGE was run following the general procedure (see Chapter 4.1.4). The cell pellets were lysed following the general procedure (see Chapter 4.1.5). A "before nickel column" aliquot of

the supernatant (20 μL) was taken and stored at -20ºC, while the remaining supernatant was loaded onto the (stripped and recharged) nickel column. An "after nickel column" aliquot of the flow-through (20 μL) was collected and stored at -20ºC. The nickel column (5 mL His-Trap column, Amersham Biosciences) was stripped and recharged in the manner described in Chapter 5.1.6. The column was run using Fast Protein Liquid Chromatography with an Amersham Biosciences GE AKTA Purifier 10 (at 4ºC, with a flow rate of 2.5 mL/min), 1 mL fractions were collected, and potential protein-containing fractions were identified by measuring the absorbance at 280 nm. A gradient run from 99% low imidazole buffer (25 mM) and 1% high imidazole buffer (250 mM) to 100% high imidazole buffer (250 mM) was used to elute the protein. SDS-PAGE was run on the fractions and those containing the protein were combined and concentrated down to a volume of 1 mL by centrifugal filtration (5,000 x g at 4°C in a 10,000 MWCO centrifugal filter). The buffer was exchanged to 50 mM PBS (pH = 7) using a PD-10 desalting column, following the manufacturer's instructions. The concentration of protein was calculated by measuring the absorbance at 280 nm and using the Beer-Lambert Law (A= εcl) as well as the extinction coefficient, ε_{280}= 94,435 $M^{-1}cm^{-1}$.[8] 1.200 mL of 42 μM EryBI was obtained and stored at -30ºC. For DesR, ε_{280}= 79,400 $M^{-1}cm^{-1}$ led to the calculation of a 311 μM protein concentration.[7] For Hsero1941, ε_{280}= 29,700 $M^{-1}cm^{-1}$ led to the calculation of a 304 μM protein concentration.[9]

5.3. Synthesis of 2,4-dinitrophenyl 2-deoxy-2-fluoro-β-D-glucopyranose (6)

Excerpts of this section were taken from the 2016 *Carbohydr Res* paper "On the phosphorylase activity of GH3 enzymes: A β-*N*-acetylglucosaminidase from

Herbaspirillum seropedicae SmR1 and a glucosidase from *Saccharopolyspora erythraea*" by Diogo R. B. Ducatti, Madison A. Carroll, and David L. Jakeman.[9]

2-deoxy-2-fluoro-3,4,6-tri-*O*-acetyl-D-manno/glucopyranose (**2**)

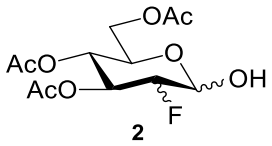

2

Compound **2**[29] was synthesized by dissolving tri-*O*-acetyl glucal **1** (7.75 mmol, 2.00 g) and Selectfluor® (1.2 eq, 9.29 mmol, 3.30 g) in acetone: water (1:1, 50 mL). The reaction mixture was stirred for 22 hours at room temperature. The solvent was removed *in vacuo*. The resulting residue was taken up in CH_2Cl_2 (25 mL) and washed with $NaHCO_3$ (sat. aq, 25 mL). A second portion of CH_2Cl_2 (25 mL) was added to the aqueous layer and extracted. The two organic phases were combined and dried using $MgSO_4$. Then, the solvent was removed *in vacuo*. R_f (hexanes: ethyl acetate 3:1) = 0.1. $^{19}F\{^1H\}$ NMR (470 MHz, $CDCl_3$) δ= -201.0, -202.4, -204.0, -219.7. A mixture of four diastereomers of 2-deoxy-2-fluoro-3,4,6-tri-*O*-acetyl-D-manno/glucopyranose was obtained (1.49 g) and subjected to the next reaction without further purification.

1,3,4,6-tetra-*O*-acetyl-2-deoxy-2-fluoro-D-glucopyranose (**3**)

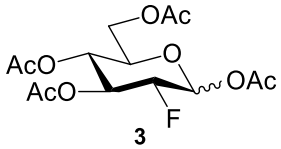

3

Compound **3**[29] was synthesized in the following manner: compound **2** (4.82 mmol, 1.49 g) was dissolved in pyridine (20 mL). DMAP (0.1 eq, 0.48 mmol, 59 mg) was added and the flask was placed under an inert atmosphere. Acetic anhydride (4 eq., 19.3 mmol, 1.82 mL) was added and the reaction was stirred for 1.5 hours at room temperature. The reaction

mixture was diluted with CH_2Cl_2 (100 mL) and washed with $NaHCO_3$ (sat. aq, 50 mL) and brine (50 mL). The organic phase was dried with $MgSO_4$ and then concentrated *in vacuo*. The crude products were purified by silica gel column chromatography in hexanes: ethyl acetate (3:2). 1,3,4,6-tetra-*O*-acetyl-2-deoxy-2-fluoro-D-mannopyranose (632 mg, 24% over the two steps) and **3** (550 mg, 21% over the two steps) were both isolated as oils. Side-product 1,3,4,6-tetra-*O*-acetyl-2-deoxy-2-fluoro-D-mannopyranose R_f (hexanes: ethyl acetate 11:9) = 0.41. Desired product **3** R_f (hexanes: ethyl acetate 11:9) = 0.53. Characterization of the desired product, 1,3,4,6-tetra-*O*-acetyl-2-deoxy-2-fluoro-D-glucopyranose **3**: $^{19}F\{^1H\}$ NMR (470 MHz, $CDCl_3$) δ= -201.0 (β), -202.3 (α). ^1H NMR (500 MHz, $CDCl_3$) δ= 6.36 (1Hα, d, $^3J_{H1\text{-}H2}$ = 4.0 Hz, H1α), 5.76 (1Hβ, dd, $^3J_{H\text{-}F}$ = 3.1 Hz, $^3J_{H1\text{-}H2}$ = 8.0 Hz, H1β), 5.49 (1Hα, dt, $^3J_{H\text{-}H}$= 9.5 Hz, $^3J_{H\text{-}F}$ = 12.2 Hz, H3α), 5.34 (1Hβ, dt, $^3J_{H\text{-}H}$ = 9.2 Hz, $^3J_{H\text{-}F}$ = 14.4 Hz, H3β), 5.02 (1Hα + 1Hβ, overlapping t, H4α, H4β), 4.61 (1Hα, ddd, $^3J_{H2\text{-}H1}$ = 4.0 Hz, $^3J_{H2\text{-}H3}$ = 9.6 Hz, $^2J_{H\text{-}F}$ = 48.5 Hz, H2α), 4.39 (1Hβ, dt, $^3J_{H\text{-}H}$ = 8.6 Hz, $^2J_{H\text{-}F}$ = 50.7 Hz, H2β), 4.23 (1Hα + 1Hβ, m, H6α, H6β), 4.05 (2Hα + 1H β, m, H5α, H6α, H6β), 3.84 (1Hβ, m, H5β), 2.01 (12Hα + 12Hβ, m, OAc).

2-deoxy-2-fluoro-3,4,6-tri-*O*-acetyl-D-glucopyranose (**4**)

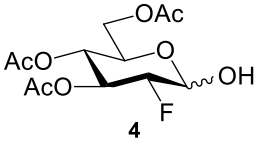

4

Compound **4**[30] was synthesized in the following manner: DMF (10 mL, anh.) and DIPEA (13.8 mmol, 2.4 mL) were added to **3** (1.57 mmol, 550 mg) and stirred until dissolution. NH_4OAc (6.28 mmol, 484 mg) was dried by prewashing with ether (50 mL, anh.), then concentrating *in vacuo* for 10 minutes. The dried NH_4OAc crystals were added to the reaction mixture and it was stirred for 24.5 hours at room temperature. It was then decanted

into a separatory funnel, leaving the NH_4OAc crystals behind. The reaction mixture was diluted with CH_2Cl_2 (300 mL) and washed with $NaHCO_3$ (sat. aq, 2 x 20 mL) and water (10 mL). The organic phase was dried using $MgSO_4$ and concentrated *in vacuo*. The product was purified using silica gel column chromatography in hexanes: acetone (7:3). The product **4** was isolated as a colourless oil (364 mg, 75%). R_f (hexanes: ethyl acetate 3:2) = 0.26. $^{19}F\{^1H\}$ NMR (470 MHz, $CDCl_3$) δ= -199.3, -199.9. ^1H NMR (500 MHz, $CDCl_3$) δ= 5.56 (1Hα, m, H3α), 5.44 (1Hα, d, $^3J_{H1-H2}$ = 3.4 Hz, H1α), 5.29 (1Hβ, m, H3β), 4.99 (1Hα + 1Hβ, m, H4α, H4β), 4.89 (1Hβ, dd, $^4J_{H1-H3}$ = 2.2 Hz, $^3J_{H1-H2}$ = 7.5 Hz, H1β), 4.48 (1Hα, ddd, $^3J_{H2-H1}$= 3.6 Hz, $^3J_{H2-H3}$= 9.6 Hz, $^2J_{H-F}$ = 49.7 Hz, H2α), 4.27 (dt, $^3J_{H-H}$ = 8.4 Hz, H2β), 4.08, 4.24 (3Hα + 2Hβ, m, H5α, H6α, H6β), 3.76 (1Hβ, m, H5β), 2.03 (9Hα + 9Hβ, m, OAc).

2,4-dinitrophenyl 2-deoxy-2-fluoro-3,4,6-tri-*O*-acetyl-D-glucopyranose (**5**)

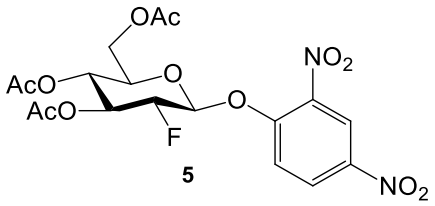

5

Compound **5**[31] was synthesized from compound **4** (1.18 mmol, 364 mg), which was dissolved in DMF (12 mL, anh.). DNFB (1.30 mmol, 163 µL) and DABCO (1.30 mmol, 146 mg) were added to the reaction mixture, which was then stirred overnight in the dark. The solvent was removed *in vacuo* and the resulting residue was taken up in ethyl acetate (20 mL). This was extracted sequentially with $NaHCO_3$ (sat. aq, 10 mL), distilled water (10 mL), and brine (10 mL). The organic phase was dried using $MgSO_4$ and then concentrated *in vacuo*. The product was purified using silica gel column chromatography in hexanes: ethyl acetate (3:2). Primarily β-configured (9β: 2α) 2,4-dinitrophenyl 2-deoxy-

2-fluoro-3,4,6-tri-O-acetyl-D-glucopyranose (**5**) was isolated as a pale yellow solid (291 mg, 52%). $^{19}F\{^{1}H\}$ NMR (470 MHz, $CDCl_3$) δ= -198.7(β), -201.7 (α). ^{1}H NMR (500 MHz, $CDCl_3$) δ= 8.82 (1Hα, m, H3'α), 8.75 (1Hβ, m, H3'β), 8.46 (1Hα + 1Hβ, m, H5'α, H5'β), 7.54 (1Hα, d, $^{3}J_{H6'-H5'}$ = 9.2 Hz, H6'α), 7.45 (1Hβ, d, $^{3}J_{H6'-H5'}$ = 9.4 Hz, H6'β), 6.03 (1Hα, d, $^{3}J_{H1-H2}$= 3.6 Hz, H1α), 5.73(1Hα, m, H3α), 5.48 (1Hβ, m, H1β), 5.44 (1Hβ, m, H3β), 5.16 (1Hα + 1Hβ, m, H4α, H4β), 4.85 (1Hα, m, H2α), 4.72 (1Hβ, dm, $^{2}J_{H-F}$ = 50.1 Hz, H2β), 4.15 (3Hα + 3Hβ, m, H5α, H5β, H6α, H6β), 2.05 (9Hα + 9Hβ, OAc).

2,4-dinitrophenyl 2-deoxy-2-fluoro-β-D-glucopyranose (**6**)

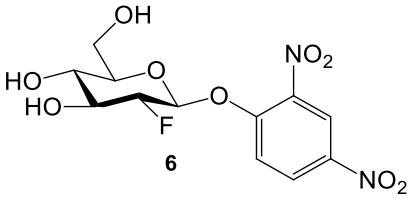

6

Compound **6**[31] was synthesized from compound **5** (0.61 mmol, 291 mg), which was suspended in methanol (8.5 mL), then cooled to 0°C. The reaction mixture was stirred while acetyl chloride (5.15 mmol, 446 µL) was added dropwise. Once the addition was complete, the reaction mixture was left at 4°C for 42 hours. The product was purified using silica gel column chromatography in ethyl acetate: methanol (19:1). Compound **6** was isolated as a pale yellow solid (198 mg, 92%). $^{19}F\{^{1}H\}$ NMR (470 MHz, CD_3OD) δ = -201.1 (β), -203.5 (α). ^{1}H NMR (500 MHz, CD_3OD) of β-configured (major): δ = 8.74 (1H, d, $^{4}J_{H3'-H5'}$ = 2.8 Hz, H3'), 8.50 (1H, dd, $^{4}J_{H5'-H3'}$ = 2.8 Hz, $^{3}J_{H5'-H6'}$ = 9.3 Hz, H5'), 7.67 (1H, d, $^{3}J_{H6'-H5'}$ = 9.4 Hz, H6'), 5.59 (1H, dd, $^{3}J_{H-F}$ = 2.9 Hz, $^{3}J_{H1-H2}$ = 7.5 Hz, H1), 4.37 (1H, dt, $^{2}J_{H-F}$ = 51.6 Hz, $^{3}J_{H-H}$ = 7.6 Hz, H2), 3.97 (1H, dd, $^{3}J_{H5-H6a}$ = 2.1 Hz, $^{2}J_{H6a-H6b}$ = 12.2 Hz, H6a), 3.80 (2H, m, H3, H6b), 3.67 (1H, m, H5), 3.52 (1H, t, $^{3}J_{H-H}$ = 9.5 Hz, H4).

5.4. Kinetic studies using 2,4-dinitrophenyl 2-deoxy-2-fluoro-β-D-glucopyranose and the three glycosidases

5.4.1. Inactivation studies

Inactivation of DesR

2,4-Dinitrophenyl 2-deoxy 2-fluoro-β-D-glucopyranose (**6**, 50 mM) and DesR (37 μM) were combined in PBS (50 mM, pH = 7.6, total volume 100 μL) and incubated at room temperature. A control was set up containing DesR (37 μM) in PBS without **6**. After various time intervals, an aliquot of the reaction mixtures (3 μM) and para-nitrophenyl glucopyranoside (pNP-glc, 50 mM) in PBS (50 mM, pH = 7.6, total volume 200 μL) were added to the wells of a 96-well plate. A microplate reader was used to measure time-dependent inhibition using the absorbance at 400 nm over a period of 5 minutes after the addition of pNP-glc.

Inactivation of Hsero 1941

Compound **6** (50 mM) and Hsero1941 (23 μM) were combined in HEPES buffer (50 mM, pH = 7.2, total volume 100 μL) and incubated at room temperature. A control was set up containing Hsero1941 (23 μM) in HEPES buffer without **6**. After various time intervals, an aliquot of the reaction mixtures (1.3 μM) and para-nitrophenyl *N*-acetyl-β-D-glucosaminide (pNP-GlcNAc, 1.0 μM) in HEPES buffer (50 mM, pH = 7.2, total volume 200 μL) were added to the wells of a 96-well plate. A microplate reader was used to measure time-dependent inhibition using the absorbance at 400 nm over a period of 5 minutes after the addition of pNP-GlcNAc.

Inactivation of EryBI

Compound **6** (9.12 mM) and EryBI (13.6 μM) were combined in PBS (225 mM, pH = 7.1, total volume 148 μL) and incubated at room temperature. A control was set up containing EryBI (13.6 μM) in PBS without **6**. After 2 hours, an aliquot of the reaction mixtures (0.75 μM) was added to the wells of a 96-well plate along with pNP-glc (6.25 mM) in PBS (225 mM, pH = 7.1, total volume 200 μL). A microplate reader was used to measure time-dependent inhibition using the absorbance at 400 nm over a period of 5 minutes after the addition of pNP-glc.

Purification and Quantification

After the inactivation studies, the remaining enzyme/**6** solutions were purified to remove any excess **6.** Solutions were centrifuged using Nanosep 10 K Ω filter devices (10,000 Da cut-off) and washing with the appropriate buffer (4 x 400 μL). Concentrations of purified, inactivated enzyme were determined using absorbance measurements at 280 nm, the Beer-Lambert Law (A= εcl), and the extinction coefficients of the enzymes (ε_{280}= 79,400 $M^{-1}cm^{-1}$ for DesR, ε_{280}= 28,700 $M^{-1}cm^{-1}$ for Hsero1941, and ε_{280}= 94,435 $M^{-1}cm^{-1}$ for EryBI).

5.4.2. Acceptor screening to reactivate DesR

Acceptor screening for the reactivation of DesR was conducted in the wells of a 96-well plate and absorbance was measured using a microplate reader. To each well, purified DesR/**6** solution (0.50 μM) (see Chapter 5.4.1) and a potential acceptor (15 mM) in PBS (50 mM, pH = 7.6) were added. The 96-well plate was incubated at room temperature for 3-24 hours. Then, pNP-glc (12.5 mM) was added and absorbance was measured at 400 nm

over a period of 5 minutes. Potential acceptors 1, 2, 3, 6, 11, 15, 16, 22-25, 27, 29, 30-33, 39, 40, 44, 48, 49, 50, 52, and 53 were screened (Table 4).

	Potential acceptors
1	4-nitrophenyl-β-D-mannopyranoside
2	α-D-glucose 1-phosphate, disodium salt
3	*p*-nitrophenyl-β-D-galactopyranoside
4	glucose-6-phosphate, barium salt
5	tyrosine methyl ester hydrochloride
6	lactose
7	D-galactose
8	methyl-β-D-glucopyranoside
9	galactosamine hydrochloride
10	D-glucosamine HCl
11	L-fucose
12	D-mannose
13	L-serine
14	D-glucose
15	*N*-acetyl glucosamine
16	p-nitrophenyl-β-D-glucoside
17	octyl-β-D-glucopyranoside
18	sodium azide (2M)
19	o-nitrophenyl-β-D-galactopyranoside
20	α-D-galactose 1-phosphate, dipotassium salt pentahydrate
21	xylose
22	4-nitrophenyl-β-D-glucuronide
23	kanamycin monosulfate
24	erythromycin (~2 mM)
25	clarithromycin
26	*N*-acetyl neuraminic acid
27	L-arabinose
28	PBS (500 mM, pH = 7.6)
29	β-gentiobiose
30	L-rhamnose monohydrate
31	sucrose
32	maltose monohydate
33	1,2-propanediol
34	benzyl alcohol

	Potential acceptors (continued)
35	3-methyl-1-butanol
36	*p*-methoxyphenol
37	2-hydroxy-5-nitrobenzyl alcohol
38	4-chloro-3,5-dimethyl phenol
39	sec butyl alcohol
40	p-nitrophenyl-β-D-fucoside
41	p-nitrophenyl-β-D-glucoside
42	p-nitrophenyl-β-D-mannoside
43	p-nitrophenyl-β-D-galactopyranoside
44	p-nitrophenyl-β-D-xylopyranoside
45	sodium fluoride (1M)
46	imido diphosphate
47	dibenzyl phosphate
48	hydroxylammonium chloride
49	Methoxyamine hydrochloride
50	*N*-benzyl hydroxylamine hydrochloride
51	benzyl phosphoric acid
52	cellobiose
53	L-threonine
54	*p*-nitrophenylphosphate
55	p-nitrophenyl-*N*-acetyl-β-D-glucosaminide
56	uridine 5'-diphosphate
57	uridine 5'-triphosphate

Table 4. Potential acceptors used in the reactivation studies of DesR, Hsero1941, and EryBI. Stock solutions of acceptors were 60 mM in ddH_2O unless otherwise indicated. 50 µL of stock solution was added to each reaction mixture.

5.4.3. Acceptor screening to reactivate Hsero1941

Acceptor screening for the reactivation of Hsero1941 was conducted in the wells of a 96-well plate and absorbance was measured using a microplate reader. To each well, purified Hsero1941/**6** (0.3 µM) (see Chapter 5.4.1) and a potential acceptor (15 µM) in HEPES buffer (50 mM, pH = 7.2) were added. The reaction mixtures were incubated at room temperature for 3 hours and then pNP-GlcNAc (1 mM) was added. Absorbance readings

were taken over a period of 5 minutes at 400 nm. Potential acceptors 1, 3-20, 22, 23, 26-36, 39, and 45 were screened (Table 4).

5.4.4. Acceptor screening to reactivate EryBI

Acceptor screening for the reactivation of EryBI was conducted in the wells of a 96-well plate and absorbance was measured using a microplate reader. Purified EryBI/**6** solution (0.75 μM) (see Chapter 5.4.1) and a potential acceptor (15 mM*) in PBS (225 mM, pH = 7.1) were added to each well. The reaction mixtures were incubated at room temperature for 2 hours and then pNP-glc (6.25 mM) was added. Absorbance was then measured at 400 nm for 5 minutes. Potential acceptors 1, 3-15, 17, 19-27, 29-44, 48-50, 52, 53, and 55 were screened (Table 4). *All acceptors were used with a final concentration of 15 mM with the exception of the following, which were used with a final concentration of 12.5 mM: 22, 42, 43, 52, and 55.

5.4.5. The inactivation of EryBI by erythromycin

EryBI (0.5 μM) was incubated with erythromycin (1 mM) in PBS (225 mM, pH =7.1) overnight in the wells of a 96 well-plate. An identical reaction mixture was set up, omitting the erythromycin, to be used as a control. pNP-glc (4 mM) was added to the reaction mixtures and absorbance vs time was measured at 400 nm over a period of five minutes.

5.5. Site-directed mutagenesis to make pET22b(+)_*pgmB*-His-W216F, digestion with restriction enzymes, and transformation of *E. coli*

5.5.1. Transformation of *E. coli* NEB 5α Cells with pET22b(+)_*pgmB*-His

A tube of *E. coli* NEB 5α cells (50 μL, New England Biolabs) was thawed on ice for 10 minutes. pET22b(+)_*pgmB*-His plasmid (2 μL, 40 ng/μL, prepared in the Jakeman lab previously[19]) was added to the cell mixture. The tube was flicked 4-6 times to mix and then

placed on ice for 30 minutes. The tube was heat shocked in a 42ºC water bath for 30 seconds and then placed on ice for 5 minutes. SOC media (950 µL, NEB) was added to the tube, which was then incubated at 37 ºC with shaking for 1 hour. Three concentrations of cell mixture (20 µL 10x diluted, 20 µL undiluted, and 200 µL undiluted) were plated on LB agar (containing 0.1 mg/mL ampicillin) and incubated overnight at 37 ºC. Colonies from the most dilute plate were used to inoculate flasks of LB_{Amp} (2 x 25 mL) which were then incubated overnight at 37ºC. Plasmids were isolated following the general procedure (see Chapter 5.1.2). The concentration of the plasmids was quantified using absorbance measured at 260 nm.

5.5.2. Digestion of pET22b(+)_*pgmB*-His with SacI and HindIII restriction enzymes

Double digestion was conducted by combining the restriction enzymes SacI (2 µL, 10 U/µL, Fermentas) and HindIII (1 µL, 20 U/µL, NEB) with pET22b(+)_*pgmB*-His plasmid (5 µL, 55 ng/µL), NEBuffer 2.1 (1 µL, 10X), and sterile water (1 µL). The reaction mixture was incubated for 1 hour at 37ºC. Agarose gel electrophoresis (1%) was performed on the digestion products following the general procedure (see Chapter 5.1.3).

5.5.3. Site-directed mutagenesis to make pET22b(+)_*pgmB*-His-W216F

Mutagenesis of pET22b(+)_*pgmB*-His to pET22b(+)_*pgmB*-His-W216F was conducted using Agilent Technologies' QuikChange Lightning Site-Directed Mutagenesis Kit. The reaction mixtures consisted of QuikChange Lightning Buffer (10X, 5 µL), pET22b(+)_*pgmB*-His plasmid (for reaction 1: 5 µL, 55 ng/µL and for reaction 2: 5 µL, 11 ng/µL), forward primer (1.25 µL, 100 ng/µL), reverse primer (1.25 µL, 100 ng/µL), dNTP mix (1 µL), QuikSolution reagent (1.5 µL), sterile water (34 µL), and QuikChange Lightning Enzyme (1 µL). The primers were obtained from Integrated DNA Technologies

(IDT). The forward primer used was 5'-TCG AGC TCT TTT TGC TTC TGC AGA **AAA** ACT TCT TTC AAA AAT TCT AAT GTA TAG TAT GAA-3' and the reverse primer used was 5'-TTC ATA CTA TAC ATT AGA ATT TTT GAA AGA AGT **TTT** TCT GCA GAA GCA AAA AGA GCT CGA-3' (where, the W216F mutation is in bold and the PstI mutation is underlined). The reaction mixtures were subjected to 20 cycles in a thermal cycler using the following program:

Segment	Cycles	Temperature (°C)	Time
Initial denaturation	1	95	2 min
Denaturation	18	95	20 s
Annealing		60	10 s
Extension		68	3 min
Final Extension	1	68	5 min

Table 5. Mutagenesis reaction thermal cycling program

After thermal cycling, the restriction enzyme *DpnI* (2 µL) was added to each reaction mixture and mixed by pipetting the solution up and down. The reaction mixture was briefly centrifuged and then incubated at 37°C for 5 minutes.

A control mutagenesis reaction was also conducted using reagents from the QuikChange Lightning kit. It contained QuikChange Lightning Buffer (10X, 5 µL), pWhitescript 4.5-kb control plasmid (5 µL, 5 ng/µL), oligonucleotide control primer #1 (1.25 µL, 100 ng/µL), oligonucleotide control primer #2 (1.25 µL, 100 ng/µL), dNTP mix (1 µL), QuikSolution reagent (1.5 µL), sterile water (34 µL), and QuikChange Lightning Enzyme (1 µL). The same thermal cycling program was used for the control except for the extension time was reduced to 2.5 minutes. Digestion with *DpnI* was conducted in the same manner.

5.5.4. Transformation of XL10-Gold Ultracompetent Cells with pET22b(+)_*pgmB*-His-W216F

A tube of XL10-Gold ultracompetent cells (135 µL, Agilent Technologies) was thawed on ice for 20 minutes. The competent cells (45 µL aliquots) were transferred to pre-chilled 1.5 mL microcentrifuge tubes. β-mercaptoethanol (2 µL) was added to each tube and gently mixed. The tubes were incubated on ice for 2 minutes. The *DpnI*-treated DNA (2 µL, from Chapter 5.5.3) was added to the mixture, which was gently mixed and then incubated on ice for 30 minutes. A transformation control was also performed where pUC18 control plasmid (1 µL, 0.01 ng/µL, Agilent Technologies) was added to an aliquot of competent cells in place of the *DpnI*-treated DNA. After the 30 minutes on ice, the tubes were heat shocked in a 42°C water bath for 30 seconds and then placed on ice for another 2 minutes. NZY^+ broth was preheated to 42°C and added to the tubes (0.5 mL each). The tubes were incubated at 37°C for 1 hour. The mutagenesis control (10 µL) and the transformation control (2.5 µL) were plated on LB_{Amp} agar containing 5-bromo-4-chloro-3-indolyl-β-D-galactopyranoside (X-gal, 80 µg/mL) and isopropyl β-D-1-thiogalactopyranoside (IPTG, 20 mM). The cell mixtures containing pET22b(+)_*pgmB*-His-W216F were plated on LB_{Amp} agar in four concentrations (20 µL 5x diluted, 200 µL 5x diluted, 20 µL undiluted, and 200 µL undiluted). The plates were incubated at 37°C overnight. Colonies from the plates were used to inoculate flasks of LB_{Amp} (2 x 25 mL) which were then incubated at 37 °C overnight. Plasmids were isolated following the general procedure (see Chapter 5.1.2). Concentration was quantified using absorbance measured at 260 nm.

5.5.5. Digestion of pET22b(+)_*pgmB*-His-W216F with PstI restriction enzyme

The digestion was conducted by combining the restriction enzyme PstI (1 µL, 10 U/µL, Fermentas), the pET22b(+)_*pgmB*-His-W216F plasmids (5 µL, 101-161 ng/µL), Buffer 0 (1 µL, 10X, Fermentas), and sterile water (3 µL). The reaction mixtures were incubated for 1 hour at 37ºC. Agarose gel electrophoresis (1%) was performed on the digestion products following the general procedure (see Chapter 5.1.3).

5.5.6. DNA Sequencing

Samples of pET22b(+)_*pgmB*-His and pET22b(+)_*pgmB*-His-W216F plasmids (10 µL each, 100-161 ng/µL) were sent to the NAPS Unit at the University of British Colombia for Sanger sequencing.

5.5.7. Preparation of *E. coli* BL21 (DE3) competent cells

E. coli BL21 (DE3) was grown overnight in LB (25 mL) supplemented with kanamycin (25 µg/mL) and chloramphenicol (25 µg/mL). This culture (1 mL) was then used to inoculate LB (25 mL) supplemented with $MgCl_2$ (20 mM). This was incubated at 37ºC with shaking (250 rpm) until OD_{600}= 0.4-0.6, followed by incubation on ice for 10 minutes. The culture was transferred to a pre-chilled centrifuge tube (Falcon, 50 mL) and centrifuged for 10 minutes (4ºC, 4000 rpm). The supernatant was discarded, whereas the pellet was taken up in cold $CaCl_2$ (10 mL, 0.1 M) and gently mixed. The tube was centrifuged for 10 minutes (4ºC, 4000 rpm) and the supernatant once again discarded. The pellet was again taken up in in cold $CaCl_2$ (10 mL, 0.1 M), gently mixed, and incubated on ice for 20 minutes. The tube was centrifuged for 10 minutes (4ºC, 4000 rpm) and the supernatant discarded. The pellet was taken up in $CaCl_2$ (5 mL, 0.1 M) and gently mixed. Aliquots of this solution (20 x 50 µL) were added to centrifuge tubes (20 x 1.5 mL)

containing sterile glycerol (20 x 50 µL) which had been pre-chilled to -30ºC. The solution was gently mixed with the glycerol by pipetting. The aliquots (20 x 100 µL) of *E. coli* BL21 (DE3) competent cells were then stored at -70ºC.

5.5.8. Transformation of *E. coli* BL21 (DE3) Competent Cells with pET22b(+)_*pgmB*-His-W216F

A tube of *E. coli* BL21 (DE3) competent cells (100 µL) was thawed on ice (for 15 minutes). pET22b(+)_*pgmB*-His-W216F plasmid (2 µL) was added to the tube and the mixture was incubated on ice for 30 minutes. The tube was heat shocked at 42ºC for 90 seconds and then incubated on ice for 2 minutes. LB (500 µL) was added to the mixture and then incubated at 37ºC for 1 hour. Aliquots of the cell mixture (2 µL, 20 µL, and 200 µL) were then plated onto LB_{Amp} agar. Plates were grown at 37ºC overnight. A single colony was used to inoculate LB_{Amp} (25 mL). The culture was grown overnight at 37ºC and then plasmids were isolated following the general procedure (see Chapter 5.1.2). Plasmid digestion with SacI and HindIII as well as plasmid digestion with PstI were conducted following the previously described procedures (see Chapters 5.5.2 and 5.5.5).

5.6. Overexpression and purification of W216F 5FWβPGM-His

Glycerol stocks were made for use in future protein productions by combining aliquots of the *E.coli* overnight culture from Chapter 5.5.8. with sterile glycerol in a 1:1 ratio. *E. coli* BL21 DE3-pET22b_*pgmB*-His-W216F from a glycerol stock (25 µL) was incubated overnight at 37ºC in LB_{Amp} (25 mL). This overnight culture (3 x 3 mL) was added to flasks of LB_{Amp} (3 x 330 mL) and incubated at 37ºC until OD_{600} = 0.6-0.8. Cultures were then centrifuged (10 minutes, 3750 rpm) to pellet the cells. The supernatant was discarded and the cell pellets were taken up in minimal media (3 flasks x 330 mL). The flasks were incubated at 37ºC for 30 minutes. An aliquot (500 µL) was taken out as a "before IPTG"

sample. Glyphosate (1 mL, 0.33 g/mL), L-phenylalanine (1 mL, 19.8 mg/mL), 5-fluorotryptophan (1 mL, 39.6 mg/mL), tyrosine (19.8 mg), and IPTG (330 µL, 1 M) were added to each flask. Incubated flasks at 20 ºC overnight. Took out an "after IPTG" sample (500 µL) the next day. The contents of the flasks were centrifuged (3700 rpm, 1 hour), the supernatant discarded, and the cell pellets stored at -70 ºC. The "before IPTG" and "after IPTG" samples were prepared for SDS-PAGE according to the general procedure and heated at 95ºC for 10 minutes. SDS-PAGE was run following the general procedure (see Chapter 5.1.4). The cells pellets were lysed following the general procedure (see Chapter 5.1.5). A "before nickel column" aliquot of the supernatant (20 µL) was taken. The supernatant was loaded onto the (stripped and recharged) nickel column (see Chapter 5.1.6). An "after nickel column" aliquot of the flow-through (20 µL) was collected. The nickel column was run by washing with 2-3 c. v. low imidazole buffer (25 mM), 10 c. v. high/ low imidazole buffer (250 mM/ 25 mM, 1:4), and 4 x 2 c. v. high imidazole buffer (250 mM). SDS-PAGE was conducted on the nickel column fractions following the general procedure (see Chapter 5.1.4). The tubes containing the desired protein were combined and concentrated down to a volume of 2.5 mL by centrifugal filtration (5,000 x g at 4°C) using a 10K MWCO filter. The buffer was exchanged to HEPES (50 mM, pH = 7.2) using a PD-10 desalting column, following the manufacturer's instructions. The concentration of protein was calculated by measuring the absorbance at 280 nm and using the Beer-Lambert Law as well as the extinction coefficient, ε_{280} = 19,940 $M^{-1}cm^{-1}$.

5.7. ^{19}F NMR spectroscopy of W216F 5FWβPGM-His Transition State Analogue complexes

The protein was concentrated down to 1.9 mM and dithiothreitol (DTT, 1 mM) was added. To obtain an NMR spectrum of the uncomplexed protein, W216F 5FWβPGM-His (final concentration of 1.6 mM), D_2O (35 µL), $MgCl_2$ (1.75 µL of 1M, final concentration: 5 mM), and NH_4F (3.5 µL of 1 M, final concentration: 10 mM) in HEPES buffer (50 mM, pH= 7.2, total volume 350 µL) were added to a Shigemi tube. To obtain the NMR spectra of the glucose-6-phosphate-MgF_3^--protein complex, the β-D-glucopyranosylmethyl-phosphonate-MgF_3^--protein complex, and the (S)-1-β-phosphonofluoromethylene-1-deoxy-D-glucopyranose-MgF_3^--protein complex, the same reagents mentionned above, along with the appropriate substrate (G6P, G1CP, or $G1CF_sP$, 5 mM final concentration), were added to a Shigemi tube. To prepare the G6P-AlF_4^--protein, G1CP-AlF_4^--protein, and $G1CF_sP$-AlF_4^--protein complexes, $AlCl_3$ (1 equivalent) was added to the Shigemi tube as well. $^{19}F\{^1H\}$ NMR spectra were obtained on the 500 MHz instrument, operating at 470 MHz for ^{19}F nuclei, with H_2O/D_2O as the solvent, and the temperature set at 278 K. For the spectra of the uncomplexed protein and of the protein with G6P, a *zgbsfhigqn* (background suppression) pulse program was used with the following parameters: 3200 or 5120 scans (for the uncomplexed protein and for the protein with G6P, respectively), 2.5 s relaxation delay (rd), 32,000 total number of data points (td), and 170 ppm sweep width, centered at -140 ppm. The $^{19}F\{^1H\}$ NMR spectra of the protein with G1CP and with $G1CF_sP$ were run using a *zgfhigqn* (no background suppression) pulse program for 31,150 scans, with a 190 ppm sweep width, centered at -140 ppm, and otherwise using the same

parameters as for the previous spectra. A HEPES buffer/ D_2O blank was run using the same parameters and subtracted from the spectra of the G1CP and $G1CF_sP$-protein complexes.

5.8. Synthesis of diammonium 3-deoxy-3-fluoro-β-D-glucopyranosylmethylphosphonate (21)

1,2: 5,6-Di-*O*-isopropylidene-α-D-*xylo*-hexofuranos-3-ulose (**8**)

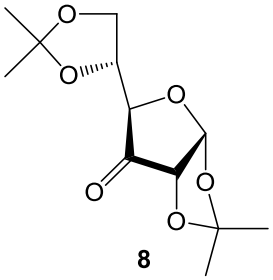

8

Compound **8**[39] was synthesized from diacetone D-glucose **7** (5.01 g, 19.2 mmol), which was dissolved in CH_2Cl_2 (40 mL, anhydrous) and placed under an inert atmosphere. Dess-Martin Periodinane (1.2 eq, 23.1 mmol, 9.78 g) and $NaHCO_3$ (1.2 eq, 23.1 mmol, 1.94 g) were dissolved in CH_2Cl_2 (40 mL, anhydrous), placed under an inert atmosphere, and cooled to 0°C. The first solution was then added to the second solution. The reaction mixture was stirred at room temperature under an inert atmosphere for 22.5 hours. It was then diluted with CH_2Cl_2 (115 mL) and cooled to 0°C. $Na_2S_2O_3$ (sat. aq, 5.3 mL) was added dropwise. The organic solution was washed with $Na_2S_2O_3$ (sat. aq, 50 mL), water (55 mL), and brine (55 mL). The organic layer was dried using $MgSO_4$ and concentrated *in vacuo*. The crude product was subjected to the next reaction without further purification.

1,2: 5,6-Di-*O*-isopropylidene-α-D-allofuranose (**9**)

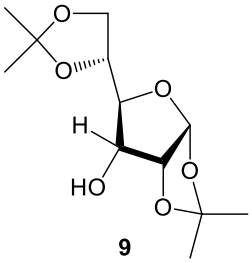

9

Compound **9**[39] was synthesized from compound **8** (19.2 mmol), which was dissolved in ethanol-water (3:1, 100 mL). Sodium borohydride (1.3 eq, 25.0 mmol, 0.94 g) was carefully added in three portions. The reaction mixture was stirred for 25 hours at room temperature, after which it was extracted with CH_2Cl_2 (4 x 133 mL). The combined organic layers were washed with water (3 x 100 mL), followed by brine (100 mL). The organic phase was dried using $MgSO_4$ and concentrated *in vacuo*. Compound **9** (4.73 g) was isolated as an off-white solid in a 94% yield over the two steps. ^{1}H NMR (500 MHz, $CDCl_3$) δ = 5.80 (d, $^3J_{H1\text{-}H2}$ = 3.7 Hz, 1H, H1), 4.61 (t, ^3J= 4.6 Hz, 1H, H2), 4.30 (m, 1H, H5), 4.04 (m, 3H, H3, H4, H6a), 3.81(dd, $^3J_{H6b\text{-}H5}$= 4.8, $^2J_{H6b\text{-}H6a}$= 8.5 Hz, 1H, H6b), 2.54 (d, $^3J_{OH\text{-}H3}$= 8.4 Hz, 1H, 3-OH), 1.57, 1.46, 1.38, 1.37 (4 x s, 4 x 3H, 4 x CH_3).

3-Deoxy-3-fluoro- 1,2: 5,6-di-*O*-isopropylidene-α-D-glucofuranose (**10**)

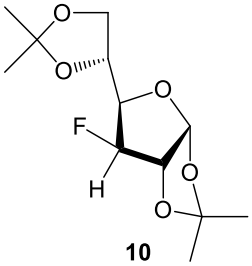

10

Compound **10** was synthesized using two different methods. In the first method,[40-42] DAST (1.1 eq, 5.79 mmol, 765 μL) was dissolved in CH_2Cl_2 (10 mL, anhydrous) and pyridine (3 mL, anhydrous), then placed under an inert atmosphere and cooled to 0°C. Compound **9**

(1.37 g, 5.27 mmol), dissolved in CH_2Cl_2 (20 mL, anhydrous), was added and the reaction mixture was stirred for 25 hours at room temperature, under an inert atmosphere. The reaction mixture was cooled to 0ºC and quenched by slowly adding methanol (0.5 mL). The solvent was concentrated *in vacuo*. The resulting residue was taken up in water (90 mL) and extracted with CH_2Cl_2 (3 x 38 mL). The combined organic layers were washed sequentially with $NaHCO_3$ (sat. aq, 3 x 15 mL), water (35 mL), and brine (35 mL). The organic phase was dried using $MgSO_4$ and concentrated *in vacuo*. Compound **10** was purified by silica gel column chromatography in hexanes: ethyl acetate (10:1 followed by 1:1). Compound **10** was isolated as an oil (618 mg, 45%) and starting material **9** was recovered (161 mg, 12%).

In the second method,[44] Compound **9** (8.35 g, 32.1 mmol) was dissolved in pyridine (64 mL, anhydrous) and placed under an inert atmosphere. The mixture was cooled to 0ºC and triflic anhydride (1.15 eq, 36.9 mmol, 6.18 mL) was added slowly. The reaction mixture was stirred until complete conversion was observed via TLC (1 hour), then it was diluted with ethyl acetate (145 mL) and washed with sodium bicarbonate (sat. aq, 145 mL) and brine (80 mL). The organic phase was dried using $MgSO_4$ and then concentrated *in vacuo*. The residue was subjected directly to the next reaction without further purification. The crude triflate was placed under an inert atmosphere and TBAF (1M in THF, 3 eq, 96.3 mmol, 96.3 mL) was added. It was stirred for 42.5 hours (at rt for the first 19 hours, then the temperature was increased to 60ºC for the remaining reaction time). The reaction mixture was cooled to 0ºC and diluted with diethyl ether (300 mL), washed with ammonium chloride (sat. aq, 3 x 200 mL) and brine (200 mL). The organic phase was dried using $MgSO_4$ and then concentrated *in vacuo*. The residue was lyophilised, taken up in

diethyl ether, and filtered to remove tetrabutylammonium salts. The filtrate was concentrated *in vacuo*, yielding **10** as an oil (3.83 g, 46%).

^{19}F NMR (470 MHz, $CDCl_3$) δ = -207.7 (ddd, $^3J_{H2\text{-}F}$= 10.6 Hz, $^3J_{H4F}$= 29.2 Hz, $^2J_{H3\text{-}F}$= 49.9 Hz). ^{1}H NMR (500 MHz, $CDCl_3$) δ = 5.95 (d, $^3J_{H1\text{-}H2}$= 3.8 Hz, 1H, H1), 5.00 (dd, $^2J_{H\text{-}F}$= 50.0 Hz, $^3J_{H\text{-}H}$ = 2.3 Hz, 1H, H3), 4.69 (dd, $^3J_{H\text{-}F}$= 10.7 Hz, $^3J_{H\text{-}H}$= 3.7 Hz, 1H, H2), 4.28 (m, 1H, H5), 4.08 (m, 3H, H4, H6a, H6b), 1.50, 1.45, 1.37, 1.33 (4 x s, 4 x 3H, 4 x CH_3).

Methyl 3-deoxy-3-fluoro-α/β-D-glucopyranoside (**11**)

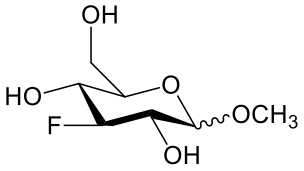

11

Compound **11** was prepared in the following manner:[43] acetyl chloride (4.3 mL) and methanol (20 mL, anhydrous) were placed under an inert atmosphere, cooled to 0°C, and stirred for 30 minutes. Then, a solution of **10** (692 mg, 2.64 mmol) in methanol (20 mL, anhydrous) was added. The reaction mixture was stirred at reflux (70°C) under an inert atmosphere for 4 hours. Then, the reaction mixture was cooled to room temperature and concentrated *in vacuo*. Silica gel column chromatography in dichloromethane: methanol (9:1) was used to isolate **11** as an oil (341 mg, 66%, 2α:1β). ^{19}F NMR (470 MHz, $CDCl_3$) δ= -196.6 (dt, $^3J_{H\text{-}H}$= 13.3 Hz, $^2J_{H\text{-}F}$= 53.0 Hz, β-anomer), -200.6 (dt, $^3J_{H\text{-}H}$= 13.3 Hz, $^2J_{H\text{-}F}$= 54.2 Hz, α-anomer). ^{1}H NMR (500 MHz, $CDCl_3$) δ= 4.82 (t, J= 3.5 Hz, 1Hα, H1α), 4.53 (dt, $^2J_{H\text{-}F}$= 54.5 Hz, $^3J_{HH}$= 9.0 Hz, 1Hα, H3α), 4.41 (dt, $^2J_{H\text{-}F}$= 53.1 Hz, $^3J_{H\text{-}H}$= 8.8 Hz, 1Hβ, H3β), 4.26 (d, $^3J_{H1\text{-}H2}$= 7.8 Hz, 1Hβ, H1β), 3.97-3.62 (m, 4Hα + 4Hβ, H2α/β, H4α/β, H6aα/β, H6bα/β), 3.58 (s, 3Hβ, OCH_3β), 3.44 (s, 3Hα, OCH_3α), 0.00-2.50 (several peaks,

impurities). The ^{19}F and ^{1}H NMR data for the α-anomer is consistent with the reported data. The β-anomer has not been reported.[53]

Methyl 2,4,6-tri-*O*-benzyl-3-deoxy-3-fluoro-β-D-glucopyranoside (**12**)

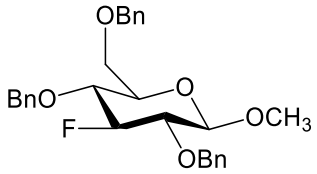

12

Compound **12** was synthesized in the following manner:[45] compound **11** (64 mg, 0.33 mmol) was dissolved in DMF (7 mL, anh.). The mixture was cooled to 0°C, and NaH was added (60% in mineral oil, 4 eq, 1.32 mmol, 52.8 mg), followed by stirring for 30 minutes at this temperature. Tetrabutylammonium iodide (TBAI, 0.01 eq, 3.3 µmol, 1.2 mg) was added and the reaction mixture was placed under an inert atmosphere. Benzyl bromide (4 eq, 1.32 mmol, 157 µL) was added dropwise to the mixture at 0°C. The reaction mixture was stirred at room temperature overnight and then cooled to 0°C. Methanol (1.6 mL) was added dropwise to quench. Extracted the reaction mixture with water (25 mL) and washed with ethyl acetate (3 x 25 mL). The organic layers were combined and washed with brine (25 mL). The organic fraction was dried over $MgSO_4$ and the solvent was removed *in vacuo*. The reaction produced a mixture of α/β methyl 2,4,6-tri-*O*-benzyl-3-deoxy-3-fluoro-D-glucopyranoside. Purification was performed using silica gel column chromatography in hexanes: ethyl acetate (7:3), to isolate the β-anomer **12** as a solid (110 mg, 72%). ^{19}F NMR (470 MHz, $CDCl_3$) δ= -188.7 (dt, $^{3}J_{H-H}$= 14.4 Hz, $^{2}J_{H-F}$ =52.1 Hz). ^{1}H NMR (500 MHz, $CDCl_3$) δ= 7.44 (m, 15H, aromatic), 5.00-4.87 (m, CH_2), 4.78 (dt, $^{3}J_{H-H}$= 8.8 Hz , $^{2}J_{H-F}$= 51.9 Hz, H3), 4.75-4.64 (m, CH_2), 4.40 (d, J= 7.8 Hz, 1H, H1), 3.85 (m, 3H, H4, H6a, H6b), 3.68 (s, 3H, OCH_3), 3.62 (dt, J= 8.4 Hz, 16.7 Hz, 1H, H2), 3.54 (m, 1H,

H5). $^{13}C\{^{1}H\}$ NMR (125 MHz, $CDCl_3$) δ= 138.3-138.0 (3 x OCH_2-Ph), 128.5-127.8 (15 x Ph) 103.8 (d, $^{3}J_{CF}$=12.3 Hz, C1), 98.1 (d, $^{1}J_{CF}$= 185.3 Hz, C3), 79.8 (d, $^{2}J_{CF}$= 17.7 Hz, C2), 76.2 (d, $^{2}J_{CF}$= 17.4 Hz, C4), 74.44 (2 x CH_2), 73.6-73.5 (1 x CH_2 + C5), 68.6 (C6), 57.3 (OCH_3). ESI-MS, *m/z* calcd for $C_{28}H_{31}FNaO_5$ [**12**+Na]$^{+}$: 489.2053, found: 489.2055.

Allyl 3-deoxy-3-fluoro-D-glucopyranoside (**13**)

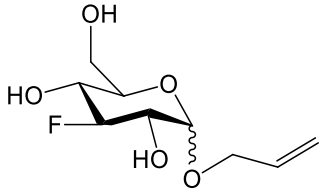

13

Compound **13** was synthesized in the following manner:[49,50] compound **10** (456 mg, 1.74 mmol) was dissolved in allyl alcohol (7.0 mL) and placed under an inert atmosphere. Concentrated HCl (1.39 mL, 2 M) was added and the reaction mixture was stirred at 80°C for 3 hours. The mixture was then cooled to room temperature and neutralized using $NaHCO_3$ (s), stirred for 20 minutes, and filtered. The filtrate was concentrated *in vacuo* and the residue was purified via silica gel column chromatography in dichloromethane: methanol (93:7 followed by 4:1) to give **13** as an oil (147 mg, 38%, 1α:1β). ^{19}F (470 MHz, $CDCl_3$) δ= -196.1 (dt, $^{3}J_{H-F}$=13.7 Hz, $^{2}J_{H3-F}$= 52.6 Hz), -200.3 (dt, $^{3}J_{H-F}$=13.0 Hz, $^{2}J_{H3-F}$= 54.3 Hz). $^{19}F\{^{1}H\}$ NMR (470 MHz, CD_3OD) δ= -195.7, -200.0. ^{1}H NMR (500 MHz, CD_3OD) δ= 5.99 (m, 2H, C<u>H</u>=CH_2 α/β), 5.37 (m, 2H, CH=C<u>H</u>$_2$ α/β), 5.21 (m, 2H, CH=C<u>H</u>$_2$ α/β), 4.91 (t, $^{3}J_{H1-H2}$= 3.5 Hz, 1H, H1α), 4.54 (dt, $^{3}J_{H-F}$= 8.7 Hz, $^{2}J_{H3-F}$= 54.5 Hz, 1H, H3α), 4.43-4.05 (m, 5H, H3β, O-C<u>H</u>$_2$-CH α/β), 4.37 (d, J= 7.9 Hz, 1H, H1β), 3.94-3.56 (m, 8H, H2α/β, H4α/β, H6aα/β, H6bα/β), 3.47 (m, 1H, H5 α or β), 3.30 (m, 1H, H5 β or α). $^{13}C\{^{1}H\}$ NMR (125 MHz, CD_3OD) δ= 135.5 and 135.2 (2 x s, 2 x <u>C</u>H=CH_2), 117.7 and 117.6 (2 x s, 2 x CH=<u>C</u>H$_2$), 102.5 (d, J= 12.2 Hz, C1), 99.2 (d, J= 10.5 Hz, C1),

98.4 (d, J= 183.1 Hz, C3), 96.6 (d, J= 180.6 Hz, C3), 76.5 (d, J= 8.1 Hz, C5), 73.5 (d, J= 17.9 Hz, C2 or C4), 73.2 (d, J= 7.2 Hz, C5), 71.7 (d, J= 17.2 Hz, C2 or C4), 71.1 (s, O-C$\underline{H}_2$), 69.8 (d, J= 14.1 Hz, C4 or C2), 69.6 (d, J= 14.3 Hz, C4 or C2), 69.4 (s, O-C$\underline{H}_2$), 62.2 and 62.1 (2 x s, 2 x C6). ESI-MS, *m/z* calcd for $C_9H_{15}FNaO_5$ [**13**+Na]$^+$: 245.0801, found: 245.0801.

Allyl 2,4,6-tri-*O*-benzyl-3-deoxy-3-fluoro-D-glucopyranoside (**14**)

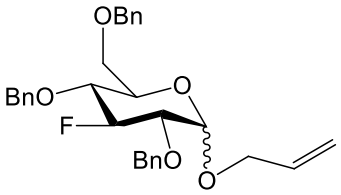

14

Compound **14** was synthesized in the following manner:[45] compound **13** (1.49 g, 6.69 mmol) was dissolved in DMF (30 mL, anh.), cooled to 0ºC, and NaH was added (60% in mineral oil, 5 eq, 33.5 mmol, 1.34 g), followed by stirring for 30 minutes. Tetrabutylammonium iodide (TBAI, 0.01 eq, 67 µmol, 25 mg) was added and the reaction mixture was placed under an inert atmosphere. Benzyl bromide (5 eq, 33.5 mmol, 3.98 mL) was added dropwise at 0ºC. The reaction mixture was stirred at room temperature overnight and then cooled to 0ºC. Methanol (24 mL) was added dropwise to quench. Water (240 mL) was added to the reaction mixture, followed by washing with ethyl acetate (3 x 180 mL). The combined the organic layers were washed with brine (180 mL). The organic phase was dried over $MgSO_4$ and concentrated *in vacuo*. Purification was performed using silica gel column chromatography in hexanes: ethyl acetate (10:1), yielding compound **14** as an oil (1.51 g, 61%, 1α:1β). $^{19}F\{^1H\}$ NMR (470 MHz, $CDCl_3$) δ= -188.7, -192.8. ^1H NMR (500 MHz, $CDCl_3$) δ= 7.34 (m, 16H, 15 Ph, $CHCl_3$), 6.00 (m, 1H, C$\underline{H}$=CH_2), 5.41 (m, 1H, CH=C$\underline{H}_2$), 5.28 (m, 1H, CH=C$\underline{H}_2$), 5.15-4.48 (m, 9H, 6 Ph-C$\underline{H}$, H3, H1, solvent/impurity),

4.21 (m, 1H, O-C<u>H</u>$_2$-CH), 4.06 (m, 1H, O-C<u>H</u>$_2$-CH), 3.87-3.47 (m, 5H, H2, H4, H5, H6a, H6b). $^{13}C\{^1H\}$ NMR (125 MHz, $CDCl_3$) δ= 138.2 (3 x quaternary Ph), 134.1 and 133.7 (<u>C</u>H=CH$_2$), 128.6-127.9 (15 x tertiary Ph), 118.2 and 117.5 (CH=<u>C</u>H$_2$), 101.9 and 96.4 (2 x d, J= 12.0 and 11 Hz, C1), 98.2 and 96.5 (2 x d, J= 184 and 183 Hz, C3), 79.9 (d, J= 17.5 Hz, C2), 77.4 and 77.1 (2 x d, J= 31 Hz, C4), 76.2, 74.6, 70.5, and 69.6 (C<u>H</u>$_2$-Ph), 73.7 and 73.2 (C5), 68.6 and 68.4 (d, J= 27 and 36 Hz, C6). ESI-MS, *m/z* calcd for $C_{30}H_{33}FNaO_5$ [**14**+Na]$^+$: 515.2210, found: 515.2191.

<u>2,4,6-Tri-*O*-benzyl-3-deoxy-3-fluoro-D-glucopyranose (**15**)</u>

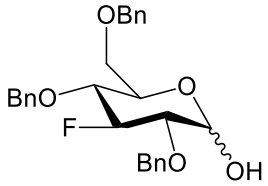

15

Compound **15** was synthesized[51] from compound **14** (96 mg, 0.19 mmol), which was dissolved in glacial acetic acid (7.6 mL). $Pd(PPh_3)_4$ (0.3 eq, 59 µmol, 68 mg) was added to the reaction mixture and the flask contents were placed under an inert atmosphere with stirring at 80°C for 23 hours. The reaction mixture was concentrated *in vacuo* and the residue was taken up in water (45 mL), extracted with ether (3 x 25 mL), and the organic fractions combined. The organic phase was washed with $NaHCO_3$ (sat. aq, 22 mL) and brine (22 mL), dried with $MgSO_4$, and concentrated *in vacuo*. Compound **15** (48 mg, 54%, 4α:1β), an oil, was purified using silica gel column chromatography in hexanes: ethyl acetate (7:1). ^{19}F NMR (470 MHz, $CDCl_3$) δ= -189.0 (dt, $^3J_{H-F}$= 13.7 Hz, $^2J_{H-F}$= 51.8 Hz, β anomer), -193.8 (dt, $^3J_{H-F}$= 13.1 Hz, $^2J_{H-F}$= 53.5 Hz, α anomer). ^1H NMR (500 MHz, $CDCl_3$, assignments are for the major α anomer) δ= 7.34 (15H, m, Ph), 5.27 (1H, t, J= 3.7 Hz, H1), 4.99 (1H, dt, $^3J_{H-H}$ = 8.7 Hz, $^2J_{H-F}$= 53.6 Hz, H3), 4.88, 4.86, 4.73, 4.64, 4.55, 4.52 (6H, 6

x d, $^{2}J_{H\text{-}H}$= 10-12 Hz, 6 x O-C<u>H</u>$_2$-Ph), 3.59-3.82 (3H, m, H5, H6a, H6b), 3.77 (1H, m, H4), 3.67 (1H, m, H2). $^{13}C\{^{1}H\}$ NMR (125 MHz, $CDCl_3$) (assignments are for α anomer) δ= 138.1 (3 x s, 3 x quaternary Ph), 128.9-127.9 (m, 15 x Ph), 96.8 (d, J= 183 Hz, H3), 92.0 (d, J= 11 Hz, C1), ~77 (obscured by $CDCl_3$ signal, H2), 76.0 (d, J= 17.0 Hz, H4), 74.7, 73.5, 73.8 (3 x s, 3 x CH_2), 69.7 (d, J= 8.6 Hz, C5), 68.4 (s, C6). ESI-MS, *m/z* calcd for $C_{27}H_{29}FNaO_5$ [**15**+Na]$^+$: 475.1897, found: 475.1884.

<u>2,4,6-Tri-*O*-benzyl-3-deoxy-3-fluoro-D-gluconolactone (**16**)</u>

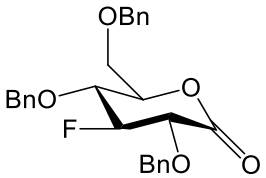

16

Compound **16** was initially synthesized via Swern oxidation.[56,57] Under an inert atmosphere, oxalyl chloride (3 eq, 0.62 mmol, 52 µL) was added to CH_2Cl_2 (anhydrous, 1.5 mL) and cooled to -78ºC. DMSO (anhydrous, 3.3 eq, 0.68 mmol, 48 µL) was added and the reaction mixture stirred (30 min) at -78ºC. Compound **15** (93.4 mg, 0.206 mmol) was dissolved in CH_2Cl_2 (anhydrous, 1 mL), was added to the oxalyl chloride solution, and stirred for an additional 30 minutes at -78ºC. Then, NEt_3 (5.1 eq, 1.05 mmol, 146 µL) was added and the reaction mixture was allowed to stir at room temperature for 3 hours. It was quenched with water (5 mL) and then extracted with CH_2Cl_2 (3 x 5 mL). The organic layers were combined, washed with brine (5 mL), dried with $MgSO_4$, and concentrated *in vacuo*. The product was purified via silica gel column chromatography in hexanes: ethyl acetate (3:1) to give **16** (9 mg, 9%).

An improved synthesis of **16** was later performed using Dess-Martin Periodinane (DMP) in CH_2Cl_2.[52] Compound **15** (243 mg, 0.539 mmol) was combined with DMP (0.3

M in CH_2Cl_2, 1.5 eq, 0.809 mmol, 2.70 mL) under an inert atmosphere. The reaction mixture was stirred for 24 hours at room temperature, then diluted with Et_2O (11 mL) and washed with $Na_2S_2O_3$ (sat. aq, 7.5 mL). The aqueous layer was extracted with Et_2O (3 x 6 mL). The combined the organic extracts were washed with water (10 mL) and brine (6 mL), dried with $MgSO_4$, and concentrated *in vacuo.* The product was purified by taking up in Et_2O (16 mL), filtering off the precipitate, and concentrating the organics *in vacuo*. Performed the purification procedure a second time, using minimal Et_2O (12 mL). Compound **16** was then isolated as a solid (235 mg, 97%, contains a small amount of DMP and/or iodinane byproduct).

$^{19}F\{^1H\}$ NMR (470 MHz, $CDCl_3$) δ= -183.5. ^1H NMR (500 MHz, $CDCl_3$) δ= 7.35 (15H, m, Ph), 5.02, 4.85, 4.77, 4.60, 4.59, 4.50 (6H, 6 x d, J= 11-12 Hz, 6 x O-C$\underline{H}_2$-Ph), 4.92 (1H, dt, $^3J_{H\text{-}H}$= 7.2 Hz, $^2J_{H\text{-}F}$= 51.0 Hz, H3), 4.39 (1H, dt, $^3J_{H5\text{-}H4}$= 8.6 Hz, $^3J_{H5\text{-}H6}$= 2.5 Hz, H5), 4.21 (1H, dd, $^3J_{H2\text{-}H3}$= 7.3 Hz, $^3J_{HF}$= 15.6 Hz, H2), 4.12 (1H, ddd, $^3J_{H4\text{-}H3}$= 7.2 Hz, $^3J_{H4\text{-}H5}$= 8.5 Hz, $^3J_{H\text{-}F}$= 16.3 Hz, H4), 3.75 (2H, m, $H6_{a\&b}$). $^{13}C\{^1H\}$ NMR (125 MHz, $CDCl_3$) δ= 168.0 (s, C1), 136.5, 137.0, 137.3 (3 x s, 3 x quaternary Ph), 128.2 (m, 15 x Ph), 93.8 (d, $^1J_{C\text{-}F}$=181 Hz, H3), 77.3 (overlapping with $CDCl_3$ peak, C5), 75.7 (d, $^2J_{C\text{-}F}$= 23.9 Hz, C2), 74.5 (d, $^2J_{C\text{-}F}$= 20.8 Hz, C4), 74.0, 73.7, 73.6 (3 x s, 3 x OCH_2), 67.7 (s, $H6_{a\&b}$). ESI-MS, *m/z* calcd for $C_{27}H_{27}FNaO_5$ [**16**+Na]$^+$: 473.1740, found: 473.1719.

1-(Dimethyl phosphonatylmethyl)-2,4,6-tri-*O*-benzyl-3-deoxy-3-fluoro-α-D-glucopyranose (**17**)

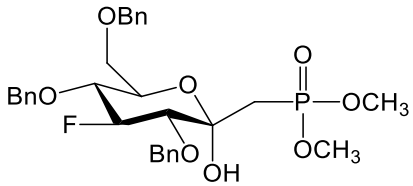

17

Compound **17** was synthesized in the following manner:[37] dimethyl methylphosphonate (distilled, 3 eq, 4.87 mmol, 0.53 mL) was combined with THF (anh., 15.5 mL) under an inert atmosphere. The solution was cooled to -78ºC and then *n*-BuLi (2.5 M in hexanes, 3 eq, 4.87 mmol, 1.95 mL) was added gradually, over one minute. The reaction mixture was stirred for 30 minutes at -78ºC. A solution of **16** (731 mg, 1.62 mmol) in THF (anh., 7.8 mL) was added. The reaction mixture was stirred for 2 h at -78ºC. Then, quenched with NH_4Cl (sat. aq, 10 mL). The contents of the flask were transferred to a separatory funnel and the two layers separated. The organic phase was washed with water (37 mL). The combined aqueous phases were washed with CH_2Cl_2 (3 x 19 mL). The combined organic phases were then dried with $MgSO_4$ and concentrated *in vacuo*. Product **17** (540 mg, 58%), a solid, was purified via silica gel column chromatography in hexanes: ethyl acetate (1:1). $^{31}P\{^1H\}$ NMR (202 MHz, $CDCl_3$) δ= 30.8 (s). $^{19}F\{^1H\}$ NMR (470 MHz, $CDCl_3$) δ= -192.2 (d, $^5J_{F-P}$= 4.1 Hz). ^{19}F NMR (470 MHz, $CDCl_3$) δ= -192.2 (dt, $^3J_{H-F}$= 13.0 Hz, $^2J_{H3-F}$= 54.0 Hz). ^1H NMR (500 MHz, $CDCl_3$) δ= 7.40-7.28 (15H, m, 15 x Ph), 5.81 (1H, s, OH), 5.11 (1H, dt, $^3J_{H-H}$= 8.6 Hz, $^2J_{H-F}$= 53.9 Hz, H3), 4.98, 4.87, 4.66, 4.58 (4 x 1H, 4 x d, J= 10.9-11.7 Hz, 4 x OC<u>H</u>-Ph), 4.49 (2H, s, OC<u>H</u>$_2$-Ph), 4.07 (1H, m, H5), 3.80 (1H, m, H4), 3.73 (1H, m, H6a), 3.68, 3.65 (2 x 3H, 2 x d, J= 4.8 Hz, P(O)(OC<u>H</u>$_3$)$_2$), 3.61 (1H, m, H6b), 3.36 (1H, dd, $^3J_{H2-H3}$= 9.1 Hz, $^3J_{H-F}$= 11.7 Hz, H2), 2.46 (1H, dd, J= 15.3Hz, J= 17.5 Hz, H1'a), 1.18 (1H, dd, J= 15.2 Hz, J= 18.6 Hz, H1'b). $^{13}C\{^1H\}$ NMR (125 MHz, $CDCl_3$) δ= 138.2, 138.0, 137.7 (3 x s, 3 x quaternary Ph), 129.0-127.9 (m, 15 x tertiary Ph), 98.2 (dd, $^2J_{C-F}$= 180 Hz, $^4J_{C-P}$= 4.3 Hz, H3), 97.1 (dd, J= 7.9 Hz, 12.2 Hz, C1), 80.3 (t, J= 15.0 Hz, C2), 76.3 (d, J= 16.9 Hz, C4), 74.6, 74.4, 73.6 (3 x O<u>C</u>H$_2$Ph), 70.2 (d, J= 8.7 Hz, C5), 68.4 (s,

C6), 53.6, 52.1 (2 x d, J= 5.6 Hz and J= 6.4 Hz respectively, 2 x P-O<u>C</u>H$_3$), 32.7 (d, J= 136.0 Hz, C1'). ESI-MS, *m/z* calcd for $C_{30}H_{36}FNaO_8P$ [**17**+Na]$^+$: 597.2030, found: 597.2017.

<u>(Methyl oxalyl) 1-(dimethyl phosphonatylmethyl)-2,4,6-tri-*O*-benzyl-3-deoxy-3-fluoro-α-D-glucopyranose (**18**)</u>

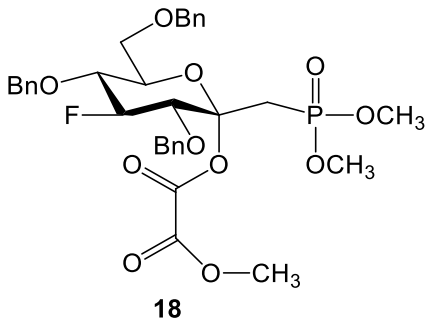

18

Compound **18** was synthesized[16] from compound **17** (71.4 mg, 0.124 mmol), which was dissolved in CH_2Cl_2 (anh., 180 µL) and pyridine (anh., 50 µL). Methyl chlorooxoacetate (10 eq, 1.24 mmol, 114 µL) was added dropwise while stirring vigorously. The reaction mixture was stirred overnight at room temperature, under an inert atmosphere. Ethanol (40 µL) was added to the reaction mixture and the solution was stirred for 10 minutes. The mixture was diluted with ethyl acetate (4 mL), washed with $NaHCO_3$ (sat. aq, 5 mL), water (4 mL), and brine (3 mL). The organic phase was dried with anhydrous $MgSO_4$ and then concentrated *in vacuo* to give **18** (crude: 70 mg, 85%). The residue was directly subjected to the next reaction without further purification. $^{31}P\{^1H\}$ NMR (202 MHz, $CDCl_3$) δ= 24.4 (s). $^{19}F\{^1H\}$ NMR (470 MHz, $CDCl_3$) δ= -193.9 (s). ESI-LRMS, *m/z* calcd for $C_{33}H_{38}FNaO_{11}P$ [**18**+Na]$^+$: 683.2, found: 683.2.

(E/Z)-1-(Dimethylphosphonomethylene)-2,4,6-tri-*O*-benzyl-1,3-deoxy-3-fluoro-D-glucopyranosyl-2-ylidene (**19**) and 2,4,6-tri-*O*-benzyl-3-deoxy-3-fluoro-β-D-glucopyranosylmethylphosphonate (**20**)

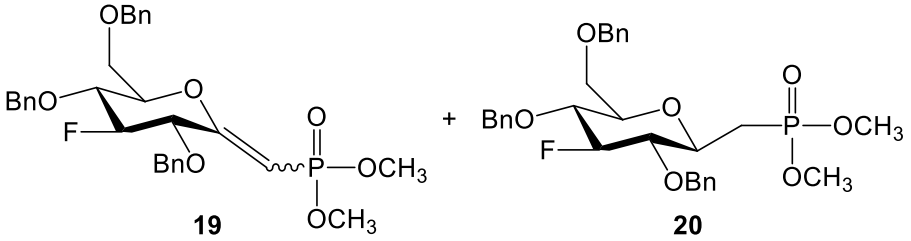

Compounds **19/20** were synthesized[16] from compound **18** (0.145 mmol), which was combined with AIBN (0.19 eq, 2.75 x 10^{-2} mmol, 4.5 mg) and dissolved in toluene (anh., 5.4 mL) under an inert atmosphere. Tributyl tin hydride (2 eq, 0.290 mmol, 78 μL) was added, and the reaction mixture was refluxed for 1 hour at 105°C under an inert atmosphere. The reaction mixture was cooled to room temperature and quenched with water (12 mL). It was then extracted with ethyl acetate (3 x 6 mL). The combined organic phases were dried with anhydrous $MgSO_4$ and then concentrated *in vacuo*. The product was purified via silica gel-KF (10% KF w/w) column chromatography[58] (dichloromethane: methanol 49:1) to give a mixture of **19** and **20** (23 mg, 28%). This chromatographic procedure was selected as a column using a silica gel-KF stationary phase has been reported to reduce organotin impurities to a level which is undetectable by ^{1}H NMR.[58] Upon running the column, the excess tributyl tin hydride reacts in a nucleophilic substitution reaction with KF, producing tributyl tin fluoride, which is insoluble in organic solvents, thus allowing for the chromatographic separation of these impurities from the organic-soluble products.[59] A fraction of pure **19** (of only one configuration, however, it is unknown as to whether it is E or Z) was isolated: $^{31}P\{^1H\}$ NMR (202 MHz, $CDCl_3$) δ= 21.9 (s). $^{19}F\{^1H\}$ NMR (470 MHz, $CDCl_3$) δ= -177.8 (s). ^{1}H NMR (500 MHz, $CDCl_3$) δ= 7.26-7.39 (17H, m, $CHCl_3$ and 15 x Ph), 5.57 (1H, dd, $^5J_{H1-H3}$= 1.4 Hz, $^2J_{H-P}$= 13.4 Hz, H1), 5.17 (1H, d, $^3J_{H2-H3}$= 6.8

Hz, H2), 4.99 (1H, dt, $^{3}J_{HH}$= 2.6 Hz, $^{2}J_{H\text{-}F}$= 46.9 Hz, H3), 4.79 (2H, s, OC<u>H</u>$_2$-Ph), 4.77, 4.64, 4.57, 4.56 (4 x 1H, 4 x d, $^{2}J_{HH}$= 11.3-12.2 Hz, 4 x OC<u>H</u>-Ph), 4.60 (1H, m, H5), 3.90 (1H, ddd, $^{3}J_{HH}$= 3.4 Hz, $^{3}J_{HH}$= 10.4 Hz, $^{3}J_{HF}$= 25.6 Hz, H4), 3.80 (1H, d, $^{2}J_{HH}$= 11.2 Hz, H6a), 3.75, 3.72 (6H, 2 x d, J= 11.4 Hz, P(OC<u>H</u>$_3$)$_2$), 3.72 (d, $^{2}J_{HH}$= 11.2 Hz, H6b). $^{13}C\{^{1}H\}$ NMR (125 MHz, $CDCl_3$) δ= 165.3 (d, $^{2}J_{CP}$= 27.2 Hz, C1), 138.0, 137.8, 137.3 (3 x s, 3 x quaternary Ph), 128.6-128.0 (m, 15 x tertiary Ph), 93.0 (d, $^{1}J_{CF}$= 182.5 Hz, C3), 92.2 (d, $^{2}J_{CF}$= 20.5 Hz, C2), 76.5 (d, $^{2}J_{CF}$= 27.2 Hz, C4), 74.3 (d, $^{3}J_{CF}$= 7.5 Hz, C5), 73.7, 72.5, 71.7 (3 x s, 3 x <u>C</u>H$_2$Ph), 72.6 (d, J= 32.7 Hz, C1'), 52.3, 52.4 (2 x d, $^{2}J_{CP}$= 6.0 Hz, 2 x P(O<u>C</u>H$_3$)). ESI-MS, *m/z* calcd for $C_{30}H_{34}FNaO_7P$ [**19**+Na]$^{+}$: 579.1924, found: 579.1906. A second fraction with a (4:1) mixture of **20** and **19** was isolated as an oil; characterization is for **20**: $^{31}P\{^{1}H\}$ NMR (202 MHz, $CDCl_3$) δ= 31.0 (s). $^{19}F\{^{1}H\}$ NMR (470 MHz, $CDCl_3$) δ= -185.3 (d, $^{5}J_{F\text{-}P}$= 3.4 Hz). Selected ^{1}H NMR (500 MHz, $CDCl_3$) δ= 2.33 (1H, ddd, J= 2.5 Hz, 15.7 Hz, 18.3 Hz, H1'a), 1.92 (1H, ddd, J= 9.2 Hz, 16.2 Hz, 25.4 Hz, H1'b). ESI-MS, *m/z* calcd for $C_{30}H_{36}FNaO_7P$ [**20**+Na]$^{+}$: 581.2080, found: 581.2063.

<u>Diammonium 3-deoxy-3-fluoro-β-D-glucopyranosylmethylphosphonate (**21**)</u>

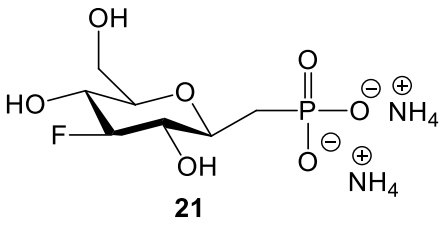

21

Compound **21** was synthesized by subsequent hydrogenation, benzyl deprotection, methyl deprotection, and ion exchange reactions.[37] First, the **19**/**20** mixture (18.3 mg, 3.29 x 10^{-2} mmol) was dissolved in ethyl acetate (0.5 mL) and methanol (0.5 mL). Palladium on carbon (10 wt. %) was added (20 mol %, 7.0 mg). The reaction mixture was degassed under vacuum (using a Schlenk line connected to a vacuum pump) and saturated with hydrogen

at atmospheric pressure. The mixture was reacted for 4 hours at room temperature, after which it was filtered through celite and washed with ethyl acetate/ methanol (1:1). The filtrate was then concentrated *in vacuo*. ^{1}H NMR ($CDCl_3$, 500 MHz) of the residue was used to confirm complete conversion to the saturated form by the disappearance of the alkenyl H1 signal. Second, the residue was subjected to benzyl deprotection without further purification. The concentrated filtrate was combined with TMSI (1 M in CH_2Cl_2, 29 eq, 0.924 mmol, 0.95 mL) at 0^{o}C under an inert atmosphere. The reaction mixture was allowed to warm to room temperature and stirred for 4 h, after which it was quenched with methanol (0.4 mL) and concentrated *in vacuo*. The residue was taken up in water (4 mL) and washed with diethyl ether (8 x 4 mL). The aqueous layer was concentrated *in vacuo* and lyophilized. ^{1}H NMR (D_2O, 500 MHz) of the residue demonstrated that benzyl deprotection had been successful by the absence of benzyl signals (both aromatic and methylene). Third, methyl deprotection was performed: HCl (6M, 1.5 mL) was added to the residue and the reaction mixture was heated at 60^{o}C for 6 hours. The reaction mixture was cooled to room temperature and concentrated *in vacuo*. Fourth, the residue was taken up in water (1 mL) and the pH adjusted to 8 using NH_4OH (2 M, aq.). The aqueous solution was concentrated *in vacuo* and lyophilized to obtain **21** as a white solid (2.7 mg, 28%). ^{31}P{^{1}H} NMR (202 MHz, D_2O) δ= 21.3 (s). ^{19}F{^{1}H} NMR (470 MHz, D_2O) δ= -192.8 (s). ^{19}F NMR (470 MHz, D_2O) δ= -192.8 (dt, $^{3}J_{H-F}$= 13.3 Hz, $^{2}J_{H-F}$= 53.0 Hz). ^{1}H NMR (500 MHz, D_2O) δ= 4.47 (1H, dt, $^{2}J_{HF}$= 53.3 Hz, $^{3}J_{HH}$= 8.5 Hz, H3), 3.96 (1H, d, J= 12.0 Hz, H6a), 3.75 (2H, m, H4, H6a), 3.67 (1H, m, H1), 3.57 (1H, m, H2), 3.49 (1H, m, H5), 2.23 (t, J= 17.4 Hz, H1'a), 1.90 (1H, m, H1'b). ^{13}C{^{1}H} NMR (125 MHz, D_2O) δ= 97.9 (d, $^{1}J_{C-F}$= 182.2 Hz, C3), 78.7 (d, $^{3}J_{C-F}$= 7.3 Hz, C5), 75.2 (d, C1), 72.8 (d, $^{2}J_{C-F}$= 17 Hz, C4), 68.3

(d, $^{2}J_{C\text{-}F}$= 16.9 Hz, C2), 60.6 (s, C6), 31.1 (C1'). ESI-MS, *m/z* calcd for $C_7H_{13}FO_7P^-$ [**21**-H]$^-$: 259.0388, found: 259.0377.

Chapter 6. Conclusion

6.1. Synthesis and application of a covalent inactivator of DesR, EryBI, and Hsero1941 glycosidases conclusion

2,4-Dinitrophenyl 2-deoxy-2-fluoro-β-D-glucopyranose (**6**) was synthesized in five steps, with an overall yield of 8%, following literature precedents.[29-31] Kinetic assays showed that DesR and EryBI were quantitatively inactivated by **6** after 2 hours of incubation. After 16 hours of incubation with **6**, Hsero1941 was inactivated by approximately 50%. This leads us to the conclusion that **6** is a much poorer inactivator of Hsero1941 than of DesR and EryBI. Considering **6** has been reported to successfully inactivate the β-*N*-acetylgucosaminidase Nag3,[60] it was somewhat unexpected that it was not capable of completely inactivating our β-*N*-acetylgucosaminidase Hsero1941. The screening of a library of potential acceptors indicated that none of them were capable of reactivating EryBI or DesR. The most promising potential acceptor for EryBI, erythromycin, was in fact shown to inhibit EryBI. It was not determined whether erythromycin was both an acceptor and an inhibitor of EryBI, or merely an inhibitor. By contrast to the lack of success reactivating the retaining glycosidases DesR and EryBI, the β-*N*-acetylglucosaminidase Hsero1941 was reactivated by several of the potential acceptors. Fifteen of the acceptors showed a percent reactivation greater than 40%, making them promising candidates as substrates for transglycosylation reactions in addition to being reactivators of Hsero1941. These results suggest that it is easier for a given acceptor to reactivate a retaining glycosidase if the covalent inactivator is more readily hydrolysed. The only enzyme in this study which demonstrated reactivation was Hsero1941 which had only been partially inhibited by **6** to begin with. In future reactivation studies of DesR and EryBI, it would be

wise to choose a compound which binds less strongly to the enzymes so that the glycosyl-enzyme bond can be more readily broken, allowing for transglycosylation.

6.2. Expression of ^{19}F-labelled β-phosphoglucomutase and the study of its transition state analogues conclusion

A ^{19}F-labelled W216F mutant βPGM was expressed and used to form analogues of both transition states 1 and 2 of the βPGM-catalyzed isomerization of βG1P to G6P. ^{19}F NMR spectroscopy proved to be a useful tool in both assigning the tryptophan residues and in monitoring TSA complexation. 5-FW24 was found to produce a single peak by ^{19}F NMR which shifted by + 2 ppm when complexed. The presence of only one peak indicated that the 5-FW24 residue exists in a single conformation in the ground state unlike the previously discovered dual conformations of 5-FW216 (which undergoes an indole ring flip). Transition state analogue 2 complexes formed readily, with all protein existing in the bound form. Transition state analogue 1 complexes formed with varied ratios of complexed to apo protein. Using the G1CP and G1CF$_s$P substrates, the AlF_4^- complexes formed more readily than those with MgF_3^-, potentially due to the charge of AlF_4^- more closely mimicking a phosphoryl group. Of all the TSA1 complexes, the AlF_4^--G1CF$_s$P-βPGM formed most readily, with a 1:1 ratio of complex to apo enzyme. In all of the TSA complex spectra acquired, comparable molar ratios of each species were found which indicates that the metal fluorides are in fact representative of the transition states.

6.3. Synthesis of diammonium 3-deoxy-3-fluoro-β-D-glucopyranosylmethylphosphonate conclusion

Diammonium 3-deoxy-3-fluoro-β-D-glucopyranosylmethylphosphonate (**21**) was successfully synthesized in twelve steps. Compound **21** will be evaluated kinetically to determine whether it will inhibit the W216F mutant β-phosphoglucomutase. Compound **21**

will also be crystallized with the aforementioned protein and the complex will be subjected to X-ray crystallography. Furthermore, formation of the **21**-W216F 5FWβPGM transition state analogue complex will be monitored using ^{19}F NMR spectroscopy. These experiments will provide us with structural information about the novel **21**-W216F 5FWβPGM transition state analogue complex as well as indicating how readily the complex forms. If complete conversion to the complex is observed, this could provide us with valuable insight into the structure of the first transition state in the βPGM-catalyzed conversion of βG1P to G6P.

References

1. AFMB-CNRS-Université d'Aix-Marseille Carbohydrate Active Enzymes. http://www.cazy.org/Glycoside-Hydrolases.html (accessed 12/01, 2016).

2. Zechel, D. L.; Withers, S. G. Glycosidase mechanisms: Anatomy of a finely tuned catalyst. *Acc. Chem. Res.* **2000**, *33*, 11-18.

3. Flos, M.; Moreno, M.; Mellet, C.; Fernandez, J.; Nierengarten, J.; Vincent, S. Potent Glycosidase Inhibition with Heterovalent Fullerenes: Unveiling the Binding Modes Triggering Multivalent Inhibition. *Chem. Eur. J.* **2016**, *22*, 11450-11460.

4. Wilkinson, S. M.; Liew, C. W.; Mackay, J. P.; Salleh, H. M.; Withers, S. G.; McLeod, M. D. Escherichia coli glucuronylsynthase: An engineered enzyme for the synthesis of beta-glucuronides. *Org. Lett.* **2008**, *10*, 1585-1588.

5. Blanchard, J. E.; Withers, S. G. Rapid screening of the aglycone specificity of glycosidases: applications to enzymatic synthesis of oligosaccharides. *Chem. Biol.* **2001**, *8*, 627-633.

6. Mackenzie, L. F.; Wang, Q.; Warren, R. A.; Withers, S. G. Glycosynthases: Mutant Glycosidases for Oligosaccharide Synthesis. *J. Am. Chem. Soc.* **1998**, *120*, 5583-5584.

7. Sadeghi-Khomami, A.; Lumsden, M. D.; Jakeman, D. L. Glycosidase inhibition by macrolide antibiotics elucidated by STD-NMR spectroscopy. *Chem. Biol.* **2008**, *15*, 739-749.

8. Jakeman, D. L.; Sadeghi-Khomami, A. A beta-(1,2)-glycosynthase and an attempted selection method for the directed evolution of glycosynthases. *Biochemistry* **2011**, *50*, 10359-10366.

9. Ducatti, D. R. B.; Carroll, M. A.; Jakeman, D. L. On the phosphorylase activity of GH3 enzymes: A β-N-acetylglucosaminidase from Herbaspirillum seropedicae SmR1 and a glucosidase from Saccharopolyspora erythraea. *Carbohydr. Res.* **2016**, *435*, 106-112.

10. Zhao, L.; Beyer, N. J.; Borisova, S. A.; Liu, H. β-Glucosylation as a Part of Self-Resistance Mechanism in Methymycin/Pikromycin Producing Strain Streptomyces venezuelae. *Biochemistry (N. Y.)* **2003**, *42*, 14794-14804.

11. Hommalai, G.; Chaiyen, P.; Svasti, J. Studies on the transglucosylation reactions of cassava and Thai rosewood β-glucosidases using 2-deoxy-2-fluoro-glycosyl-enzyme intermediates. *Arch. Biochem. Biophys.* **2005**, *442*, 11-20.

12. Scaffidi, A.; Stick, R. V.; Stubbs, K. A. Synthesis of Some Glycosylated Derivatives of 2-Deoxy-2-fluoro-β-laminaribiosyl Fluoride: Another Success for Glycosynthases. *Aust. J. Chem.* **2007***, 60*, 83-88.

13. Syson, K.; Stevenson, C. E. M.; Rashid, A. M.; Saalbach, G.; Tang, M.; Tuukkanen, A.; Svergun, D. I.; Withers, S. G.; Lawson, D. M.; Bornemann, S. Structural Insight into How Streptomyces coelicolor Maltosyl Transferase GlgE Binds α-Maltose 1-Phosphate and Forms a Maltosyl-enzyme Intermediate. *Biochemistry* **2014***, 53*, 2494-2504.

14. De Cesco, S.; Kurian, J.; Dufresne, C.; Mittermaier, A. K.; Moitessier, N. Covalent inhibitors design and discovery. *Eur. J. Med. Chem.* **2017***, 138*, 96-114.

15. Vaishnavi, R.; Kumar, A.; Saravanakumar, A. Cloning, expression and comparative study of white spot syndrome virus (WSSV) thymidine kinase gene during infection in Penaeus monodon. *Int. J. Curr. Microbiol. Appl. Sci.* **2016***, 5*, 405-412.

16. Jin, Y.; Bhattasali, D.; Pellegrini, E.; Forget, S. M.; Baxter, N. J.; Cliff, M. J.; Bowler, M. W.; Jakeman, D. L.; Blackburn, G. M.; Waltho, J. P. α-Fluorophosphonates reveal how a phosphomutase conserves transition state conformation over hexose recognition in its two-step reaction. *PNAS* **2014***, 111*, 12384-12389.

17. Allen, K. N.; Dunaway-Mariano, D. Phosphoryl group transfer: evolution of a catalytic scaffold. *Trends Biochem. Sci.* **2004***, 29*, 495-503.

18. Burroughs, A. M.; Allen, K. N.; Dunaway-Mariano, D.; Aravind, L. Evolutionary Genomics of the HAD Superfamily: Understanding the Structural Adaptations and Catalytic Diversity in a Superfamily of Phosphoesterases and Allied Enzymes. *J. Mol. Biol.* **2006***, 361*, 1003-1034.

19. Ampaw, A. The Expression of ^{19}F labelled beta-phosphoglucomutase and the evaluation of its inhibitors, MSc. thesis, Dalhousie University. **2016**.

20. Lahiri, S. D.; Zhang, G.; Dunaway-Mariano, D.; Allen, K. N. Caught in the Act: The Structure of Phosphorylated β-Phosphoglucomutase from Lactococcus lactis. *Biochemistry* **2002***, 41*, 8351-8359.

21. Dai, J.; Finci, L.; Zhang, C.; Lahiri, S.; Zhang, G.; Peisach, E.; Allen, K. N.; Dunaway-Mariano, D. Analysis of the Structural Determinants Underlying Discrimination between Substrate and Solvent in β-Phosphoglucomutase Catalysis. *Biochemistry (N. Y.)* **2009***, 48*, 1984-1995.

22. Zhang, G.; Dai, J.; Wang, L.; Dunaway-Mariano, D.; Tremblay, L. W.; Allen, K. N. Catalytic Cycling in β-Phosphoglucomutase: A Kinetic and Structural Analysis, *Biochemistry (N. Y.)* **2005***, 44*, 9404-9416.

23. Schramm, V. L. Enzymatic transition states and transition state analogues. *Curr. Opin. Struct. Biol.* **2005***, 15*, 604-613.

24. Schramm, V. L. Transition States and Transition State Analogue Interactions with Enzymes. *Acc. Chem. Res.* **2015***, 48*, 1032-1039.

25. Svensson, F.; Engen, K.; Lundback, T.; Larhed, M.; Skold, C. Virtual Screening for Transition State Analogue Inhibitors of IRAP Based on Quantum Mechanically Derived Reaction Coordinates. *J. Chem. Inf. Model.* **2015***, 55*, 1984-1993.

26. Graham, D. L.; Lowe, P. N.; Grime, G. W.; Marsh, M.; Rittinger, K.; Smerdon, S. J.; Gamblin, S. J.; Eccleston, J. F. MgF3− as a Transition State Analog of Phosphoryl Transfer. *Chem. Biol.* **2002***, 9*, 375-381.

27. Baxter, N. J.; Blackburn, G. M.; Marston, J. P.; Hounslow, A. M.; Cliff, M. J.; Bermel, W.; Williams, N. H.; Hollfelder, F.; Wemmer, D. E.; Waltho, J. P. Anionic Charge Is Prioritized over Geometry in Aluminum and Magnesium Fluoride Transition State Analogs of Phosphoryl Transfer Enzymes. *J. Am. Chem. Soc.* **2008***, 130*, 3952-3958.

28. Baxter, N. J.; Olguin, L. F.; Goličnik, M.; Feng, G.; Hounslow, A. M.; Bermel, W.; Blackburn, G. M.; Hollfelder, F.; Waltho, J. P.; Williams, N. H. A Trojan horse transition state analogue generated by MgF3− formation in an enzyme active site. *PNAS* **2006***, 103*, 14732-14737.

29. Bucher, C.; Gilmour, R. Fluorine-Directed Glycosylation. *Angew. Chem. Int. Ed.* **2010***, 49*, 8724-8728.

30. Zamyatina, A.; Gronow, S.; Puchberger, M.; Graziani, A.; Hofinger, A.; Kosma, P. Efficient chemical synthesis of both anomers of ADP l-glycero- and d-glycero-d-manno-heptopyranose. *Carbohydr. Res.* **2003***, 338*, 2571-2589.

31. Damager, I.; Numao, S.; Chen, H.; Brayer, G. D.; Withers, S. G. Synthesis and characterisation of novel chromogenic substrates for human pancreatic α-amylase. *Carbohydr. Res.* **2004***, 339*, 1727-1737.

32. Edward, J. T.; Puskas, I. Stereochemical studies. IV. Acid-catalyzed equilibration of α- and β-forms of 3-alkoxy-4-oxa-5α-cholestanes. The anomeric effect. *Can. J. Chem.* **1962***, 40*, 711-17.

33. Qian, N.; Stanley, G. A.; Bunte, A.; Raadstroem, P. Product formation and phosphoglucomutase activities in Lactococcus lactis: cloning and characterization of a novel phosphoglucomutase gene. *Microbiology (Reading, U. K.)* **1997***, 143*, 855-865.

34. Crowley, P. B.; Kyne, C.; Monteith, W. B. Simple and inexpensive incorporation of 19F-Tryptophan for protein NMR spectroscopy. *Chem. Commun. (Cambridge, U. K.)* **2012***, 48*, 10681-10683.

35. Alibhai, M. F.; Stallings, W. C. Closing down on glyphosate inhibition- with a new structure for drug discovery. *Proc. Natl. Acad. Sci. U. S. A.* **2001***, 98*, 2944-2946.

36. Ampaw, A.; Carroll, M.; Velsen, J.; Bhattasali, D.; Cohen, A.; Bowler, M.; Jakeman, D. L. Observing enzyme ternary transition state analogue complexes by ^{19}F NMR spectroscopy. *Chem. Sci.* **2017***, 8*, 8427.

37. Forget, S. M.; Bhattasali, D.; Hart, V. C.; Cameron, T. S.; Syvitski, R. T.; Jakeman, D. L. Synthesis and enzymatic evaluation of ketose phosphonates: the interplay between mutarotation, monofluorination, and acidity. *Chem. Sci.* **2012***, 3*, 1866-1878.

38. Zhu, J.; McCormick, N. E.; Timmons, S. C.; Jakeman, D. L. Synthesis of α-deoxymono and difluorohexopyranosyl 1-phosphates and kinetic evaluation with thymidylyl- and guanidylyltransferases. *J. Org. Chem.* **2016***, 81*, 8816-8825.

39. Wang, A.; Liu, C.; Yang, S.; Zhao, Z.; Lei, P. An efficient method to synthesize novel 5-O-(6'-modified)-mycaminose 14-membered ketolides. *Tetrahedron* **2016***, 72*, 285-297.

40. Tewson, T. J.; Welch, M. J. New approaches to the synthesis of 3-deoxy-3-fluoro-D-glucose. *J. Org. Chem.* **1978***, 43*, 1090-2.

41. Danac, R.; Ball, L.; Gurr, S. J.; Fairbanks, A. J. Synthesis of UDP-glucose derivatives modified at the 3-OH as potential chain terminators of β-glucan biosynthesis. *Carbohydr. Res.* **2008***, 343*, 1012-1022.

42. Liu, Z.; Jenkinson, S. F.; Vermaas, T.; Adachi, I.; Wormald, M. R.; Hata, Y.; Kurashima, Y.; Kaji, A.; Yu, C.; Kato, A.; Fleet, G. W. J. 3-Fluoroazetidinecarboxylic Acids and trans,trans-3,4-Difluoroproline as Peptide Scaffolds: Inhibition of Pancreatic Cancer Cell Growth by a Fluoroazetidine Iminosugar. *J. Org. Chem.* **2015***, 80*, 4244-4258.

43. Kovac, P.; Yeh, H. J.; Glaudemans, C. P. Synthesis and n.m.r. spectra of methyl 2-deoxy-2-fluoro- and 3-deoxy-3-fluoro-alpha- and beta-D-glucopyranosides. *Carbohydr. Res.* **1987***, 169*, 23-34.

44. Egli, M.; Pallan, P. S.; Allerson, C. R.; Prakash, T. P.; Berdeja, A.; Yu, J.; Lee, S.; Watt, A.; Gaus, H.; Bhat, B.; Swayze, E. E.; Seth, P. P. Synthesis, Improved Antisense Activity and Structural Rationale for the Divergent RNA Affinities of 3'-Fluoro Hexitol Nucleic Acid (FHNA and Ara-FHNA) Modified Oligonucleotides. *J. Am. Chem. Soc.* **2011***, 133*, 16642-16649.

45. Vallinayagam, R.; Schmitt, F.; Barge, J.; Wagnieres, G.; Wenger, V.; Neier, R.; Juillerat-Jeanneret, L. Glycoside Esters of 5-Aminolevulinic Acid for Photodynamic Therapy of Cancer. *Bioconjugate Chem.* **2008***, 19*, 821-839.

46. Lin, G.; Sun, H. G.; Liu, H. Study of uridine 5'-diphosphate (UDP)-galactopyranose mutase using UDP-5-fluorogalactopyranose as a probe: Incubation results and mechanistic implications. *Org. Lett.* **2016***, 18*, 3438-3441.

47. Stick, R.; Williams, S. Ethers. In *Carbohydrates: The Essential Molecules of Life* Elsevier Ltd.: Oxford, UK, 2009; pp 43.

48. Jambal, I.; Kefurt, K.; Hlavackova, M.; Moravcova, J. Synthesis of 2-fluoro and 4-fluoro galactopyranosyl phosphonate analogs of UDP-Gal. *Carbohydr. Res.* **2012***, 360*, 31-39.

49. Deller, R. C.; Congdon, T.; Sahid, M. A.; Morgan, M.; Vatish, M.; Mitchell, D. A.; Notman, R.; Gibson, M. I. Ice recrystallisation inhibition by polyols: comparison of molecular and macromolecular inhibitors and role of hydrophobic units. *Biomater. Sci.* **2013***, 1*, 478-485.

50. Greene, T.; Wuts, P., Eds.; In *Protective Groups in Organic Synthesis;* John Wiley & Sons, Inc.: 1991; .

51. Nakayama, K.; Uoto, K.; Higashi, K.; Soga, T.; Kusama, T. A useful method for deprotection of the protective allyl group at the anomeric oxygen of carbohydrate moieties using tetrakis(triphenylphosphine)palladium. *Chem. Pharm. Bull.* **1992***, 40*, 1718-20.

52. Csuk, R.; Prell, E. Unexpected formation of oxetanes from a geminal difluorinated δ-lactone. *Tetrahedron* **2010***, 66*, 1313-1318.

53. Umemura, E.; Tsuchiya, T.; Kobayashi, Y.; Tanaka, K. A synthetic study of methyl 3-deoxy-3-fluoro-α-D-glucopyranosides from methyl 2,3-anhydro-α-D-allopyranosides, and synthesis of 3'-deoxy-3'-fluorokanamycin A and 3'-chloro-3'-deoxykanamycin A. *Carbohydr. Res.* **1992***, 224*, 141-63.

54. AnonymousAIST: Integrated Spectral Database System of Organic Compounds. (Data were obtained from the National Institute of Advanced Industrial Science and Technology (Japan)). (accessed 06/28, 2017).

55. Dondoni, A.; Marra, A.; Pasti, C. Stereoselective synthesis of C-glycosyl phosphonates from their ketols. Reconsideration of an abandoned route. *Tetrahedron: Asymmetry* **2000***, 11*, 305-317.

56. Mancuso, A. J.; Brownfain, D. S.; Swern, D. Structure of the dimethyl sulfoxide-oxalyl chloride reaction product. Oxidation of heteroaromatic and diverse alcohols to carbonyl compounds. *J. Org. Chem.* **1979***, 44*, 4148-50.

57. Corcilius, L.; Elias, N. T.; Ochoa, J. L.; Linington, R. G.; Payne, R. J. Total synthesis of Glycinocins A-C. *J. Org. Chem.* **2017**, Ahead of Print.

58. Harrowven, D. C.; Guy, I. L. KF-Silica as a stationary phase for the chromatographic removal of tin residues from organic compounds. *Chem. Commun. (Cambridge, U. K.)* **2004**, 1968-1969.

59. Leibner, J. E.; Jacobus, J. Facile product isolation from organostannane reductions of organic halides. *J. Org. Chem.* **1979***, 44*, 449-50.

60. MacDonald, S. S.; Blaukopf, M.; Withers, S. G. N-Acetylglucosaminidases from CAZy Family GH3 Are Really Glycoside Phosphorylases, Thereby Explaining Their Use of Histidine as an Acid/Base Catalyst in Place of Glutamic Acid. *J. Biol. Chem.* **2015***, 290*, 4887-4895.

Appendix A. ^{19}F NMR spectra of synthetic products

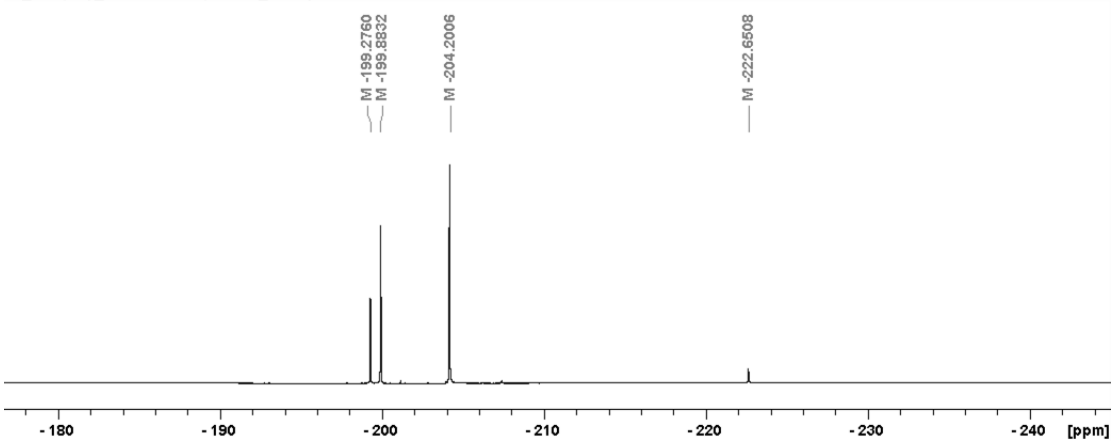

$^{19}F\{^{1}H\}$ NMR spectrum (470 MHz, $CDCl_3$) of 2-deoxy-2-fluoro-3,4,6-tri-*O*-acetyl-D-manno/glucopyranoside (**2**)

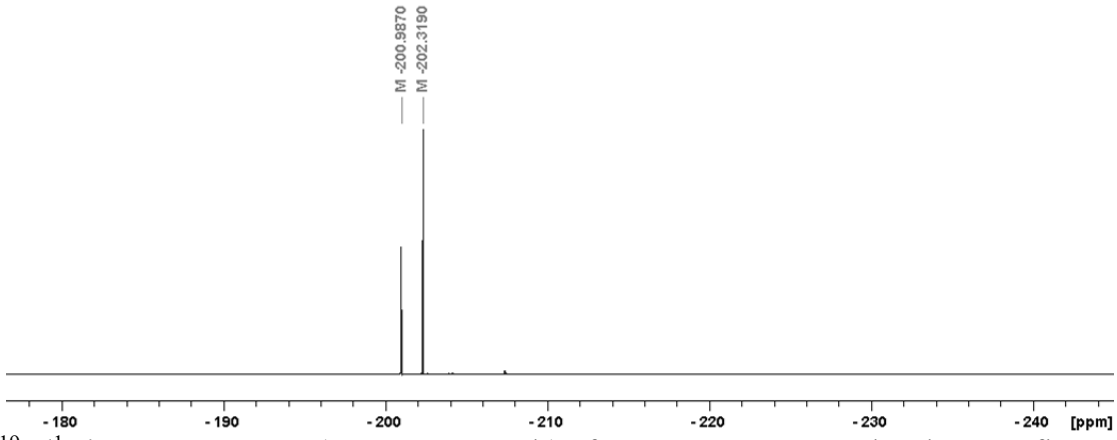

$^{19}F\{^{1}H\}$ NMR spectrum (470 MHz, $CDCl_3$) of 1,3,4,6-tetra-*O*-acetyl-2-deoxy-2-fluoro-D-glucopyranose (**3**)

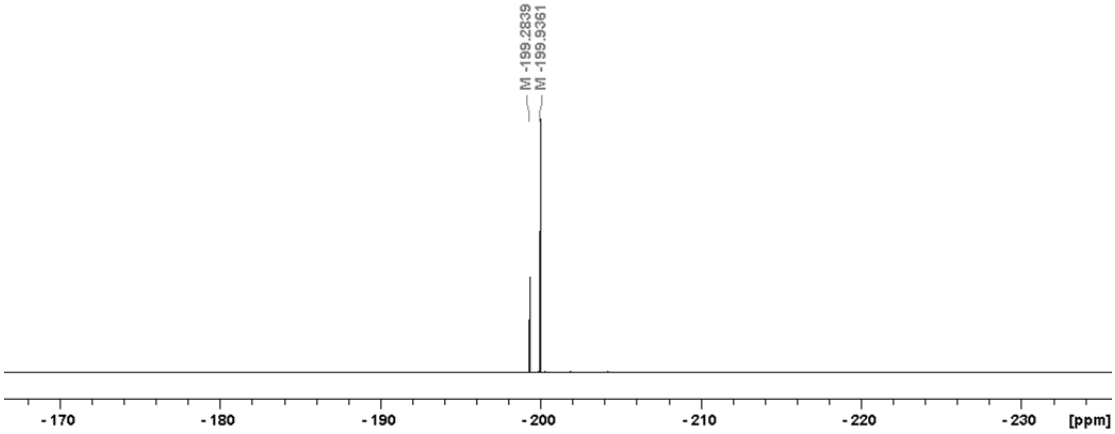

$^{19}F\{^{1}H\}$ NMR spectrum (470 MHz, $CDCl_3$) of 2-deoxy-2-fluoro-3,4,6-tri-*O*-acetyl-D-glucopyranose (**4**)

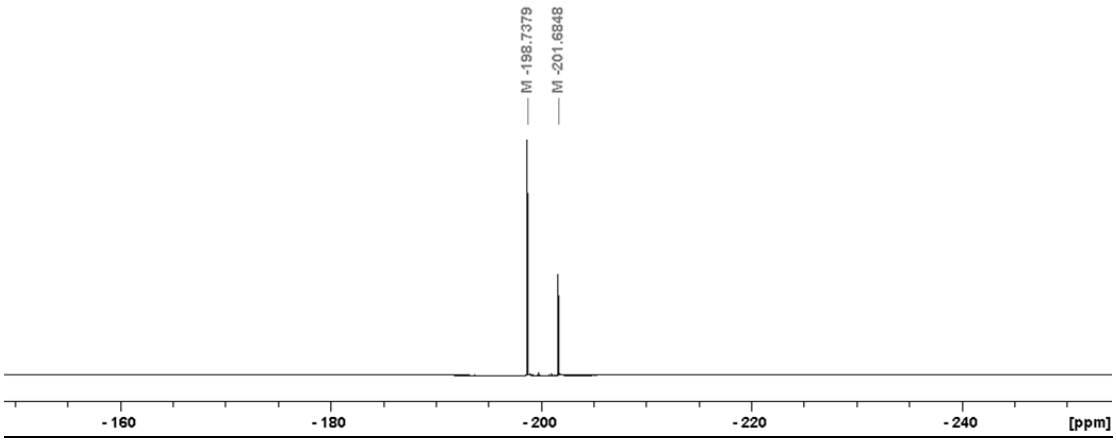

$^{19}F\{^{1}H\}$ NMR spectrum (470 MHz, $CDCl_3$) of 2,4-dinitrophenyl 2-deoxy-2-fluoro-3,4,6-tri-*O*-acetyl-D-glucopyranose (**5**)

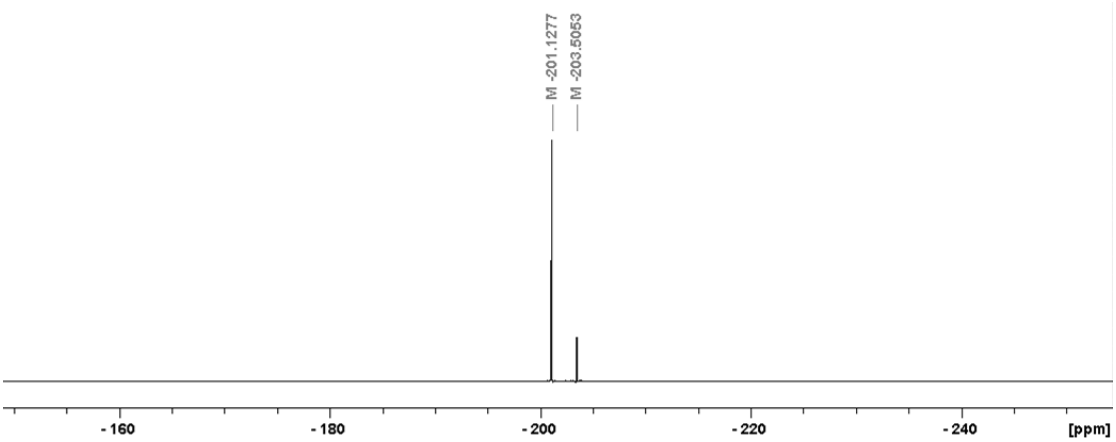

$^{19}F\{^{1}H\}$ NMR spectrum (470 MHz, CD_3OD) of 2,4-dinitrophenyl 2-deoxy-2-fluoro-β-D-glucopyranose (**6**)

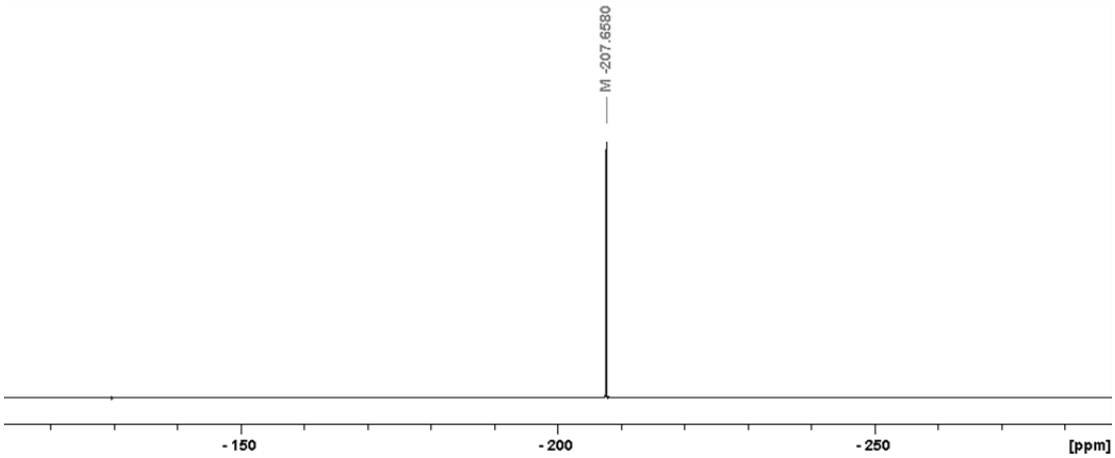

^{19}F NMR (470 MHz, $CDCl_3$) spectrum of 3-deoxy-3-fluoro- 1,2: 5,6-di-*O*-isopropylidene-α-D-glucofuranose (**10**)

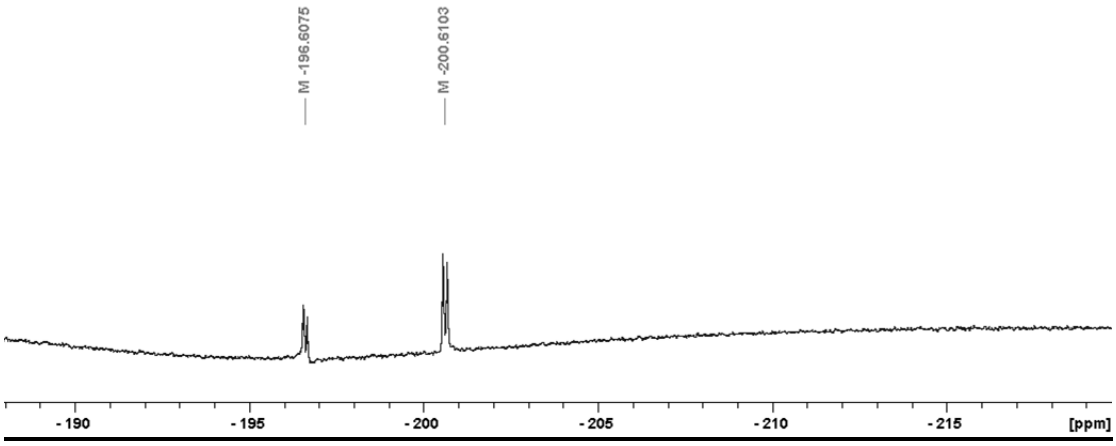

^{19}F NMR (470 MHz, $CDCl_3$) spectrum of methyl 3-deoxy-3-fluoro-α/β-D-glucopyranoside (**11**)

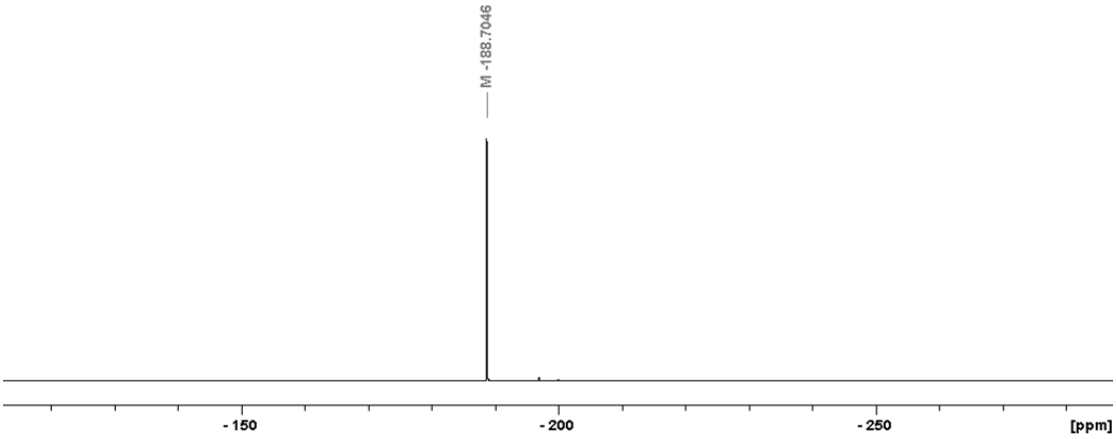

^{19}F NMR spectrum (470 MHz, $CDCl_3$) of methyl 2,4,6-tri-*O*-benzyl-3-deoxy-3-fluoro-β-D-glucopyranoside (**12**)

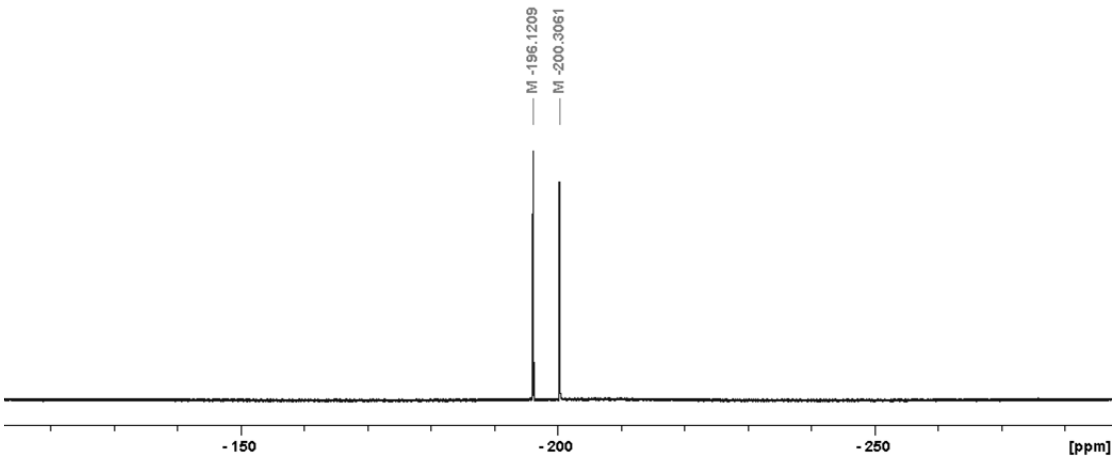

^{19}F NMR spectrum (470 MHz, $CDCl_3$) of allyl 3-deoxy-3-fluoro-D-glucopyranoside (**13**)

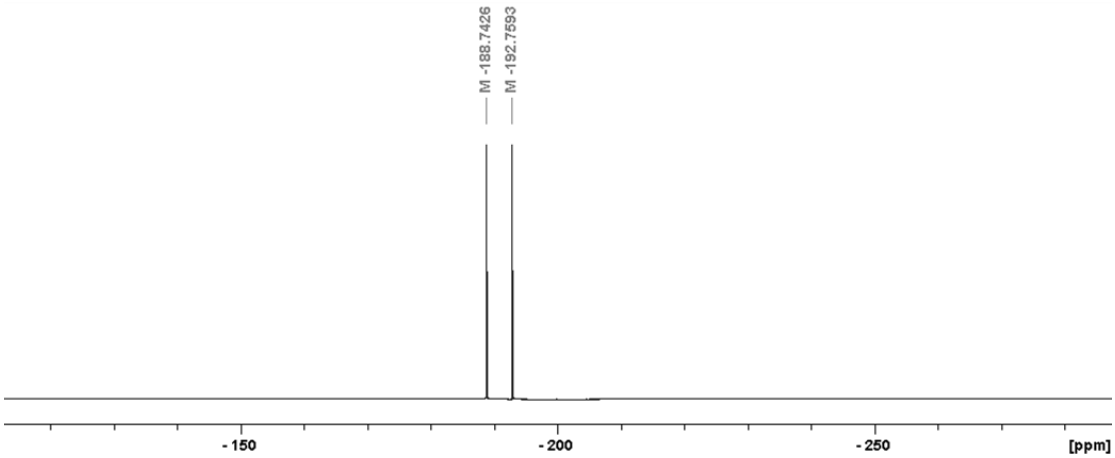

$^{19}F\{^{1}H\}$ NMR spectrum (470 MHz, $CDCl_3$) of allyl 2,4,6-tri-*O*-benzyl-3-deoxy-3-fluoro-D-glucopyranoside (**14**)

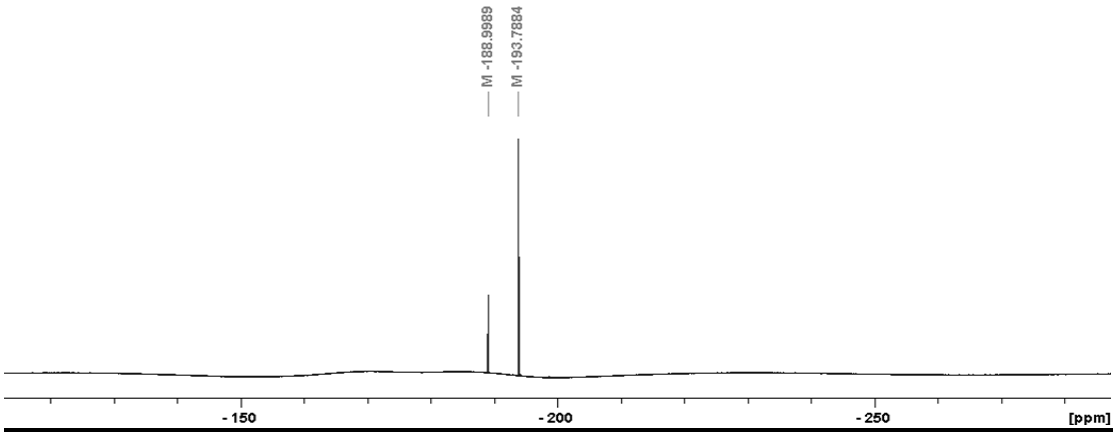

^{19}F NMR spectrum (470 MHz, $CDCl_3$) of 2,4,6-tri-*O*-benzyl-3-deoxy-3-fluoro-D-glucopyranose (**15**)

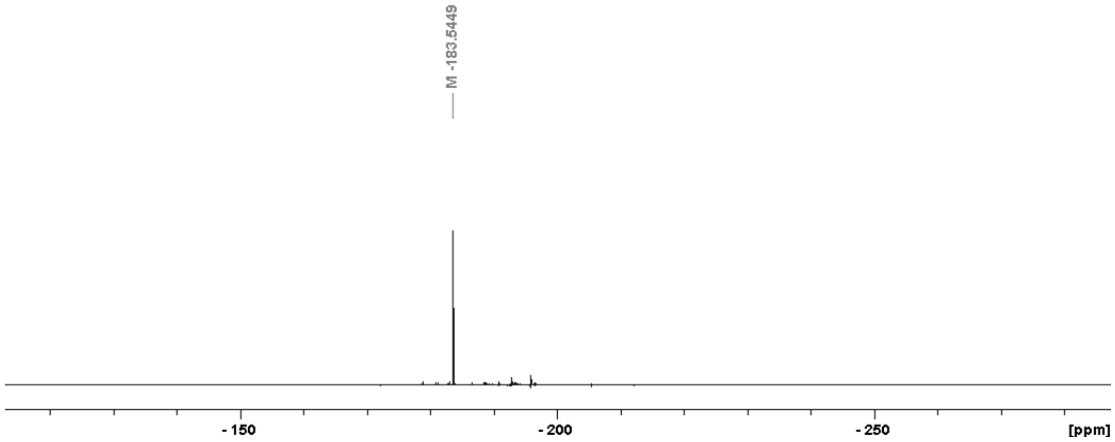

$^{19}F\{^{1}H\}$ NMR spectrum (470 MHz, $CDCl_3$) of 2,4,6-tri-*O*-benzyl-3-deoxy-3-fluoro-D-gluconolactone (**16**)

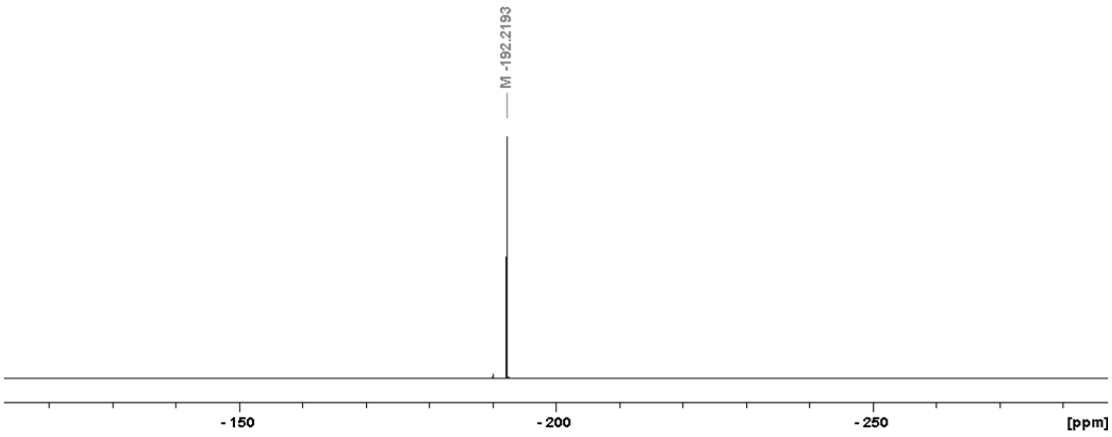

$^{19}F\{^{1}H\}$ NMR spectrum (470 MHz, $CDCl_3$) of 1-(dimethyl phosphonatylmethyl)-2,4,6-tri-*O*-benzyl-3-deoxy-3-fluoro-α-D-glucopyranose (**17**)

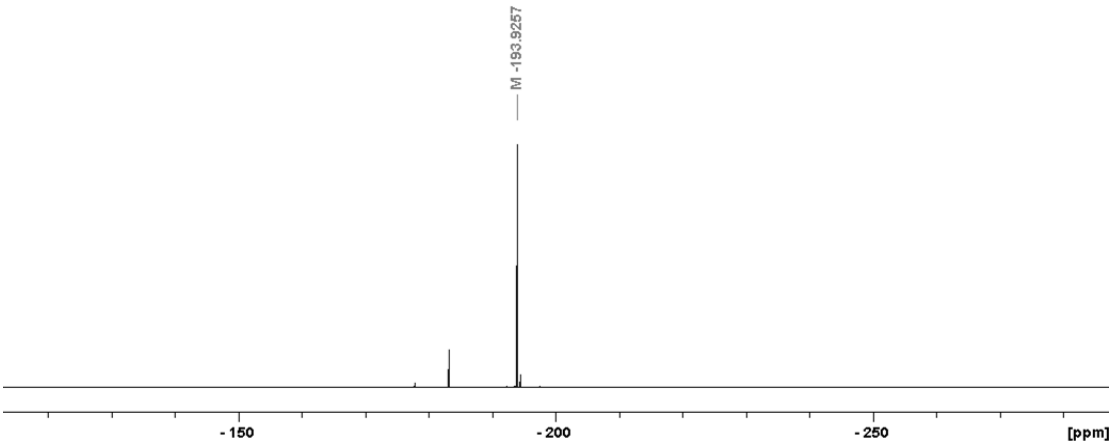

$^{19}F\{^{1}H\}$ NMR spectrum (470 MHz, $CDCl_3$) of (methyl oxalyl) 1-(dimethyl phosphonatylmethyl)-2,4,6-tri-*O*-benzyl-3-deoxy-3-fluoro-α-D-glucopyranose (**18**)

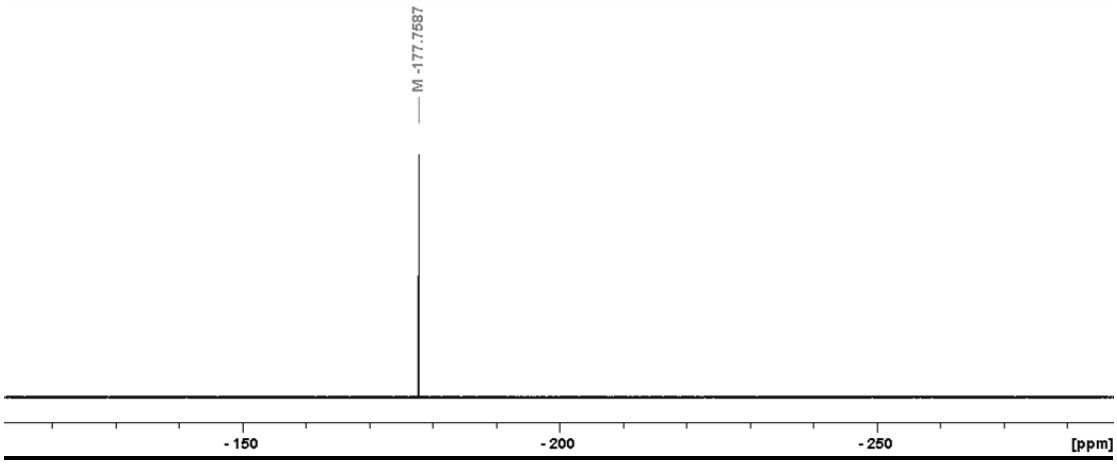

$^{19}F\{^{1}H\}$ NMR spectrum (470 MHz, $CDCl_3$) of (E/Z)-1-(dimethylphosphonomethylene)-2,4,6-tri-*O*-benzyl-1,3-deoxy-3-fluoro-D-glucopyranosyl-2-ylidene (**19**)

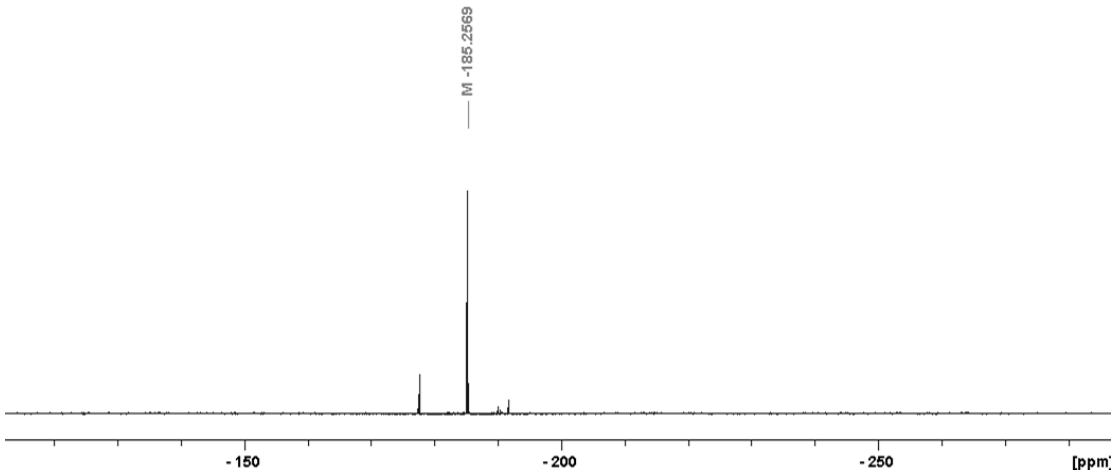

$^{19}F\{^{1}H\}$ NMR spectrum (470 MHz, $CDCl_3$) of (E/Z)-1-β-dimethylphosphonomethylene-2,4,6-tri-*O*-benzyl-1,3-deoxy-3-fluoro-D-glucopyranosyl-2-ylidene (**19**) and 2,4,6-tri-*O*-benzyl-3-deoxy-3-fluoro-β-D-glucopyranosylmethylphosphonate (**20**) mixture

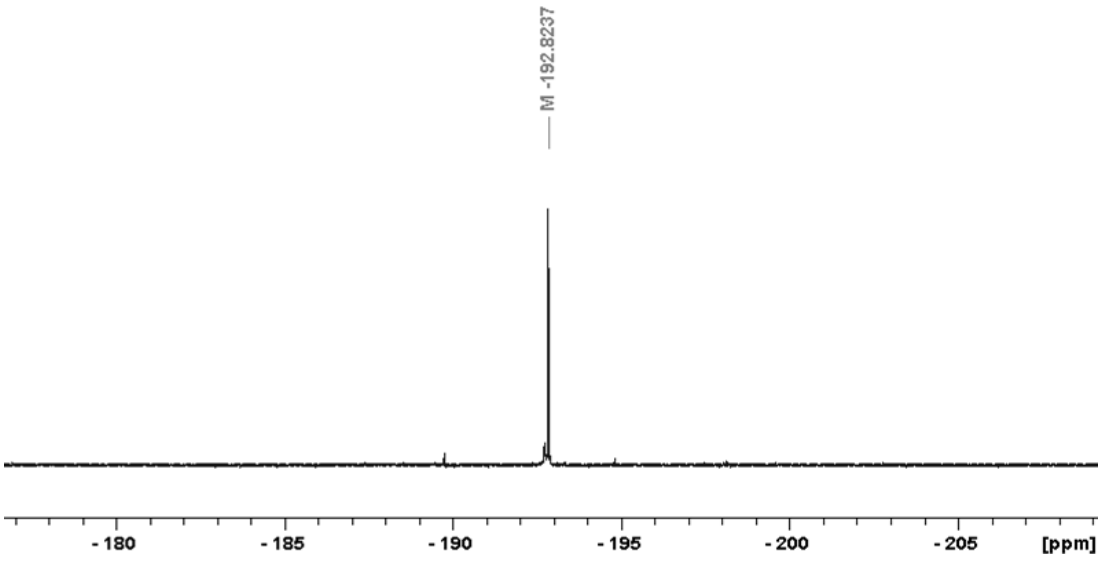

$^{19}F\{^{1}H\}$ NMR spectrum (470 MHz, D_2O) of diammonium 3-deoxy-3-fluoro-β-D-glucopyranosylmethylphosphonate (**21**)

Appendix B. Full range ^{1}H NMR spectra of synthetic products

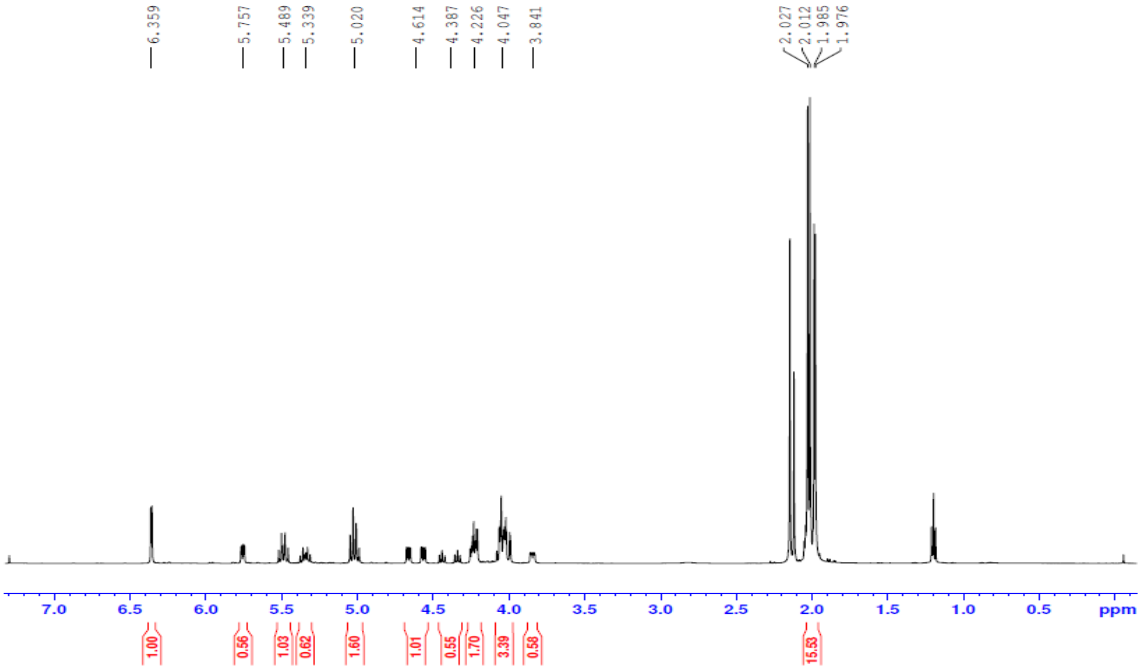

^{1}H NMR (500 MHz, $CDCl_3$) spectrum of 1,3,4,6-tetra-*O*-acetyl-2-deoxy-2-fluoro-D-glucopyranose (**3**)

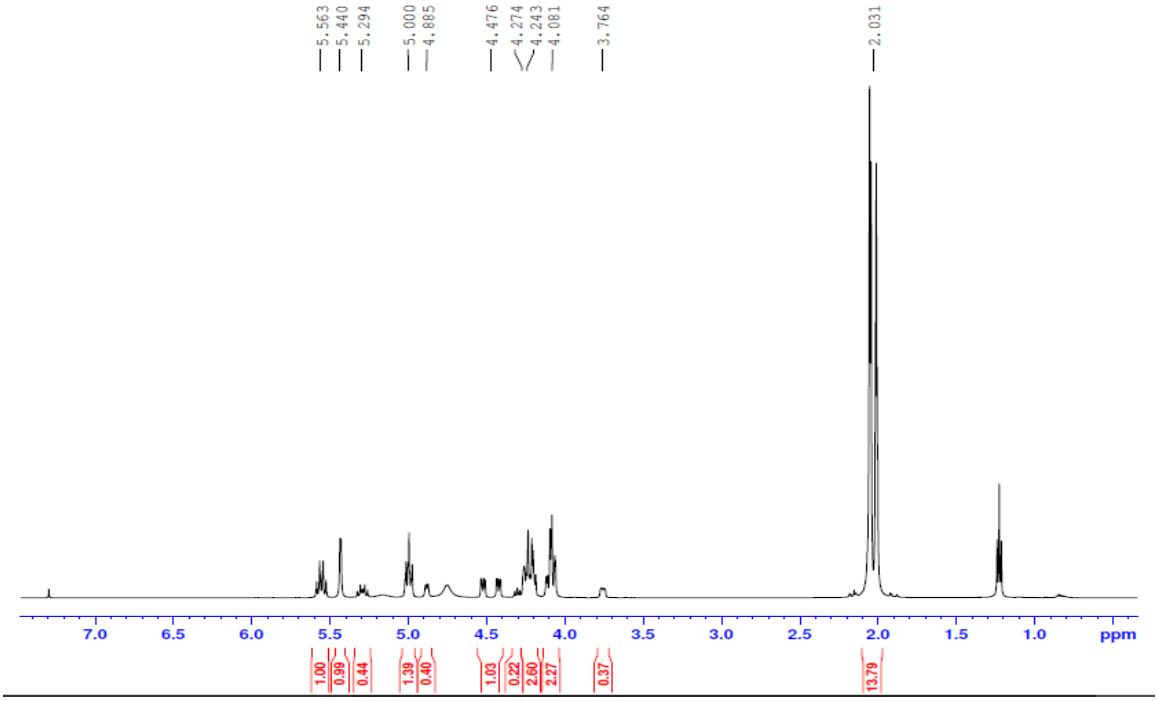

^{1}H NMR (500 MHz, $CDCl_3$) spectrum of 2-deoxy-2-fluoro-3,4,6-tri-*O*-acetyl-D-glucopyranose (**4**)

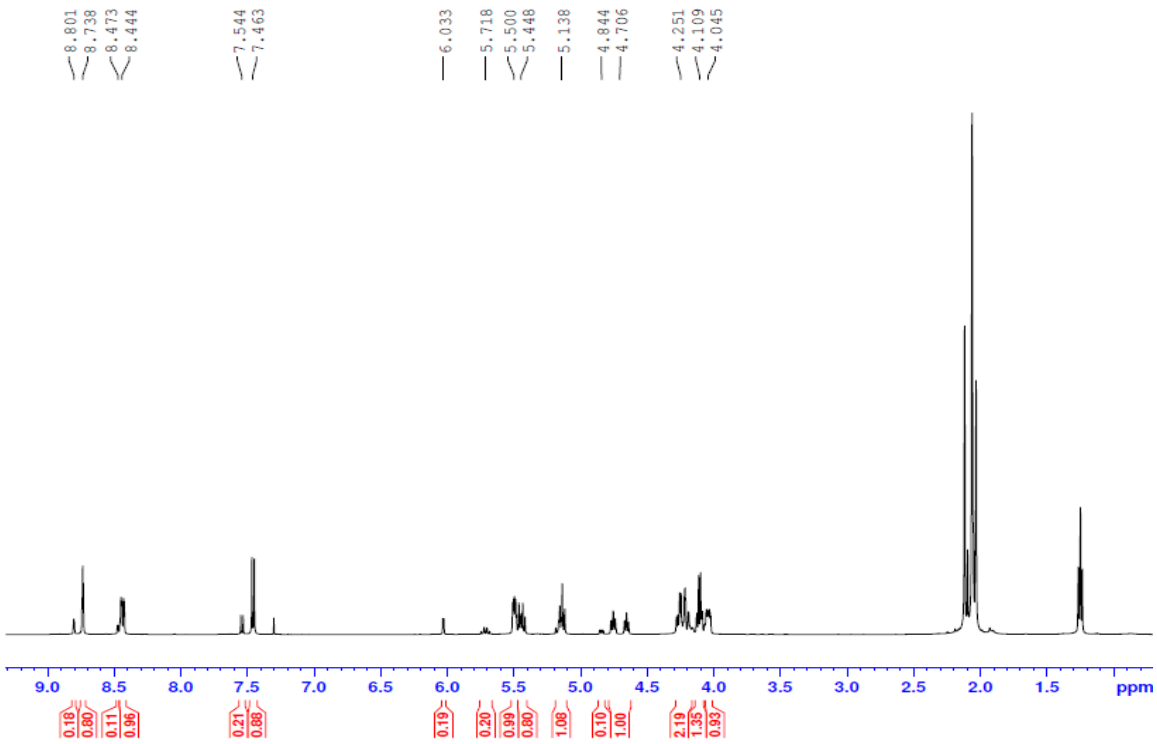

^{1}H NMR (500 MHz, $CDCl_3$) spectrum of 2,4-dinitrophenyl 2-deoxy-2-fluoro-3,4,6-tri-*O*-acetyl-D-glucopyranose (**5**)

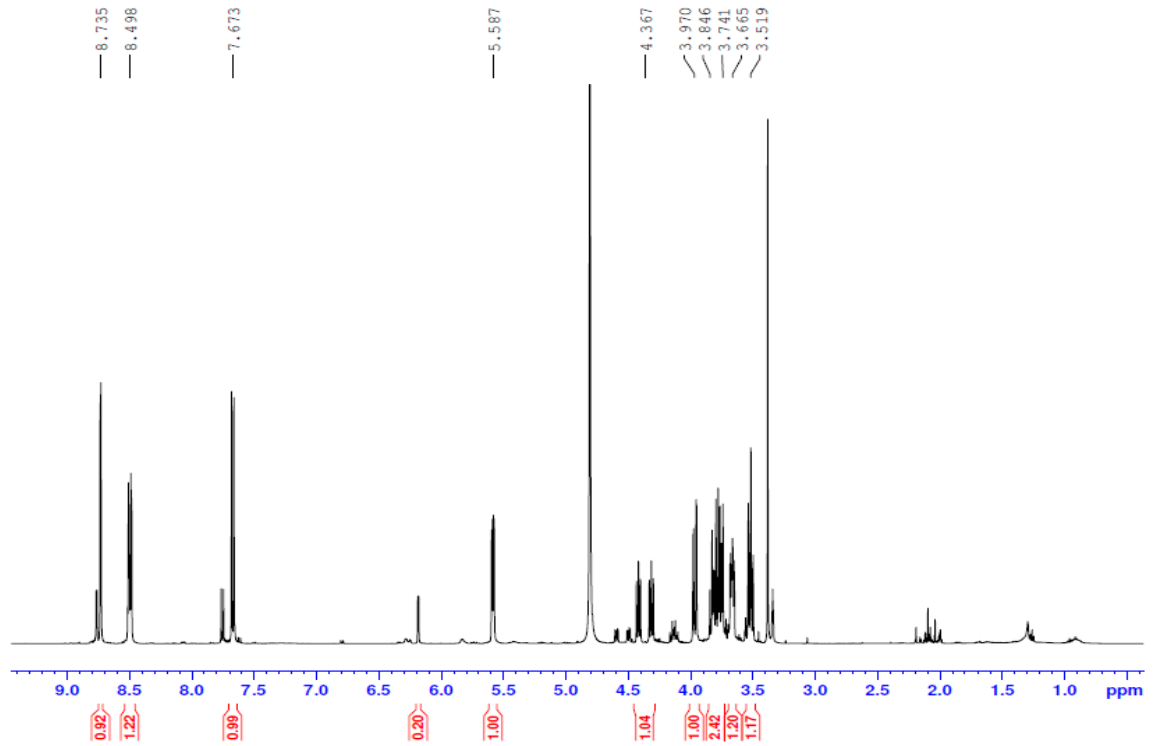

^{1}H NMR spectrum (500 MHz, CD_3OD) of 2,4-dinitrophenyl 2-deoxy-2-fluoro-β-D-glucopyranoside (**6**)

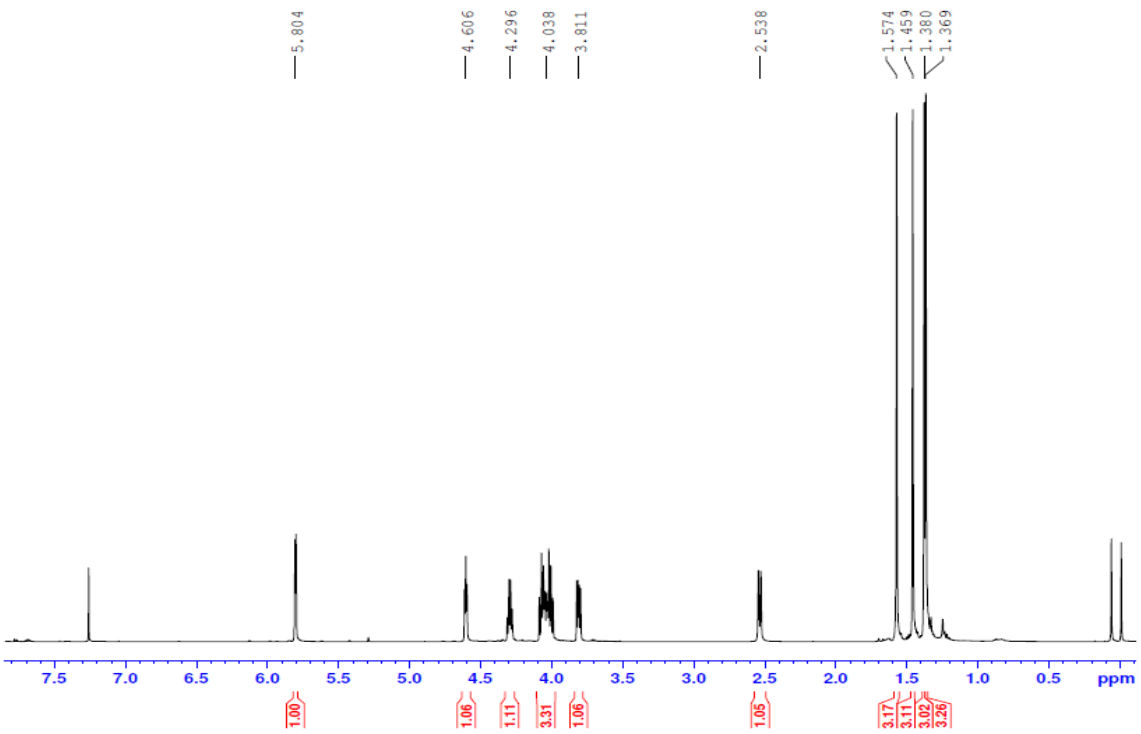

^{1}H NMR (500 MHz, $CDCl_3$) spectrum of 1,2:5,6-di-*O*-isopropylidene-α-D-allofuranose (**9**)

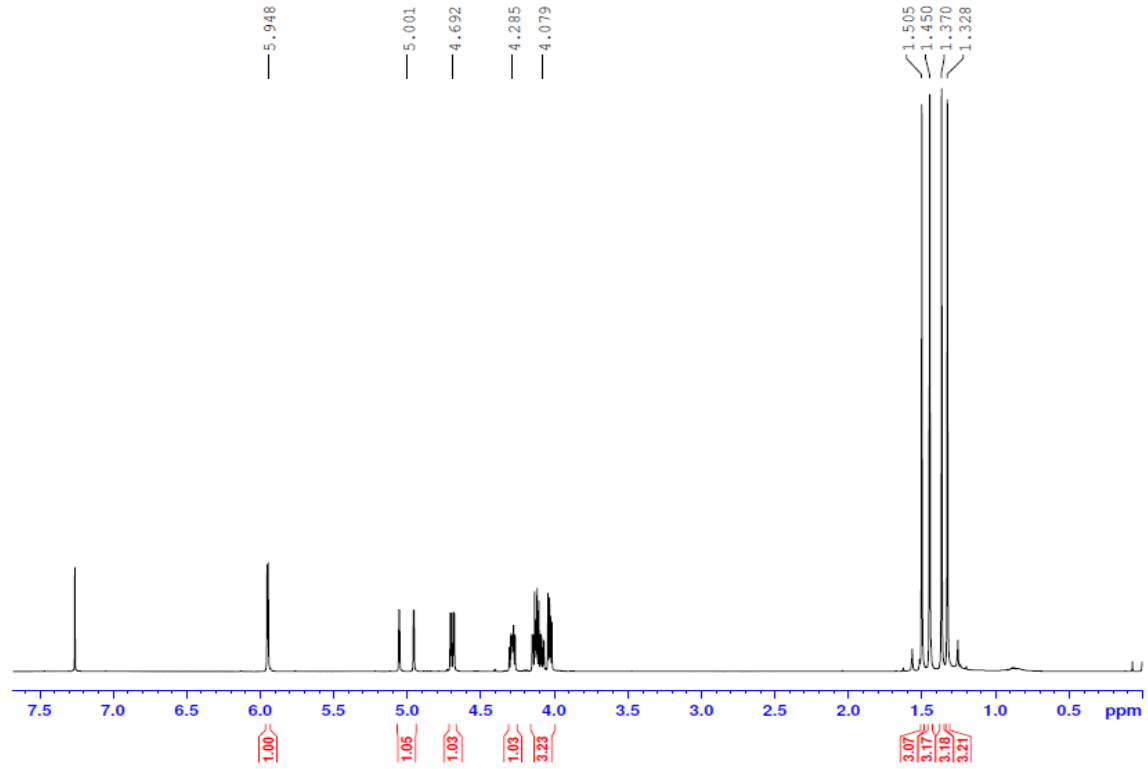

^{1}H NMR (500 MHz, $CDCl_3$) spectrum of 3-deoxy-3-fluoro- 1,2: 5,6-di-*O*-isopropylidene-α-D-glucofuranose (**10**)

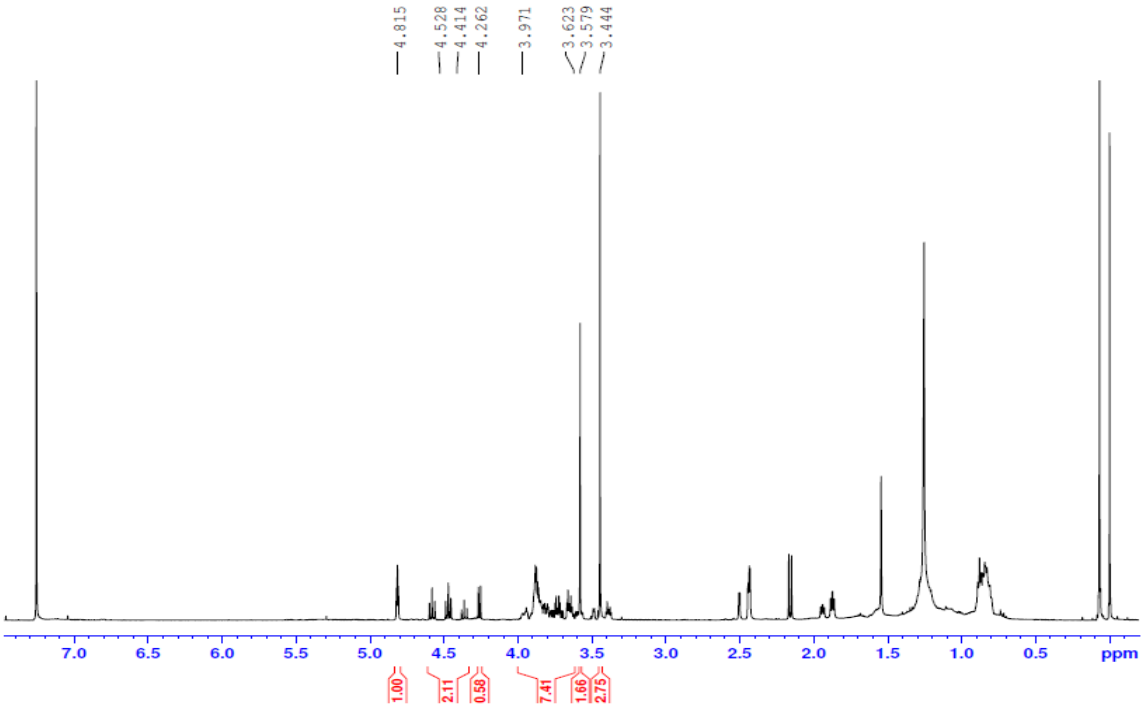

^{1}H NMR (500 MHz, $CDCl_3$) spectrum of methyl 3-deoxy-3-fluoro-α/β-D-glucopyranoside (**11**)

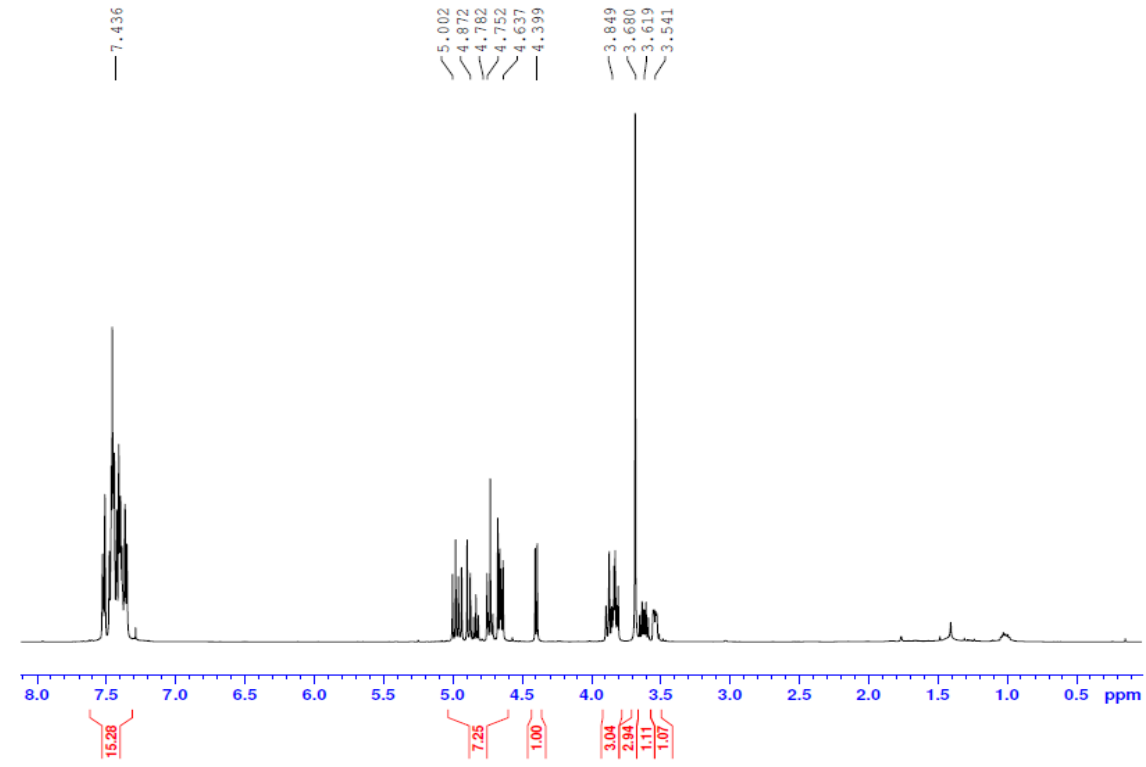

^{1}H NMR (500 MHz, $CDCl_3$) spectrum of methyl 2,4,6-tri-*O*-benzyl-3-deoxy-3-fluoro-β-D-glucopyranoside (**12**)

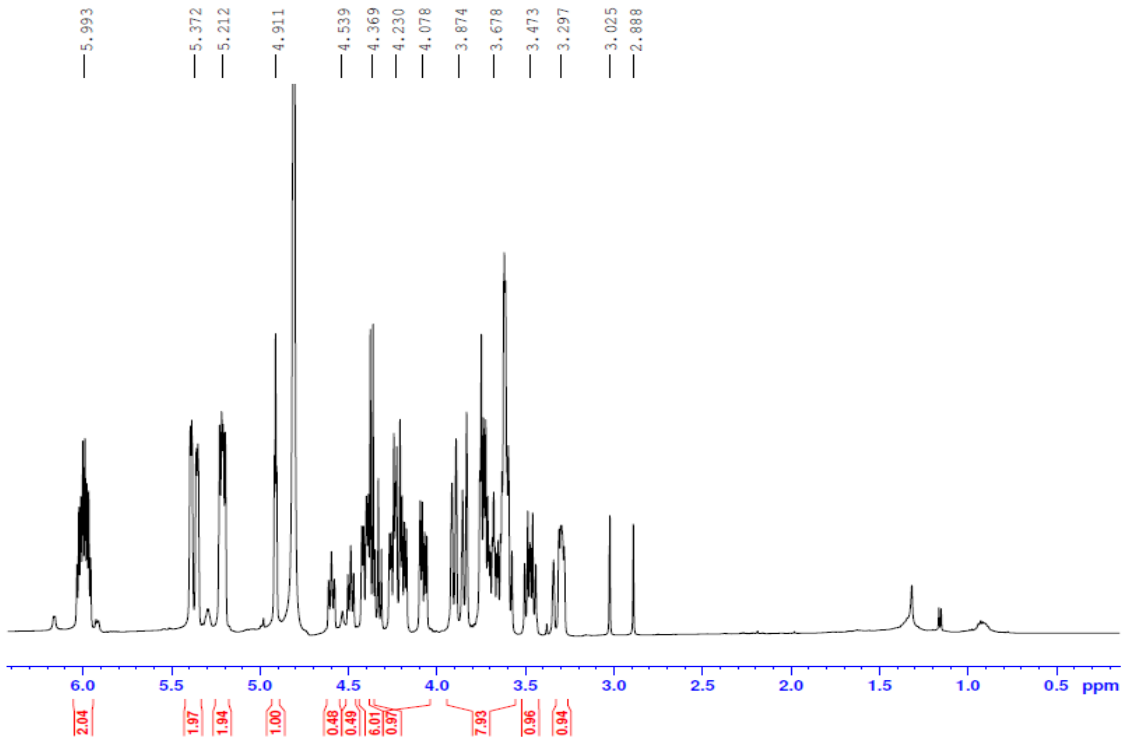

^{1}H NMR (500 MHz, CD_3OD) spectrum of allyl 3-deoxy-3-fluoro-D-glucopyranoside (**13**)

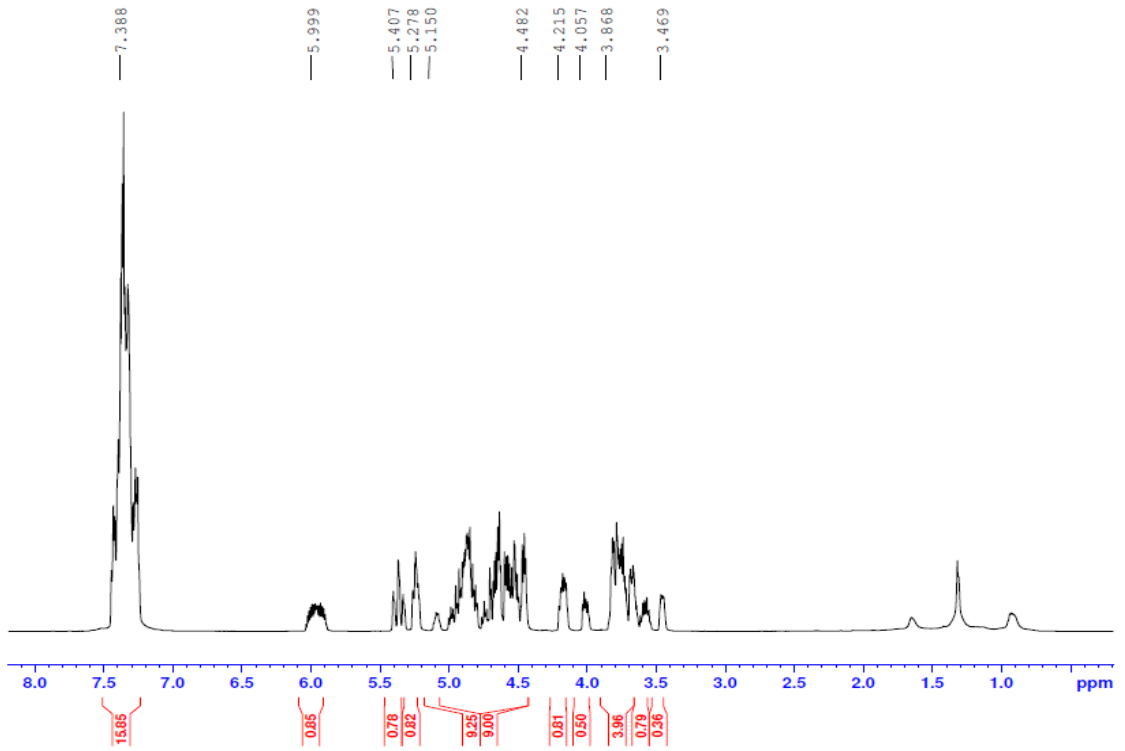

^{1}H NMR spectrum (500 MHz, $CDCl_3$) of allyl 2,4,6-tri-*O*-benzyl-3-deoxy-3-fluoro-D-glucopyranoside (**14**)

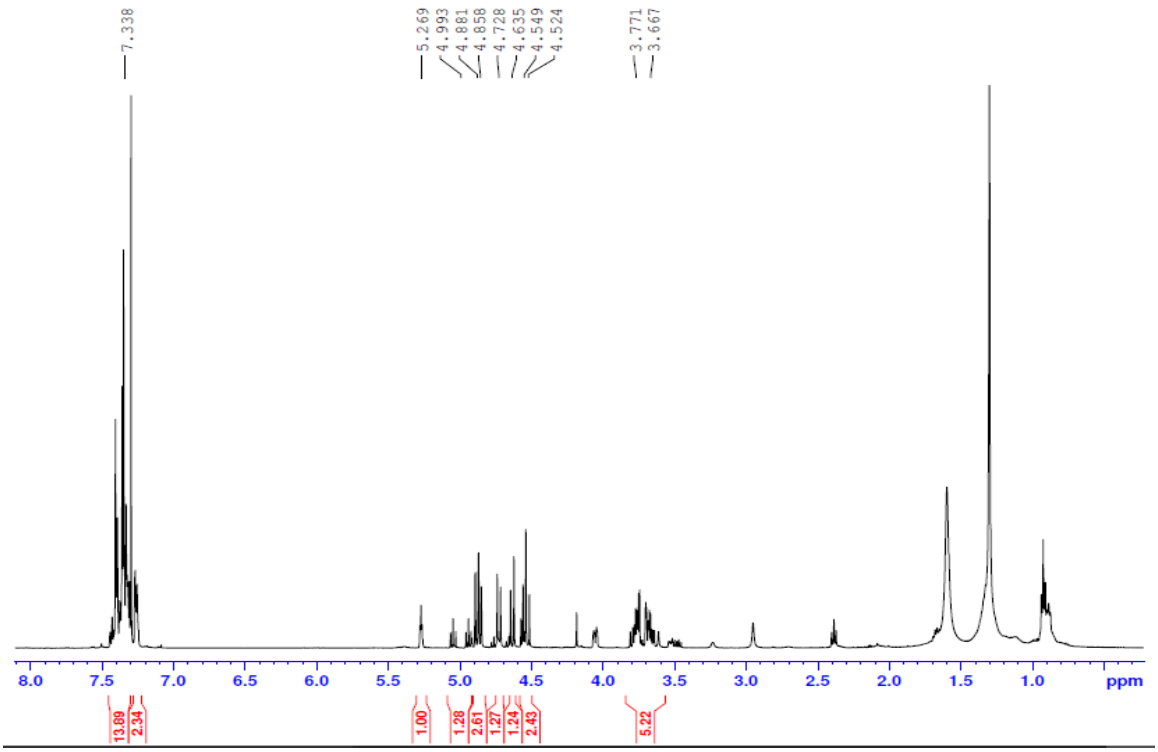

^{1}H NMR spectrum (500 MHz, $CDCl_3$) of 2,4,6-tri-*O*-benzyl-3-deoxy-3-fluoro-D-glucopyranose (**15**)

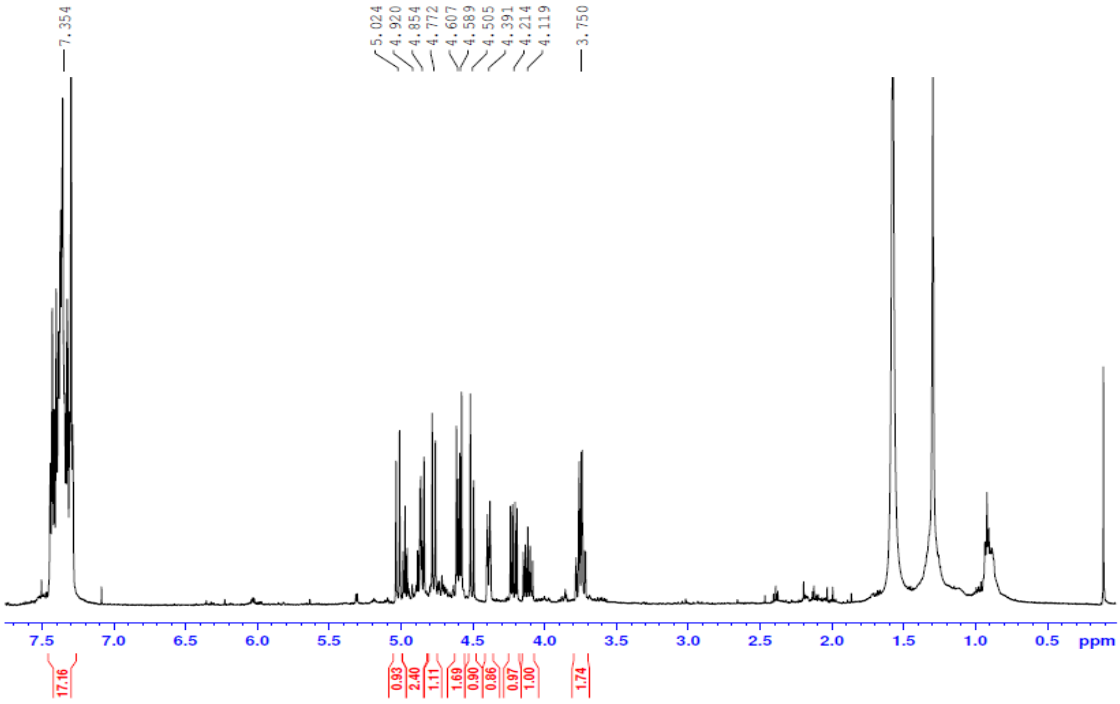

^{1}H NMR spectrum (500 MHz, $CDCl_3$) of 2,4,6-tri-*O*-benzyl-3-deoxy-3-fluoro-D-gluconolactone (**16**)

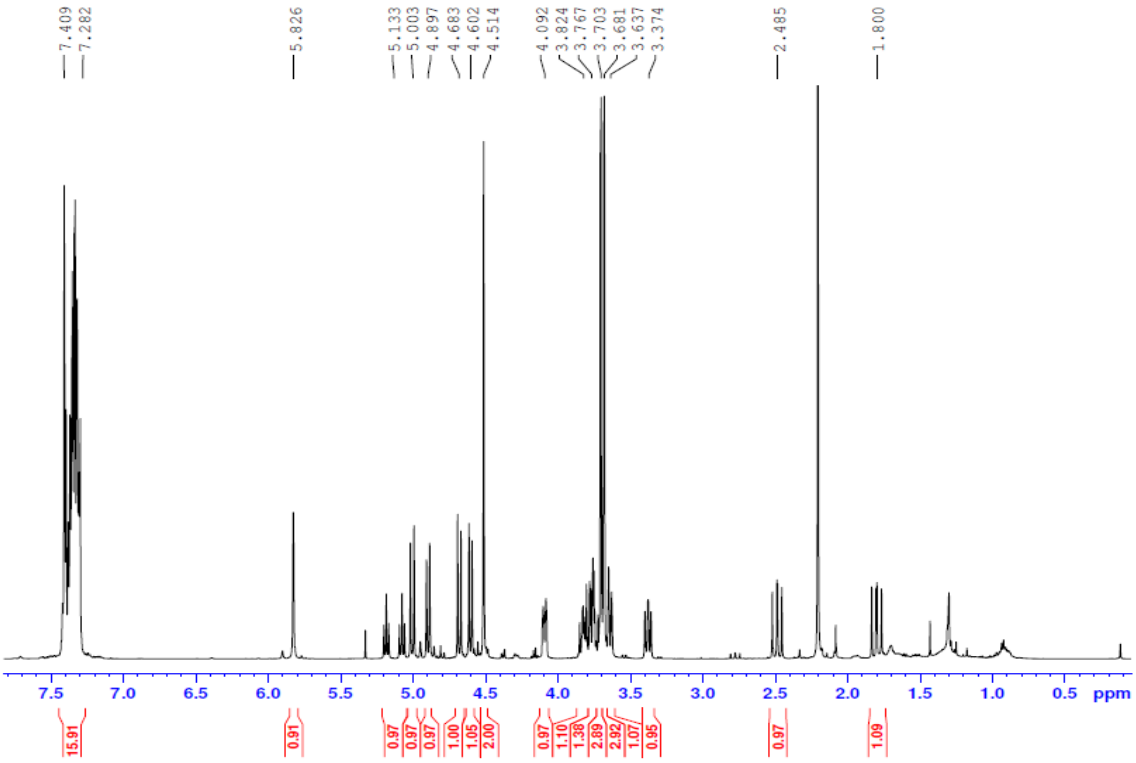

^{1}H NMR spectrum (500 MHz, $CDCl_3$) of 1-(dimethyl phosphonatylmethyl)-2,4,6-tri-*O*-benzyl-3-deoxy-3-fluoro-α-D-glucopyranose (**17**)

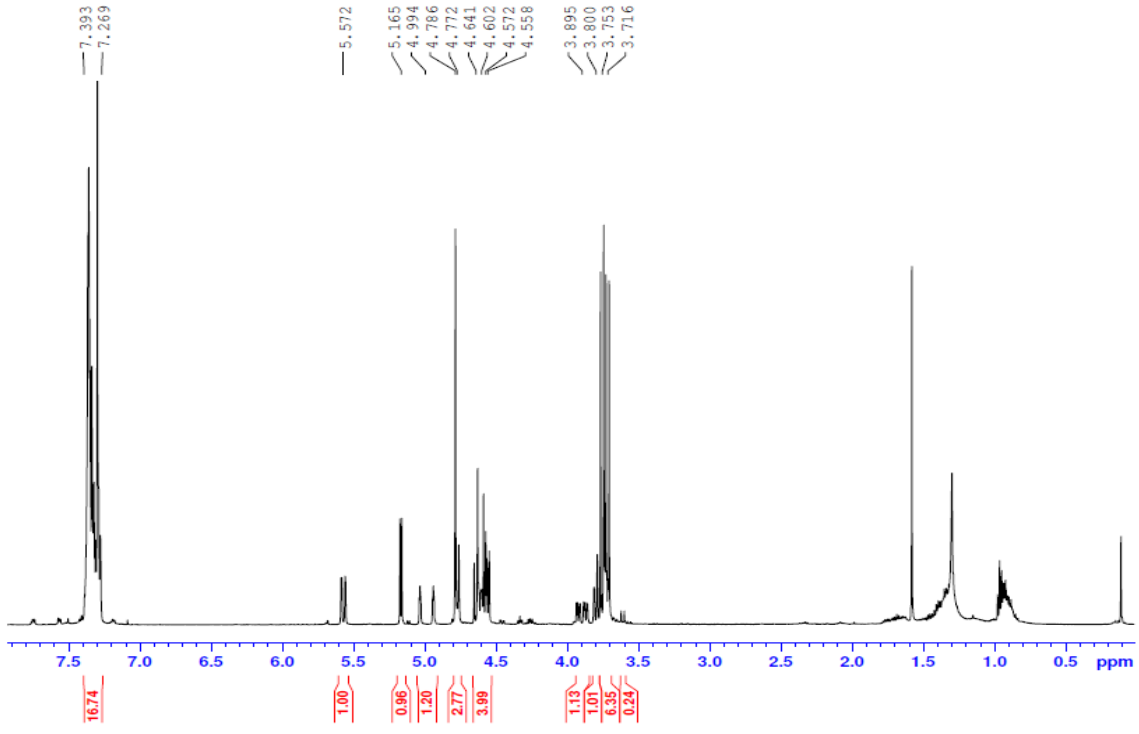

^{1}H NMR spectrum (500 MHz, $CDCl_3$) of (E/Z)-1-β-dimethylphosphonomethylene-2,4,6-tri-*O*-benzyl-1,3-deoxy-3-fluoro-D-glucopyranosyl-2-ylidene (**19**)

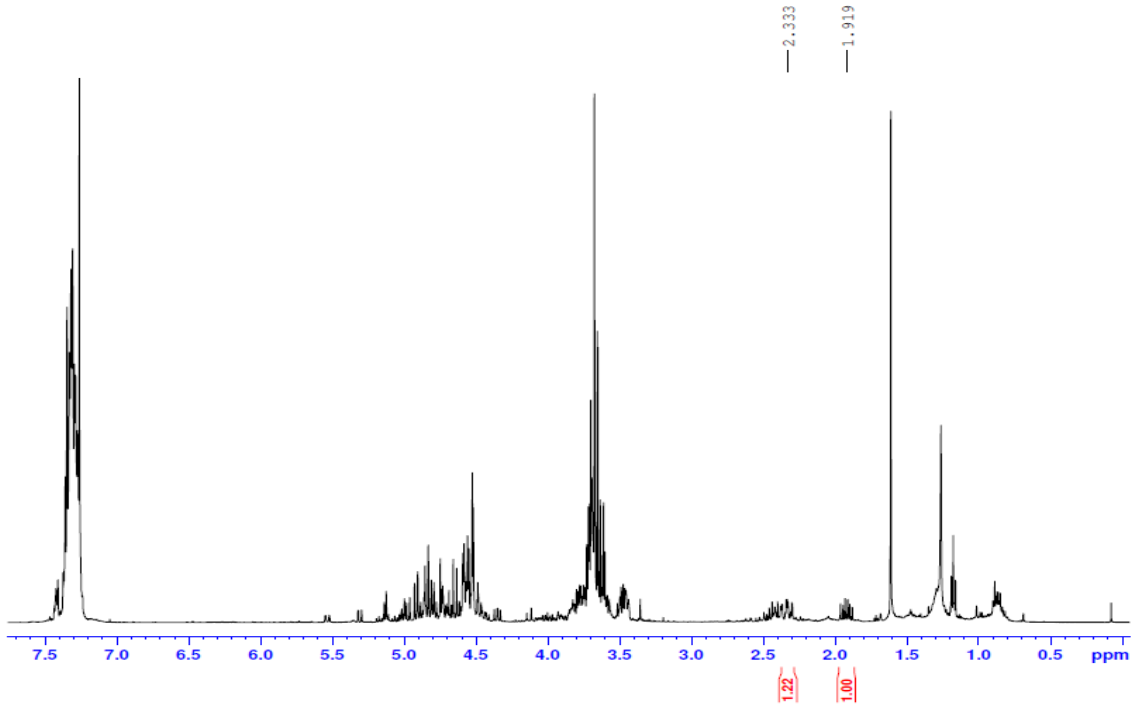

^{1}H NMR spectrum (500 MHz, $CDCl_3$) of (E/Z)-1-(dimethylphosphonomethylene)-2,4,6-tri-*O*-benzyl-1,3-deoxy-3-fluoro-D-glucopyranosyl-2-ylidene (**19**) and 2,4,6-tri-*O*-benzyl-3-deoxy-3-fluoro-β-D-glucopyranosylmethylphosphonate (**20**) mixture

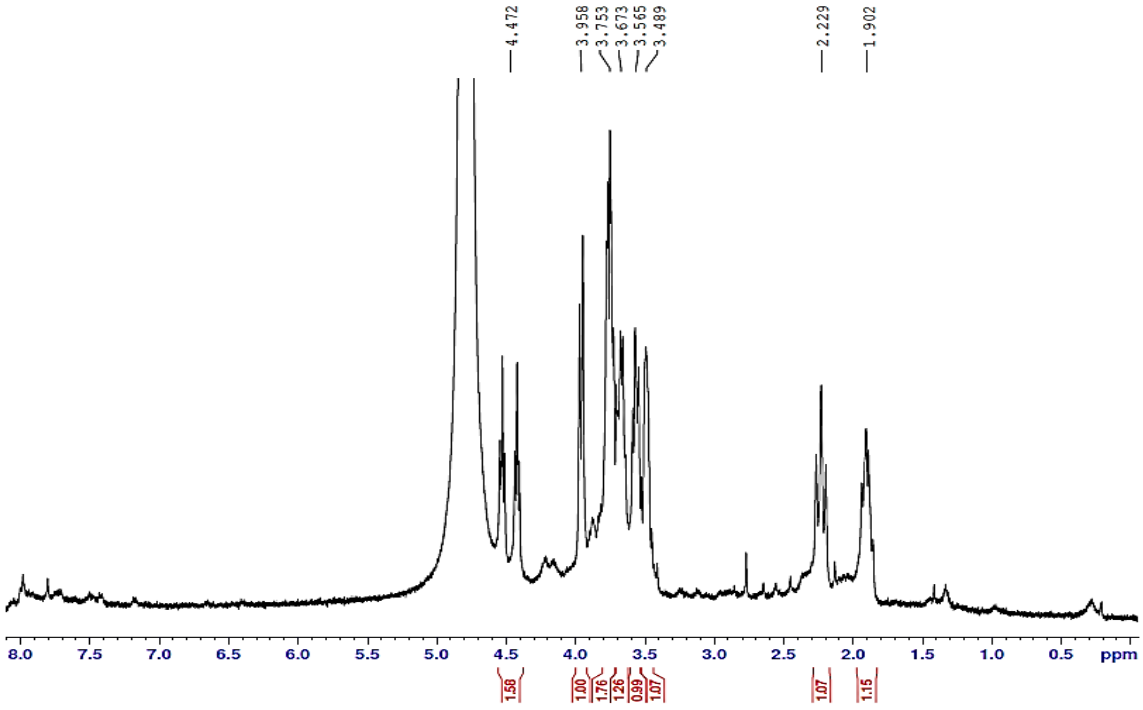

^{1}H NMR spectrum (500 MHz, D_2O) of diammonium 3-deoxy-3-fluoro-β-D-glucopyranosylmethylphosphonate (**21**)

Appendix C. $^{13}C\{^{1}H\}$ NMR spectra of synthetic products

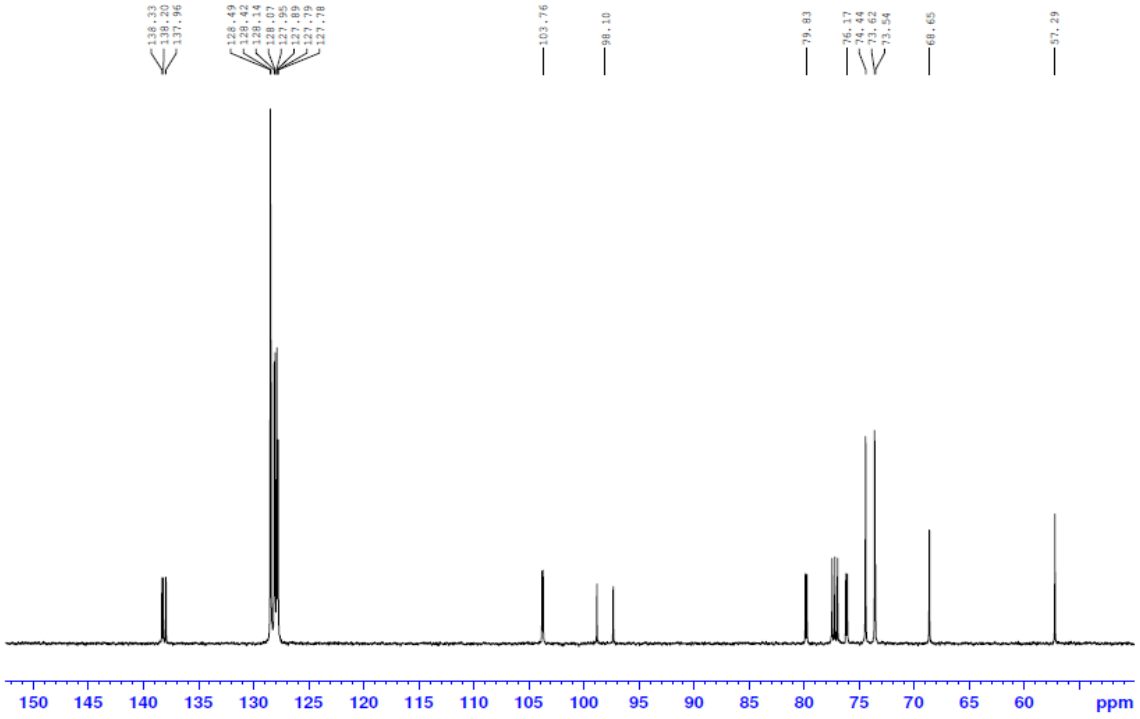

$^{13}C\{^{1}H\}$ NMR (125 MHz, $CDCl_3$) spectrum of methyl 2,4,6-tri-*O*-benzyl-3-deoxy-3-fluoro-β-D-glucopyranoside (**12**)

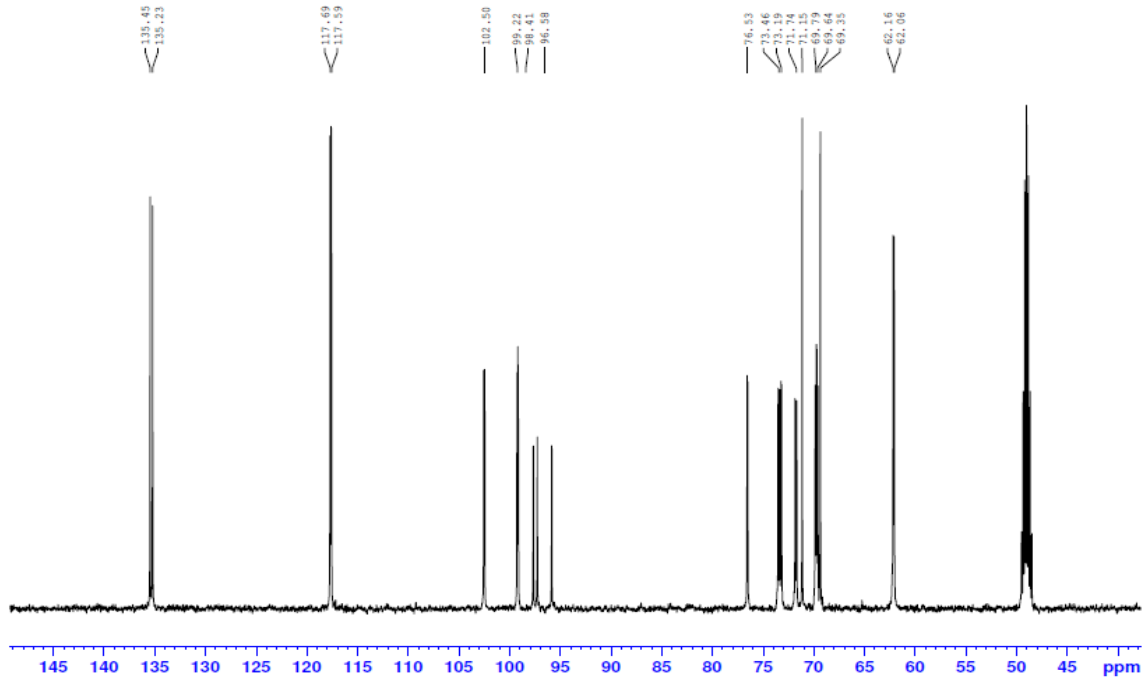

$^{13}C\{^{1}H\}$ NMR (125 MHz, CD_3OD) spectrum of allyl 3-deoxy-3-fluoro-D-glucopyranoside (**13**)

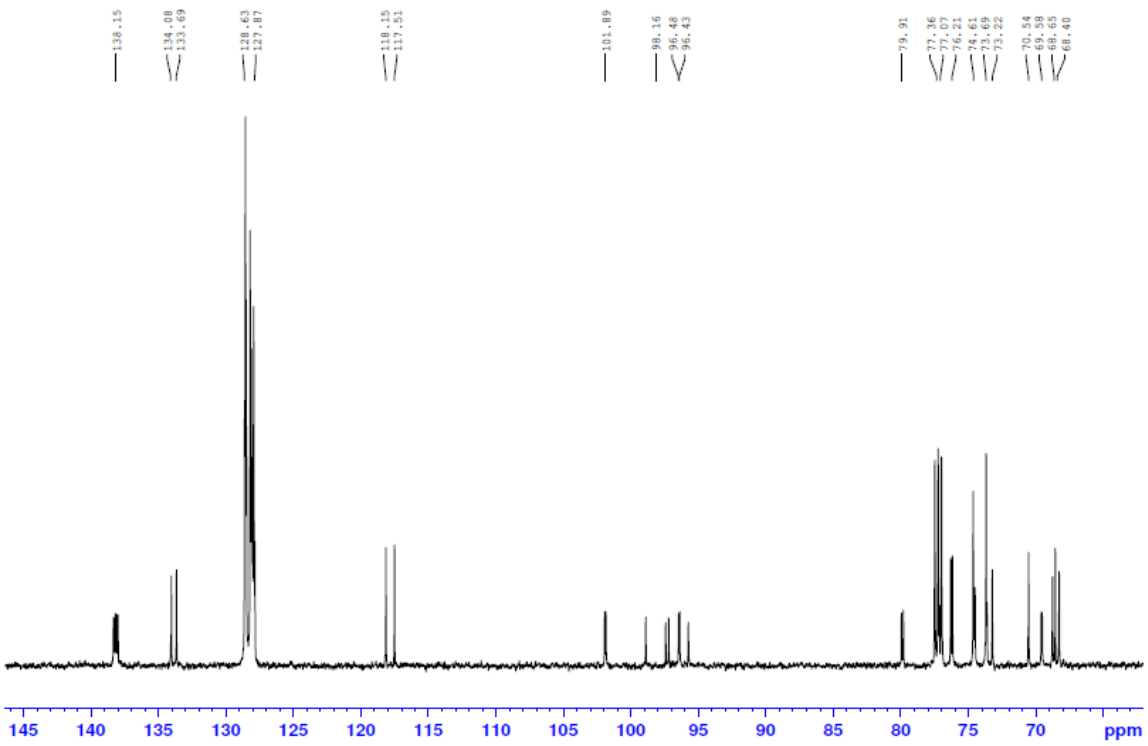

$^{13}C\{^{1}H\}$ NMR (125 MHz, $CDCl_3$) spectrum of allyl 2,4,6-tri-*O*-benzyl-3-deoxy-3-fluoro-D-glucopyranoside (**14**)

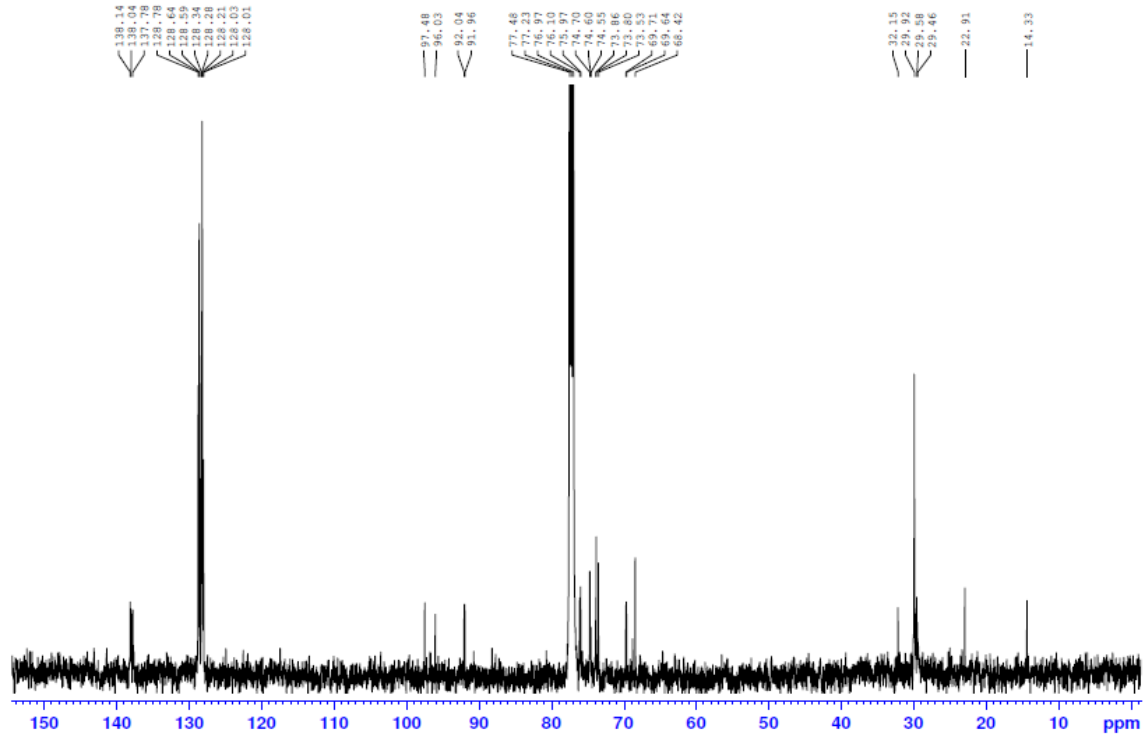

$^{13}C\{^{1}H\}$ NMR (125 MHz, $CDCl_3$) spectrum of 2,4,6-tri-*O*-benzyl-3-deoxy-3-fluoro-D-glucopyranose (**15**)

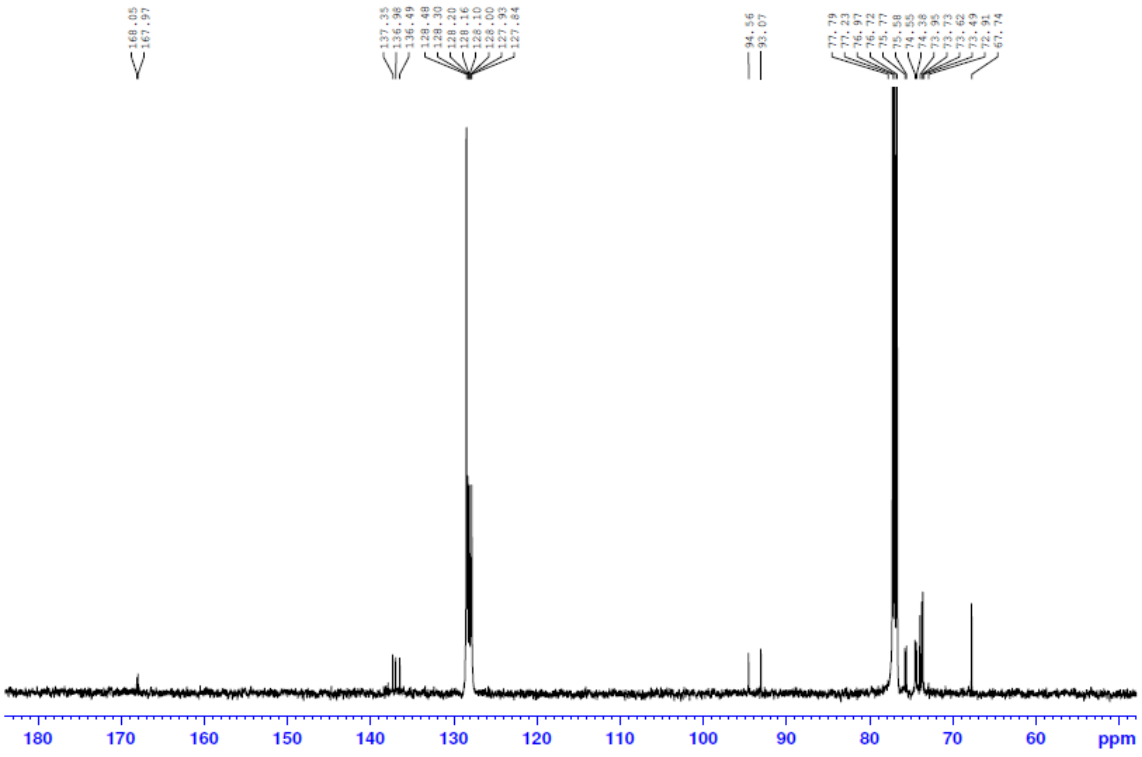

$^{13}C\{^{1}H\}$ NMR (125 MHz, $CDCl_3$) spectrum of 2,4,6-tri-*O*-benzyl-3-deoxy-3-fluoro-D-gluconolactone (**16**)

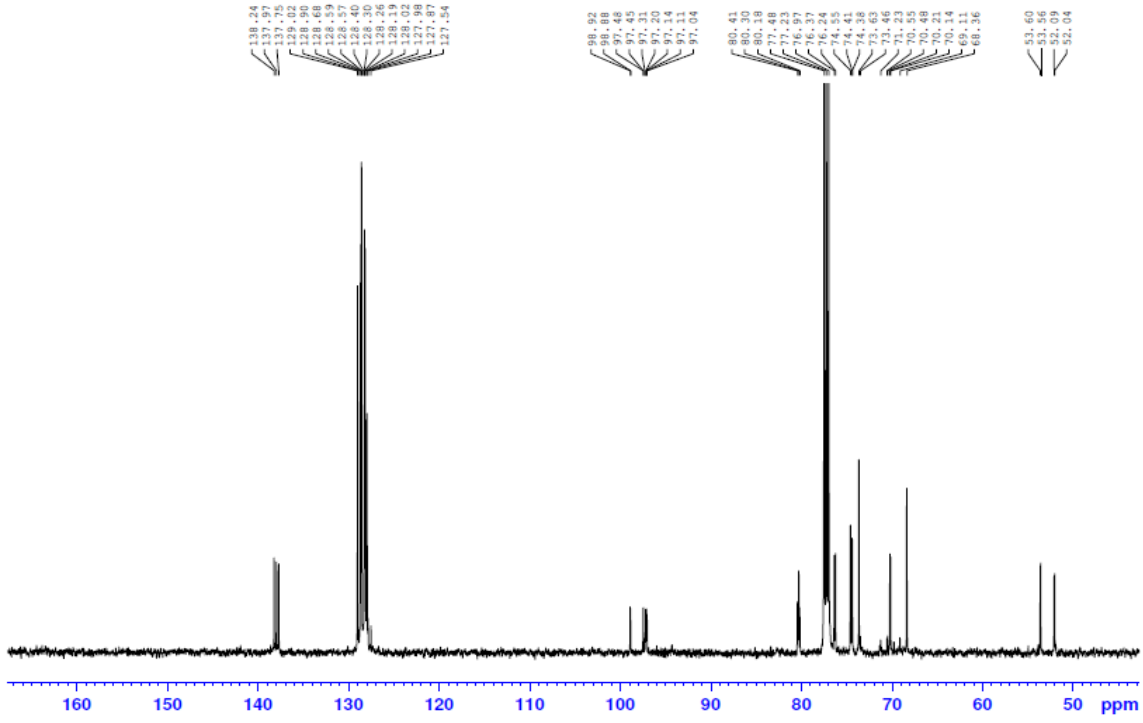

$^{13}C\{^{1}H\}$ NMR (125 MHz, $CDCl_3$) spectrum of 1-(dimethyl phosphonatylmethyl)-2,4,6-tri-*O*-benzyl-3-deoxy-3-fluoro-α-D-glucopyranose (**17**)

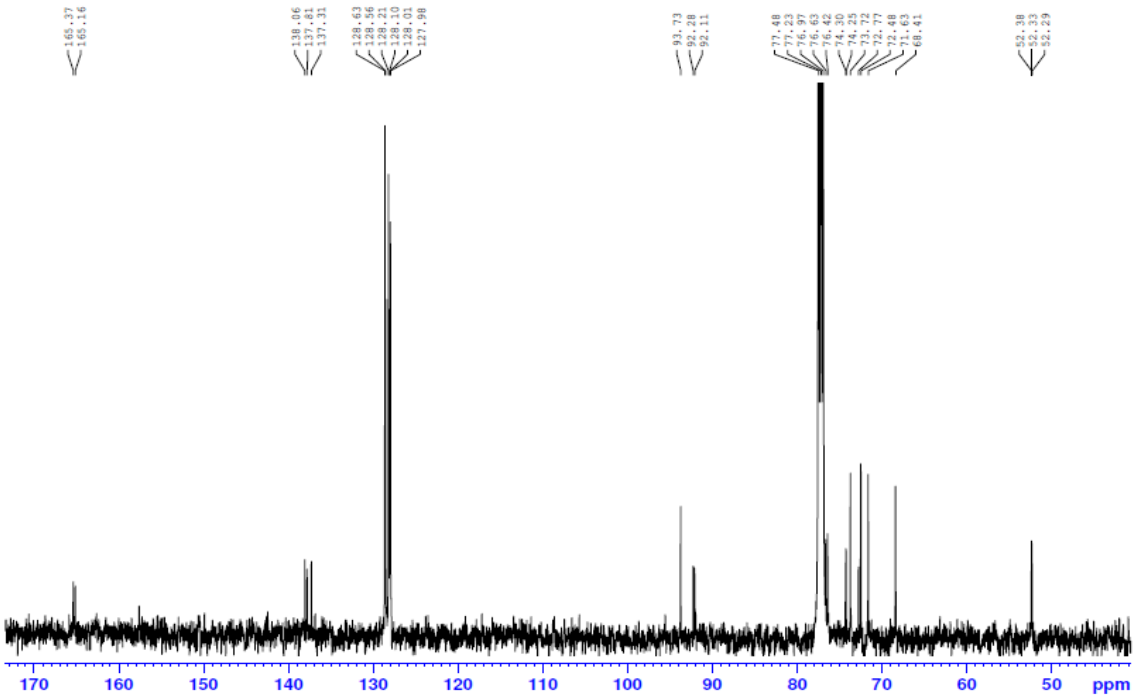

$^{13}C\{^{1}H\}$ NMR (125 MHz, $CDCl_3$) spectrum of (E/Z)-1-β-dimethylphosphonomethylene-2,4,6-tri-*O*-benzyl-1,3-deoxy-3-fluoro-D-glucopyranosyl-2-ylidene (**19**)

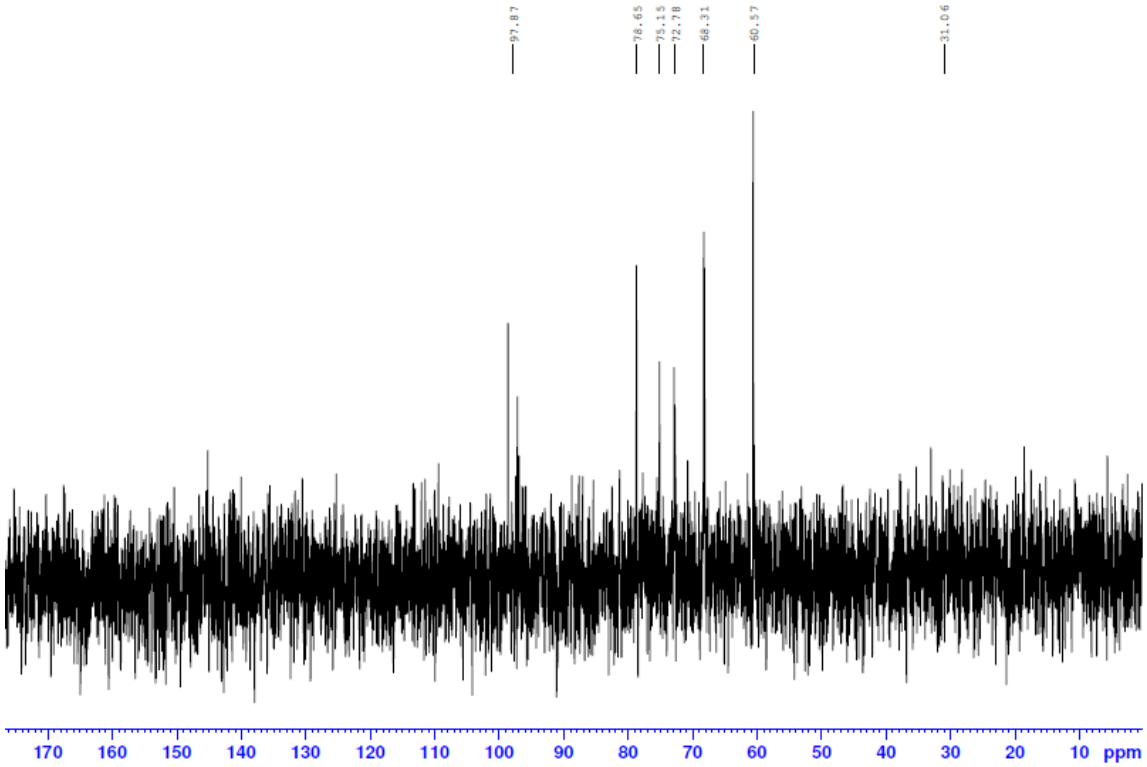

$^{13}C\{^{1}H\}$ NMR (125 MHz, D_2O) spectrum of diammonium 3-deoxy-3-fluoro-β-D-glucopyranosylmethylphosphonate (**21**)

Appendix D. Mass spectra

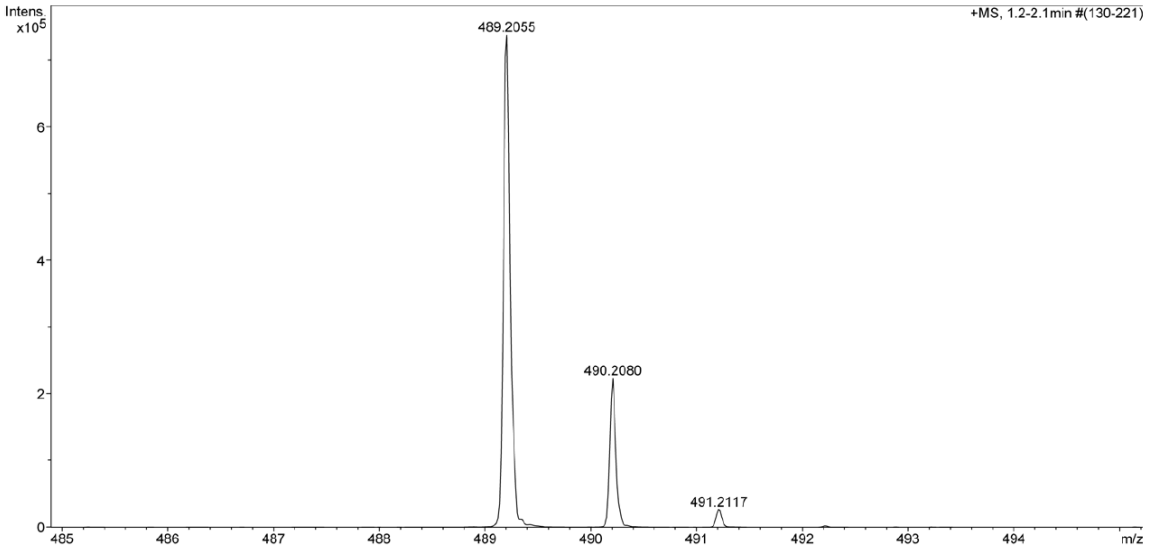

ESI+ high resolution mass spectrum of methyl 2,4,6-tri-*O*-benzyl-3-deoxy-3-fluoro-β-D-glucopyranoside (**12**), where *m/z* found = $[\mathbf{12}+Na]^+$ = 489.2055.

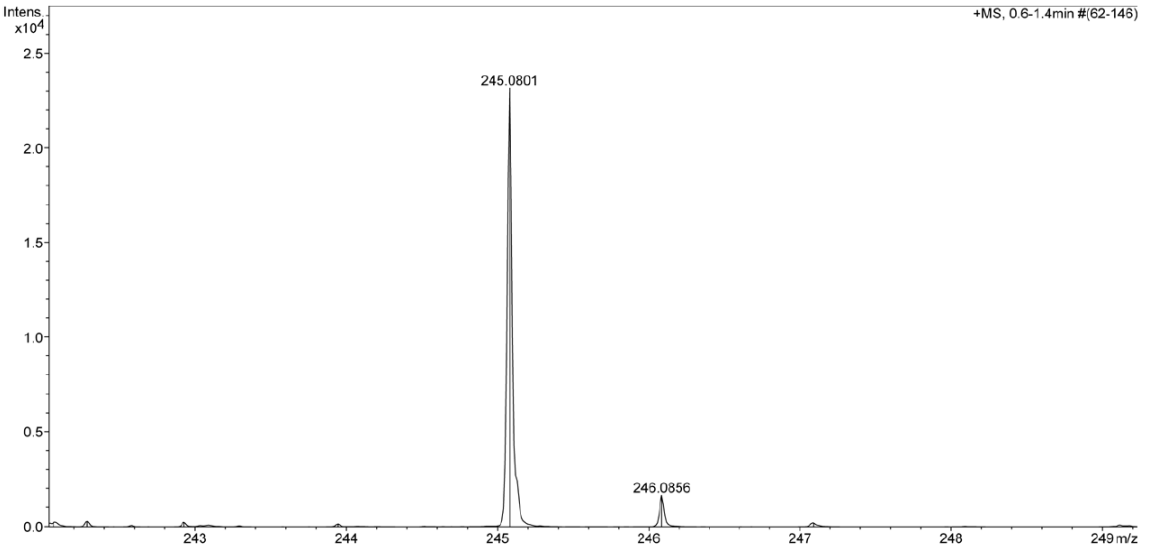

ESI+ high resolution mass spectrum of allyl 3-deoxy-3-fluoro-D-glucopyranoside (**13**), where *m/z* found = $[\mathbf{13}+Na]^+$ = 245.0801.

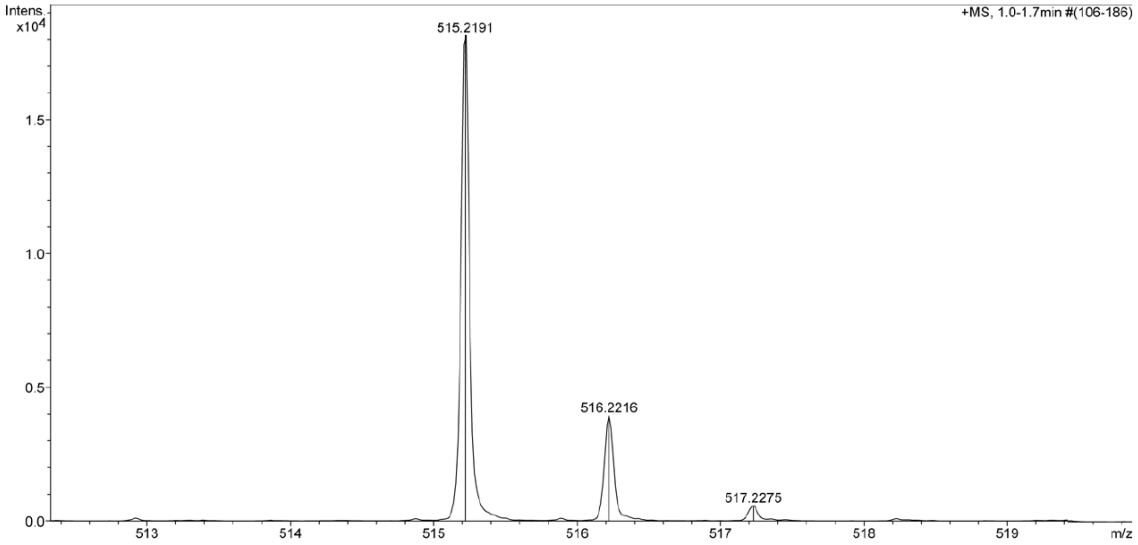

ESI+ high resolution mass spectrum of allyl 2,4,6-tri-*O*-benzyl-3-deoxy-3-fluoro-D-glucopyranoside (**14**) where *m/z* found = $[\mathbf{14}+Na]^+$ = 515.2191.

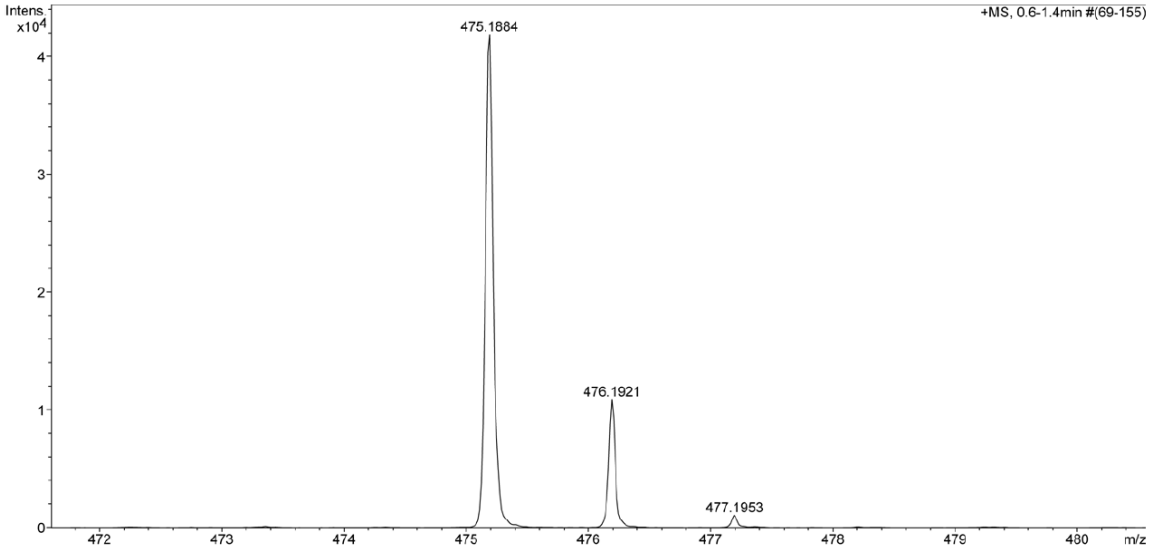

ESI+ high resolution mass spectrum of 2,4,6-tri-*O*-benzyl-3-deoxy-3-fluoro-D-glucopyranose (**15**) where *m/z* found = $[\mathbf{15}+Na]^+$ = 475.1884.

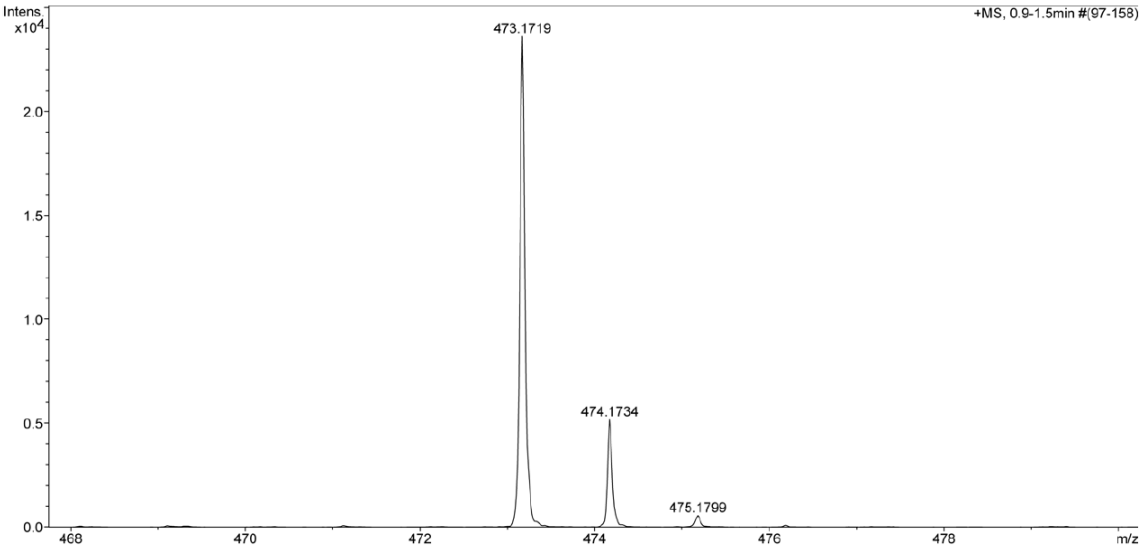

ESI+ high resolution mass spectrum of 2,4,6-tri-*O*-benzyl-3-deoxy-3-fluoro-D-gluconolactone (**16**) where *m/z* found = [**16**+Na]$^+$ = 473.1719.

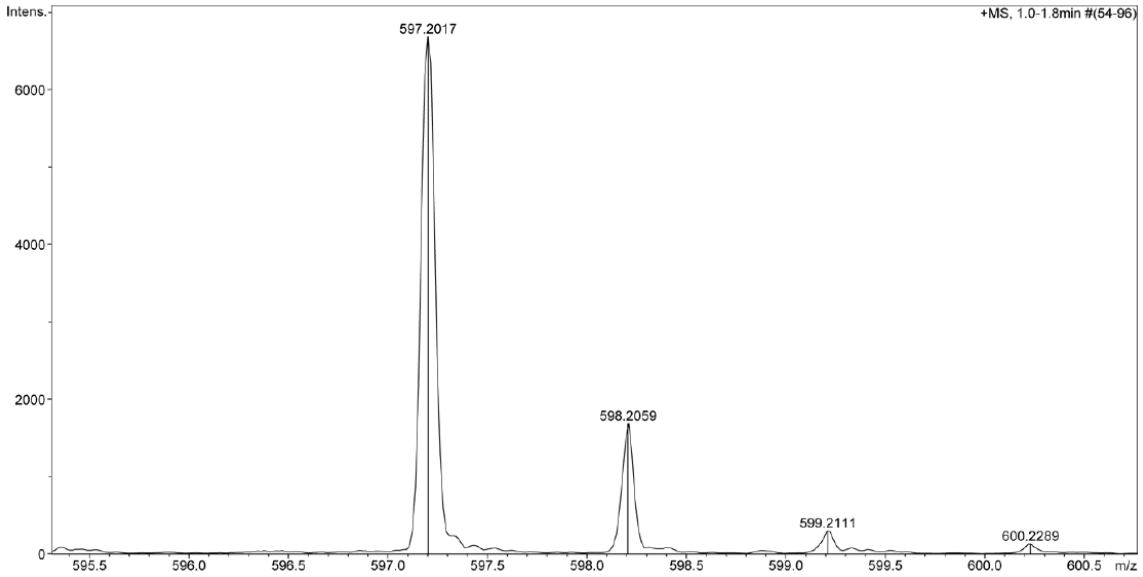

ESI+ high resolution mass spectrum of 1-(dimethyl phosphonatylmethyl)-2,4,6-tri-*O*-benzyl-3-deoxy-3-fluoro-α-D-glucopyranose (**17**) where *m/z* found = [**17**+Na]$^+$ = 597.2017.

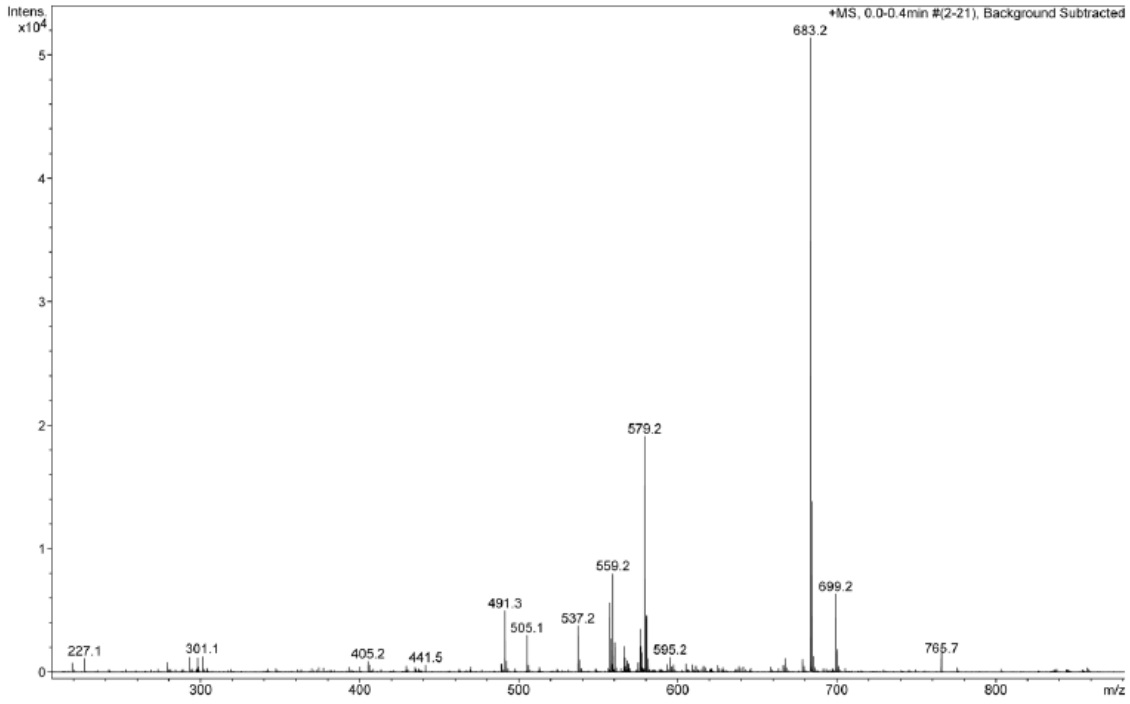

ESI+ low resolution mass spectrum of (methyl oxalyl) 1-(dimethyl phosphonatylmethyl)-2,4,6-tri-*O*-benzyl-3-deoxy-3-fluoro-α-D-glucopyranose (**18**) where *m/z* found = $[\mathbf{18}+Na]^+ = 683.2$.

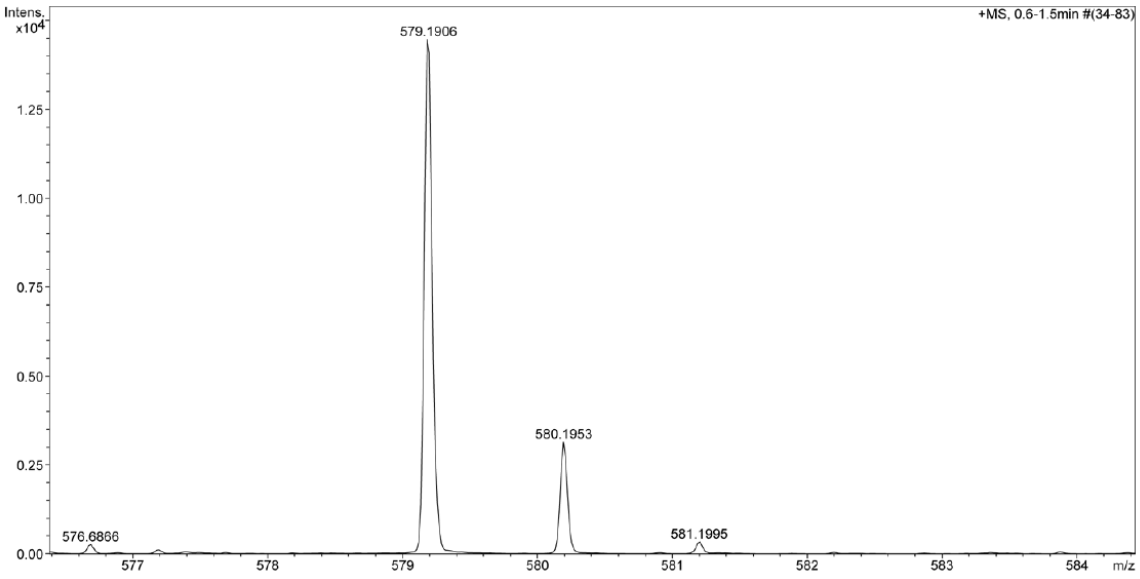

ESI+ high resolution mass spectrum of (E/Z)-1-(dimethylphosphonomethylene)-2,4,6-tri-*O*-benzyl-1,3-deoxy-3-fluoro-D-glucopyranosyl-2-ylidene (**19**) where *m/z* found = $[\mathbf{19}+Na]^+ = 579.1906$.

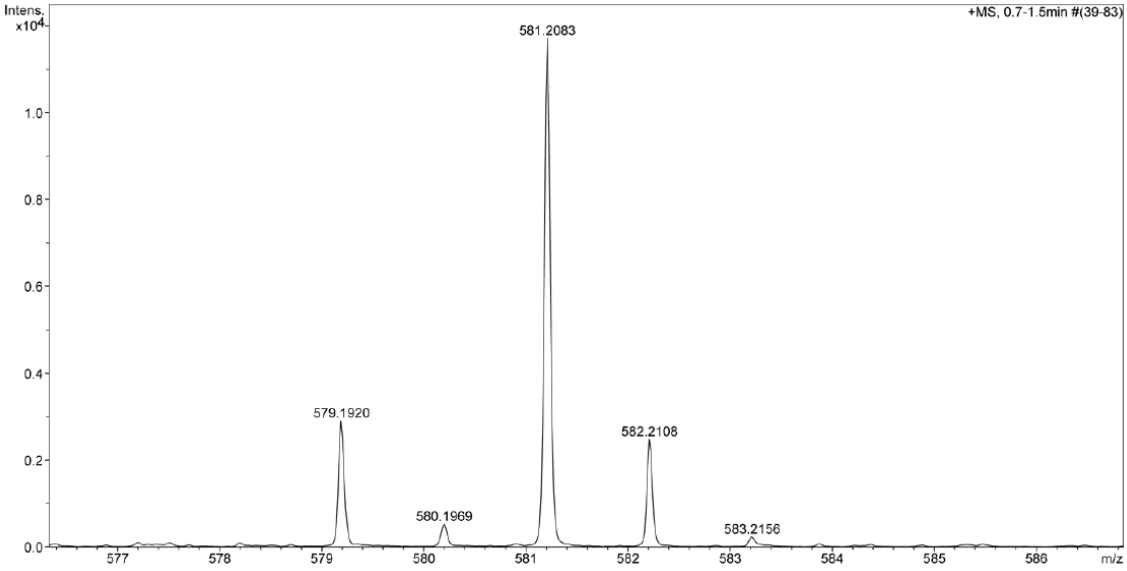

ESI+ high resolution mass spectrum of (E/Z)-1-β-dimethylphosphonomethylene-2,4,6-tri-*O*-benzyl-1,3-deoxy-3-fluoro-D-glucopyranosyl-2-ylidene (**19**) and 2,4,6-tri-*O*-benzyl-3-deoxy-3-fluoro-β-D-glucopyranosylmethylphosphonate (**20**) mixture where *m/z* found = $[\mathbf{20}+Na]^+ = 581.2063$.

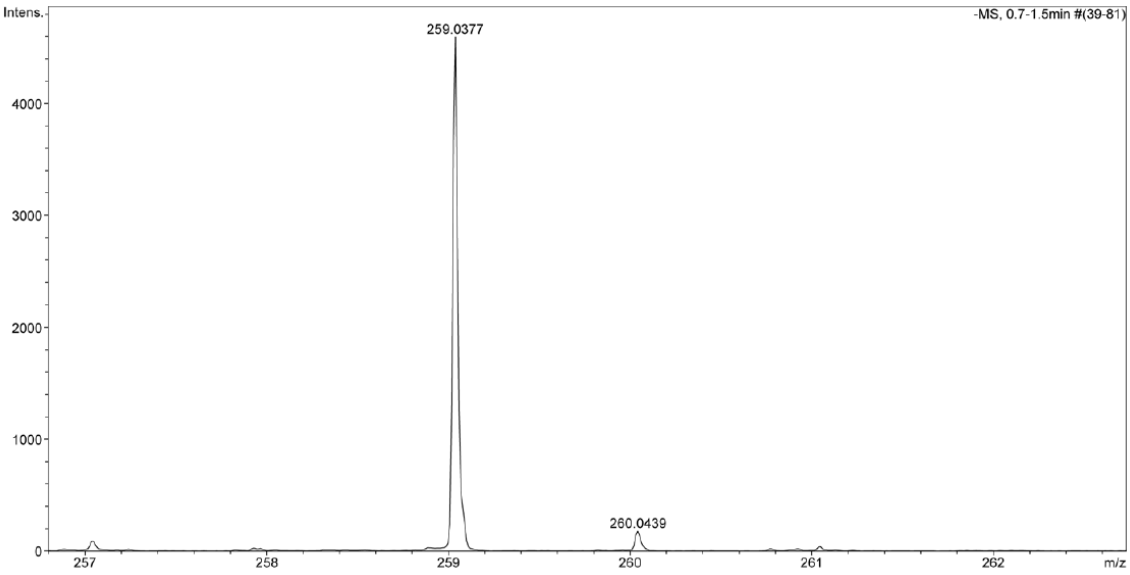

ESI- high resolution mass spectrum of diammonium 3-deoxy-3-fluoro-β-D-glucopyranosylmethylphosphonate (**21**) where *m/z* found = $[\mathbf{21}-H]^- = 259.0377$

Appendix E. ^{31}P NMR spectra of Synthetic Products

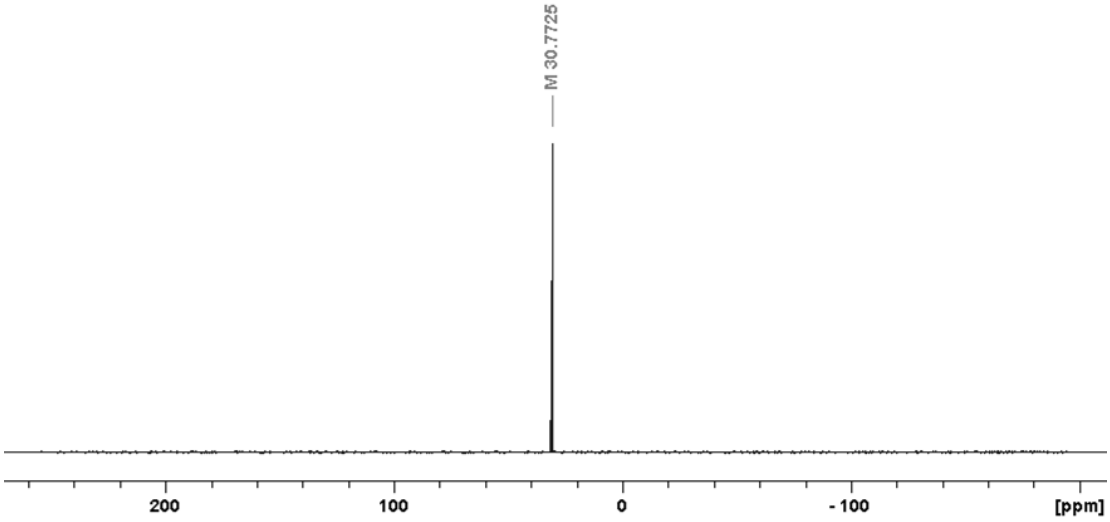

$^{31}P\{^{1}H\}$ NMR (202 MHz, $CDCl_3$) spectrum of 1-(dimethyl phosphonatylmethyl)-2,4,6-tri-*O*-benzyl-3-deoxy-3-fluoro-α-D-glucopyranose (**17**)

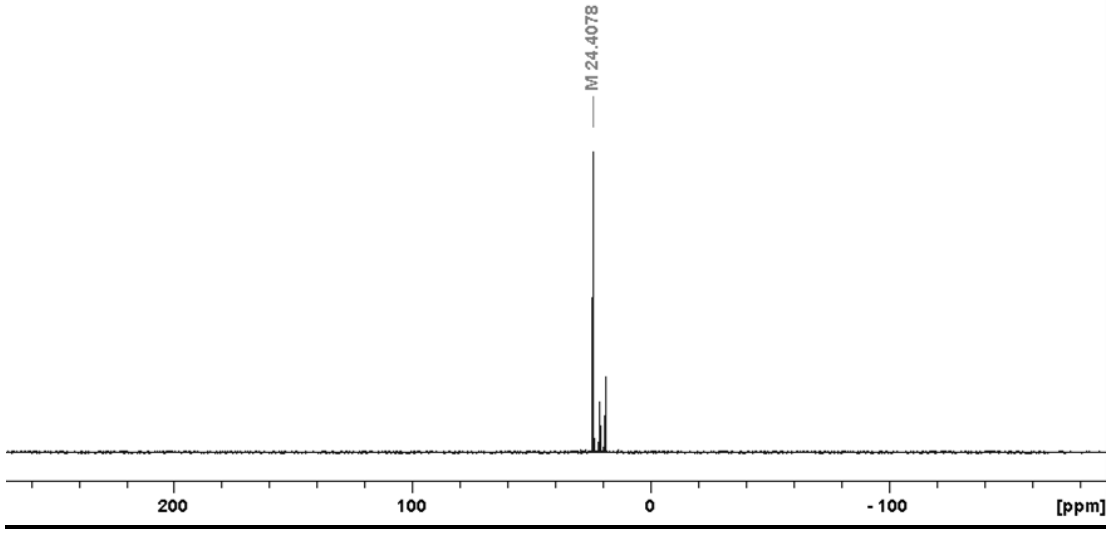

$^{31}P\{^{1}H\}$ NMR (202 MHz, $CDCl_3$) spectrum of (methyl oxalyl) 1-(dimethyl phosphonatylmethyl)-2,4,6-tri-*O*-benzyl-3-deoxy-3-fluoro-α-D-glucopyranose (**18**)

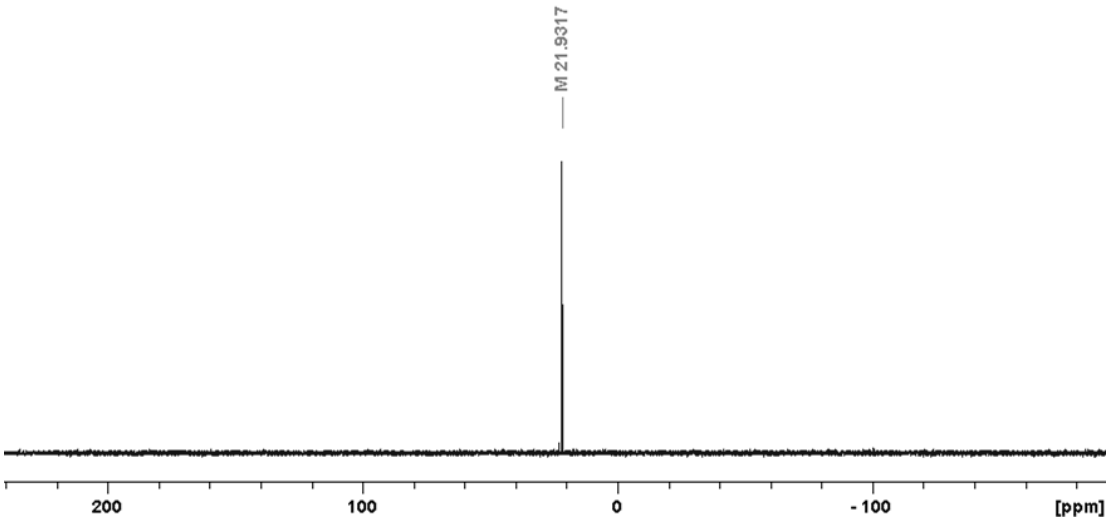

$^{31}P\{^{1}H\}$ NMR (202 MHz, $CDCl_3$) spectrum of (E/Z)-1-(dimethylphosphonomethylene)-2,4,6-tri-*O*-benzyl-1,3-deoxy-3-fluoro-D-glucopyranosyl-2-ylidene (**19**)

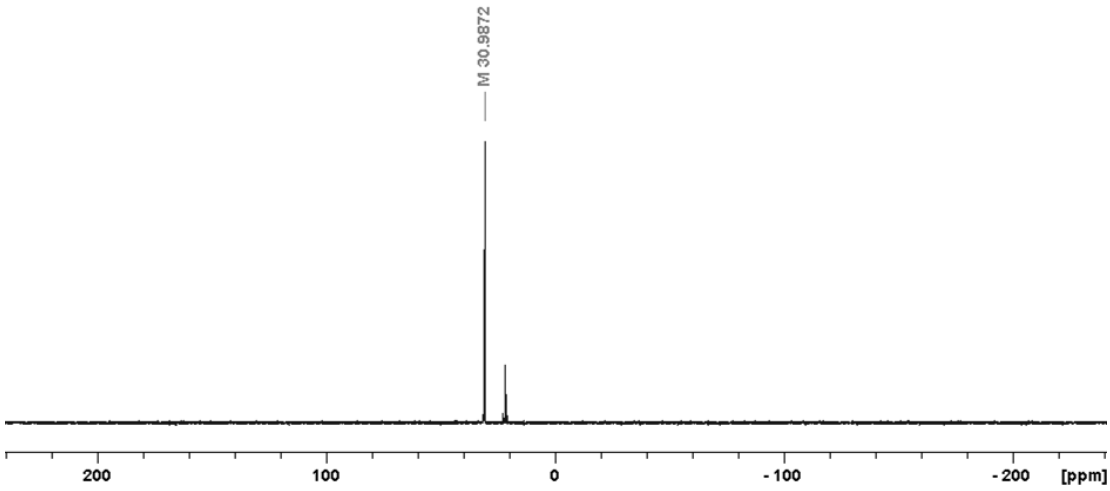

$^{31}P\{^{1}H\}$ NMR (202 MHz, $CDCl_3$) spectrum of (E/Z)-1-β-dimethylphosphonomethylene-2,4,6-tri-*O*-benzyl-1,3-deoxy-3-fluoro-D-glucopyranosyl-2-ylidene (**19**) and 2,4,6-tri-*O*-benzyl-3-deoxy-3-fluoro-β-D-glucopyranosylmethylphosphonate (**20**) mixture

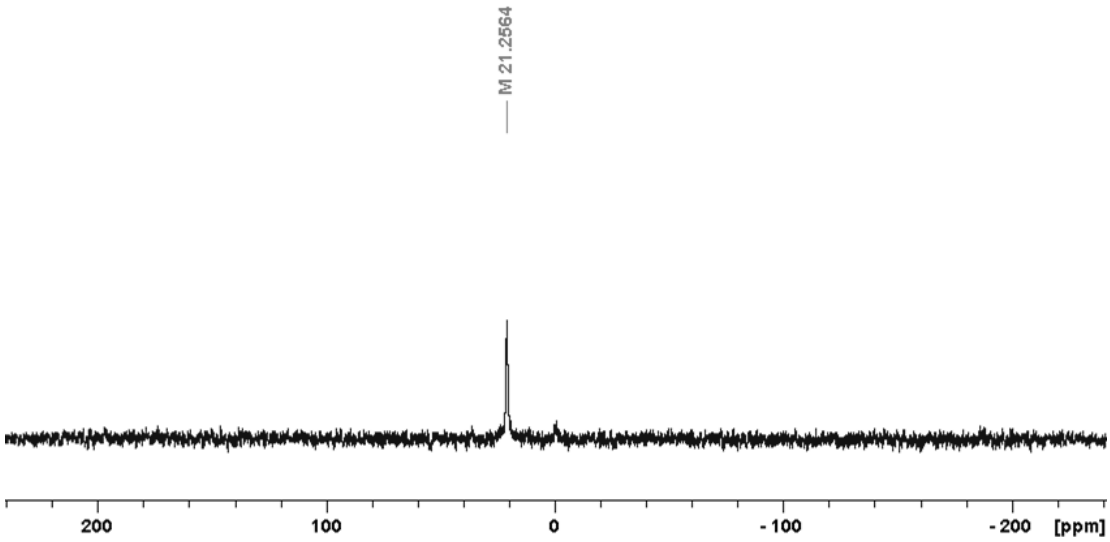

$^{31}P\{^{1}H\}$ NMR (202 MHz, D_2O) spectrum of diammonium 3-deoxy-3-fluoro-β-D-glucopyranosylmethylphosphonate (**21**)

Appendix F. HSQC NMR spectrum of 21

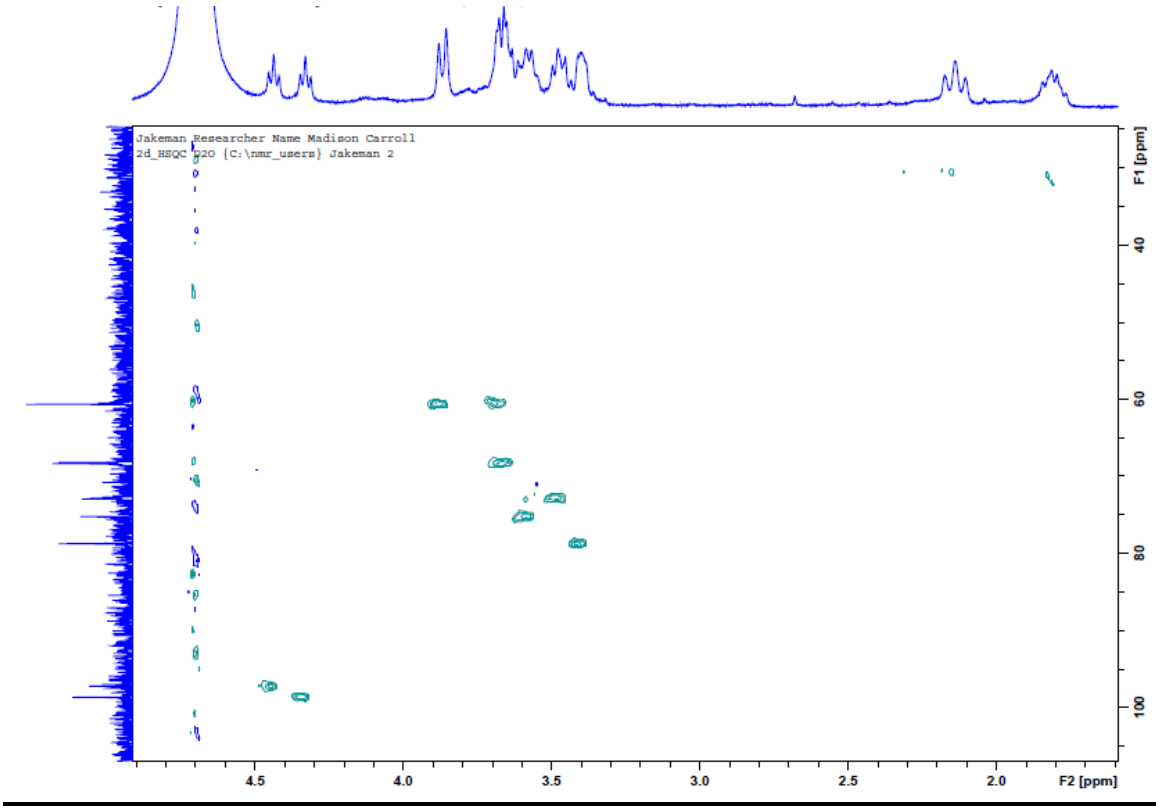

HSQC NMR spectrum (500 MHz, D_2O) of diammonium 3-deoxy-3-fluoro-β-D-glucopyranosylmethylphosphonate (**21**)